Project no. 044132
AFISA
Automated FISh Ageing

Instrument: **STREP**

Thematic Priority: **8.1** Policy-oriented researches

Final Activity Report

Period covered: from 01/04/2007 to 31/03/2009

Date of preparation: 04/2009

Start date of project: 01/04/2007

Duration: 24 months

Project coordinator: Kélig Mahé
Project coordinator organisation: Ifremer

Revision: draft 1

CONTENTS

Publishable executive summary

Most of the fish stocks are assessed using age-based models, however age estimations using otoliths costs several million euros annually. In this context, Automatic Fish Ageing (EU Project) aimed at providing means to standardize ageing among laboratories and build interpreted image databases ensuring the information conservation. It falls within the framework of the quality approach for ageing and storage. Automation should improve growth studies while reducing the cost of the acquisition of age data.

The overall objectives of this project were (i) the development of algorithms for fish ageing automation from otolith features (ii) the implementation of these automated ageing modules in a software platform dedicated to otolith imaging (iii) a cost-benefit analysis of the proposed automated ageing systems.

The Afisa project focused on three case studies : a) Cod (*Gadus morhua* ; Faeroes, North Sea, North East Arctic) b) Anchovy (*Engraulis encrasicolus* ; Bay of Biscay) c) Plaice (*Pleuronectes platessa*, Eastern Channel, Iceland).

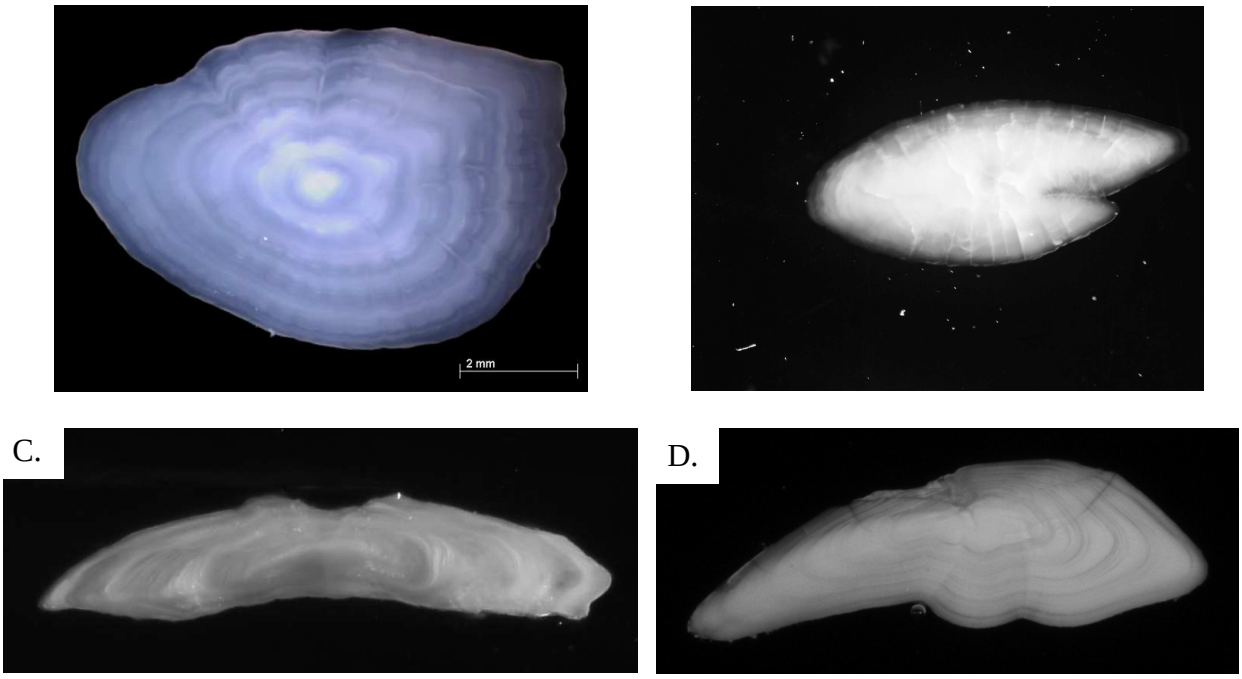

Images of three case studies : Whole otolith of plaice (A.), Whole otolith of anchovy (B.), Thin transverse section of plaice otolith (C.) and Thin transverse section of cod otolith (D.)

A total of 6729 otoliths were collated from surveys and commercial landings. The associated data were specifically made available for the AFISA project (Area, Year, Quarter, Total Length, Weight, Sex, Maturity). Using TNPC software, images were acquired (calibrated images under reflected and transmitted light, otolith features). Age estimates were provided by readers each otolith. All images and data were compiled in the same format.

The consortium developed two different approaches to realise an automated fish age estimation :

- a classifier that estimates individual ages based on intensity profiles along radials of the images of otolith sections.

- ❖ models that estimates age proportion based on the otolith and fish features. Conditional and Mixture models were used.

The estimation of individual ages from otolith images involved a series of image processing methods, specifically designed for the considered case studies (morphological segmentation and nucleus detection, 2D ring detection contrast enhancement) and a nearest neighbour classification method. The angular sectors, that a priori contain the best growth marks, are selected, an intensity profile is computed in each sector and the fish's age is estimated by searching for the k most similar intensity profiles among those stored in a reference database (RDB), which has been calibrated by experts. To reduce the effects of non-linear growth the profiles are aligned elastically before measuring the differences between them.

The estimation of age proportion based on morphologic descriptors of the fish and its otolith are estimated by the probability that a fish belongs to a certain age group.
The conditional model is based on the principle that the probability is computed from the distance between the descriptors of the fish of unknown age and the ones with known ages in the calibration set. For a given production set, the age-class proportions are estimated by the sum of the individual classification probabilities.
The mixture model used discriminant analysis which was considered to estimate the unknown age distribution in a production sample including covariates (features) based on a calibration sample for which age as well as covariates were known. For the calibration sample the linear discriminant analysis procedure was used to predict the posterior probabilities and the averages (procedure was repeated 500 times) were used for the age composition. To test and validate the conditional and mixture models, the available data set was randomly divided the into a training set of 50% and a testing set of 50%.

The results of the automatic estimation of individual age showed agreement percentages with the age estimated by the readers from 90.9% (Iceland Plaice) to 33.2% (North East Arctic Cod). Conditional and mixture models were applied for automatic estimation of age structure starting from the features of fish (TL and W) and otolith (TL, W, Area, Major and Minor Axis Length, Perimeter) and showed very strong variations between the cases of study.

These differences could be due to the difficult discrimination of the growth rings for some species (anchovy for example), because of the poor quality of the images, and also the poor representation of some age groups…

Automatic Fish Ageing algorithms (estimation of individual ages and age proportioned), were integrated in the software TNPC 5.0 developed by the Noesis company. The software now allows automated procedures for the acquisition of otolith image series and for age estimation (individual or age proportions)

A cost/benefit analysis was carried out for the 3 automated methods and the traditional ALK (Age Length Key). Two measures have been applied as measure of goodness: Mean squared error (MSE) and relative bias (RB). Cost associated to the different age estimation methodologies are worked out.
The cost/benefit results showed large differences between species and stocks. By comparing the bias between the automatic methods and the traditional ALK, they are low for the plaice (Eastern Channel, Iceland) and the North East Artic cod whereas they are very significant for anchovy (Bay of Biscay) and cod (Faeroes, North Sea). Moreover, the cost analysis presented the same results. It is important to note that bias can exist for the age estimation among the

international readers. For example, inter-reader bias test during the international otolith exchange of NEA Cod, showed that there are significant differences in age estimates among readers from different institutions.

In conclusion, the AFISA project resulted in advances in computer vision which provide more reliable methods to extract information from otoliths in order to estimate the individual age and the age structure. These methods are operational using TNPC software. How ever such methods should not be seen as being able to fully substitute to experts. They should rather been seen as tools to provide automatically extracted information that requires a subsequent control by experts for the estimations of individual age and age structure. For some species such as plaice, these methods could be usable from the perspective of bias and costs.

Project information

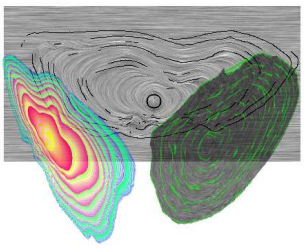

Co-ordinator : Ronan Fablet (from 01/04/07 to 25/02/08)
Kélig Mahé (from 26/02/08 to 01/04/09)

Kelig.Mahe@ifremer.fr
IFREMER, Centre Manche-mer du Nord, Laboratoire Ressources Halieutiques, 150 quai Gambetta, BP 699, 62321 Boulogne sur mer, France

Contractors Involved : Institut Français de Recherche pour l'Exploitation de la Mer (IFREMER, France), Fundacion AZTI-AZTI Fundazioa (AZTI, Spain), The Centre for Environment Fisheries & Aquaculture Science (CEFAS, United Kingdom), Danish Institute for Fisheries Research (DTU, Denmark) , Institute of Marine Research (IMR, Norway), Marine Research Institute (MRI, Iceland), University Polytechnic of Catalonia (UPC, Spain)

Deliverables List

List all deliverables, giving date of submission and any proposed revision to plans.

Del. no.	Deliverable name	WP no.	Date due	Actual/Forecast delivery date	Estimated indicative person-months *)	Used indicative person-months *)	Lead contractor
D0.1	Consortium Agreement	WP0	31/06/2007	31/02/2008	-	-	1
D0.2	Facilities for disseminating data sets and analyses (FTP, Web site or CD)	WP0	31/12/2007	31/12/2007	-	-	1
D0.3	Reports: all reports as specified in Article II.7.2 of Annex II of the contract	WP0	31/03/2008	31/03/2008	-	-	1
D0.4	Reports: all reports as specified in Articles II.7.2, II.7.3 and II.7.4 of Annex II of the contract	WP0	31/03/2009	31/03/2009	-	-	1
D0.5	Policy Implementation Plan	WP0	31/03/2009	31/03/2009	-	-	1
D0.6	Audit certificates to each participant	WP0	31/03/2009	31/03/2009	-	-	1
D1.1	Provide settings for protocols and database structure for images and associated otolith and biological information, for cod, plaice and anchovy otoliths	WP1	31/07/2007	31/07/2007	-	-	3
D1.2	Database of otolith images and associated otolith and biological information for cod, plaice and anchovy otoliths	WP1	31/12/2007	31/12/2007	-	-	3
D1.3	Age distribution of the selected case studies based on expert readers and otolith weight for comparison with the result from the automated ageing	WP1	31/12/2007	31/12/2007	-	-	3
D1.4	Comprehensive cost –budgets for processing otoliths enabling calculation of a population age distribution for traditional ageing, otolith weight and automated ageing	WP1	31/12/2007	31/12/2007	-	-	3
D2.1.a	Automated system for the acquisition of series of otolith images	WP2	31/12/2007	31/12/2007	-	-	1
D.2.2.a	a 2D forward-growth model of otolith morphology	WP2	31/03/2008	31/03/2008	-	-	1
D.2.2.b	Probabilistic 2D growth consistency-checking model	WP2	31/03/2008	31/03/2008	-	-	1
D2.3.a	Algorithm for nucleus detection	WP2	31/12/2007	31/12/2007	-	-	1
D2.3.b	Algorithm for the reconstruction of dense growth direction fields from images	WP2	31/12/2007	31/12/2007	-	-	1
D2.3.c	Algorithm for locally adapting directional filters with variable bandwidth for ring enhancement and detection	WP2	31/12/2007	31/12/2007	-	-	1
D 2.3.d	Algorithm for the detection of reference growth axes	WP2	31/03/2008	31/03/2008	-	-	1
D2.3.e	Algorithm for the 1D detection of otolith rings	WP2	31/03/2008	31/03/2008	-	-	1

D2.3.f	Algorithm for the 2D segmentation of partial otolith rings	WP2	31/08/2008	31/08/2008	-	-	1
D2.3.g	Contrast-invariant representation of otolith ring-based information	WP2	31/08/2008	31/08/2008	-	-	1
D2.4.a.	Feature discrimination algorithm	WP2	31/12/2007	31/12/2007	-	-	1
D2.4.b.	Feature discrimination algorithm code and report, following modifications suggested from its evaluation during the 2nd project meeting at month 9	WP2	31/03/2008	31/03/2008	-	-	1
D2.4.c.	Statistical learning algorithm for automated fish ageing	WP2	31/08/2008	31/08/2008	-	-	1
D2.4.d.	Statistical learning algorithm for automated fish ageing, following modifications suggested from its evaluation during the 3rd project meeting at month 17	WP2	30/09/2008	30/09/2008	-	-	1
D2.5.a	Mixture model for age structure estimation from global otolith features and physical fish characteristics	WP2	31/03/2008	31/03/2008	-	-	1
D2.5.b	Conditional model for age structure estimation from global otolith features and physical fish characteristics	WP2	31/08/2008	31/08/2008	-	-	1
D3.1	TNPC module automating the acquisition of series of otolith images	WP3	31/03/2008	31/03/2008	-	-	1
D3.2	TNPC module for the automated estimation of individual ages	WP3	31/12/2008	31/12/2008	-	-	1
D3.3	TNPC module for the automated estimation of age structures	WP3	31/12/2008	31/12/2008	-	-	1
D4.1.a	Template for cost-benefit analysis based on different objective functions	WP4	31/11/2007	31/11/2007	-	-	4
D4.1.b	Parameterization, to case-studies I, II and III, of the automated estimations of individual ages	WP4	31/07/2008	31/07/2008	-	-	4
D4.1.c	Parameterization, to case-studies I, II and III, of the automated estimation of age structures	WP4	30/11/2008	30/11/2008	-	-	4
D4.2	Cost-benefit analysis for case study I (cod)	WP4	31/03/2009	31/03/2009	-	-	4
D4.3	Cost-benefit analysis for case study II (plaice)	WP4	31/03/2009	31/03/2009	-	-	4
D4.4	Cost-benefit analysis for case study III (anchovy)	WP4	31/03/2009	31/03/2009	-	-	4

*** If available**

Milestones List

List all milestones, giving date of achievement and any proposed revision to plans.

Mlst no.	Milestone name	WP no.	Date due	Actual/Forecast delivery date	Estimated indicative person-months *)	Used indicative person-months *)	Lead contractor
M0.1	Project meetings (at the start and then at approximately 8 month intervals thereafter)	WP0	31/11/2007	31/11/2007	-	-	1
M1.1	Agree list of procedures for standardisation of protocols	WP1	31/06/2007	31/07/2007	-	-	3
M1.2	Review of data complied and identification of any weaknesses and remedial action	WP1	31/08/2007	31/12/2007	-	-	3
M1.3	Acceptance of finalised databases with associated data (including acquisition costs/budgets)	WP1	31/12/2007	31/01/2008	-	-	3
M2.1	Definition of code formats and prototypes	WP2	31/04/2007	31/04/2007	-	-	1
M2.2	Review of information extraction in otolith images	WP2	31/12/2007	31/01/2008	-	-	1
M2.3	Review of the automated ageing systems	WP2	31/08/2008	31/01/2009	-	-	1
M3.1	Define software specifications	WP3	31/03/2008	31/03/2008	-	-	1
M3.2	Beta-version Release	WP3	31/09/2008	31/01/2009	-	-	1
M3.3	Software release	WP3	31/12/2008	31/03/2009	-	-	1
M4.1	Agree template for cost analysis	WP4	31/04/2007	31/05/2007	-	-	1
M4.2	Define objective functions for precision and accuracy using different strategies	WP4	31/10/2007	31/10/2007	-	-	4
M4.3	Parameterization of the automated ageing systems for case-studies I, II and III	WP4	31/08/2008	31/08/2008	-	-	4
M4.4	Cost-benefit analyses for case studies I, II and III	WP4	31/03/2009	31/03/2009	-	-	4

WP1 - Collation of otolith material and creation of databases of annotated images of otoliths

Scientific teams involved: Partner 1, Ifremer; Partner 2, Azti, Partner 3, Cefas (coordinator); Partner 4, Difres; Partner 5, IMR; Partner 6, MRI
Institute: Person (1) Kélig Mahé, André Ogor, Romain Elleboode, Jean Louis Dufour, Marie Line Manten ; Erwan Duhamel (2) Unai Cottano; (3) Richard Millner, Sally Warne; (4) Karin Hűssy; (5) Hans Høie; Alf Harbitz; (6) Elías Guðmundsson.

Overall objectives: Collect otolith images and associated otolith and biological parameters for the three species selected under this project and to make these available in a suitable database.
Create a cost-budget for all steps involved in making data available for the estimation of an age distribution (by traditional ageing; otolith weight/morphological features; and automated ageing respectively).

Deliverables:

1. Provide settings for protocols and database structure for images and associated otolith and biological information, for cod, plaice and anchovy otoliths
2. Database of otolith images and associated otolith and biological information for cod, plaice and anchovy otoliths
3. Age distribution of the selected case studies based on expert readers and otolith weight for comparison with the result from the automated ageing
4. Comprehensive cost –budgets for processing otoliths enabling calculation of a population age distribution for traditional ageing, otolith weight and automated ageing

WP1: Collation of otolith material and creation of databases of annotated images of otoliths

Start date: month : 1
Completion date: month : 9

Partner responsible: Partner 3 (Cefas)
Partners involved: All partners except UPC
Person-months: 34.75
Status of progress: This WP has been successfully completed.

Workpackage 1 Objectives

The key aims of this work package were to:

- Collect otolith images and associated otolith and biological parameters for the three species selected under this project and to make these available in suitable databases.
- Create a cost-budget for all steps involved in making data available for the determination of an age distribution (by traditional ageing; otolith weight/morphological features; and automated ageing respectively).

The aim was to assemble all the basic material required for the remainder of the project. This means collecting together both images and associated biological parameters from otoliths of the three selected species and five sea areas. The otoliths will be representative of the

exploited age range and area from which they come. Apart from the FAbOSA material from the Faeroes, there is no other known age material and all the otoliths will be aged by expert readers. In the case of cod, slides will then be used in processing but in plaice the image analysis will be carried out on both sections and whole otoliths as a means of comparing the two widely used techniques. For anchovies, only whole material will be used. In order to ensure standardisation across the images methodologies will be developed at the start of the project for ensuring that images are obtained in a standardised form for each species with respect to the illumination, magnification and resolution. Data will be assembled in a simple database holding the images an associated biological data which will be made available to all participants. The second aim of this project will be to create an exhaustive cost-budget for all the steps involved in handling the otoliths from collection, weighing through to the capture of the image for analysis. The cost benefit will also look at factors such as equipment costs and staff training which may have an impact on comparing routine ageing with computer assisted age reading.

Progress towards Objectives WP1

During this first year, the entirety of the Workpackage 1 was carried out with 4 following tasks:

- **Provide settings for protocols and database structures for images and associated otolith and biological information, for cod, plaice and anchovy otoliths.**

INTRODUCTION

The aim of this work was to ensure standardisation of methods across the different institutes. At the outset, methodologies and protocols were developed to ensure that the images were obtained in a standardised form for each species with respect to the illumination, magnification and resolution.

RESULTS

Following the first meeting in April 2007, a set of agreed protocols was outlined defining a number of the key procedures including:

1. **Acquisition system: minimum requirements**
   - Greyscale digital camera, 1000x1000, >= 1Megapixels
   - Binocular equipped with transmitted and reflected light
   - Known calibration for any magnification

2. **Image format and naming convention**
   - Uncompressed tiff images, conversion to .im6 format (to be checked with Noesis for a conversion application)
   - Naming convention:
     Species_stock_YearQuarter_Whole/Section_Left/Right_Number.tiff: e.g.,
     plaice_NS_2006_Q1_TL_WR_999.tiff

3. **Acquisition settings**

- One magnification for all samples
- Determine an optimal incident lighting (reflected light) from test images
- Avoid image saturation, allowed/expected modification of lighting/acquisition time settings
- Acquiring reflected light and transmitted light images during the same session (exact overlapping of the images) (not for NEA cod, only transmitted light images)

4. **Interpretation acquisition**
   - interpretation: .rad + .iid file (for TNPC), both for annual rings and checks, on at least one reference axis (routine to be developed)
   - Naming convention: image name_suffix.rad (suffix: CEFASJS_RefAxis, for CEFAS John Smith)
   - Export to the database: .rad, .iid, estimated age

5. **Database**
   - TNPC database structure
   - One instance for each image
   - Proposed database structure:
     - Fish information
     - Otolith information: left/right, weight
     - Image information: lighting, calibration
     - Interpretation (graphic overlay (.rad file), inter[retation ascii file (.iid file)) associated to the reflected or transmitted light image (to be normalised for each CS)

   For each otolith: 3 instances in the DB
   - an otolith image acquired under transmitted light
   - an otolith image acquired under reflected light
   - a saturated otolith image acquired under reflected for background subtraction issue

CONCLUSION

The work was completed within the agreed timescale. The protocols and methodologies for standardisation of image capture, image format and naming convention were used and applied to subsequent deliverables within WP1.

▪ Database of otolith images and associated otolith and biological information for cod, plaice and anchovy otoliths

INTRODUCTION

The aim of this work was to provide a full set of digitized images covering all three case studies. The images were annotated with marks to indicate the position of the annual rings. These annotated images will provide the basis for work in all the other workpackages.

METHODS

Otolith Preparation

In all cases, the Sagitta otoliths were used. Otoliths from anchovy and Icelandic plaice were analysed whole and no sections were taken. Cod otoliths were analysed as sections only except that for North Sea cod otolith weight was measured on the whole otoliths. In the case of plaice otoliths from VIId, the full analysis was carried out on both the whole otoliths and sections.

Prior to digitising the whole cod and plaice otoliths, the samples were cleaned to remove any adhering blood or tissue, by soaking in water or in physiological Ringer (milliQ and PSU- 8 g salt per liter milliporewater) and dried.

Otoliths from anchovy collected on the market were stored in glass vials and then each pair was transferred directly to plastic slides in which 25 small depressions had been drilled. The otolith pairs were aligned vertically with the thin end uppermost and the sulcus side lying against the plastic slide. Clear polyester resin was then poured into the slides and the slide covered in a glass cover slip. Once the resin had dried, the slides were ready for image capture.

Otolith sections were used for all the cod samples and also for VIId plaice. The sections from North Sea cod were prepared by embedding the otoliths in polyester resin and taking a transverse section through the *nucleus* following the procedures in Bedford (1983) and Easey and Millner (2008). Section thickness was kept standard within species. Thin sections (0.45-0.5mm) were accurately cut through the *nucleus* and placed on a glass slide. The sections were covered in a thin layer of UV stabilised resin and covered with a glass cover slip. Similar methods were used for cod samples from the north-east Arctic. The sections of cod from the Faeroes were of poor quality, many not through the centre and most were too thick for transmitted light analysis. Therefore, these sections were ground and polished by hand prior to image acquisition using a series of grinding and polishing films with decreasing grain sizes from 30 µm to 0.3 µm.

Image Capture: Standard settings for otolith examination

The procedure for North Sea cod is described in detail but similar approaches were taken for the other species. The North Sea cod otoliths were digitised under reflected light using standard settings (as described below) in a stereo microscope (Leica MZ6) connected with a digital camera (Leica DFC320) and a framegrabber (software Leica IM 50).

Illumination influences the appearance of daily as well as annual growth structures and thereby potentially affects the visual interpretation and age estimation of the otoliths. Thus prior to measurements of optical density of individual cod otoliths, the effect of preparation and illumination on measurements of cod otolith optical density was examined. In this section, optical density is measured using reflected light. High optical density is related to high protein content and in reflected light these areas return high values as they reflect more light than areas with less protein content. In contrast, when using transmitted light, areas with high protein returns low grey values as these areas appear non-transparent and thus black.
In a standard set-up with a dissection microscope connected to monitor using a digital camera (Leica DC300F) and a frame grabber (software Leica IM 50) cod otoliths were digitized using

a standard set exposure time (e.g. 107.9 ms, 8 bit/channel) with a frame of 1300x1030 pixels. To examine the effect of light intensity, angle of light source, and direction of light a series of images were taken of the same otolith using following combinations of setups:

- Fixed angles and distances, varying light intensity
- Varying angles and distances and light intensity
- Varying angles, light direction and light intensity

The opacity of the otolith was measured using the "line profile" tool of IMAGE PRO version 5.0 which returns the distribution of grey values within a selected area of interest, increasing from 0 (black) to 255 (pure white), These absolute values are a measure of the luminescence of the otolith in transmitted light and in the case of reflected light; the grey values represent the light transmitted through the otolith. The increase in grey values is directly proportional to the increase in light (Fig. 1), thus varying light intensity is easily calibrated when the light angle and direction is constant. The light angle and direction of light source had a less predictable influence on the opacity.

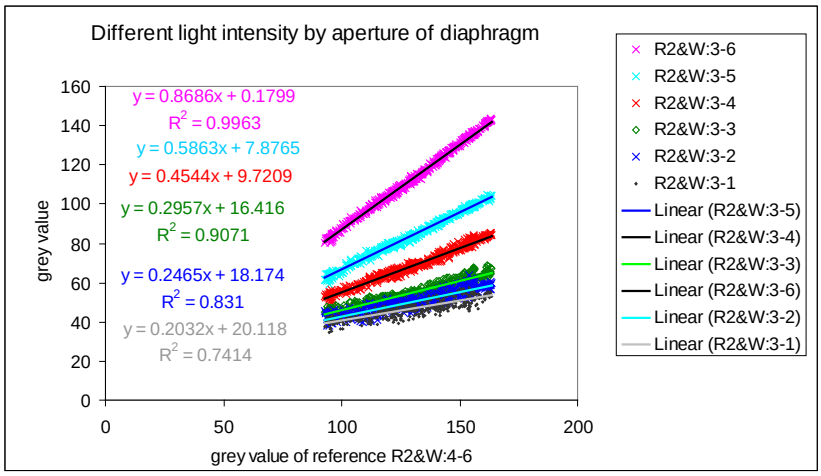

Figure 1. Correlation of the grey value of varying light intensities.

Thus the set-up concerning light settings were highly influential on the opacity measure and were very well defined and all measurements of opacity were done using a standard set-up in which the magnification, the light settings, position of light-source and otolith under the light and the setting of the frame-grabber system was kept constant between all otoliths.

When measuring opacity, the alignment of the profiles was kept as constant as possible between the individual sections. For the TS the profiles were positioned along the longest dorsal axis and for the SS the profiles were set along the longest axis of the rostrum. For all profiles the starting point was defined as the edge of the otolith moving inwards.

To ensure that all otolith images were digitized with the same settings, a "calibration otolith" was used. This otolith was digitized and its grey values measured along a predetermined axis at the beginning and end of each series. An example of otolith image from a Faeroe Island (FAbOSA) otolith following this procedure is shown in Figure 2.

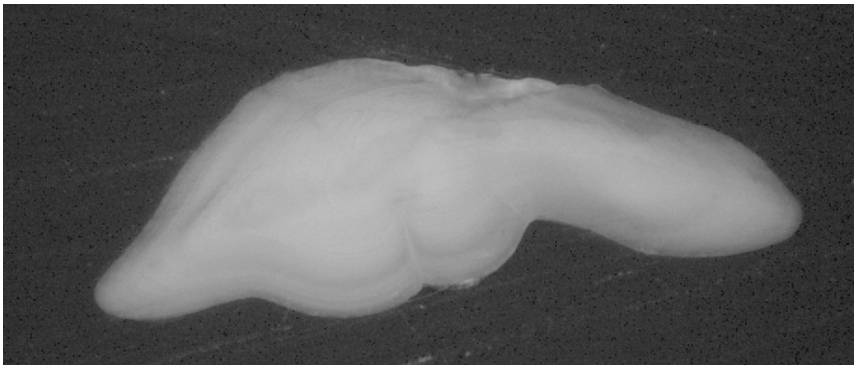

Figure 2. Example of Faeroe Island (FAbOSA) otolith image.

Image annotation

The procedures used for annotating the images were similar for all species. The age for each otolith was initially decided by viewing the whole otolith or section under a light microscope. In addition to recording the age, each reader graded the otolith using a three stage numeric scale with 1 corresponding to “good”, 2 “average” and 3 “bad”. After ageing under a microscope, the image captured using reflected light was examined in TNPC. The main growth axis was identified and if suitable for ageing, a radius marked in TNPC. The centre of each translucent band was then marked along the radius out to the tip. The number of marks should correspond to the age determined under the microscope even if this was not clear in the digitized image. The main growth axis was marked even in cases where the reader considered it to be unsuitable. In these cases a second axis was also marked at a more suitable location on the section. Once satisfied with the marks, the annotations were saved as a .rad file into a new folder using the agreed file naming convention together with the readers' initials at the end.
For example, species_stock_YearQuarter_Whole/Section_Left/Right_Number_reader’s initials.rad: e.g., plaice_VIId_2006_Q1_TL_WR_999_BH.rad

RESULTS

Otolith collection

The table below (Tab. 2) summarizes the otoliths collected by species and area:

institute	species	area	year	quarter	proposed	delivered
Cefas	cod	NS	1998	3	400	400
Cefas	cod	NS	1999	3	400	347
Cefas	cod	NS	2000	3	400	400
Cefas	cod	NS	2001	3	400	400
IMR	cod	NEA	2000	1 - 4	500	494
IMR	cod	NEA	2001	1 - 4	500	498
IMR	cod	NEA	2004	1 - 4	500	500
IMR	cod	NEA	2005	1 - 4	500	500
Difres	cod	Faroes	1996-2001		255	255
Ifremer	plaice	VIId	2006	1	250	248
	plaice	VIId	2006	2	250	249
	plaice	VIId	2006	3	250	195
	plaice	VIId	2006	4	250	237
MRI	plaice	Iceland	2006	1-4	1000	1000
AZTI	anchovy	Bay of Biscay	1998	1-3	500	500
	anchovy	Bay of Biscay	1999	1-3	500	500
	anchovy	Bay of Biscay	2004	2	500	500
	anchovy	Bay of Biscay	2005	1-3	500	500

Case Study 1: Cod

North Sea: Otoliths were collected from research vessel surveys carried out by Cefas in quarter 3 in the periods 1998, 1999, 2000 and 2001. A total of 1600 otoliths were planned but insufficient otoliths were available in all years, and a total of 1553 otoliths were provided for the project. Otoliths were available as sections only.

North East Arctic: Otoliths were from surveys. A total of 500 otoliths from each year 2000-2004 were planned but as there were insufficient otoliths in the archive, an additional 48 from 1999 were also included. A total of 1992 otoliths were available for the project as sections.

Faeroes: 255 otoliths from the FAbOSA project (FAbOSA, 2002) were available as sections. These otoliths were from fish which had been reared, tagged and released so that they were all validated known-age samples.

Case Study 2: Plaice

VIId: Otoliths were collected from research vessel surveys as well as from the market, covering all four quarters in 2006. Otoliths were provided whole and as sections in order to compare the two methods of age reading.

Iceland: Samples of plaice were obtained from markets covering all four quarters in 2006. Only sections were analyzed.

Case Study 3: Anchovy

Biscay: A full set of otoliths were collected from commercial landings except in 2005 when 200 of the 500 samples came from survey samples. The otoliths were embedded whole in clear resin.

Image Annotation

Case Study 1: Cod
North Sea: The aim was to have 400 otoliths from each year over the period 1998-2001. There was a shortfall of 53 otoliths in 1999 but in all other years the full numbers were achieved. There were considerable problems obtaining clear and well-defined images and the position, angle and intensity of the lighting was found to be critical to obtaining good quality images.
North-east Arctic: The total number of otoliths annotated was 1992 which was very close to the planned number of 2000. In cases where the dorsal axis was poor, annotations were applied to the distal or median axis.
Faeroes: All 255 otoliths planned were annotated. Initially, the sectioning was considered poor and all sections were ground and polished by hand to obtain a much improved image for annotation.

Case Study 2: Plaice
VIId: It was not possible to collect the full 250 otoliths in each quarter of 2006 but in quarters 1, 2 and 4, the numbers obtained were very close to the estimated totals. In quarter 3 it was only possible to collect 195 otoliths. In total 929 otoliths were annotated whole and 908 as sections compared with 1000 planned. Obtaining good quality whole images proved very difficult. The initial batch of images proved to be of poor quality and subsequent images although greatly improved were not as clear as images viewed directly under the microscope.
Iceland: All 1000 otoliths planned were annotated successfully.

Case Study 3: Anchovy
Biscay: Five hundred otoliths were collected from each of the years1998, 1999, 2004 and 2005 as planned. All 2000 otoliths were annotated successfully.

CONCLUSION

A total of 6729 otoliths out of a proposed 6855 have been digitized and annotated for further analysis by subsequent work packages. There were initially considerable problems in obtaining satisfactory images for a number of the species but in all cases the problems have been overcome and the only deviation from the deliverable has been a delay of one month for VIId plaice. This will not affect the delivery of subsequent work packages.

REFERENCES

Bedford, B. C. 1983. A method for preparing sections of large numbers of otoliths embedded in black polyester resin. *Journal du Conseil International pour l'Exploration de la Mer*, 41: 4-12.

Easey, M.W. & Millner, R.S., 2008. Improved methods for the preparation and staining of thin sections of fish otoliths for age determination. *Sci. Ser. Tech Rep., Cefas Lowestoft*, 143: 12p.

▪ Age distribution of the selected case studies based on expert readers and Otolith weight for comparison with the result from the automated ageing

INTRODUCTION

The aims of this work were to provide otolith ages and weights corresponding to the full set of digitised and annotated otoliths.

METHODS

Age reading
All age readings were carried out by reading the otoliths under a binocular microscope at the magnification best suited to the particular species. All fish were aged to a January 1st birthday.

Weighing
Before weighing, the otoliths were checked and any chipped, damaged or crystalline otoliths were rejected. Plaice otoliths were washed in water to remove any adhering blood or tissue. Since washing ads significantly to the time taken to analyse large numbers of otoliths it was decided that an alternative approach would be tried for cod. In this case, any tissue on the surface of the otolith was carefully removed using cotton gloves but no washing was carried out.

For plaice, either the left (asymmetric) or right (symmetric) otolith could be selected. For standardisation, it was agreed that the symmetric otolith should be used. In cod there were no differences between right or left otoliths and either one was acceptable.

Otoliths were weighed dry to a relative precision of at least 0.1% of the total otolith weight. In most cases this should be to the nearest 0.1mg but where balances automatically weigh to 0.01mg this was regarded as acceptable to avoid manual rounding errors.

The time taken to weigh otoliths was recoded for use with the cost benefit analyses under WP4.

RESULTS

A summary of the otoliths aged and weighed is shown below:

North Sea cod: 1553 otoliths aged and weighed.
North East Arctic cod: 1607 otoliths from a total of 1992 were weighed. The remainder were broken and it was not possible to obtain weights. All 1992 otoliths were aged.
Faeroes cod: Weights were not required but all 255 otoliths were aged.

VIId plaice: 929 otoliths were weighed and aged whole. 908 were aged as sections.
Icelandic Plaice: 1000 otoliths were weighed and aged.

Biscay anchovy: weights were not required but all 2000 were aged.

CONCLUSION

This work has been completed. There were only a small number of samples where it was not possible to obtain weights and all samples were aged. In addition the time taken to weigh samples was recorded and will provide data for the cost benefit analysis in WP4.

▪ Comprehensive cost–budgets for processing otoliths enabling calculation of a population age distribution for traditional ageing, otolith weight and automated ageing

INTRODUCTION

The second aim of this work was to create a cost-budget for the main steps involved in handling the otoliths from weighing through to the capture of the image for analysis.

METHODS

A cost budget template was developed to summarise the main costs involved in the routine ageing otoliths. Initially it was intended to only cover the processes involved in handling the otoliths from weighing through to image capture. However, it was decided that in order to enable a full cost benefit analysis of routine age reading to be compared with computer assisted age reading (CARR), the initial steps in the process of collection should also be included. If the CARR process results in a reduction in the number of otoliths collected, then it will be necessary to reflect this in the cost benefit analysis. The analysis should include both the staff costs and the time involved in all aspects of work leading up to the estimation of a population age distribution. The only area where full costs have not been applied was for otoliths collected by research vessel survey. In these cases, there is a very large capital and operating cost for the vessel and re-allocating a proportion of this onto the small amount of time used to collect otoliths would be very difficult to standardise across different vessels. For this reason, only the staff time required to collect the otoliths has been used.

RESULTS

A detailed list of costs has been completed by each participant. The main areas covered include:

- Equipment costs (capital items with estimated depreciation). In the case of items used only partly in handling otoliths, the proportion of time in use has also been included.
- Equipment costs for consumable items such as otolith packets measuring equipment etc
- Preparation of known age material
- Staff training including fish measuring and collection of otoliths, otolith preparation and sectioning, image acquisition, age reading and data handling
- Direct variable costs involved in the collection, preparation, age reading and image acquisition

CONCLUSION

A full breakdown of the costs involved in all aspects of the collection, handling and analysis of otoliths for the preparation of population age distributions has been collected by each participant. This information will provide the essential data used in WP4 to develop cost benefit analyses of the age reading processes.

Deviations from the project work programme in WP1

This work package has been successfully completed and all information relating to the otolith images is now available in a web-based database accessible to all partners. The full images are stored in separate databases with links to the web site. Information necessary to describe the full cost benefit of each step in the process has been collected for each of the three case studies.

WP2 - Develop efficient algorithms for automated fish age estimation

Scientific teams involved: Partner 1, Ifremer (coordinator); Partner 4, Difres; Partner 5, IMR; Partner 7, UPC

Institute: Person (1) Sébastien Carbini; Anatole Chessel; Ronan Fablet; Kélig Mahé; Hélène De Pontual; (4) Henrik Mosegaard; Asbjorn Christensen (5) Hans Høie; Alf Harbitz; (7) Vicenc Parisi, Antonio Soria, Père Marti

Overall objectives: The overall objective of this workpackage is to develop efficient algorithms for fully automating fish age estimation. This includes:

- Task 2.1 Automated acquisition of series of otolith images
- Task 2.2 Otolith growth modelling
- Task 2.3 Automated extraction of structures of interest in otolith images
- Task 2.4 Automated estimation of individual fish ages
- Task 2.5 Automated estimation of age structures from statistical distribution of otolith features

Deliverables:

1.a Automated system for the acquisition of series of otolith images – M9 (Month 9)

2.a 2D forward-growth model of otolith morphology – M12

2.b Probabilistic 2D growth consistency-checking model – M12

3.a Algorithm for nucleus detection – M9

3.b Algorithm for the reconstruction of dense growth direction fields from images – M9

3.c Algorithm for locally adapting directional filters with variable bandwidth for ring enhancement and detection – M9

3.d Algorithm for the detection of reference growth axes – M12

3.e Algorithm for the 1D detection of otolith rings – M12

3.f Algorithm for the 2D segmentation of partial otolith rings – M17

3.g Contrast-invariant representation of otolith ring-based information – M17

4.a. Feature discrimination algorithm M9

4.b. Definite feature discrimination algorithm code and report, following modifications suggested from its evaluation during the 2nd project meeting at month 9 – M12

4.c. Statistical learning algorithm for automated fish ageing – M17

4.b. Statistical learning algorithm for automated fish ageing, following modifications suggested from its evaluation during the 3rd project meeting at month 17 – M18

5.a Mixture model for age structure estimation from global otolith features and physical fish characteristics – M12

5.b Conditional model for age structure estimation from global otolith features and physical fish characteristics - M17

Start date: month 1
Completion date: month 24

Partner responsible: Partner 1 (Ifremer)

Partners involved: Partner 1 (Ifremer); Partner 4 (Difres); Partner 5 (IMR); Partner 7 (UPC)

Person-months:

Status of progress: this WP has been successfully completed.

.

Workpackage 2 Objectives

The aim of this work package is to develop the algorithms which will be the different components of the automated ageing systems. These algorithms will mainly cope with three different issues:

- Automating the acquisition of image series using a system combining a motorized stage to a digital camera. In terms of image processing, this issue will rely on object detection and segmentation in image mosaic built from the motorized stage. More precisely, morphological approaches will be investigated especially parameter less ones with a view to increasing robustness and reducing user interaction.
- Automating the extraction of image structures. The methods dedicated to automated ageing primarily rely on an extraction of relevant features. Depending on the methods, these features include global image descriptors (e.g., shape descriptors as well as global and compact representation of otolith structural information) and local image features (*nucleus*, growth axis, rings...). It should be pointed out that these issues are complex and the developed solutions will rely on advanced computer vision and pattern recognition techniques, such as variational (Fablet *et al*., 2007) and contrary (Cao & Fablet, 2005) framework as well as statistical analysis. Otolith growth models will be developed to parameterize the scale-space analysis of image structures. Whereas almost all existing prototypes are computer-aided tools since user interaction is required (e.g., to determine the position of the *nucleus* or the reference growth axis), our objective is to fully automate this information extraction stage.
- Automating ageing issues. Given databases of otolith features (including both otolith features automatically extracted from otolith images and global features such as fish length and otolith weight), algorithms will be developed to infer individual ages as well as age structures. These algorithms will mainly rely on statistical learning and Bayesian modelling. The estimation of individual fish ages will be stated either as a classification issue or as an actual Bayesian image segmentation in terms of growth ring structures. The estimation of age structures will mainly rely on statistical inference.

Progress towards Objectives WP2

During this first year, work was developed on the Automated system for the acquisition of series of otolith images and the development of algorithms for otolith morphology, *nucleus* detection, the reconstruction of dense growth direction fields from images, locally adapting directional filters with variable bandwidth for ring enhancement and detection, the detection of reference growth axes and the 1D detection of otolith rings.

During this second year, work was developed on the Algorithm for the 2D segmentation of partial otolith rings, Contrast-invariant representation of otolith ring-based information, Statistical learning algorithm for automated fish ageing, Statistical learning algorithm for automated fish ageing, following modifications suggested from its evaluation during the 3rd project meeting at month 17, Conditional model for age structure estimation from global otolith features and physical fish characteristics

▪ Automated system for the acquisition of series of otolith images.

INTRODUCTION

To help the otolith images acquisition, TNPC software enables the operator to acquire several otoliths with one operation. The otoliths lay on a grid and the microscope is automatically moved to take several shots inside a rectangle defined by the operator. The set of images are

aligned to create a mosaic (Fig. 3). Then a computer vision algorithm is used on this mosaic to segment otoliths and output an image per otolith. All images are then automatically added to a database and can be annotated.

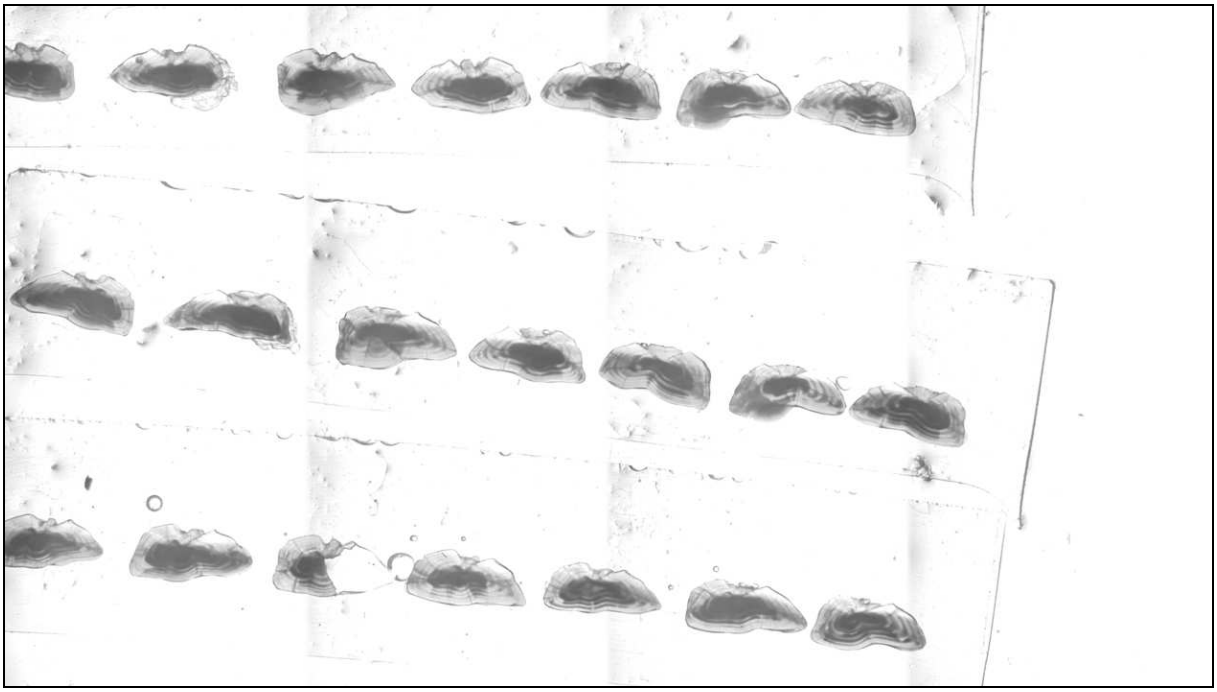

Figure 3. Series of otolith images acquired with TNPC.

METHODS

Segmentation algorithm

A previous algorithm used a simple threshold on luminance to segment otolith from background. The method proposed here is based on the FLST (Fast Level Set Transform). The goal of the algorithm is to estimate a bounding box around each otolith to crop an image of each. The following algorithm is used:

- *Downsize the mosaic image by a factor z (fixed in our experiments at a value of 0.1).*
- *Compute FLST on downsized image and retrieve the tree of shapes.*
- *Scan the tree of shapes and keep only shapes with characteristics a priori similar to an otolith.*
- *Reconstruct the image from the filtered tree of shapes (inverse FLST).*
- *Detect bounding box of each shapes and resize them to the initial mosaic resolution.*
- *Add some margin to each bounding box and crop corresponding images.*

The acquired mosaic image has a very high resolution and is first downsized to speed other treatments. The other steps are detailed on following sections.

Fast Level Sets Transform

The Fast Level Sets Transform (FLST) is a decomposition of an image into "shapes", based on connected components of level sets and on level lines [12; 13; 2]. The result of FLST is an inclusion tree of shapes (Fig. 4) where each shape is included in his parent shape.

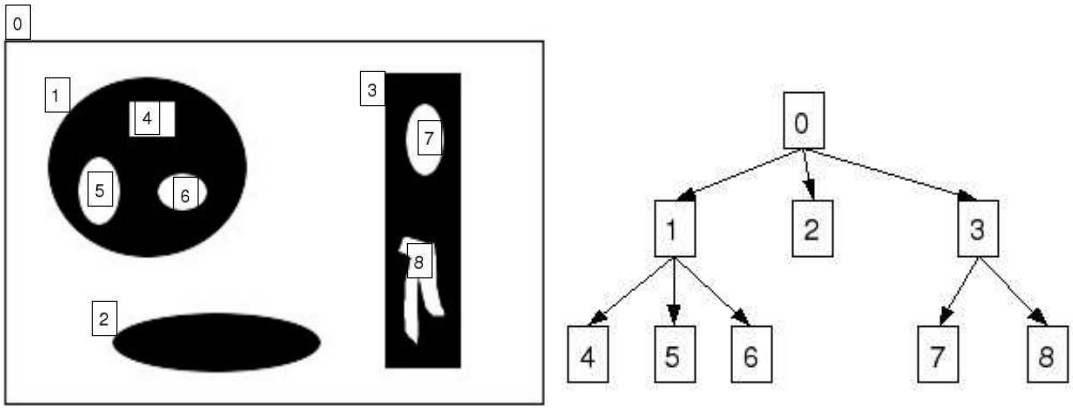

Figure 4. FLST tree of shapes result. The root of the tree (shape 0) represents the whole image.

Scan and filter the tree of shapes

The filter is a recursive function that scans the tree to select the shape similar to an otolith. The filters test the following characteristics:

```
Function Test (a shape)
{
IF shape area is between areamin and areamax
AND the shape doesn't meet the border of the image
AND the high/width ratio of the shape is between ratiomin and ratiomax
AND the ratio between the shape area and its bounding box area is between pmin and pmax
    THEN
        Select the shape
    ELSE IF shape area if superior to airemin
        call Test ( first son of current shape )
ENDIF
call Test ( next sibling shape )
}
```

The algorithm scan recursively the shapes of the tree. It starts with the first son of the tree root and then, for each shape, iterates on its son if the shape is not an otolith and if the shape area is big enough to contain an otolith. The shapes that meet the border of the mosaic image are discarded because only images showing an entire otolith are kept. The parameters have been empirically fixed to the following values:

- areamin = 25000 and areamax = 170000 (pixels)
- ratiomin = 1.6 and ratiomax = 3.2
- pmin = 0.3 and pmax = 0.98

The parameters areamin and areamax can be adapted to the mosaic resolution. The other parameters are dimensionless and lead to a result independent of the mosaic resolution.

RESULTS

Figure 5 shows the result of the segmentation obtained with the segmentation algorithm running under TNPC. One can notice that two otoliths on the left border of the mosaic and a broken otolith are discarded thanks to the conditions imposed by the recursive. The border of otolith's receptacle is discarded as well. Once the otolith are segmented, a TNPC pre-existing module finds the bounding box of each shape (Fig. 6) and save each image to a database.

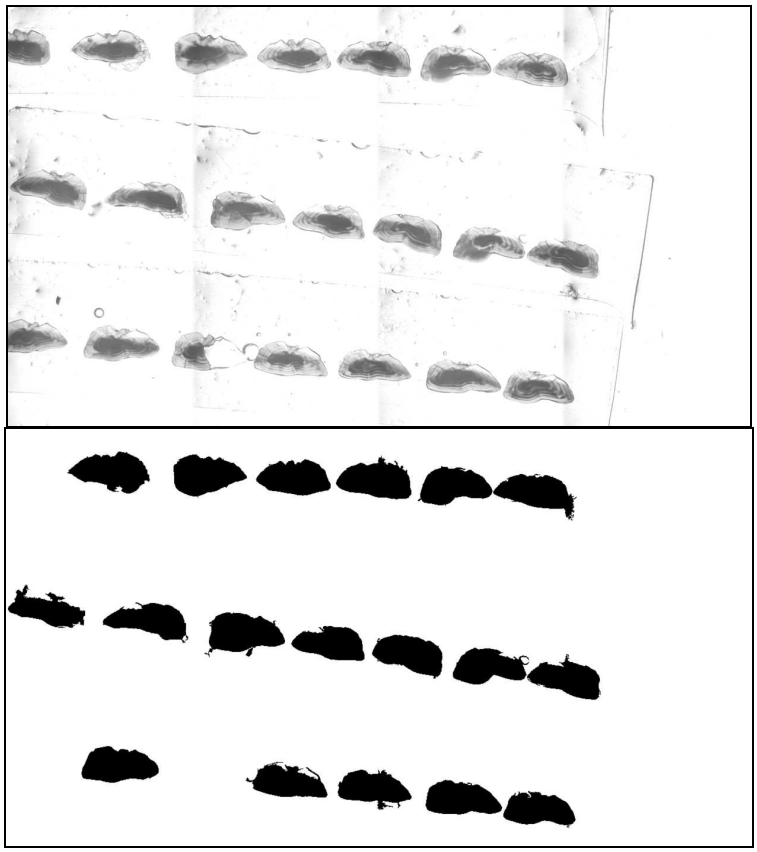

Figure 5. Result of segmentation.

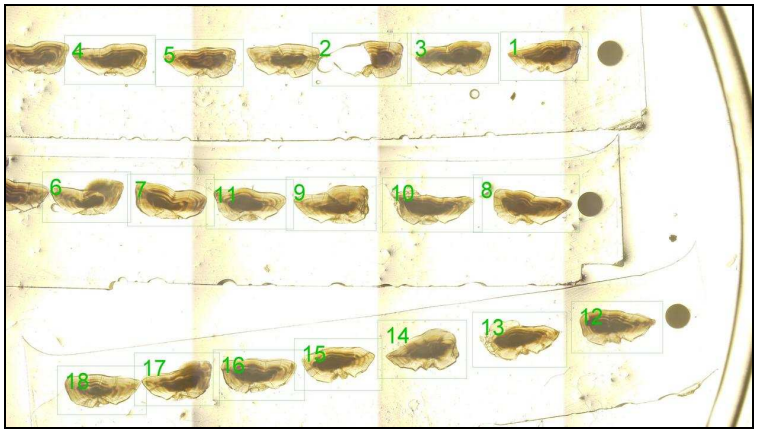

Figure 6. Otolith mosaic labelling result. On this result, two otoliths on the left border are discarded as well as the three dark circles on the right but an otolith is missed (between otolith number 5 and 2).

CONCLUSION

This algorithm has been implemented on software TNPC (see Workpackage 3).

- ## A 2D forward-growth model of otolith morphology

INTRODUCTION

Fish otoliths grow according to an accretion process. In other words, they can be viewed as a succession of three-dimensional layers (with respect to an initial core). The composition of these layers, in terms of crystalline organization and chemical features, vary according to endogenous and exogenous factors. further, the accretion process is associated with periodic patterns, both daily and seasonal, reflecting the fish life cycle and seasonal cycle in exogenous factors. Cutting the otolith allows the observation of these biological structures in an observation plane going through the initial core depict concentric ring patterns, also called growth marks, as illustrated in figure 7 (left)

Figure 7. Right: characteristic ring structure in a cut otolith. Left: optical and virtual (intermediate) ring structures obtained by image analysis and growth model interpolation.

These characteristics provide the basis for exploiting these structures as biological archives to define environmental proxies (e.g., for instance to reconstruct temperature and salinity sequences) or to reconstruct individual life traits (e.g., individual age and growth information or migration paths). Therefore reliable forward-growth models play an important role in the suite of algorithms needed to facilitate automated fish ageing from otolith image analysis. The main output of growth models is growth pattern extraction/mapping and validation of automated shape inference. Two related and complementary variants of forward models has been developed in the present project, both aiming at predicting the *arrival time surface T(x,y)* as sketched below in Figure 8. The characteristic otolith ring structures are derived from *T(x,y)* by solving the equation

$$T(x, y) = T_0 \qquad (1)$$

for any T_0. The solution of this equation corresponds to the otolith surface at time T_0 (which are embedded but further growth layers at times $t > T_0$).

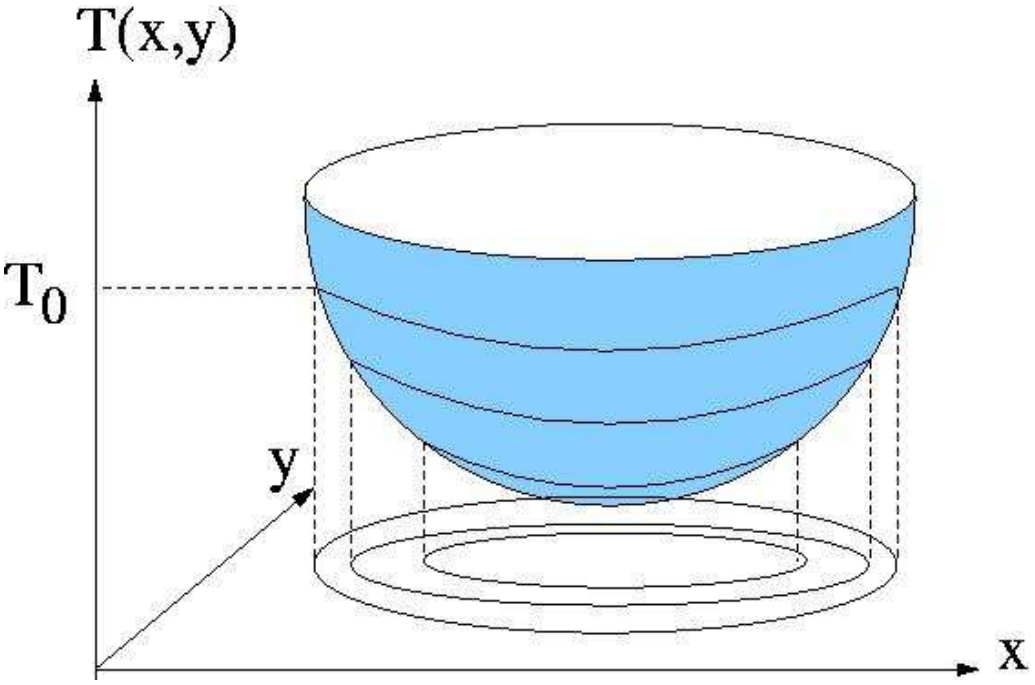

Figure 8. The arrival time surface *T(x,y)* and the relation to observed otolith ring structures.

METHODS

If the arrival surface *T(x,y)* can be resolved, simple geometric considerations show that the otolith growth history *F(x,y)* is recovered by

$$\begin{aligned} F(x,y) &= \frac{1}{|\nabla T(x,y)|} \\ \nabla T(x,y) &= n(x,y)\frac{1}{F(x,y)} \end{aligned} \qquad (2)$$

where *n(x,y)* is a normal vector corresponding to the contour $T(x,y)=T_0$ crossing the point *(x,y).* The arrival time surface *T(x,y)* determined by solving a minimal surface problem. The functional *R[T]* generating the surface *T(x,y)* is decomposed in two positive definite parts

$$R_\lambda[T] = P[T] + \lambda K[T] \qquad (3)$$

The first part *P[T]* is a shape penalty functional that penalises unlikely features of the arrival time surface. *K[T]* is a constraint penalty functional that penalises deviations from direct constraints on the arrival time surface, e.g. boundary conditions and other prior knowledge. λ is a relative weight that balances importance of violations of shape feature knowledge and direct constraints. Typically, λ is chosen as the minimal value that keeps *K[T]* below a tolerance limit, which is adjusted iteratively when minimizing $R_\lambda[T]$. The simplest positive definite form satisfying elementary mathematical properties is the gradient penalty

$$P[T] = \int \nabla T(x,y) \bullet \nabla T(x,y) dxdy \qquad (4)$$

For point wise direct constraints, e.g. a sampling set $\{x_i, y_i\}_{i=1..k}$ of an otolith ring attributed to time $t=t_i$, the simplest well conditioned penalty functional is

$$K[T] = \sum_{i=1}^{k} w_i (t_i - T(x_i, y_i))^2 \qquad (5)$$

where w_i is a confidence weight associated with each sampling point (x_i, y_i).

EXAMPLES

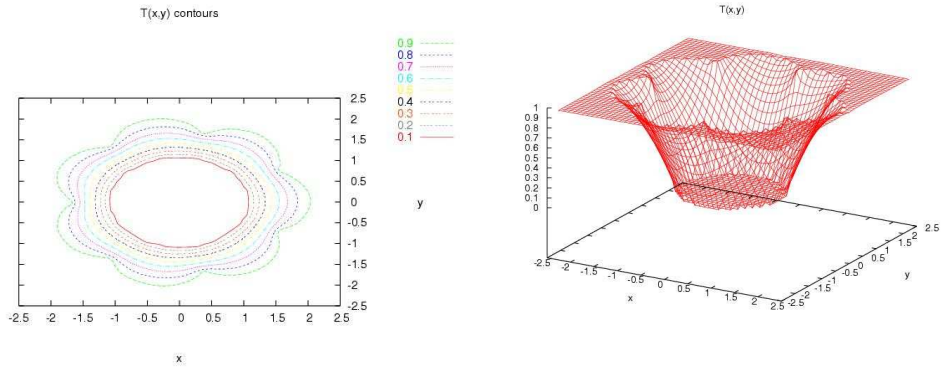

Figure 9. Right: Model prediction of a test otolith contour. Left: the arrival time surface *T(x,y)* corresponding to the right set of test otolith rings, as obtained by Eqs. 3-5.

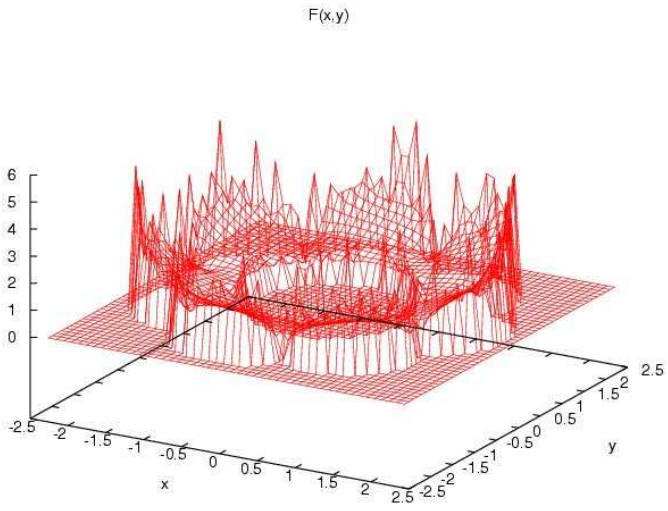

Figure 10. Model prediction of a test otolith growth *F(x,y)*, as obtained from Eqs 2 and corresponding to Figure 9.

▪ Probabilistic 2D growth consistency-checking model

INTRODUCTION

The forward growth model described previously deliverable 2.2.b requires a skill assessment tool for calibration and validation. In the light of the current level of understanding otolith growth processes and their coupling to physiological state of the host fish as well as abiotic factors, skill assessment is best performed by a data driven approach, based on a representative reference set of otolith shapes for the fish stocks in question. The optimal reference set consists of an ensemble of otolith shape histories, i.e. a set of mappings of the otolith of same individuals at different ages. Such reference sets are generally expensive to establish. It is easier to establish a reference set of otolith shapes corresponding to different ages. The crucial difference is that individual-level correlations can not be addressed by the age-pooled reference set. A validation is more powerful, if it includes the life (and otolith growth) history as prior in the validation. In this task, we will describe a generic validation frame work based on an age-pooled reference set which is most likely to be of practical use because it has less demands on the reference set. The question about the potential bias created by neglecting individual-level correlations is left as a topic for future research

METHODS

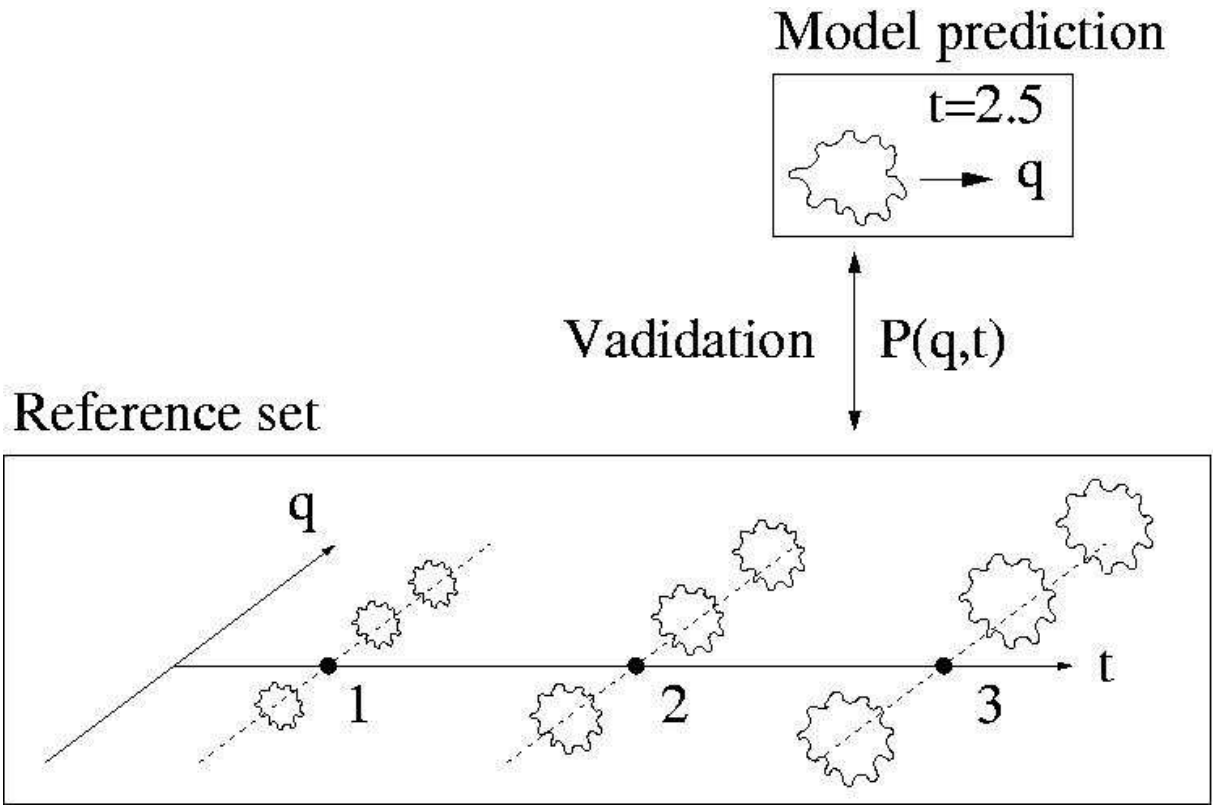

Figure 11. Probabilistic 2D growth consistency-checking model.

The idea of the overall framework is sketched above in Figure 11. The reference set is structured in age-layers (*t*) of reference shapes. However, the age-layering is not a necessary assumption in the framework. Otolith shapes are aligned by a standard procedure and mapped onto a suitable shape representation (*q*). In this setup, we apply spectral analysis of shapes,

but other and/or hybrid shape representations (q) are feasible in the current framework. The contact function between the reference set and a virtual otolith shape predicted another submodel in the TNPC framework is the likelihood function $P(q,t)$, which assigns a likelihood that a given shape (q) occurs at a given age(t), with no further priors in the current set-up. Therefore a robust definition of $P(q,t)$ is pivotal for the usefulness of the current framework.
We define the likelihood function $P(q,t)$ as

$$P(q,t) = \sum_{i=1}^{N} \omega_i(t) P_i(q) \qquad (1)$$

where i indicates the age-layers and $P_i(q)$ measures the likelihood in age-layer i. The age-layer likelihoods are expressed as

$$P_i(q) = \frac{1}{M_i} \sum_{j=1}^{M_i} \frac{1}{\Delta_{ij}^n \pi^{n/2}} \exp[-\frac{|q - q_{ij}|^2}{\Delta_{ij}}] \qquad q \in R^n \qquad (2)$$

where M_i is the number of entries in reference age-layer i, n is the dimensionality of the representation q, q_{ij} is the representation of entry j in age-layer i, and Δ_{ij} a smearing range of of entry j in age-layer i. The age-layer structure in the reference set warrants the following definition of the weights $\omega_i(t)$ for age-layer i at time t:

$$\omega_i(t) = \begin{cases} 0 & i \neq (n(t), m(t)) \\ \dfrac{t - t_n}{t_m - t_n} & i = m(t) \\ \dfrac{t_m - t}{t_m - t_n} & i = n(t) \end{cases} \qquad t \in R \qquad (3)$$

where the functions $n(t)$ and $m(t)$ points to the age layer below and above t corresponding to t_n and t_m, respectively, so that $t_n < t < t_m$. This definition is linked to the age-layering ansatz, but can easily be generalized by a suitable redefinition of weights $\omega_i(t)$. Obviously the definitions (1)-(3) satisfies the necessary normalization conditions

$$\sum_{i=1}^{N} \omega_i(t) = 1 \qquad t \in R \qquad (4)$$

and

$$\int P_i(q) dq = 1 \qquad i = 1..N \qquad (5)$$

implying

$$\int P(q,t) dq = 1 \qquad t \in R \qquad (6)$$

so that $P(q,t)$ is a proper likelihood.

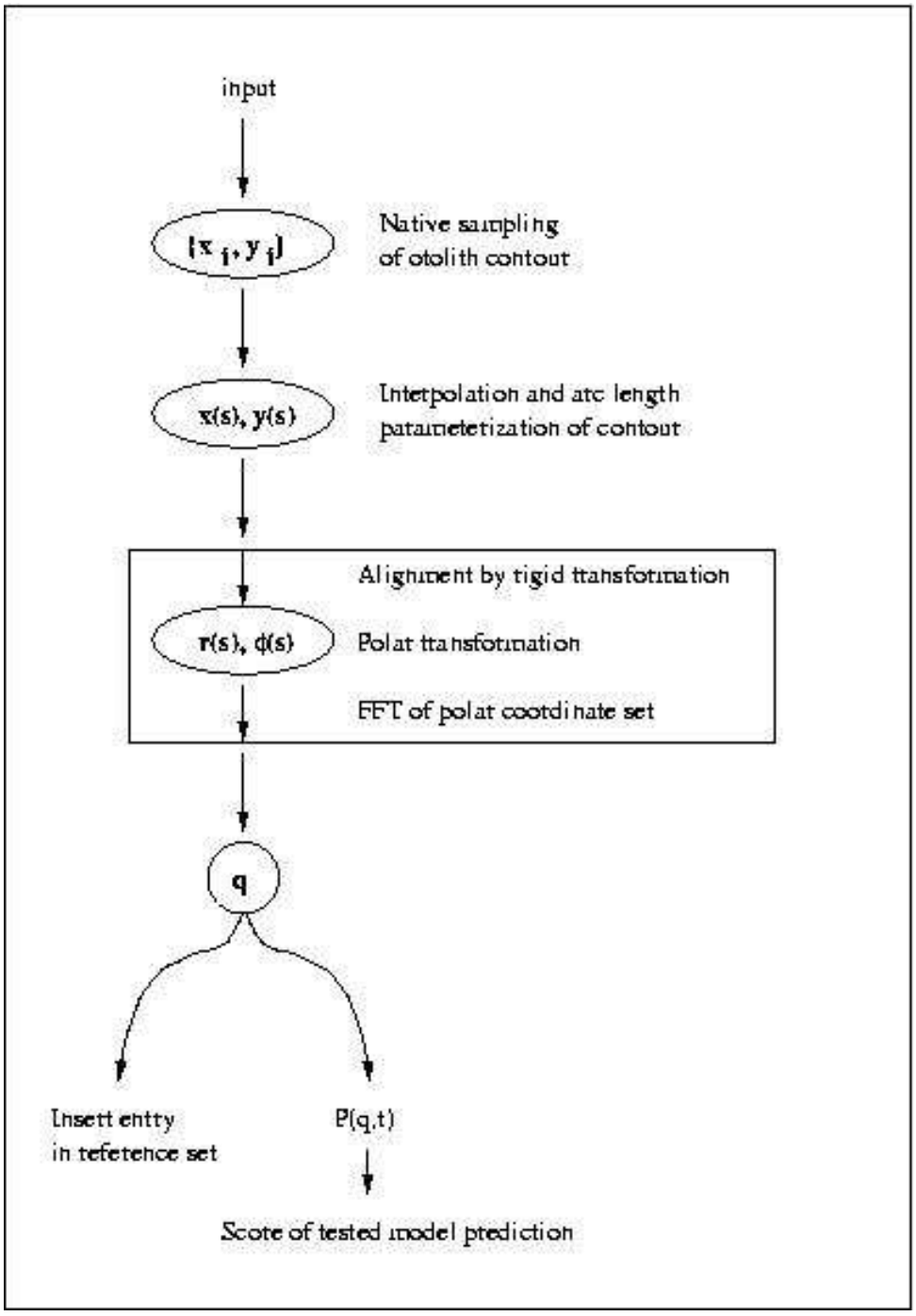

Figure 12. Processing of an arbitrary otolith contour.

The detailed flow in the processing of an arbitrary otolith contour is illustrated in Figure 12 above. The native sampling $\{x_i,y_i\}$ is raw points representing the otolith shape with sufficient resolution to include all important features. The sampling is not assumed to be equidistant and may be infected by discretization noise and is insensitive to rotation and translation in the image capture process. To have a proper basis for generating the representation *q*, the native sampling $\{x_i,y_i\}$ is interpolated and reparameterized according to arc length, to remove sensitivity to the position of the sampling points. On generating the representation *q*, the contour is aligned by a standardizing rigid transformation (in the present setup locating the longest axis in the shape, fixing the Cartesian origo to the centre of the axis and orienting the axis along the first Cartesian axis). In this Cartesian frame the contour is transformed to polar

representation, including both radius r and angle φ, because r(φ) can not be assumed to be single valued for many otoliths. In the current setup, we use spectral representation as q, which in many cases are converges relatively fast (and provides a well defined shape smoothing facility).

▪ Algorithm for *nucleus* detection

INTRODUCTION

The automatic determination of the otolith growth center is of key importance both for ageing automation and computer-assisted otolith interpretation since it serves as the reference point for further analysis (automated extraction of interpretation axis, 2D ring segmentation, age and growth estimation ...).

METHODS

i) Morphological approach

In order to detect the *nucleus*, we propose to select the best shape with respect to a few criteria. Let us state the following qualitative facts: otoliths are vaguely elliptic, and *nucleus* corresponds to a dark region close to the longest principal axis of the otolith. This region is also basically elliptic and no too eccentric. From these qualitative descriptions, we have to make quantitative arguments.

We proceed as follows: we start by removing shapes that definitely cannot be *nucleus* (it was checked on 100% of the observed images). We then introduce features measuring the previous qualitative properties. This will allow us to define a functional, and we will keep the shape that minimizes this functional. But contrarily to usual variational methods, this functional will have a quantitative meaning. It will tell how likely a shape will satisfy our geometric criteria only by chance. We will then see that it is possible to fix a robust automatic threshold to validate the detection. Besides, we will detail a refinement of the proposed approach based on a priori information on nucleus position. The proposed approach is summarized in Figures 13 and 14.

ii) Alternative approach based on ellipse geometry

This is a global method based on the assumption that the location of the core relative to a best fitted ellipse with origin in the area centroid is rather constant from one otolith to another, on a standardized scale. The criterion is motivated by experiences from more than 2000 cod otoliths (NEA cod as well as NS cod), where it appeared that the detected cores by the readers were close to the minor ellipse axis. Let L denote the distance between the area centroid and the intersect point between the contour and the minor ellipse axis, as shown in Figure 15. Empirically the core will then be close to a point on the minor ellipse axis at a distance $0.4585L$ from the area centroid. The advantage of the method is that it is rather robust with regard to image quality and the accuracy of the contour detection. The method can easily be generalized and tried on any species by allowing the core in general to not lie on any ellipse axis.

iii) Statistical Prediction approach

The method for the statistical prediction of the otolith *nucleus* is based on the assumption that the *nucleus* position can be regressed with a polynomial function that depends on the bounding box dimensions of the otolith contour. To estimate such function a database of otolith images and the manually estimated position of the *nucleus* is required as input data.

Each image is preprocessed to segment the otolith background and project the otolith to a common reference axis; in this case we use the Principal Component Axis of each otolith image.

RESULTS

i) Morphological approach

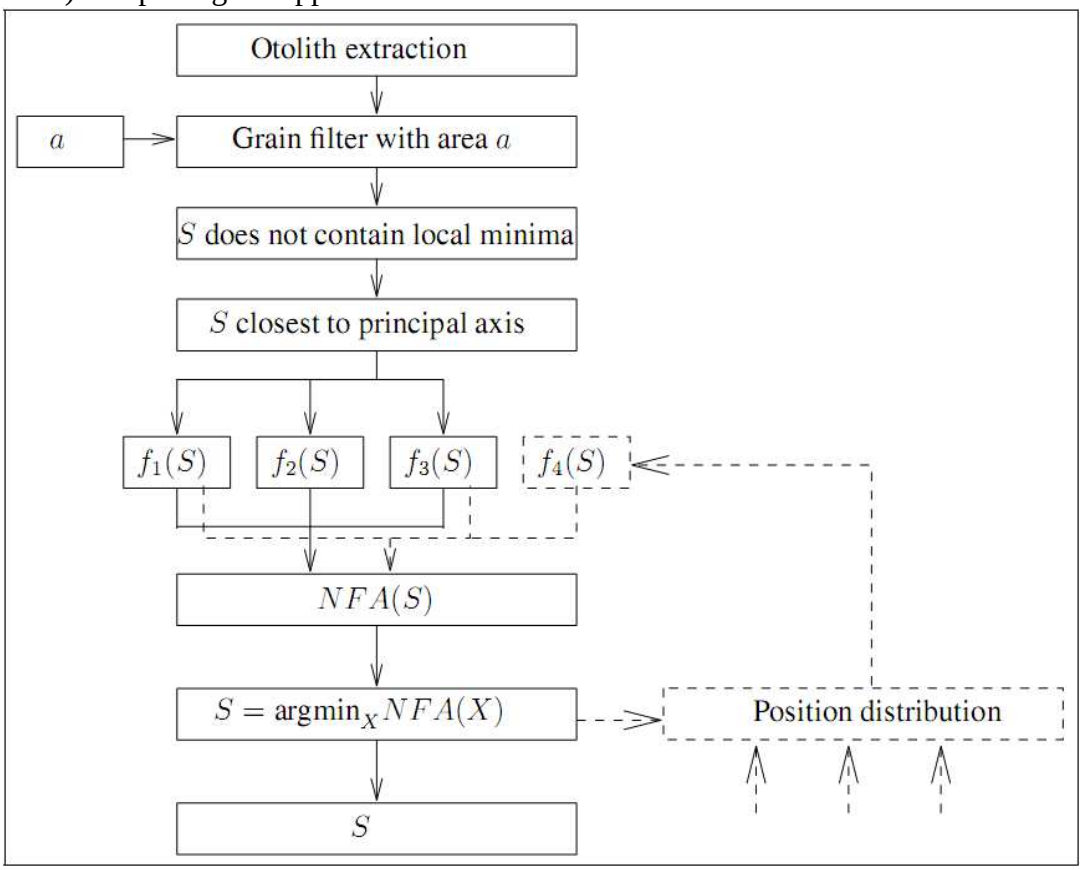

Figure 13. Diagram of the *nucleus* detection algorithm. The first step is the otolith extraction. Local extrema are filtered out by a grain filter with area parameter a. Shapes that contain local maxima or that are not the closest to the principal axis cannot be the *nucleus*. (This is only heuristic, but was satisfied for nearly all the images of the database.) Then three features f1, f2, f3 allow to compute the NFA (Number of False Alarm). The best candidate is the one with the lowest NFA. In dashed lines, an optional loop: the position of the detections for a large database can be learned. It permits to propose a refinement of the proposed method using a feature f4 which is more accurate than f2, and leads to another NFA which experimentally gives better result.

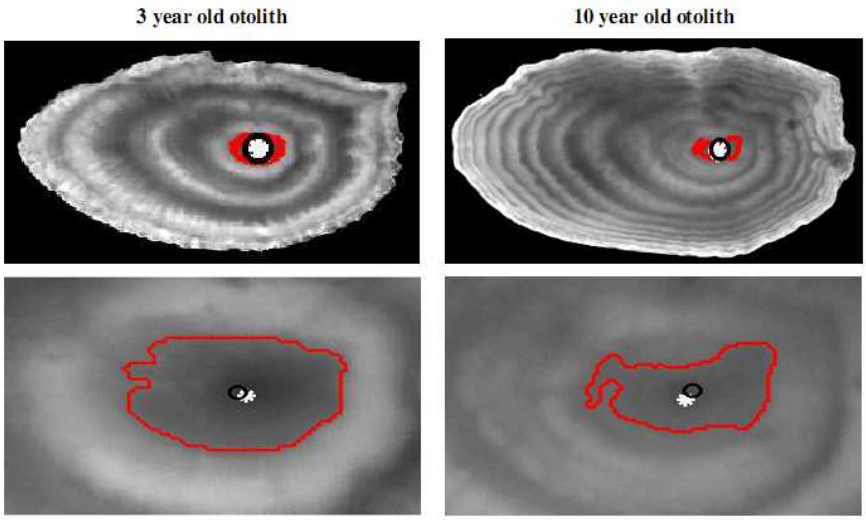

Figure 14. Two examples of the detection of otolith center using our morphological approach: the line superimposed to the image depicts the contour of the selected shape, marker o (black) the estimated position of the otolith center, and marker * (white) its true position. The first row displays the image of the whole otolith, while the second row zooms in to the region close to the otolith center.

ii) Alternative approach based on ellipse geometry

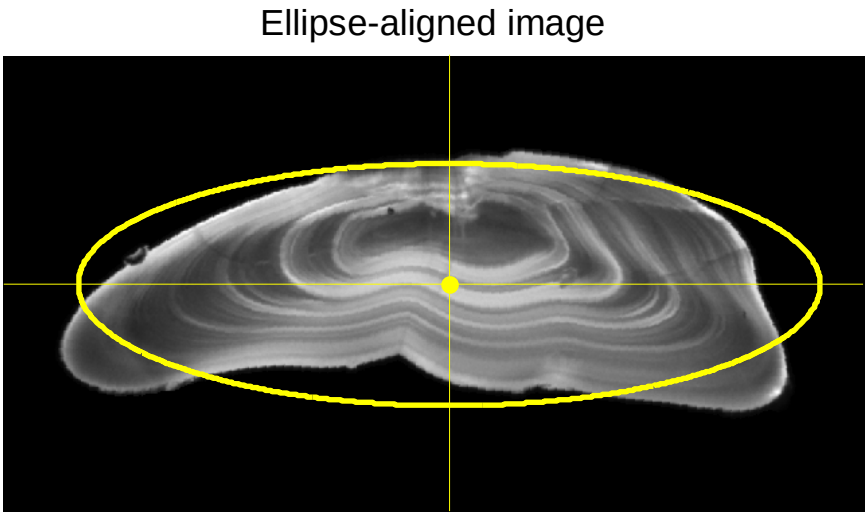

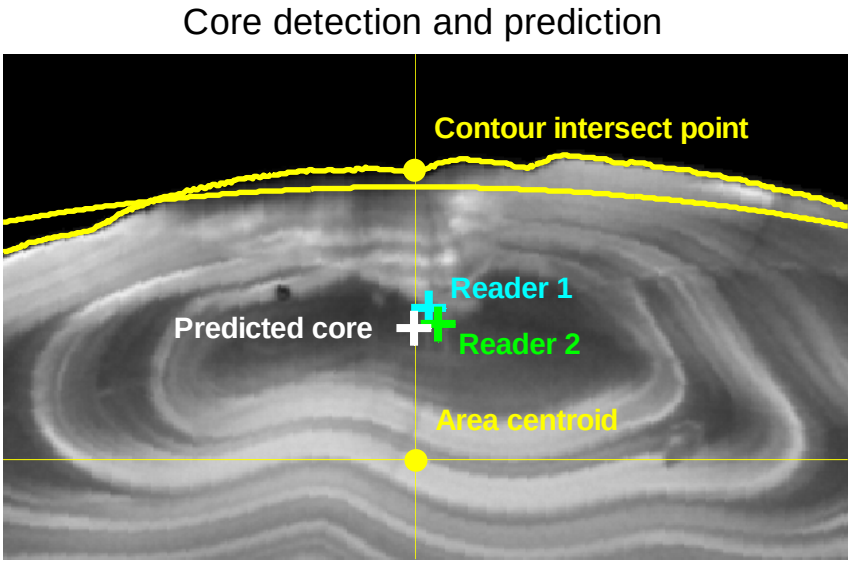

Figure 15. Upper panel: NEA cod otolith aligned along best fitted ellipse through the area centroid. Lower panel: Enlarged part of upper image showing the core points detected by reader 1 and 2 along with the automatically predicted core point. The latter is located at a distance 0.4585*L* from the area centroid, where *L* is the distance along the minor ellipse axis from the centroid to the intersection between the contour and the minor ellipse axis.

iii) Statistical Prediction approach

Cod2000 Test Case: Figure 16. Shows the position of the horizontal coordinate of the *nucleus* (column) w.r.t. the width of the otolith bounding box, for a set of 411 Cod images and a polynomial curve fitted to these points. In this case, the 1st order polynomial adjusts to the data with a mean error equal to 27 pixels for a mean otolith width of 990 pixels. The standard deviation of the error is: 32 pixels and the ratio of the mean error to the mean width of the otolith is: 2.69 %.

Cod2000 Test Case: Figure 17. Shows the position of the vertical (row) coordinate of the *nucleus* w.r.t. the height of the otolith bounding box, for a set of 411 Cod images and a polynomial curve fitted to this points. In this case, a 3rd order polynomial adjusts to the data with a mean error equal 17 pixels for a mean otolith height of 491 pixels. The standard deviation of the error is: 28 pixels and the ratio of the mean error to the mean width of the otolith is: 3.38 %.

PlaiceQ32000 Test Case: Figure 18. Shows the position of the horizontal (column) coordinate of the *nucleus* w.r.t. the width of the otolith bounding box, for a set of 196 Plaice images and a polynomial curve fitted to this points. In this case, a 1st order polynomial adjusts to the data with a mean error equal to 16 pixels for a mean otolith width of 631 pixels. The standard deviation of the error is: 21 pixels and the ratio of the mean error to the mean width of the otolith is: 2.58 %.

Plaice Q32000 Test Case: Figure 19. Shows the position of the vertical (row) coordinate of the *nucleus* w.r.t. the height of the otolith bounding box, for a set of 196 Plaice images and a polynomial curve fitted to this points. In this case, a 1st order polynomial adjusts to the data with a mean error equal 17 pixels for a mean otolith height of 398 pixels. The standard

deviation of the error is: 7 pixels and the ratio of the mean error to the mean width of the otolith is: 1.89 %.

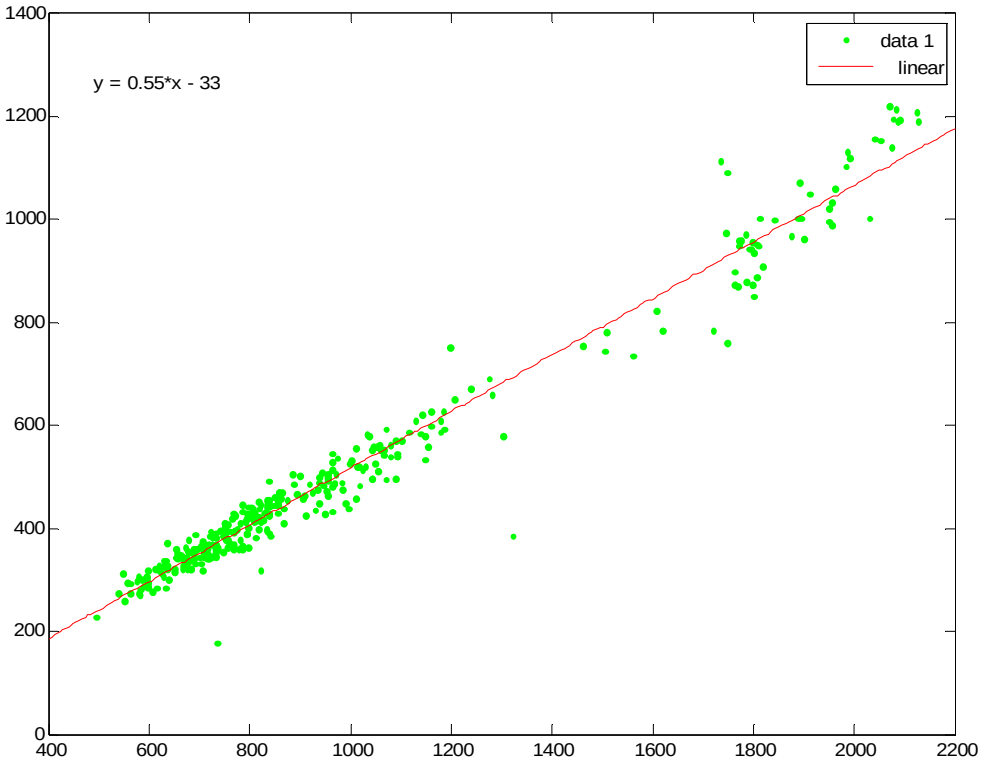

Figure 16. Cod image dataset. Plot of the horizontal (column) *nucleus* position versus the otolith width (pixels).

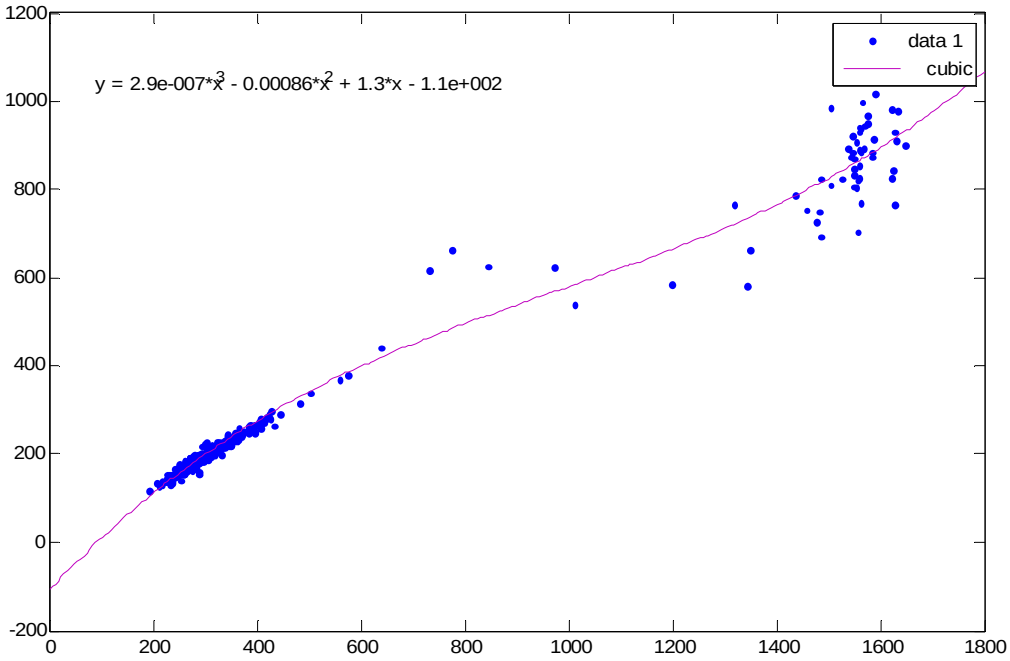

Figure 17. Cod image dataset. Plot of the vertical (row) *nucleus* position versus the otolith height (pixels).

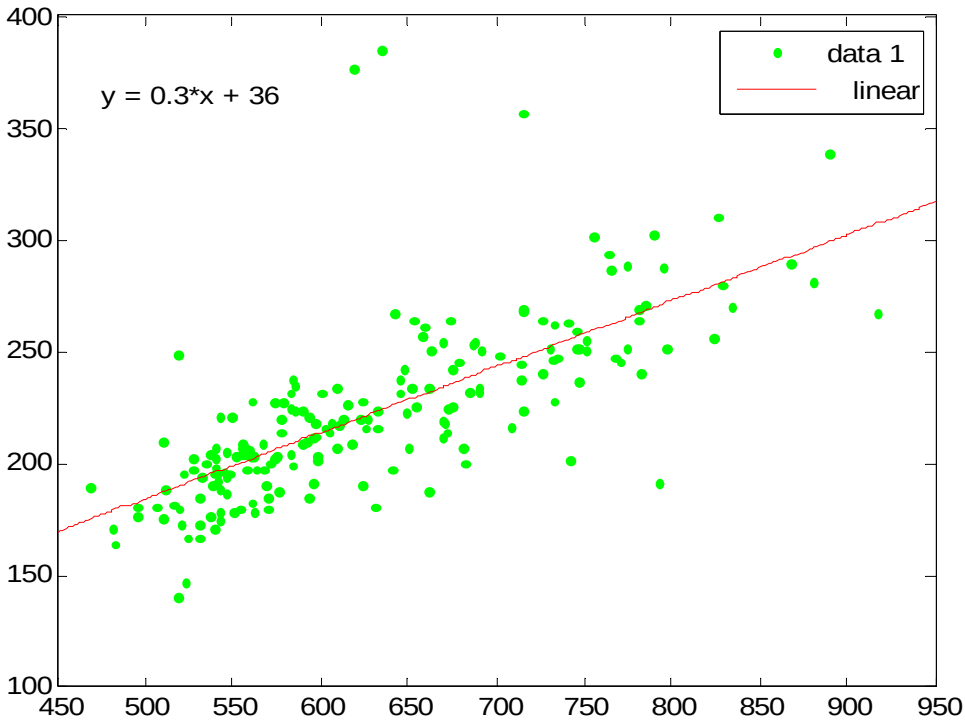

Figure 18. Plaice image dataset. Plot of the horizontal (column) *nucleus* position versus the otolith width (pixels).

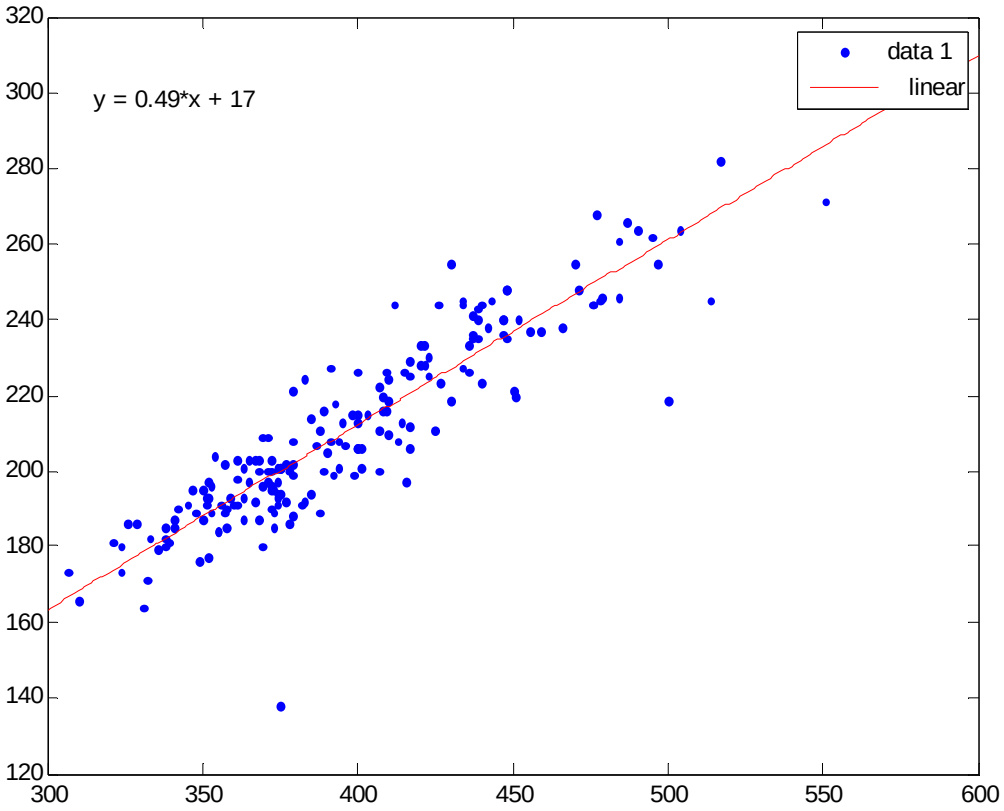

Figure 19. Plaice image dataset. Plot of the vertical (row) *nucleus* position versus the otolith height (pixels).

▪ Algorithm for the reconstruction of dense growth direction fields from images

INTRODUCTION

The reconstruction of the dense growth direction fields from images is an important pre-processing step required by other algorithms such as the directional filtering (D2.3.c), the detection of reference growth axis (D2.3.d), the detection of otolith rings (D2.3.f). Indeed, the dense growth direction fields give a representation that best fit the otoliths accretion process.

METHOD

The first step is to extract a sparse edged field from the image. The growth direction is known on the otolith border and *nucleus*. The aim of our method is then to find the growth direction on the whole otolith by interpolation.
The interpolation is done by an axiomatic approach known as the Absolutely Minimizing Lipschitz Extension (AMLE). It's a well studied operator for which existence and unicity results are known. In particular it satisfies a maximality principle which guarantees that the solution is oscillation free.

Let $\Omega \subset \mathbb{R}^2$. Let S^1 be parametrized by angles in $[0, 2\pi[$. Let $D \subset \Omega$ be a set of curves and/or points and $\theta_0 : D \to S^1$. Then $\theta : \Omega \to S^1$ is the AMLE of θ_0 in Ω if:

$$\begin{cases} D^2\theta(D\theta, D\theta) = 0 \text{ in } \Omega, \\ \theta|_D = \theta_0 \text{ on } D, \end{cases} \quad (1)$$

I.e. if the second derivative in the direction of the gradient is null. The mathematical theory only holds if the data θo is not surjective, i.e. if it takes value in S1 minus one point. If it is not the case, singularities are bound to appear, which the operator, looking for Lipschitz solutions, cannot handle. The AMLE is a laminar flow orientation operator, not a turbulent flow one. In practice we are interested in geometric structures, which give rise to regular orientation field. Thus this necessary condition will be locally fulfilled.
This equation has been implemented using the associated evolution problem combined to a finite difference scheme. Due to the specificity of angular data and the iterative nature of such a scheme, a multiresolution procedure was used to initialise the numerical resolution. Typical computational time is about a minute for 512x512 images on Pentium IV 2.5 GHz, and the interpolation process is parameter-less.

RESULTS

In Figure 20, the computed field is shown for an otolith image. The dense field obtained by our method is visualised via its flow line using the LIC (line integral convolution). It follows when possible the geometry of the image. For topological reason, singularities are unavoidable. Thus in absence of clear constraints or if they conflict with each other, chaotic zones akin to turbulence flows are created.

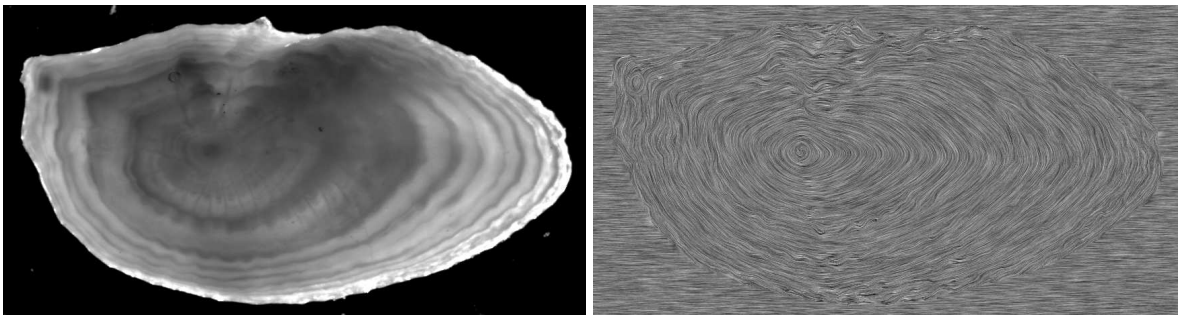

Figure 20. Left: original image, right: obtained dense orientation field visualised by LIC.

CONCLUSION

The dense growth direction field can be improved by adding some constraints where the direction is known. For example, once some rings are detected, their orientation can be used as constraints to re-estimate a better direction field.

- **Algorithm for locally adapting directional filters with variable bandwidth for ring enhancement and detection**

INTRODUCTION

When applying image filtering techniques, one is required to define the width and the orientation of the filter. If no specific a priori information is available, one typically consider an isotropic smoothing such as a Gaussian filter. It is obvious that an isotropic filtering is not adapted to otolith images. On the one hand, otolith images depict clearly oriented ring structures. And, on the other hand, as the otolith growth acts as a frequency modulation law on the widths of the opaque and translucent rings, ring structures are also associated with different image scales. Estimated potential function U provides the both types of information. The orientation of the gradient of U is an estimate of the orientation of ring structures and its magnitude is directly related to the width of the associated ring structures. Therefore, the level-set representation U provides the basis for applying an orientation-driven and scale-adapted filtering of otolith images.

METHODS

For each pixel *p* of the mask, the filter first defines a neighbourhood *Np* by retrieving *nt* pixels around *p* following the orientation of ring structures. The obtained curve is then shifted by no pixels around *p* in the orthogonal direction. The new luminance value of pixel *p* is computed as a weighted mean:

$$l(p) = \sum_{n}^{Np} w_n l(n)$$

where *l(p)* and *l(n)* are respectively the luminance value of pixel *p* and neighbour *n*, and *wn* the weight of neighbour *n* defined as the product of two Gaussian functions:

$$w_n = G_o G_t = \frac{1}{2\pi\sigma_o^n \sigma_t} e^{-\frac{d_o^2}{2\sigma_o^{n\,2}} - \frac{d_t^2}{2\sigma_t^2}}$$

with *σt* (respectively *σo*) the standard deviation of the tangent (respectively orthogonal) Gaussian function. *σo* is a function of *p* and is previously estimated using a two step algorithm based on the otolith growth law (figure 17-up-left). A first step estimates the value of *σo* on each radial by a linear interpolation between the value on the border *σb* and the *nucleus σc*.
σb and *σc* correspond to the quarter of a ring width and thus value on the border is smaller than on the *nucleus*: *σb*<*σc*. The second step interpolates the values between the *nucleus* and the border using AMLE with the first step resulting image as an initial condition.

RESULTS

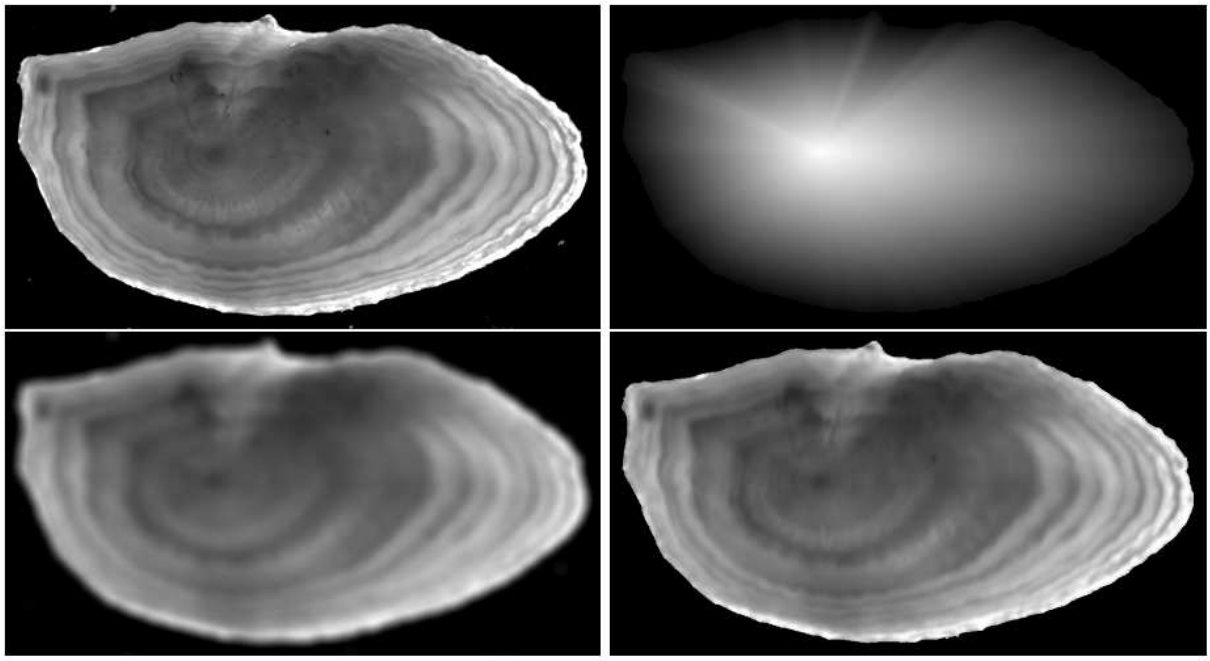

Figure 21. Comparison of two smoothing methods. Up-left: original image, Up-right: sigma image, Bottom-left: isotropic Gaussian filtering (with σ = 10), Bottom-right: orientation-based filtering (with σt = 7 and σo ranging from 5 on the border to 45 on the *nucleus*).

CONCLUSION

The image obtained by this adaptative filter better fit the otolith structure. One of the difficulties was to choose correctly the parameters of the filter but the quality of the result is less sensitive to this choice than a classical Gaussian filter.

▪ Algorithm for the detection of reference growth axes

INTRODUCTION

Usually biological studies on otoliths are based on the extraction of a one-dimensional line or curve going from the otolith *nucleus* to the border. These growth axes can be defined as curves linking the *nucleus* to the border with a path tangent to growth structure. Usually these axes are manually defined. Thus to normalise these biological studies, retrieving automatically these axes in a standard way is an important issue.

METHOD

Given a point on the otolith border, a point on the *nucleus* and the 2D growth model (given by D2.2.a), our method can link these two points following the growth axis.

First, a vector field u is constructed from the gradient of the 2D growth model. Then using minimal path formulation, given two points M0 and M1 and this vector field u, the extraction

of the curved growth axis Γ_{M_0,M_1} is stated as minimising a given metric $F(u,\Gamma)$. The axis Γ_{M_0,M_1} is defined by:

$$\Gamma_{M_0,M_1} = \arg \min_{\tilde{\Gamma} \in C(M_0,M_1)} E_{F(u,\tilde{\Gamma})}(M_0,M_1)$$

with $C(M_0,M_1)$ the set of continuous curves from M_0 to M_1. To solve for it, we compute:

$$E_{M_0}(x) = \min_{\tilde{\Gamma} \in C(M_0,x)} E_{F(u,\tilde{\Gamma})}(M_0,x), \qquad x \in \Omega .$$

$E_{M_0}(x)$ is a convex function whose only minimum is in M_0, thus it leads to Γ_{M_0,M_1} by a simple gradient descent on E_{M_0} from M_1 to M_0.

To actually compute E_{M_0}, the Fast Marching algorithm is used. It is based on a front propagation of equation:

$$\frac{\partial C}{\partial t}(c(\lambda,t)) = \frac{1}{F\left(u,\Gamma_{M_0,C(\lambda,t)}\right)} n(C(\lambda,t)),$$

with C the front, initially an infinitesimal circle around M_0, λ an Euclidean parameterisation of C and n the outward normal to the front. $E_{M_0}(x)$ is then defined as the arrival time of the front at each point. Thus at any given time, minimal paths have been computed from M_0 to all the points already visited by the front at that time, they can then be used to further propagate it.

The proposed function F is:

$$F(u,\Gamma)(y) = \left\langle \frac{\partial \Gamma(\lambda)}{\partial \lambda}(y), u^{\perp}(y) \right\rangle^2 ,$$

with λ an Euclidean parameterisation of Γ, $u^{\perp}$ the orthogonal of u and $< .,. >$ the usual scalar product of R^2. It is by definition null if u is tangent to Γ and maximum if it is orthogonal.

RESULTS

Figure 22 display the growth axis obtained with a point M0 on the *nucleus* and the point M1 taken successively on a subset of otolith border.

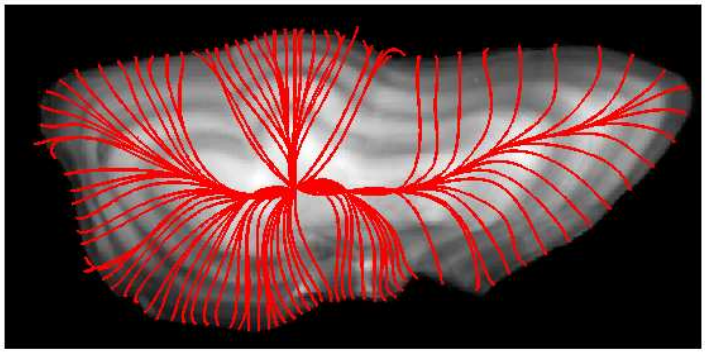

Figure 22. Example of growth axis extraction.

▪ Algorithm for the 1D detection of otolith rings

INTRODUCTION

The 1D detection of otolith rings can be done on a radial extracted by expert or on automatically retrieved growth axis.

❖ Method based on the radial intensity extrema

The extraction of local elementary ridge or valley segments proceeds as follows. Given an image and the position (xO,yO) of the growth centre O, its external shape is initially extracted. The number of sampling points of the external shape is denoted by NC and their polar coordinates by $\left\{\left(\rho_C^k, \theta_C^k = 2k\pi / Nc\right)\right\}_{k\in[1,Nc]}$, in the framework of the two principal axes centred in the growth centre. The semi-local detection of ridge and valley structures is performed within N_{SL} overlapping angular sectors, referenced by their angular coordinate $\left\{\theta_{SL}^n = 2n\pi / N_{SL}\right\}_{n\in[1,N_{SL}]}$ and their angular width $2\Delta\theta_{SL}$. To ensure overlapping of the angular sectors, $\Delta\theta_{SL}$ is set such that $\Delta\theta_{SL} > \pi / N_{SL}$. Given an angular sector $\theta_{SL}^n \pm \Delta\theta_{SL}$, the associated semi-local template model is defined by its polar coordinates $\left\{\left(\rho_C^k, \theta_C^k = 2k\pi / Nc\right)\right\}_{k\in\kappa^n}$.

Our goal is to determine the scaling factors $\alpha \in [0,1]$ such that the scaled template, defined by the polar coordinates $\left\{\left(\alpha\rho_C^k, \theta_C^k\right)\right\}_{k\in\kappa^n}$ with $\kappa^n = \left\{[1, Nc] / \left|\theta_C^k - \theta_{SL}^n\right| < \Delta\theta_{SL}[2\pi]\right\}$, fit the local ridge and valley segments within the angular sector $\theta_{SL}^n \pm \Delta\theta_{SL}$. Different features computed from the derivatives of the intensity function along and normal to the local template can be used as the measure of the strength of local ridges or valleys. However, a simpler and more robust feature is preferred: the median value of the intensity along the scaled local template. It comes to define the following intensity function $s_{SL}^n(\alpha)$ for given angular sector $\left(\theta_{SL}^n, \Delta\theta_{SL}\right)$ and scaling factor α:

$$(1)\quad s_{SL}^n(\alpha) = med\left(\left\{I\left(x_0 + \alpha\rho_C^k \cos\theta_C^k, x_0 + \alpha\rho_C^k \sin\theta_C^k\right)\right\}_{k\in\kappa^n}\right)$$

Where med() is the median estimator and I the image intensity function. The extraction of the elementary ridge and valley segments then resorts to the detection of the extrema of the intensity function s_{SL}^n. Thus, one aims at computing the scaling factors α verifying:

$$(2)\quad \frac{ds_{SL}^n(\alpha)}{d\alpha} = 0$$

Solving for Eq2 requires computing the derivatives $\frac{ds_{SL}^n(\alpha)}{d\alpha}$ at relevant scales. In addition, specific time-frequency features of the images of biological hard tissues have to be considered. First, smooth variations of material density (for instance, otolith are usually thicker close to the edge) might result in a continuous evolution of the mean intensity values from the growth centre to the edge. Second, the width of translucent and opaque rings is directly related to the underlying growth pattern. Growth patterns are mainly non-linear. Images of biological hard tissues then involve a frequency modulation applied to the ring

structures. The actual growth pattern is obviously unknown, but a mean *a priori* growth model can be used for demodulation purposes. This idea was first applied to 1D intensity signals using an exponential model. Here, a mean growth model is derived from the growth patterns associated to images interpreted by an expert. Mathematically, the mean growth model is defined by the function $L = \phi(t)$, where L is the distance to the otolith centre, and t the time variable in years.

The framework used to solve for Eq2 then initially demodulates $ds^n_{SL}(\alpha)$ w.r.t. the growth model ϕ. The resulting demodulated signal $s^n_{DM}(t)$ is given by:

$$(3)\quad s^n_{DM}(t) = s^n_{SL}\left(\frac{\rho^n_C}{\rho^{n*}_C}\phi(t)\right),$$

Where n* refers to the point of the external shape on the main reading axis (for instance, $\theta^{n*}_C = \pi$ for plaice otoliths). Let us point out that $\phi(t)$ is normalized w.r.t. ρ^{n*}_C since the mean growth model is learned along the main reading axis.

To remove the trend s^n_{TDM} from the intensity signal s^n_{DM}, s^n_{TDM} is estimated using a convolution to a Gaussian kernel $g_{\sigma TDM}$ with a large variance $\alpha^2_T : s^n_{TDM} = g_{\sigma T} * s^n_{DM}$. Then, the detection of the positions of the local ridges and valleys involves the computation of the derivative $d_t s^n_{DM}$ of the intensity function $s^n_{DM} - s^n_{TDM}$. $d_t s^n_{DM}$ is estimated using a Gaussian kernel $g_{\sigma D}$ with a low variance σ^2_D :

$$(4)\quad d_t s^n_{DM} = \frac{d\left[g_{\sigma D} * \left(s^n_{DM} - s^n_{TDM}\right)\right]}{dt}$$

To actually determine the extrema of $s^n_{DM} - s^n_{TDM}$, the zero crossings of its first derivative $d_t s^n_{DM}$ are detected for time values uniformly sampled within $[0, t_{\max}]$, with $t_{\max}$ computed such that $\phi(t_{\max}) = \rho^{n*}_C$. The scaling factors solving for Eq2 are then computed from the inverse transform ϕ^{-1}. Typically, the sampling rate is set to 0.01, σ_D to 0.1 and σ_{TDM} to 1.5 (all these values are given in years since they are used in the demodulated domain).

The detection of the elementary ridge and valley segments arose from the adapted filtering of the semi-local template-based function s^n_{SL} is shown (Fig. 23). This example stresses that the growth-adapted demodulation eases the detection of ridge and valley structures close to edge and avoids over detections close to the centre.

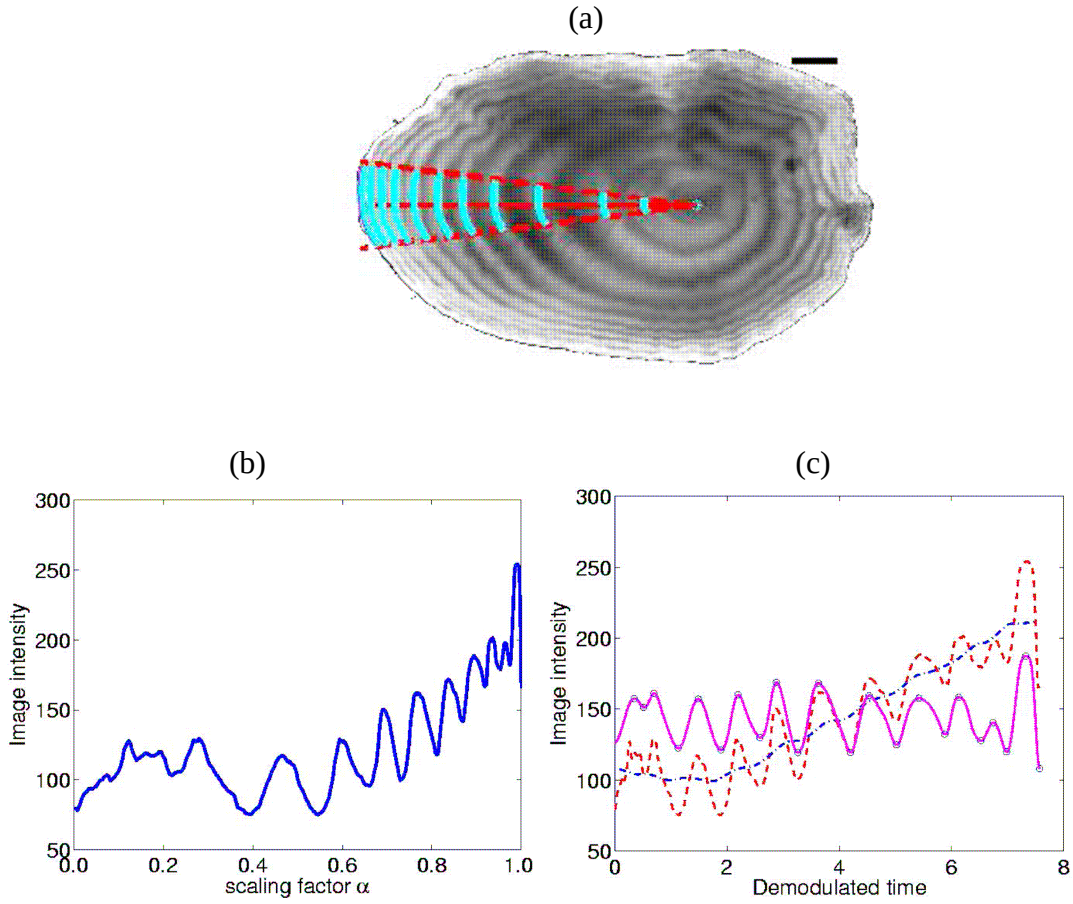

Figure 23. Detection of elementary ridge segments: (a) the processed image with the extracted elementary ridge segments (thick line) within the angular sector $\theta_{SL}^{n} = \pi$ (Bar = 1 mm); (b) the intensity function s_{SL}^{n}, c) the demodulated version (red dashed line) using the mean growth law, the estimated tendency (blue dashed-dotted line), the filtered signal (magenta solid line) and the estimated extrema positions (o symbols).

❖ Method based on the radial autocorrelation

Otolith growth is non-linear and is influenced by environmental conditions of fish habitat, such as water temperature, diet and light, among other factors. This means that the location of season related peaks and valleys along the radial intensity profiles appears with unalignments of the seasonal structures, even if they belong to otoliths of the same age class, and follows a quasi-exponential growth law. Figure 24 shows a section of a 3-year old fish otolith image on which the experts have manually plotted red dots to mark the position of the successive annual rings. The radial, from the *nucleus* to the edge, is represented with a green line and Figure 25 shows the intensity profile r along this radial with red stem marks on the annual rings.

The growth rate is non-uniform and generally follows frequency modulated behaviour and therefore the radial length can be expressed as an exponential law of the fish age. To obtain a linear growth law version of the intensity profile we must demodulate this signal using an optimal function, which yields an almost periodic repetition of the seasonal structures. This demodulating function can be calculated in an optimisation process which measures the signal

periodicity. Figure 26 shows the demodulated intensity profile and the red stem marks on the annual rings are equally distributed along the radial axis. The periodicity is measured by the inverse of the normalised entropy of a histogram of the intensity profile short term autocorrelation lags above a certain threshold. The annual rings correspond to the maxima of the short term autocorrelation histogram (Fig. 27).
Optionally, there is the possibility to remove the effects of the image non-uniform contrast on the intensity profile. To do this we use a Gaussian lowpass filter to detrend the intensity profile.

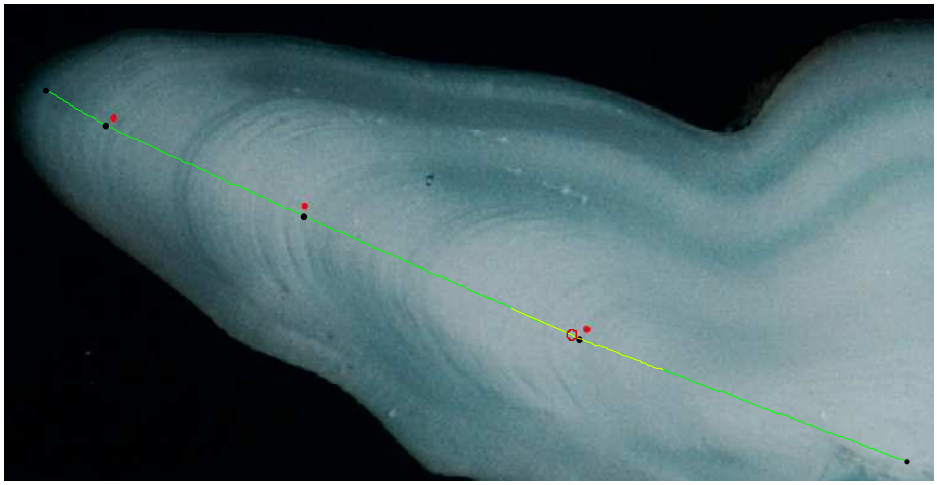

Figure 24. Section of a 3 year old Cod otolith. The red dots, from left to right, are the *nucleus* and successive year marks, placed manually by an expert. The green line represents the radial used to extract the intensity profile. The red circle is the position of the computed first annual ring along this intensity profile.

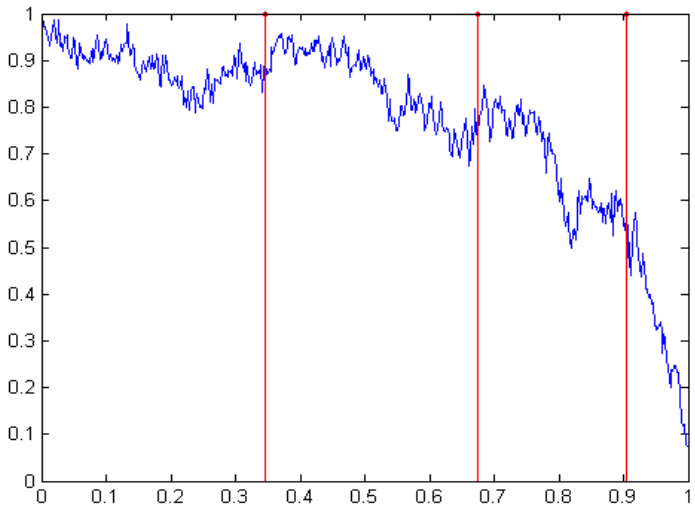

Figure 25. Intensity profile along the radial growth axis.

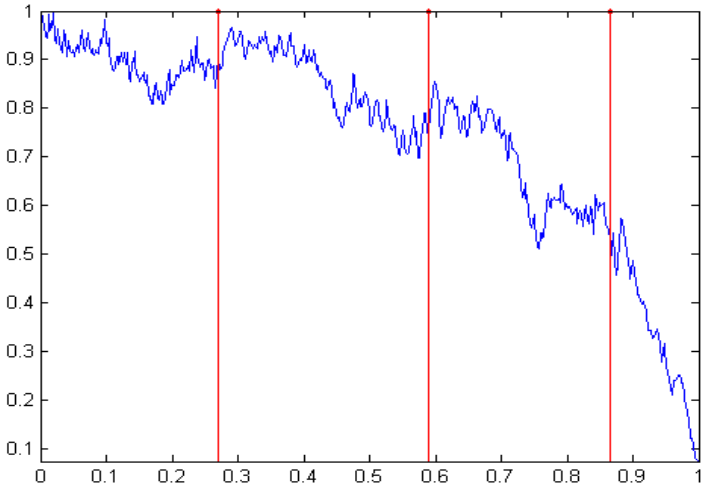

Figure 26. Demodulated Intensity Profile. The equally spaced red stems correspond to the annual growth marks.

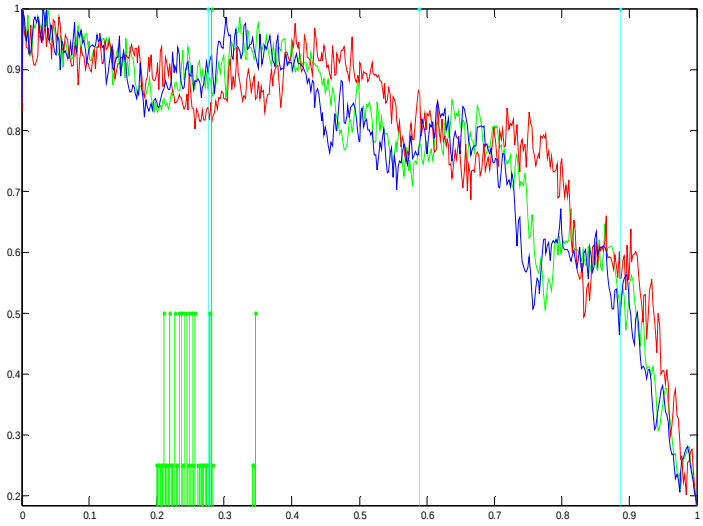

Figure 27. Original (red) intensity profile, Linear growth (green) intensity profile and demodulated (blue) intensity profile. The green stems are the histogram of the normalized autocorrelation lags above 0.8, computed using a 64 samples window length. The maximum of the histogram is the position of the first annual ring.

▪ Algorithm for the 2D segmentation of partial otolith rings

Problem statement

The shape and position of seasonal rings is of great interest to estimate fish age and growth history, but detecting automatically this dark rings from image is challenging. Intuitively, ridges and valleys (together known as creases) of a grey level image are the relief curves of the landscape obtained when the image intensity is seen as a height map. A rigorous, efficient and general purpose computer vision implementation of that intuition has however proved to be a challenge because, as for the other perceptual structures so clear for the human vision

(edges, shapes, objects etc...), they are the result of a lot of grouping laws which interact globally in non-trivial ways [1]. In our case, ridges and valleys can be seen as the results of two grouping process. One is contrast-based, and locates the creases locally at the locus of high curvature of the image. The second, the good continuity, is more global and group together those loci which constitute a curve smooth and long enough.

In this study, the detection of partial otolith rings is limited to the case of valleys detection (the case of ridge detection being solved in a similar way). The problem is formulated in term of energy minimization and consist in finding a labelling l that assigns each pixel $p \in P$ a label $l_p \in L$ where $l_p = 1$ if pixel p is located on a valley and $l_p = 0$ elsewhere. The goal is to find the labelling l that minimizes the following energy[2]:

$$E(l) = E_d(l) + E_s(l)$$

The data energy term $E_d(l)$ measures the disagreement between the labelling l and the observed data and the smooth energy term $E_s(l)$ measures the extend to which l is not piecewise smooth. Thus, minimizing this energy tends to emulate the grouping laws involved in human perception process. The observed data are the intensity curvature and the orientation of the structure. The first eigenvalues of the Hessian is computed to estimate the main intensity curvature at each pixel while the orientation of intensity gradient is used to estimate the orientation of the structure.

Energy minimization via graph cuts

In the field of computer vision, graph cuts can be employed to efficiently solve a wide variety of low-level computer vision problems (stereo correspondence, smoothing) that can be formulated in terms of energy minimization. Such energy minimization problems can be reduced to instances of the maximum flow problem in a graph (and thus, by the max-flow min-cut theorem, define a minimal cut of the graph). Under most formulations of such problems in computer vision, the minimum energy solution corresponds to the maximum a posteriori estimate of a solution.

To formulate our problem of valleys detection in term of energy minimization with graph cuts, we must define both an adapted graph topology and energy. Figure 28 presents a general graph topology. For legibility, the topology is illustrated in the binary case (2 labels) and in 4-connexity.

[1] G. Kanizsa. La grammaire du voir. Diderot, 1996.

[2] Yuri Boykov, Olga Veksler, and Ramin Zabih. Fast approximate energy minimization via graph cuts. IEEE transactions on Pattern Analysis and Machine Intelligence, 23(11):1222–1239, November 2001.

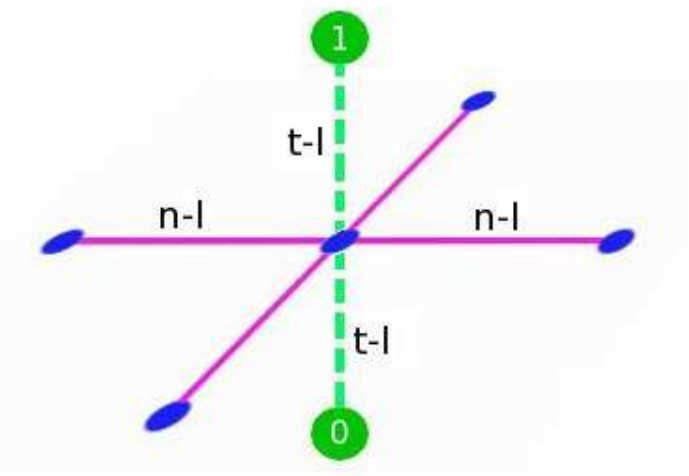

Figure 28: Graph cuts topology. Each node of the graph (blue) is linked to each labels (0 or 1 in green) with terminal links (t-l) and to its neighbour nodes (here in 4-connexity) with neighbour links (n-l).

Each node of the graph is linked to labels with terminal links (t-l) and to its neighbour nodes with neighbour links (n-l). The data energy on terminal links represents the cost of assigning a label to a pixel, the lower the data energy Ed_p^{lp}, the more appropriate the label l_p for pixel p according to the observed data. In our binary case and for a given labelling l, data energy can be decomposed as follow:

$$Ed(l) = \sum_{p \in P} l_p Ed_p^1 + \sum_{p \in P} (1 - l_p) Ed_p^0$$

The smooth energy on neighbour links tends to give the same label to the pixels belonging to the same neighbourhood. It is defined by the following equation:

$$Es(l) = \sum_{p \in P} \sum_{q \in Np} Wl_{pq} Wk_{pq}$$

Where N_p is the neighbourhood of pixel p, Wk_{pq} is a weighting term representing the a priori knowledge on the link between pixels p and q, Wl_{pq} is the weighting term depending only on the label of pixels p and q and is defined by a table which has the following general form:

$l_p \cdot \cdot l_q$	0	1
0	α_{00}	α_{01}
1	α_{10}	α_{11}

Table 3: Labels (Wl)

Once the energy and the topology are defined, the graph energy can be minimized. The methods to minimize this energy with graph cut are described in [Boykov 2004][3], [Boykov 2001][4].

[3] Yuri Boykov and Vladimir Kolmogorov. An experimental comparison of mincut/max-flow algorithms for energy minimization in vision. IEEE transactions on Pattern Analysis and Machine Intelligence, 26(9):1124–1137, September 2004.

They are implemented using the C++ libraries provided by authors[5]. The following sections present two different implementations of graph cut algorithm using different topology and energy definitions.

Pixel node graph

This first algorithm use graph cuts to label pixels as valley (with label 1) or not (label 0). A node of the graph corresponds to a pixel and a link of the graph defines the relation between two pixels. The data energy is related to Hessian and the smooth energy is related to orientation.

Energy definition

Concerning data energy, a normalised histogram H_n of Hessian value is computed satisfying:

$$\sum_{p=1}^{N} H_n(\mu_p) = 1$$

where μ_p is the Hessian value for pixel p and N is the number of pixels inside the otolith. Then, for each pixel inside the otolith, the data energy Ed is computed as follow[6]:

$$Ed_p^1 = -\log(P_{\mu_p}).\alpha_{data}$$
$$Ed_p^0 = -\log(1-P_{\mu_p}).\alpha_{data}$$
$$\text{with} \qquad P_{\mu_p} = P(\mu \le \mu_p) = \int_{\mu=0}^{\mu_p} H_n(\mu)d\mu$$

The smooth energy Es is divided in two terms, the term Es_{pq}^t defines the energy on the neighbour links tangent to local image structure while Es_{pq}^o defines the energy on those orthogonal :

$$Es_{pq}^t = Wl_{pq}\left[\frac{1}{2}\left|\cos\left(\gamma_{pq}-\gamma_p+\frac{\pi}{2}\right)\right|+\frac{1}{2}\left|\cos\left(\gamma_{pq}-\gamma_q+\frac{\pi}{2}\right)\right|\right]$$
$$Es_{pq}^t = Wl_{pq}\left[\frac{1}{2}\left|\cos\left(\gamma_{pq}-\gamma_p\right)\right|+\frac{1}{2}\left|\cos\left(\gamma_{pq}-\gamma_q\right)\right|\right]$$

with γ_{pq} the orientation of the line between pixels p and q, and Wl_{pq} the label dependent term defined by the following table :

---

[4] Yuri Boykov, Olga Veksler, and Ramin Zabih. Fast approximate energy minimization via graph cuts. IEEE transactions on Pattern Analysis and Machine Intelligence, 23(11):1222–1239, November 2001.

[5] http://www.csd.uwo.ca/faculty/olga/code.html}{http://www.csd.uwo.ca/faculty/olga/code.html

[6] R. Azencott, B. Chalmond, and F. Coldefy. Markov fusion of a pair of noisy images to detect intensity valleys. Int. J. Comput. Vision, 16(2):135–145, 1995.

$l_p \cdot \cdot . l_q$	0	1
0	0.5	2
1	2	1

Table 4: Labels (Wl) for pixel node graph

The coefficients in table 2 are higher when p and q have different labels and result in penalizing this configuration in the smooth energy. The second part of smooth energy results from the scalar product between the link pq and the vector defined by the mean structure orientation in p and q.

Results

The figure 29 presents the result obtains on a North-Sea cod otolith. The pixels detected as valleys are near or on the true valleys of the images. But the result is not completely satisfying because, due to the smooth energy definition, valley pixels are grouped in blob whereas a valley corresponds to a curved and thin line.

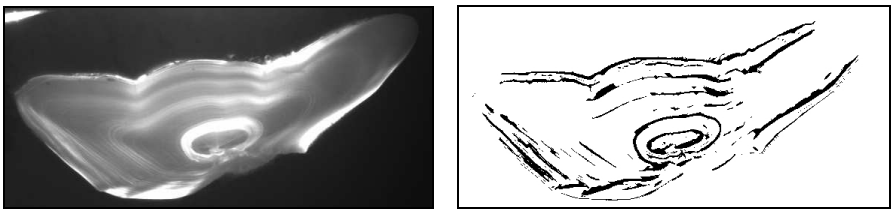

Figure 29: Result of valley detection using pixel node graph. Pixels detected as valleys are black (label 1) while the rest of the image is white (label 0).

We would have prefer a smooth energy definition closer to the one defined in [Azencott1995][7] so that 3x3 pixels cliques are given a lower energy when containing only a line of 3 pixels (with label 1), whereas in our case the lower energy is given when all the pixels of the 3x3 clique are at the label 1 or 0. But even if the energy defined in [Azencott1995] is more suitable for our case, it results in an energy function that does not satisfy the submodular criterion[8]. This criterion guarantees that the minimization process can converge in polynomial time whereas the problem is N-P hard in the general case.

Another problem is also that with this energy definition, the smooth energy term contains orientation information that would better correspond to data energy term. The next section introduces another topology and energy definition that try to overcomes theses problems.

[7] R. Azencott, B. Chalmond, and F. Coldefy. Markov fusion of a pair of noisy images to detect intensity valleys. Int. J. Comput. Vision, 16(2):135–145, 1995.

[8] Vladimir Kolmogorov and Ramin Zabih. What energy functions can be minimized via graph cuts? IEEE transactions on Pattern Analysis and Machine Intelligence, 26(2):147–159, February 2004.

Curve node graph

This second algorithm use graph cuts to labels curves as valley (label 1) or not (label 0). Whereas in the pixel node graph, the topology of the image directly map the topology of the graph, in this case, a node of the graph corresponds to a curve and a link of the graph defines the relations between two neighbour's curves.

Energy definition

To obtain a network of curves on which we can apply this graph cuts labelling, we first compute local maximums of Hessian, keeping only the maximum in each 20x20 pixels window (figure 3-Middle-left). These maximums are then linked with curves that follow the image structures by using the fastmarching distance (figure 3-Middle-right). This initial network of curves is used as input for our graph cuts algorithm.

$$Ed_p^1 = \sum_{c \in C} \sum_{p \in c} -\log(P_{\mu_p})$$

$$Ed_p^0 = \sum_{c \in C} \sum_{p \in c} -\log(1 - P_{\mu_p})$$

with $$P_{\mu_p} = P(\mu \le \mu_p) = \int_{\mu=0}^{\mu_p} H_n(\mu) d\mu$$

Where c is a curve in the set of initial curves C and p is a pixel of the curve c (see previous section for definition of H_n.

The smooth energy Es is defined by:

$$Es_{cd} = Wl_{cd}[\cos(\gamma_c - \gamma_d)]$$

with γ_c (respectively γ_d) is the orientation of the curve c (respectively d) computed in the neighbourhood of the curves intersection, and Wl_{cd} the label dependent term defined by the following table:

Table 5. Labels (Wl) for pixel node graph

$l_c \ddots l_d$	0	1
0	1	2
1	2	1

This table coefficients are higher when curves c and d have different labels and result in penalizing this configuration in the smooth energy.

Results

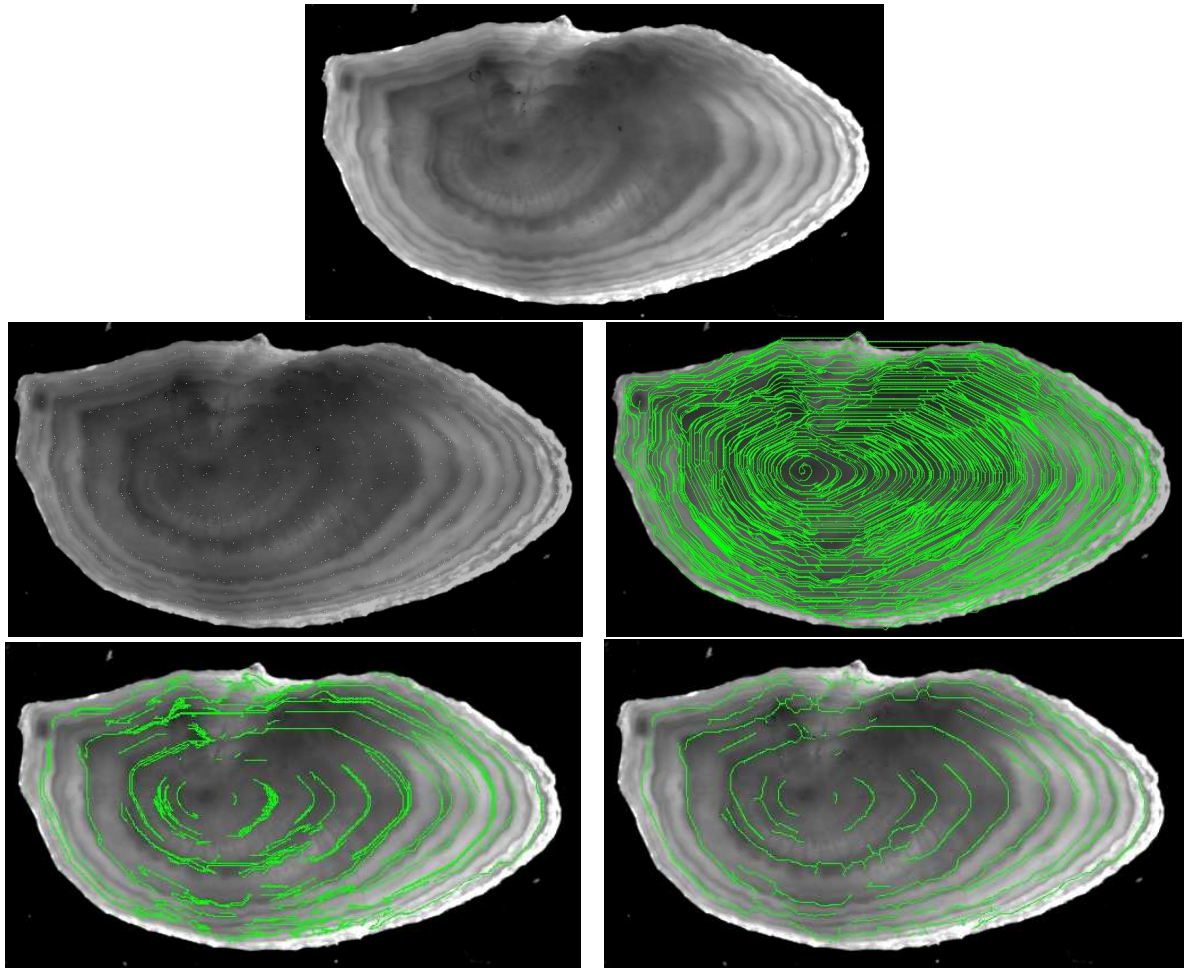

Figure 30:. Result of valley detection using curve nodes graph. Top: original image, Middle-left: Hessian maximums, Middle-right: initial network of curves, Bottom-left: output curves labelled as valleys (label 1) after graph cuts minimization. Bottom-right: output resulting curves after grouping process.

The curves labelled as valleys (label 1) after graph cuts (figure 3-Bottom-left) are grouped in blobs and several tangent resulting curves are found for each valley. Like in pixel node graph algorithm, the problem comes from the fact that smooth energy cannot satisfy submodular criterion while solving exactly our valley detection problem. To overcome this problem, each curve blobs are detected and a new curve passing in the middle of each blob is computed. The result gives an estimation of the valley position (figure 3- *Bottom-right*).

Conclusion

To our knowledge, this study is a first attempt to use graph cut for otolith ring detection and thus must be considered as a preliminary study. The first results present here are promising but still too noisy to be directly used for age estimation. In is current development, this method would be more efficient for example to improve the orientation field estimation.
One of the main issues of future works should be to formulate the problem so that it both fit the frame of graph cut energy minimization theory and the perceptual grouping laws of our particular ring detection problem. But graph cuts can be a powerful new tool for 2nd ring segmentation and this method should be investigated further.

- **Contrast-invariant representation of otolith ring-based information**

Method

Seasonal rings are of key interest for ageing and are visible on otolith because they induce variations in opacity that can be seen as variations of luminance signal on an otolith image. However, this luminance signal is also a product of several other processes, for example: acquisition noise, local growth anisotropy and even otolith thickness in the case of whole otolith images. The contrast-invariant representation proposed here try to best separate the otolith ring-based information from the other type of information merged in the luminance signal.

The method consists in using the advection-diffusion principle to propagate along the structure orientation field the partial ring information issued from local extraction of ridges and valleys structures. In a first step the orientation field is estimated (Figure 31) by the direction of the gradient. Then local ridges and valleys are extracted using multiple 1D detection of extremums along several radials. Then a map of ridge and valley points is built with 1 at ridge points, -1 at valley points and 0 elsewhere. This map is used to initialize the potential function of the advection-diffusion algorithm.

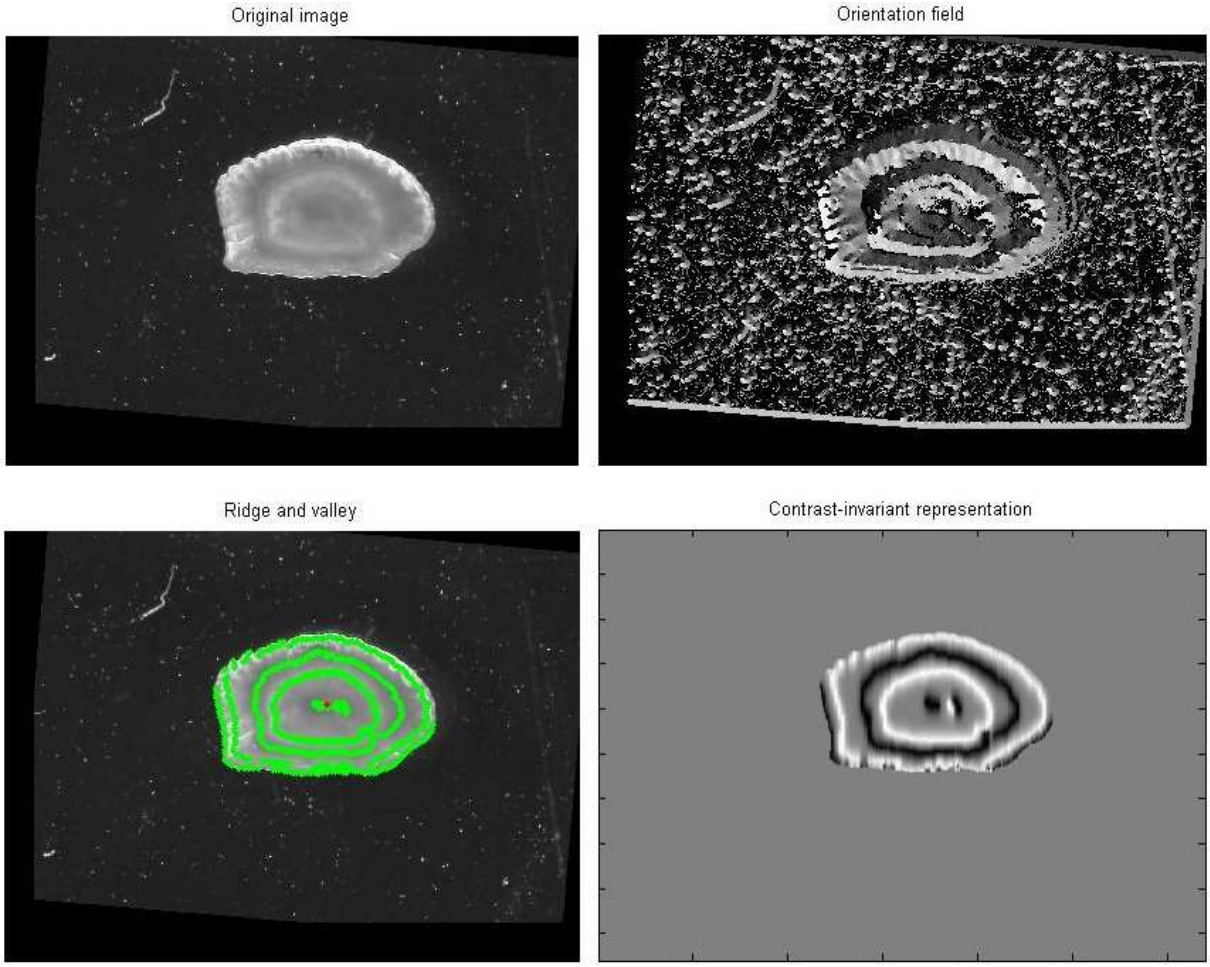

Figure 31: The different steps of the Contrast-invariant representation method on an Eastern Channel plaice otolith.

The advection-diffusion algorithm is based on a partial differential equation (PDE) scheme that makes a potential function U evolves according to the field lines of the orientation field. This PDE-scheme can be described by the following equations:

$$\begin{cases} U_O \\ \dfrac{dU}{dt} = \alpha_1 \Delta U + \alpha_2 div\left(\omega \langle \nabla U, \omega \rangle\right) \\ U_{t+1} = U_t + \Delta t \dfrac{dU}{dt} \end{cases}$$

Where U_t (respectively U_{t+1}) is the potential function at time t (respectively $t+1$), U_0 is the initial value of the potential function initialised with the map of ridges and valleys points, α_1 and α_2 are two weighting coefficients that respectively control the isotropic diffusion and the diffusion along field lines (Figure 32).

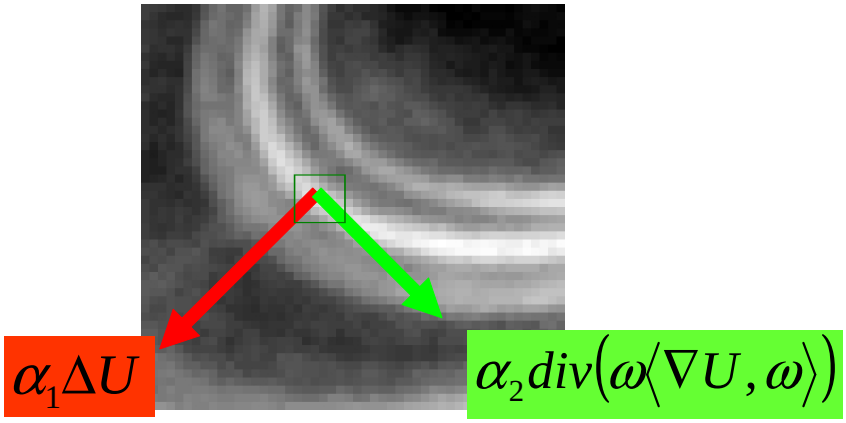

Figure 32: Visualisation of the advection-diffusion principle on a zoomed part of the otolith image. Red : isotropic diffusion. Green : diffusion along field lines.

Results

The results obtained on Eastern Channel plaice (Figure 31 and Figure 33) are quite good and stable among all the images of the species. Thus the contrast-invariant representation has been used successfully in the pre-processing step of an individual age estimator.

The results on Icelandic plaice are quite good for some images but the result is not stable among all images, so that it was not possible to include this method in automatic age estimation. The figure 34 presents an example of result for Icelandic plaice. On this image, the local extraction of ridges and valleys structures fails on the part of the images where the rings are not well contrasted, resulting in a partial contrast-invariant representation. The part of the ring missed by the local extractor is too important to be completed by the advection-diffusion algorithm.

The results on cod are very poor (Figure 35 and Figure 36). On both North-Sea cod and North-East Arctic cod, we observe the same problem regarding the failure of the local ridge

and valley extractor caused by the lake of contrast in some parts of the rings. But added to this problem, the local extractor is also distract by local variation due to impacts on otolith slices (Figure 5) and important local variation of luminance that are not related to rings (Figure 6).

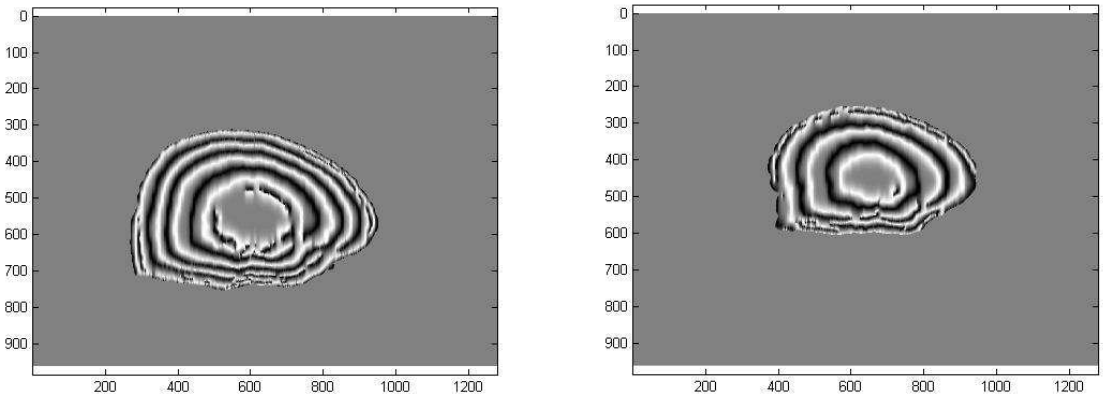

Figure 33: Examples of contrast-invariant representation results for Eastern-Channel plaice.

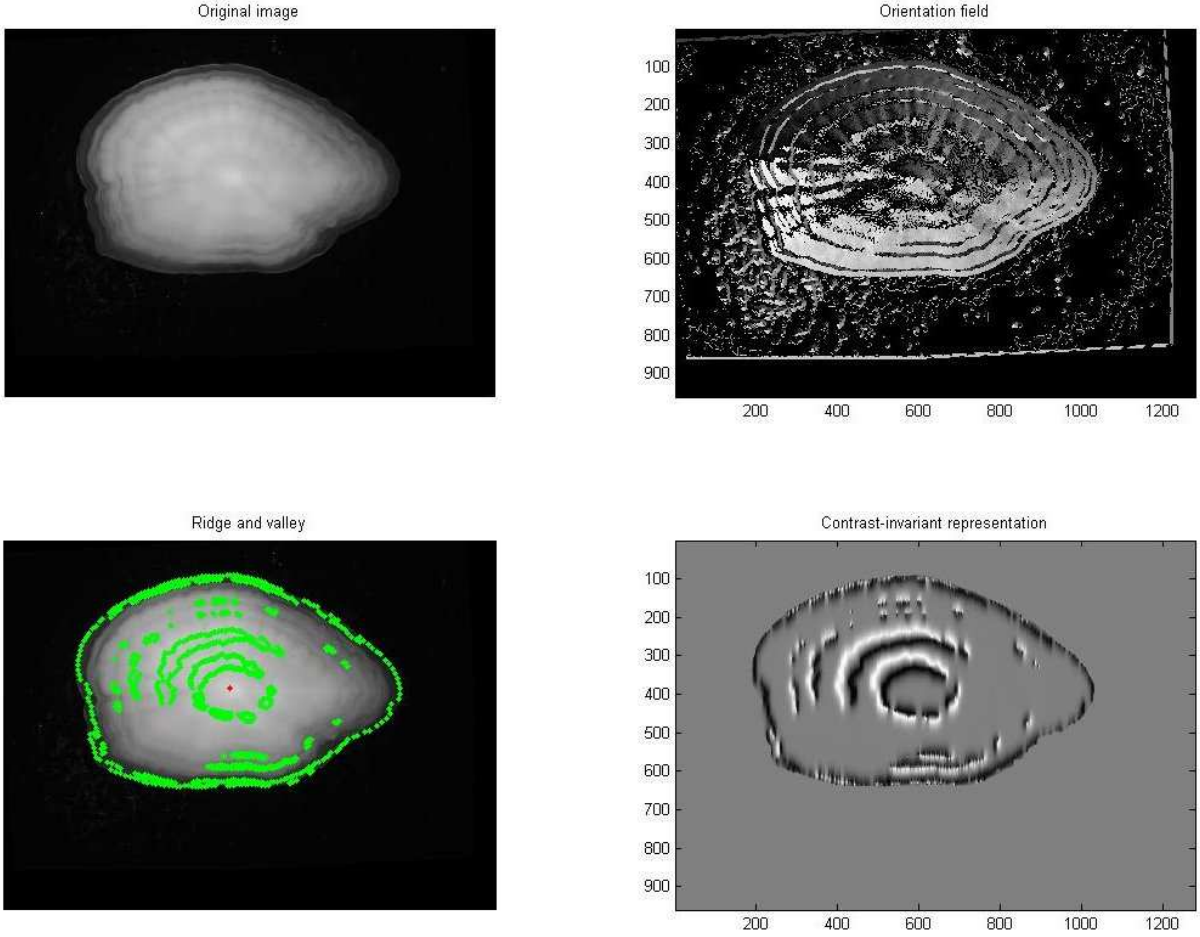

Figure 34: Example of contrast-invariant representation result for Icelandic plaice.

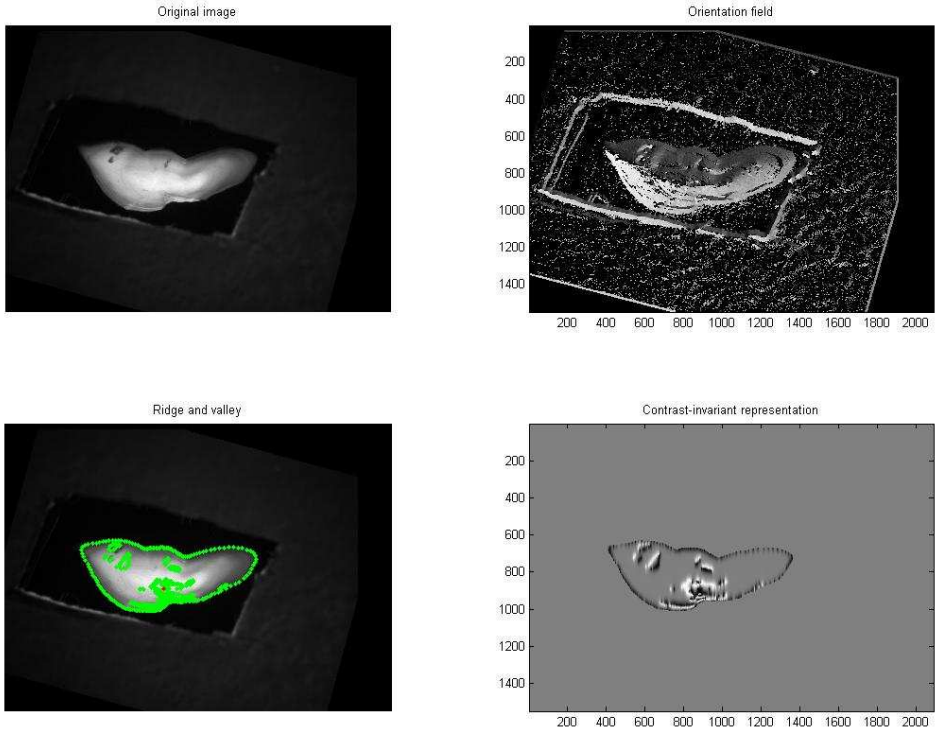

Figure 35: Example of contrast-invariant representation result for North Sea cod.

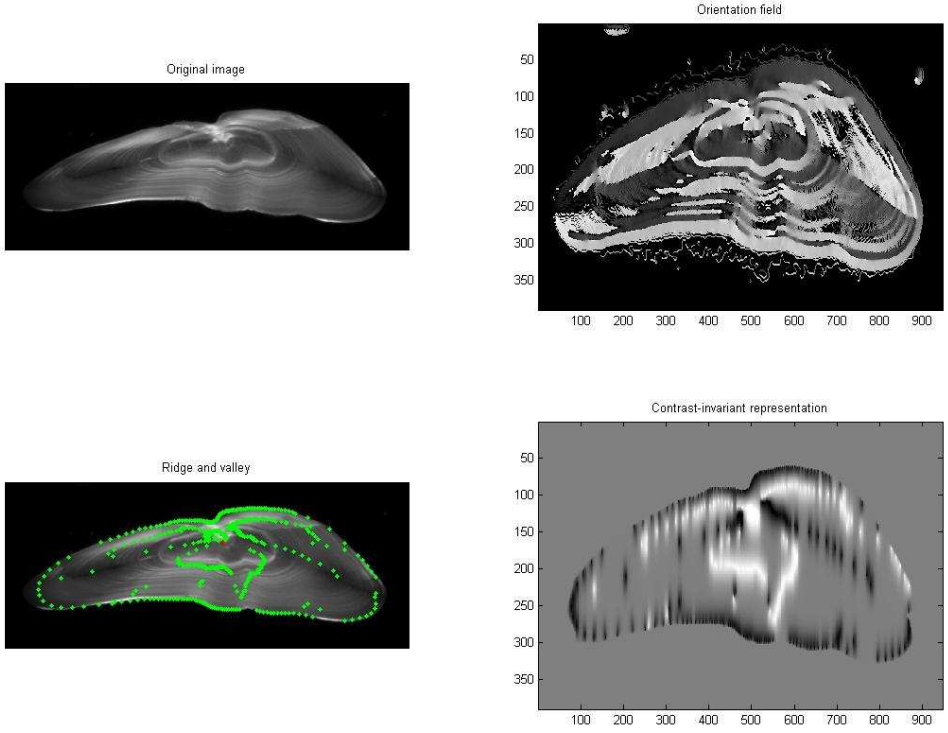

Figure 36: Example of contrast-invariant representation result for North-East Arctic cod.

Conclusions

The method proposed here works well on Eastern Channel plaice, mainly because the rings are large and well contrasted but still failed on other species.

The general scheme proposed here can be improved by using a more complex method of ridges and valleys detection, for example the method proposed in deliverable 2.3.f, once this method will be in a more advanced stage to be applied on a large amount of images and species.

The method to estimate the orientation field used here is also rather simple and the contrast-invariant representation can also benefit from better orientation field estimation. Though, even with a best orientation field, the advection-diffusion will hardly recover from a bad initialisation caused by the local ridges and valleys extractor.

We tried to use the locally adapting directional filter (Deliverable 2.3.c), as a pre-processing step, to enhance the ring information. But the benefit of this pre-processing on the result is hard to evaluate because it was hard to find a generic set of parameters for the whole stock. Moreover, the change on the final result is hard to evaluate even qualitatively.

Despite its defects, this method offers a promising scheme that uses all available 2D information to enhance the ring information.

▪ Feature discrimination algorithm

INTRODUCTION

Fish automatic age estimation methods normally extract the intensity profile from otolith section images to extract age structures that appear in the form of peaks and valleys, which also represent seasonal events. This signal is the radial grey level value from the *nucleus* to the edge of the otolith section. Feature extraction methods, normally use traditional signal processing techniques to yield new signals with suitable size in order to train a classifier and enhance its performance.

METHOD

Given a set of intensity profile signals and knowing the year classes they belong to, we use the LDB. This approach combines *Wavelet Packet transform* (WPT) and discriminant analysis to reduce dimensionality selecting the basis functions (or filters) which highlight class differences.

First, the LDB decomposes the original signal space x_i using WPT to obtain its projection in multiresultion spaces $\Omega_{j,k}$ computing the coefficients $w_{j,k,l}\,x_i$ where $w_{j,k,l}$ is the l-th base of the space denoted by j and k (j=0,…,J; k=0,…, 2^J-1), being J the maximum decomposition level (or scale). These spaces can be symbolised in the form of a tree similar to the shape in figure 28. Then, class energy maps are computed by means of:

$$\Gamma_{j,k,l}^{(c)} = \frac{\sum_{i=1}^{N_c} \left(w_{j,k,l} x_i^{(c)} \right)^2}{\sum_{i=1}^{N_c} \left\| x_i^{(c)} \right\|^2}$$

Where Γ_c denotes the energy pap of class c, N_c is the number of signal in each class and the notation $x_i^{(c)}$ is used to specify class signal. Next, pairwise combinations of the symmetric relative entropy are accumulated for evaluating discrepancies among classes. This measure is given by :

$$D_{j,k,l} = \sum_{i=1}^{C-1} \sum_{j=i+1}^{C} D\left(p^{(i)}, p^{(j)} \right)$$

where $D(\cdot,\cdot)$ is the symmetric relative entropy between two equivalent tree samples of the energy maps in two different classes ($p^{(c)} = \Gamma_{j,k,l}^{(c)}$), and C is the number of classes. At this point, the node discrimination power is computed by means of :

$$D_{j,k} = \sum_{l=0}^{2^{n_0}-1} D_{j,k,l}$$

Where 2^{n_0} is the signal length.

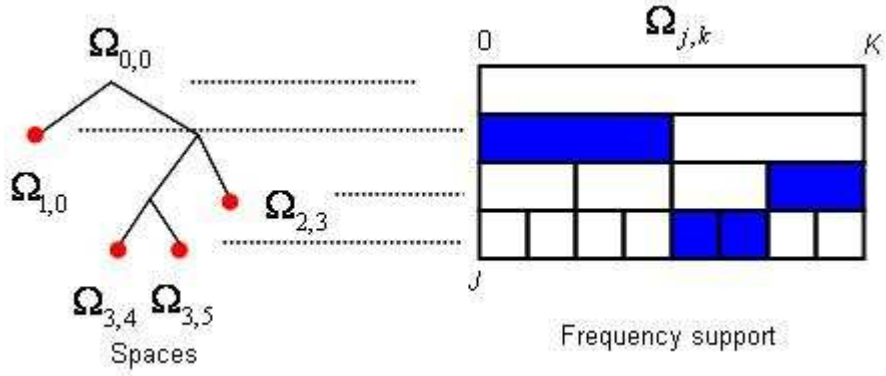

Figure 37: Relation between node position in the WPT tree and their frequency support in a space selection example.

With this measure, the LDB algorithm selects the most discriminant nodes of the tree (red dotted nodes in Figure 37). Each parent node is compared against its two children in all levels to obtain the most discriminant space $A_{0,0}$. The LDB algorithm is the following:

1. Choose a dictionary
2. For every class c = 1,…, C construct time-scale energy maps $\Gamma_{j,k,l}^{(c)}$
3. Calculate $D_{j,k}$ in all nodes.
4. For k = 0, …, 2^J-1 set:

   $A_{J,k} = B_{J,k}$
   and
   $\Delta_{J,k} = D_{J,k}$

where $B_{J,k}$ represents the time-scale coefficients of space $\Omega_{J,k}$

5. For $j=J\text{-}1,\ldots,0$ and $k=0,\ldots,\ 2^{J}\text{-}1$ determine the 'best subset' $A_{j,k}$ by the following rule:

If $\Delta_{j,k} \geq \Delta_{j+1,2k} + \Delta_{j+1,2k+1}$

$A_{j,k} = B_{j,k}$

else

$A_{j,k} = A_{j+1,2k} \cup A_{j+1,2k} + 1$

and

$\Delta_{j,k} = \Delta_{j+1,2k} + \Delta_{j+1,2k+1}$

The main outputs of the algorithm are the selected coefficients $A_{0,0}$ and the discrimination value $\Delta_{0,0}$ that can serve to evaluate the dictionary. With these coefficients, the input signal space can be reconstructed with no lose of information. Nevertheless, we are only interested with the reconstruction of discriminant features for this reason, there is an additional evaluation step in which all spaces in $A_{0,0}$ are arranged according to its $D_{j,k,l}$ value.

RESULTS

Figure 38 displays the reconstruction of 2-year and 3-year class cod otoliths with the four most discriminant bases selected by LDB using the *Daubechies4* wavelet dictionary. Figure 30 shows the power discrimination profile of all selected spaces.

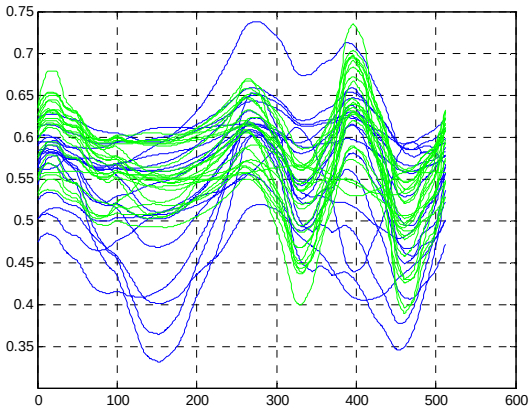

Figure 38: Profile reconstruction of 2-year (blue) and 3-year (green) class otoliths using the four most discriminant bases (red rows in figure 39).

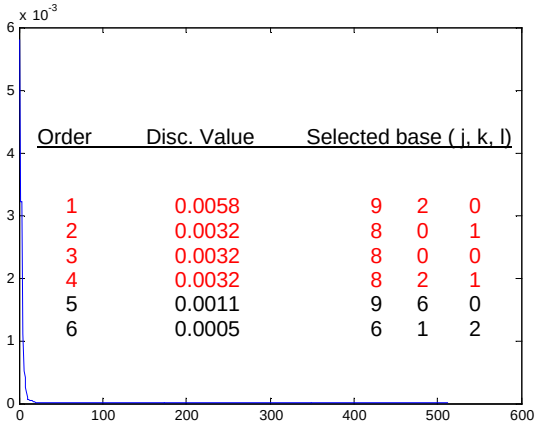

Figure 39: Discrimination profile.

▪ Feature discrimination algorithm following modifications suggested from its evaluation during 2nd. project meeting at month 9

INTRODUCTION

When the class number increases or the input signals contain modulations and other kind of non-linear structures, LDB doesn't perform optimally. In otolith age identification, this scenario occurs when the location of age structures (radial structures in the form of 'peaks' and 'valleys') varies along the intensity profile, even when otoliths are of the same age class. These misalignments affect negatively the process of dimensional reduction since they force the LDB to use more bases to represent each intensity profile.

METHOD

In order to achieve generalisation in front of the otolith non-linear growth with LDB, we use two pre-processing methods before computing LDB: Given a set of intensity profile signals, we study the use of two preprocessing methods for compensating the effects of this non linearity before using LDB.

- 1st method**.** *Intensity profile demodulation* and contrast cancellation

The goal of this method consists in obtain a new representation of the seasonal structures distributed uniformly along the radial before using the LDB. Given the intensity profile *r*, its radial length *l*(*a*) can be expressed as a non-uniform growth rate function that follows an exponential behaviour ϕ, by means of:

$$l = \phi(a) = L_{\infty}\left(1 - e^{-k/a}\right)$$

Where *a* denotes the fish age, and (L_{∞},*k*) are two growth parameters.

To obtain a linear growth law version of the intensity profile we must demodulate r computing $r(\phi^{-1})$ with an optimal (L_∞,k) that yields al almost periodic repetition of the seasonal structures. Since L_∞ represent the longest radial length, it can be set to a normalised value in order to decrease execution time of the optimisation process. In this case, the algorithm measures the signal periodicity in order to find the growth parameter k. To obtain this measure we build a histogram τ_n containing the short-term autocorrelation lags above a fixed threshold and, then, we compute its normalised entropy $H(\tau_n)$ given by:

$$H(\tau_n) = -\frac{1}{\ln(\tau_N)}\sum_{n=1}^{N}\tau_n \ln(\tau_n)$$

where N is used to specify the largest short-term autocorrelation lag, being τ_N the histogram value for this lag. With a demodulated version of the intensity profile, image non-uniform contrast can be removed additionally by means of a *Gaussian* low-pass filter.

- 2nd method. MLDB (or *LDB with customised paraunitary filter banks*)

Although WPT method contains a rich library of wavelet dictionaries which can be used to describe signal features, another option is to consider the inclusion of paraunitary filter banks as new 'customised' wavelet dictionaries in the LDB. The associated LDB using these dictionaries is called MLDB (*Modified Local Discriminant Bases*) since the shape of the wavelet packets is adapted to the tree adjustment. We use this technique to obtain customised filter which is described as follows.

The real coefficients of two-channel paraunitary bank can be obtained by means of:

$$H_i(z) = H_{i0}(z^2) + z^{-1}H_{i1}(z^2) \quad (i = 0,1)$$

where $H_i(z)$ denotes the associated discrete transfer function of the *lowpass* ($i=0$) and *highpass* (i=1) filters; and $H_{i0}(z^2)$, $H_{i1}(z^2)$ are entries obtained from the *polyphase matrix*:

$$H_{pol}(z) = \begin{pmatrix} H_{00}(z) & H_{01}(z) \\ H_{10}(z) & H_{11}(z) \end{pmatrix} = \left(\prod_{k=0}^{K-1}\begin{pmatrix} \cos v_k & \sin v_k \\ -\sin v_k & \cos v_k \end{pmatrix}\begin{pmatrix} 1 & 0 \\ 0 & z^{-1} \end{pmatrix}\right)\begin{pmatrix} \cos v_K & \sin v_K \\ -\sin v_K & \cos v_K \end{pmatrix}$$

where $v_k \in [0,\pi)$ (k= 0,…, K-1) being k the coefficient index of the FIR filters of order $2K$+1, and v_K is obtained computing the residue $\pi/4 - \sum_{k=0}^{K-1} v_k$ modulo 2π in $[0,2\pi)$.

Assuming this scenario, the space:

$$P^K = \{v = (v_0,...,v_{K-1}) : v_k \in [0,\pi)\}$$

serves to parameterise two-channel filter banks where each angle vector $v \in P^K$ defines a different dictionary. The discriminatory power of the dictionary is given by $\Delta_{0,0}(v)$ computed by LDB. Thus, the MLDB is obtained estimating v by means of :

$$\hat{v} = \arg\max_{v \in P^K} \Delta_{0,0}(v)$$

In order to search $\hat{v}$, we use a discretized parameter space N of the form:

$$P_K^N = \left\{ \left(\frac{\pi}{N} (i_0, ..., i_{K-1}) : i_k \in (0, ..., N-1) \right) \right\}$$

If parameters K and N are of moderate size, (e.g. K=2, N=10) this method is suitable for (1D data) like the otolith intensity profiles considered in this project.

RESULTS

Figure 40 shows the LDB results with 74 otoliths ageing from one to five years, using the best standard wavelet dictionary (*Biorthogonal3.1*). It can be seen that, it is impossible to distinguish class singularities even though the 7 most discriminant bases of this dictionary were used in the reconstruction process (see 3-year and 4-year class reconstructed profiles in 31. c) and 31. d)).

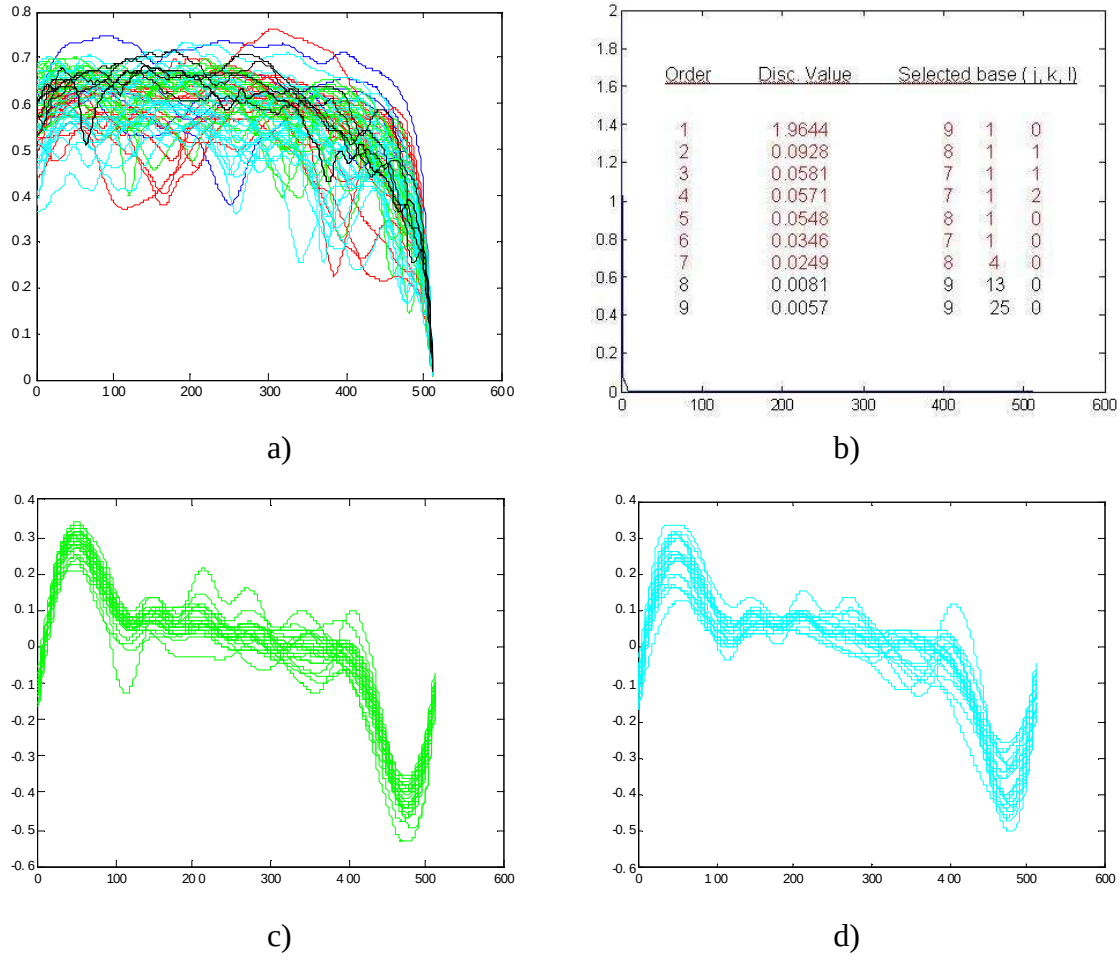

Figure 40: ***LDB using original intensity profiles from 74 otoliths of 1-year*** **(blue),** ***2-year*** **(red),** ***3-year*** **(green),** ***4-year*** **(cyan)** ***and 5-year*** **(black)** ***class.*** **a) Original profiles, b) Dictionary discrimination profile with the 9 most discriminant bases. c) and d) Profile reconstruction of 3-year and 4-year otoliths, only, using 7 most discriminant bases (red rows in b)).**

In order to study this poor performance of LDB we consider the removal of contrast and growth non-linearities. We process data, cancelling out these two effects, manually. We consider two cases: 1) – Contrast removal (or *detrending*); and 2) – Both detrending and growth removal. It can be seen that not only the discriminant values of selected bases increase (37.75: Case 1, and 92.72: Case 2, see Table 6) but also seasonal structures can be distinguished in every year class (Figure 32), which demonstrates that the performance of LDB can improve if input data is 'detrended' and 'demodulated' previously by using automated techniques, such as the one explained in method 1.

So next, we pre-process all intensity profiles with method 1 before passing them through LDB (see Figure 38). In this case, it can be seen in Table 6 a much higher discriminant value than using the original radials (45.38 – Method 1; 1.96 - Original radials). Additionally, one can appreciate when using automated pre-processing methods for detrending and demodulation, $\Delta_{0,0}$ value goes towards the same value using manual methods ($\Delta_{0,0}$ = 92.72) which indicates certain improvement in the feature extraction process performed by LDB

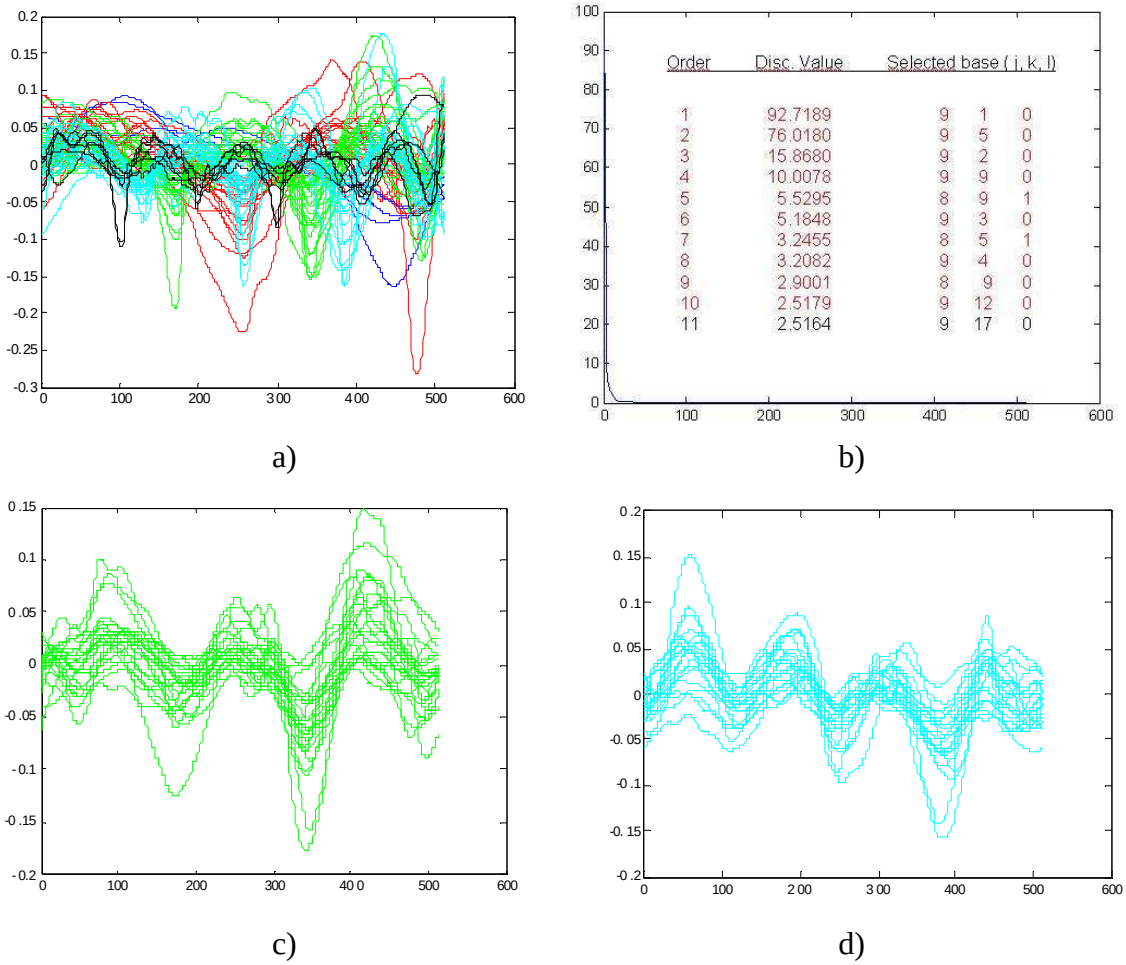

Figure 41: LDB after 'detrending' and 'demodulating original intensity profiles'. a) Pre-processed profiles, b) Dictionary discrimination profile with the 11 most discriminant bases. c) and d) Profile reconstruction of 3-year and 4-year otoliths, only, using 10 most discriminant bases (red rows in b)).

Table 6: LDB comparison of different pre-processing methods.

Processing Type	Pre-processing	Best dictionary	$\Delta_{0,0}$
Manual	Original signals	Bior.3.1	1.96
	1)	Reverse Bior.3.1	37.75
	2)	Bior.3.1	9.78
	1) and 2)		92.72
Automated	1)		19.95
	2)		3.76
	1) and 2)		45.38

1. Trend extraction
2. Growth extraction (Method 1)

▪ Statistical learning algorithm for automated fish ageing

INTRODUCTION

The statistical learning algorithm consists in a chain of image and signal processing steps, developed 'adhoc' in the frame of this project, and a classifier that estimates the age class of a given otolith sample image.

The preprocessing steps basically try to improve the classification performance, by highlighting those parts of the otolith images that carry information about the annual structures and discarding other regions of the image that could lead to confusions. To build the classifier we need two phases: learning and test. The learning procedure quantizes the information brought by the features of each calibration otolith and creates codevectors (arrays of features). These codevectors are representatives of each class, and to choose the age class of a given test sample, one needs to compute the distance between the features of the sample and those of all the codevectors. The class of the most similar codevector is assigned to the otolith under test.

METHOD

The design of the classifier uses all the preprocessing methods created in this project and a Learning Vector Quantization method. Creates calibration and production sets, in a random manner, to test the performance of the preprocessing and statistical learning methods and to adjust the parameters.

Namely, the steps for each test are:

Radial Extraction

- Preprocess the otolith images to extract the intensity profile of the radials
  1.1. Background substraction
  1.2. *Nucleus* detection
  1.3. Enhance the image using Advection/Diffusion
  1.4. Extract radials at 3 angular sectors
- Nonlinear growth demodulation
  2.1. Compute the parameters using the marks from the experts
  2.2. Use a median value for the sector radials
  2.3. Compute the parameters adaptively
  2.4. Demodule using a median value and module using a random set of parameters that follow the same distribution obtained in 2.1.

Classifier construction

- Choose randomly a calibration and production set for the species used as study cases.
- Compute Local Discriminant Bases (LDB) for the calibration set.
- Project the intensity profiles of the production set on the LDB.
- Create a training set with the coefficients of the calibration otoliths and their ages (as estimated) by experts.
- Train the Codebook to learn the Codevectors
- Test the accuracy of the classifier, using the production set coefficients.

All the steps are implemented in Matlab and C, using the functions created specifically for the AFISA library and public domain functions to build the classifier. Lately, the definite version of the classifier (Deliverable 2.4.d.) will use only functions created in AFISA project.

For each species we have created a Matlab script that implements the steps mentioned above and serve to compute the best combination of methodologies and set the needed parameters.

The common version of the basic script is as follows:

```
% Matlab Script to test the Preprocessing part and classification methods
% in AFISA Project.

% Vicenç Parisi / Jose Antonio Soria, UPC


%%%%%%%%%%%%%%%%%%%%%%%%%%%%%%%%%%%%%%%%%%%%%%%%%%%%%%%%%%%%%%%%%%%%%%%%%%%%%%%%
% Folder with the signals

RADIALS_DIR='';   % Set to the folder that contains the radials

% Name extension of the files to be processed

% Choose between:
% 'rip': Radial Intensity Profiles
% 'rip.ide': Demodulation with the iid files
% 'rip.ade': Adaptive Demodulation

EXTENSION = 'rip';
xiidfiles = dir('*.iid'); % The iid files contain the experts readings

%%%%%%%%%%%%%%%%%%%%%%%%%%%%%%%%%%%%%%%%%%%%%%%%%%%%%%%%%%%%%%%%%%%%%%%%%%%%%%%%
% Age classes:  Set sminage and smaxage to the Min and Max age classes
%               For example, to use 2-,3,4 and 5+

sminage = 2;
smaxage = 5;

%%%%%%%%%%%%%%%%%%%%%%%%%%%%%%%%%%%%%%%%%%%%%%%%%%%%%%%%%%%%%%%%%%%%%%%%%%%%%%%%
% Parameters

sNSamples = 512;;       % Number of samples per radial
snc = 64;      % Number of radial coeffitients to use;

saw = 20;               % Width of the angular sectors
rsa =[000 090 180];     % This is the central angle of the angular sector
rsaSTR =['000' ; '090' ; '180']; % Last part of the name of the files

sntrials = 10; % Number of classifications to do:
sn_test = 10;  % Number of test files (per age group) to be used


%%%%%%%%%%%%%%%%%%%%%%%%%%%%%%%%%%%%%%%%%%%%%%%%%%%%%%%%%%%%%%%%%%%%%%%%%%%%%%%%
% CODE
%%%%%%%%%%%%%%%%%%%%%%%%%%%%%%%%%%%%%%%%%%%%%%%%%%%%%%%%%%%%%%%%%%%%%%%%%%%%%%%%

rl = [0:1/(sNSamples-1):1];
xaccuracy =[];
rage = [];
xr_000 = [];
xr_090 = [];
xr_180 = [];
rip_used = [];

%%%%%%%%%%%%%%%%%%%%%%%%%%%%%%%%%%%%%%%%%%%%%%%%%%%%%%%%%%%%%%%%%%%%%%%%%%%%%%%%
% LDB + LVQ
%%%%%%%%%%%%%%%%%%%%%%%%%%%%%%%%%%%%%%%%%%%%%%%%%%%%%%%%%%%%%%%%%%%%%%%%%%%%%%%%
% Fill the matrices that contain the radials for each sector

sniidfiles = length(xiidfiles);
sid =0;
for si=1:sniidfiles

    fnom_000 = [xiidfiles(si).name(1:end-4),'_a_000',EXTENSION];
    fnom_090 = [xiidfiles(si).name(1:end-4),'_a_090',EXTENSION];
    fnom_180 = [xiidfiles(si).name(1:end-4),'_a_180',EXTENSION];
```

```
     rip_used = [rip_used si];
     sid = sid+1;
     rage = [rage read_iid_age([xiidfiles(si).name])];

     rr = load(fnom_000);
     xr_000= [ xr_000 , rr'];

     rr = load(fnom_090);
     xr_090= [ xr_090 , rr'];

     rr = load(fnom_000);
     xr_180= [ xr_180 , rr'];
end

%%%%%%%%%%%%%%%%%%%%%%%%%%%%%%%%%%%%%%%%%%%%%%%%%%%%%%%%%%%%%%%%%%%%%%%%%%%%%%%%%%%%
% Set the age class, between sminage and smaxage

rage(find(rage < sminage))=sminage;
rage(find(rage > smaxage))=smaxage;
rclass = rage - sminage + 1;
cages = rclass';

%%%%%%%%%%%%%%%%%%%%%%%%%%%%%%%%%%%%%%%%%%%%%%%%%%%%%%%%%%%%%%%%%%%%%%%%%%%%%%%%%%%%
% Compute the Local Discriminant Bases using a Daubechies 4 mother wavelet
% xip_s is a cell containing the coefitients of the Intensiry Profiles


 xr_000=(resample(xr_000,snc,512))';
 xr_090=(resample(xr_090,snc,512))';
 xr_180=(resample(xr_180,snc,512))';

 [Bspaces_000 D_Ranking]=f_mlldb2(xr_000,rclass,9,'Std','c_db4');
 [Bspaces_090 D_Ranking]=f_mlldb2(xr_090,rclass,9,'Std','c_db4');
 [Bspaces_180 D_Ranking]=f_mlldb2(xr_180,rclass,9,'Std','c_db4');

 xip_000=(Bspaces_000(:,5:end))';
 xip_090=(Bspaces_090(:,5:end))';
 xip_180=(Bspaces_180(:,5:end))';

 xip_s(:,:,1)=xip_000;
 xip_s(:,:,2)=xip_090;
 xip_s(:,:,3)=xip_180;


%%%%%%%%%%%%%%%%%%%%%%%%%%%%%%%%%%%%%%%%%%%%%%%%%%%%%%%%%%%%%%%%%%%%%%%%%%%%%%%%%%%%
% Perform n trials

for strial = 1:sntrials

    xip_test_files = {};
    xno = {};
    xclass = [];
    sin = 0;

    % Choose randomly a training and test set
    for sage = min(cages):max(cages)
        r_age = (find(cages==sage));
        sl=length(r_age);
        rrpsl = randperm(sl);
        xno{sage} = rrpsl;
        for si = 1:sn_test
            sin = sin +1;
            xip_test_files{sin,1}=xiidfiles(rip_used(r_age(rrpsl(si)))).name;
            sfage = read_iid_age(xip_test_files{sin,1});
            if sfage < sminage
                sfage = sminage;
            elseif sfage > smaxage
                sfage = smaxage;
```

```
        end
        xip_test_files{sin,2} = sfage;
        if sfage ~= (sage+sminage-1)
            disp('Error in radial selection');
            return;
        end
    end
end

% Test the radials at each sector
for ss = 1:3
    xip = xip_s(:,1:snc,ss);
    xip_age = [xip cages];
    sdim = length(xip(1,:));
    sn_vectors = length(xip(:,1));

    xip_test=[];
    xip_train=[];
    xip_test_R = [];
    sin = 0;
    cages_R = [];

    for sage = min(cages):max(cages)
        r_age = (find(cages==sage));
        xip_a = xip_age(r_age,:);
        sl=length(r_age);
        rno = xno{sage};
        for si = 1:sn_test
            xip_test=[xip_test ; xip_a(rno(si),:)];
        for si = sn_test+1:sl
            xip_train=[xip_train ; xip_a(rno(si),:)];
        end
    end
    xr_test = xip_test(:,end);
    xr_test_DTW = xip_test(:,end);

    % Save the training and test set in files for the LVQ routines

    save(['xip_test_',rsaSTR(ss,:),'.txt'],'xip_test','-ASCII');
    save(['xip_train_',rsaSTR(ss,:),'.txt'],'xip_train','-ASCII');
    sl_test = length(xip_test(:,1));
    sl_train = length(xip_train(:,1));

    fid = fopen('.\xip_test.txt','wt');
    fprintf(fid,'%d \n',sdim);
    for si = 1:sl_test
        for sj = 1:sdim
            fprintf(fid,'%3.8f \t',xip_test(si,sj));
        end
        fprintf(fid,'%d \n',xip_test(si,sdim+1));
    end
    fclose(fid);

    fid = fopen('.\xip_train.txt','wt');
    fprintf(fid,'%d \n',sdim);
    for si = 1:sl_train
        for sj = 1:sdim
            fprintf(fid,'%3.8f \t',xip_train(si,sj));
        end
        fprintf(fid,'%d \n',xip_train(si,sdim+1));
    end
    fclose(fid);

    %%%%%%%%%%%%%%%%%%%%%%%%%%%%%%%%%%%%%%%%%%%%%%%%%%%%%%%%%%%%%%%%%%%%%%%%%%%%%%%%%
    % Perform Learning Vector Quantization

    % Compute an initial codebook
    disp(['Creating LVQ Codebook for Radial at sector ',num2str(ss)]);
```

```
        !c:/lvq_pak-3.1/elimin -din xip_train.txt -cout xip_train_e.txt -knn 10 -v 0
         [xip_train_e,sdim] = fReadDataFile('xip_train_e.txt');
         save(['xip_train_e_',rsaSTR(ss,:),'.txt'],'xdata','-ASCII');
         !c:/lvq_pak-3.1/eveninit -din xip_train_e.txt  -cout xip.cod -noc 100 -v 0
         !c:/lvq_pak-3.1/mindist  -cin xip.cod -v 0
         !c:/lvq_pak-3.1/balance  -din xip_train_e.txt  -cin xip.cod  -cout
          xip_bc.cod -v 0

         % Train the codevectors
         disp('Training the LVQ Codevectors');
         !c:/lvq_pak-3.1/lvqtrain -type lvq1  -din xip_train_e.txt  -cin xip.cod
          -cout xip_o.cod -rlen 10000 -alpha 0.05 -v 0

         % Compute the classification performance
         disp('Computing classification performance');
         !c:/lvq_pak-3.1/classify  -din xip_test.txt -cin xip_o.cod -dout
          dataires.clf -cfout resultat.clf -v 0

          % Save Codebook for each sector
         [xip_codebook,sdim] = fReadCodebook('xip_o.cod');
         save(['CodeBook_',rsaSTR(ss,:),'.cod'],'xip_codebook','-ASCII');

         %%%%%%%%%%%%%%%%%%%%%%%%%%%%%%%%%%%%%%%%%%%%%%%%%%%%%%%%%%%%%%%%%%%%%%%%%%%%
         % Accumulate the classification performance

         cres = load('./resultat.clf');
         xr_test = [xr_test cres];
         xclass = [xclass cres];


     end

     % Once each sector is classified, let's figure out the exactitude
     xMclass = median(xclass,2);
     sb = 0;
     slt = length(xMclass);
     for sp = 1:slt
         xip_test_files{sp,3} = xMclass(sp)+sminage-1;
         if (xMclass(sp)+sminage-1)==xip_test_files{sp,2}
             sb = sb+1;
             xip_test_files{sp,4} = 'B';
         else
             xip_test_files{sp,4} = 'KK';
         end
          xip_test_files{sp,5} = xMcorr(sp)+sminage-1;
     end
     sexac = sb/slt * 100;
disp(['Mean Exa LVQ: ',num2str(smexac), 'Mean Exac kNN: ',num2str(smexac_e)]);

%%%%%%%%%%%%%%%%%%%%%%%%%%%%%%%%%%%%%%%%%%%%%%%%%%%%%%%%%%%%%%%%%%%%%%%%%%%%%%%%%%%
%% End
```

RESULTS

The evaluation of the preliminary design of the statistical learning algorithm has been done using a dataset of North Sea Plaice otoliths that belong to the 3rd quarter. The age histogram of the dataset is shown in figure 42

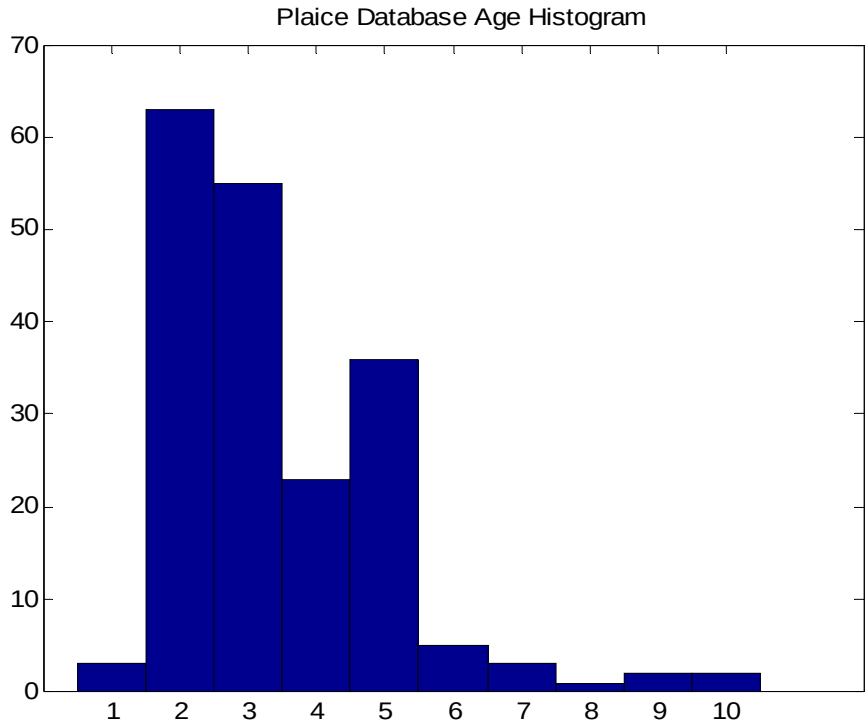

Figure 42: Histogram of the plaice database

Given that age distribution we decided to use age classes 2- to 5+, in order to have a more homogeneous number of otoliths/age.
From each otolith we extracted 3 radials, at the sectors corresponding to 0, 90 and 180º (counter clockwise), with an angular width of 10º. Each radial is the median of 10 radials distributed uniformly in the angular sector. All the radials have been finally resampled to 512 points.
For each radial we compute a growth demodulated version, using various approaches to estimate the growth law parameters ($l(t) = L - (L - Lo) \exp(-kt)$) (We assume $Lo = 0$) :

- Compute the parameters using the marks from the experts, for each radial
- Use a median value for all the radials
- Compute the parameters adaptively
- Demodule using a median value and module using a random set of parameters that follow the same distribution obtained in 2.1.

The distribution of parameters and median values appear in figure 43

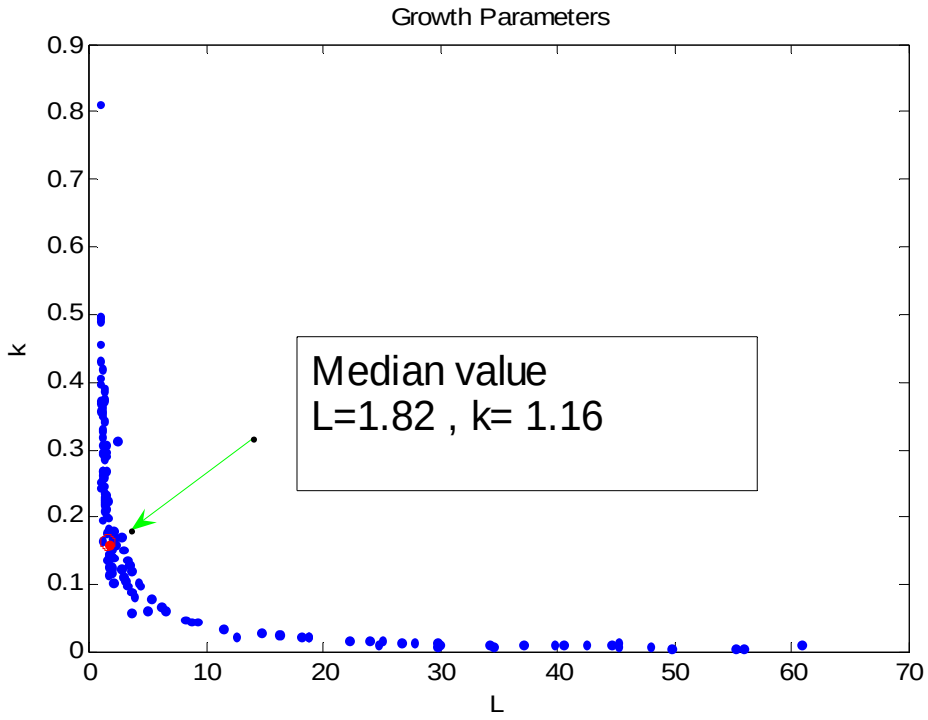

Figure 43: Distribution of the growth parameters (Von Bertalanffy function) for the NS Plaice dataset.

We did, for each approach, 100 trials, and at each instance we randomly chose 10 otoliths per age class, to be used as test set. The other otoliths were the training set.

First, to have a reference of the best results that we can achieve, we worked with the set of radials, at the angular sector used by the experts. This information is available at the '.iid' files associated to each otolith. Besides, these radials growth law can be directly computed from the annual growth marks, and the first 64 LDB coefficients, retain most of the discriminant information. With this conditions, the classifier gave an 82% of accuracy for this data, but this is an ideal case, since we do not have normally this information, for the production set. Thus, we compute the adaptive demodulation of the radials and, after several runs of the test, we have never been able to obtain more than 65% of accuracy. The demodulation with a median value or the demodulation/modulation strategy, to artificially increase the dataset, gave always worse results.

After these results, it seemed reasonable to conclude that the misalignment of the annual structures in the radials, due to differences in growth, affects negatively both the LDB algorithm, that is non invariant to translation, and the measurement of the distance between a radial and a codevector. The adaptive demodulation is not capable to fix this non linearity in a satisfactory amount. On the other hand, the projection of the radials onto a 2 dimensional space, using the Sammon mapping, revealed that the features are very mixed, and that is difficult to find clusters of data for each class. This might also pose problems to the vector quantization algorithm, when it tries to compute a set of codevectors representative of each class.

Under these circumstances, we propose an alternative classification method, based on the k-nearest neighbours scheme and a signal warping algorithm to counter effect the differences in growth. The classifier and its evaluation are reported in Deliverable 2.4.d.

- **Statistical learning algorithm for automated fish ageing, following modifications suggested from its evaluation during the 3rd project meeting at month 17**

This report contains the code for the final version of the statistical learning algorithm, following the modifications suggested after the initial tests, with a database of plaice otoliths.

The main modification consists in the use of a warping function and a nearest neighbour classifier, due to the difficulties to automatically demodulate the non linear growth effects and to find age clusters that pose bounds to the performance of other classification schemes (neural networks as learning vector quantization or support vector machunes).
All the steps are implemented in Matlab and C, using the functions created specifically for the AFISA library, and available at the afisa_tnpc8 suite of functions.

The principal function is 'EstimateAge'. It loads the otolith image , performs the preprocessing steps, extracts the radials and searches the most similar exemplars in the CodeBooks created ad-hoc for each species (year and quarter). These codebooks are ASCII files containing a set of exemplar radials that we call codevectors, with the age estimated by expert reader. Each row of the file contains a codevector, and the last column is the age class.

```
Codevector_1 Age_1
Codevector_2 Age_2
Codevector_3 Age_3
   ...       ...
```

Once the radials to be classified are extracted, for each angular sector, EstimateAge calls to function '`fDTW_kNN'`. The function name is the acronym for 'Function Dynamic Time Warping and k Nearest Neighbours'. It warps the radial to all the codevectors in the codebook and then computes their normalized cross correlation. Finally it sorts the codevectors to find the 'k' most correlated ones. The estimated age for a given radial in an angular sector is the median age of these k nearest codevectors, and the estimated age of the otolith is the median of the ages of all the sectors.

Below you can find the most important functions of the statistical learning algorithm:

1) age=EstimateAge(imagename, level , light) (Matlab)
2) [sclass] = fDTW_kNN(xCodeBook,rrdp,snknn) (Matlab)
3) void **fDTW_C** (double *d, double *P, double *D, double *R, double *T, long LR, long LT) (C Language)

```
function age=EstimateAge( imagename, level , light)
%
% Return the estimated age of an otolith image
% Inputs:
% - imagename:  name of the otolith image
% - level:      level for the background subtraction algorithm (between 0
%               and 1). The value of level depends on the stock an also on
%               the image acquisition settings.
%
% Ouput:
% - age:        the estimated age of the fish
%
%  Ifremer/UPC
%

% -- Initialisation and default parameters --
age=0;                  % Initialise age to 0
radius=10;              % Default parameter for background subtraction
sNSamples = 512; % Number of samples per intensity profile
rsa =[0 90 180]; % This is the central algle of the angular sector
rsaSTR = ['000' ; '090' ; '180'];
saw = 20; % This is the witdh of the angular sector
snc = 64; % This is the number of LDB or signal components used
snknn = 10; % Number if nearest neighbours to compute


%%%%%%%%%%%%%%%%%%%%%%%%%%%%%%%%%%%%%%%%%%%%%%%%%%%%%%%%%%%%%%%%%%%%%%%%%%%%%%%%%%

xclass = []; % Empty matrix to hold the classification of each sector

% Load the codebooks for the otolith species
for sai = 1:length(rsa)
    CCodeBook{sai} = load(['CodeBook_',rsaSTR(sai,:)],'-ASCII');
end

%%%%%%%%%%%%%%%%%%%%%%%%%%%%%%%%%%%%%%%%%%%%%%%%%%%%%%%%%%%%%%%%%%%%%%%%%%%%%%%%%%
% Main code

image = loadImage( imagename );

% -- Pre-processing step --
% Compute background subtraction
mask = BackgroundSubtraction3(image, level, radius);

% Align the image and the mask to its principal axes
[image_PA, xMPA, yMPA] = RotateImageToPrincipleAxis(image,mask);
[mask_PA, xMPAm, yMPAm]  = RotateImageToPrincipleAxis(mask, mask);

% Estimate otolith nucleus position (same in original image than in image
% in the principle axis)
nuc=computeNucleusImage(image);
[sxn syn]=findNucleusInNucleusImage(nuc,mask);

% Transform to uint8 data type
image_PA=uint8(image_PA);
mask_PA=uint8(mask_PA);
```

```
% Extract border, beginning at the [rightmost, yMPA] pixel location
[rir,ric]=find(mask_PA);
rirr = find(rir == round(yMPA));
xdummy=[ric(rirr),rir(rirr)];
[smx,sim] = max(xdummy(:,1));
smy = xdummy(sim,2);
xbt= bwtraceboundary(mask_PA,[smy,smx],'N',8,Inf,'counterclockwise');
cx = xbt(:,2);
cy = xbt(:,1);

% Compute orientation field (can be replaced by a more advanced method later)
orientation_PA = SimpleOrientation( image_PA );

% Compute Advection-Diffusion algorithm
advection_PA = AdvectionDiffusion(image_PA,sxn,syn,mask_PA,orientation_PA,cx,cy');

% Compute the angle of each contour point in xbt
cbta = 180/pi * atan2(syn-xbt(:,1),xbt(:,2)-sxn);
icbta = find(cbta < 0);
cbta(icbta)=cbta(icbta)+360;
xbt_pa = [xbt cbta];

% Process each radial
for sai = 1:length(rsa)
    sa = rsa(sai);
    % Extract the radial
    [rr,rixb] = fExtractRadialSector(advection_PA,sxn,syn,xbt_pa,sa,saw,sNSamples);
    % Resample to the chosen number of coefficients (snc)
    rrdp = resample(rr,snc,sNSamples);
    % Classify the radial
    xCodeBook = CCodeBook{sai};
    [sclass] = fDTW_kNN(xCodeBook,rrdp,snknn);
    xclass = [xclass sclass];
end

% The result is the median of the classes at each sector
age = median(xclass,2);
```

%%

```
function [cr] = fDTW_kNN(xip_codebook,xIP,sknn)
%
% Return the estimated age class of an intensity profile
% Inputs:
% - xip_codebook: CodeBook of Intensity Profiles
% - xIP: Intensity Profile to estimate the age
%
% Ouput:
% - cr:        the estimated age class
%
%  Ifremer/UPC


snCodeVectors = length(xip_codebook(:,1));
sdim = length(xip_codebook(1,:)) - 1;
cdiff =[];

for si = 1:length(xIP(:,1))
    rr = xIP(si,1:sdim);
    for sj = 1:snCodeVectors
        [sd,rP,rc] = fDTW_C(rr,xip_codebook(sj,1:sdim));
        cdiff=[cdiff;(1-1/sdim*((rr-mean(rr))*(rcmean(rc))')/(std(rr)*std(rc)))];
```

```
    end
    [Y,I] = sort(cdiff);
    cclasses = xip_codebook(I(1:sknn),sdim+1);
    cr(si,1) =  floor(median(cclasses));
    cdiff = [];
end
```

%%

```
/*****************************************************************************/
/* This is a MEX file that implements the Dynamic Time Warping */
/* To compile it, type mex fDTW_C.c at the matlab command window prompt */
/* To execute, use it as a conventional matlab function: [d,rP] = fDTW_C(rR,rT) */


/* Author: Vicenç Parisi */
/* Date: 12/12/08 */

/*****************************************************************************/
#include "matrix.h"
#include "mex.h"
#include <math.h>

#define BIG_VALUE 1e30

void fDTW_C(double*d,double *P,double *D,double *R,double *T,long LR,long LT);
double *Alloc_1_Double(long d0);
double **Alloc_2_Double(long d0, long d1);
void *Allocate_Something(long hm);
void Free_1_Double(double *f);
void Free_2_Double(double **f, long d0);

/*****************************************************************************/
void fDTW_C(double *d,double *P,double *D,double *R, double *T, long LR, long LT)
{
    double **g,**t, g1,g2,g3,dl;
    long i,j,ir,it,iw;
    int old_path, old_path_2, old_path_3;
    short ts;

    g=Alloc_2_Double(LT+1, LR+1);
    t=Alloc_2_Double(LT+1, LR+1);

    for (i=1; i<=LR; i++) g[0][i]=BIG_VALUE;
    for (i=1; i<=LT; i++) g[i][0]=BIG_VALUE;
    g[0][0]=0.0;

    /*********************************************************/
    /* Compute cumulated distances */
    for (i=1; i<=LT; i++) {
        for (j=1; j<=LR; j++)  {
            dl=(double)pow((T[i-1]-R[j-1]),2.0);
            g2=g[i-1][j] + dl;
            g3=g[i][j-1] + dl;
            g1=g[i-1][j-1] + dl;
            if (g1 <= g2 && g1 <= g3) {
                g[i][j] = g1;
                t[i][j] = 1.0;
            }
            else
                if (g2 < g3) {
                    g[i][j] = g2;
                    t[i][j] = 2.0;
                }
```

```
                else {
                    g[i][j] = g3;
                    t[i][j] = 3.0;
                }
            }
        }
        /*************************************************************/
        /* Compute the path */
            ir=LR; it=LT;
            P[ir-1] = (double)(it-1);
            old_path   = 1;
            old_path_2 = 0;
            old_path_3 = 0;

            while ((it + ir > 2) && (it > 1) && (ir > 1)) {
                ts = (short)(t[it][ir]);
                switch (ts) {
                    case 1: it--; ir--; old_path=1; old_path_2=0; old_path_3=0; break;
                    case 2: if ((old_path == 2) && (old_path_2==2))
                    {
                        it--; ir--; old_path_2=0; old_path_3=0 ; old_path=1;
                    }
                    else
                    {
                        it--; old_path_2++; old_path_3=0; old_path=2;
                    }
                    break;
                    case 3: if ((old_path == 3) && (old_path_3==3))
                    {
                        it--; ir--; old_path_2=0; old_path_3=0; old_path=1;
                    }
                    else
                    {
                        ir--; old_path_3++; old_path_2=0; old_path=3;
                    }
                    break;
                }
                P[ir-1] = (double)(it-1);
            }
            for (j=ir;j>=1;j--) P[j-1] = P[ir-1];
            P[LR-1] = (double)(LT-1);

        /*************************************************************/

        dl=0.0;
        for (i=0; i< LR; i++)
        {
            iw = (long)P[i];
            dl+=pow((T[iw]-R[i]),2.0);
            D[i] = T[iw];
        }
        dl=(double) sqrt(dl) * 1/LR ;

        *d = dl;

        Free_2_Double(g, LT+1);
        Free_2_Double(t, LT+1);

}

/*****************************************************************************/

double *Alloc_1_Double(long d0)
{
   double *f;
   f=(double*)Allocate_Something(d0*sizeof(double));
   return (f);
}
```

```
double **Alloc_2_Double(long d0, long d1)
{
   long i;
   double **f;
   f=(double**)Allocate_Something(d0*sizeof(double*));
   for (i=0; i<d0; i++) f[i]=Alloc_1_Double(d1);
   return (f);
}

void *Allocate_Something(long hm)
{
   void *ptr;
   if ( (ptr=malloc(hm)) == NULL )
   {
      fprintf(stderr,"\n!!! Problem of allocation of %ld elements - EXITING
!!!\n\n",hm);
      fflush(stdout); exit(1);
   }
   return(ptr);
}

void Free_1_Double(double *f)
{
   free (f);
}
void Free_2_Double(double **f, long d0)
{
   long i;
   for (i=0; i<d0; i++) Free_1_Double(f[i]);
   free (f);
}
/*****************************************************************************/

void mexFunction(int nlhs, mxArray *plhs[], int nrhs, const mxArray *prhs[])
{
    double *d,*P,*R,*T,*D;
    long LR,LT;

    LR =  (long)mxGetN(prhs[0]);
    LT =  (long)mxGetN(prhs[1]);

  /* Create matrices for the return arguments */

    plhs[0] = mxCreateDoubleMatrix(1, 1, mxREAL);
    d = mxGetPr(plhs[0]);

    plhs[1] = mxCreateDoubleMatrix(1, (int)LR, mxREAL);
    P = mxGetPr(plhs[1]);

    plhs[2] = mxCreateDoubleMatrix(1, (int)LR, mxREAL);
    D = mxGetPr(plhs[2]);

  /* Assign pointers to each input*/

     R = mxGetPr(prhs[0]);
     T = mxGetPr(prhs[1]);

  /* Call the subroutine. */

     fDTW_C (d, P, D, R, T, LR, LT);
}
```

▪ Mixture model for age structure estimation and software integration of the developed automated ageing systems

Introduction

Data from the English Ground Fish Surveys (EGFS) 1998-2001 were analysed. For each year the surveys took place in August/September. For all surveys the age was read, the length of the fish and the weight of the otoliths were measured and recorded. Hence the samples must be regarded as random samples representing the general distribution of fish in the North Sea of age, length and otolith weight at the time of the sampling. As the distribution among hauls varies, it is important that sufficiently many samples (hauls) are taken to cover the total population.

The annual numbers of hauls available for 1998-2001 are 391, 314, 395 and 417 for 1998-2001 respectively. Data are summarized in figure 44 showing that there is a close relationship between length and otolith weight. For ages larger than zero and for the age range considered (age groups less than 6 years) the relationship seems to be linear. The correlation is about 0.97 for each year. Hence, besides the fish length the otolith weight does not seem to contain much information about the age due to the close relationship between the two quantities.

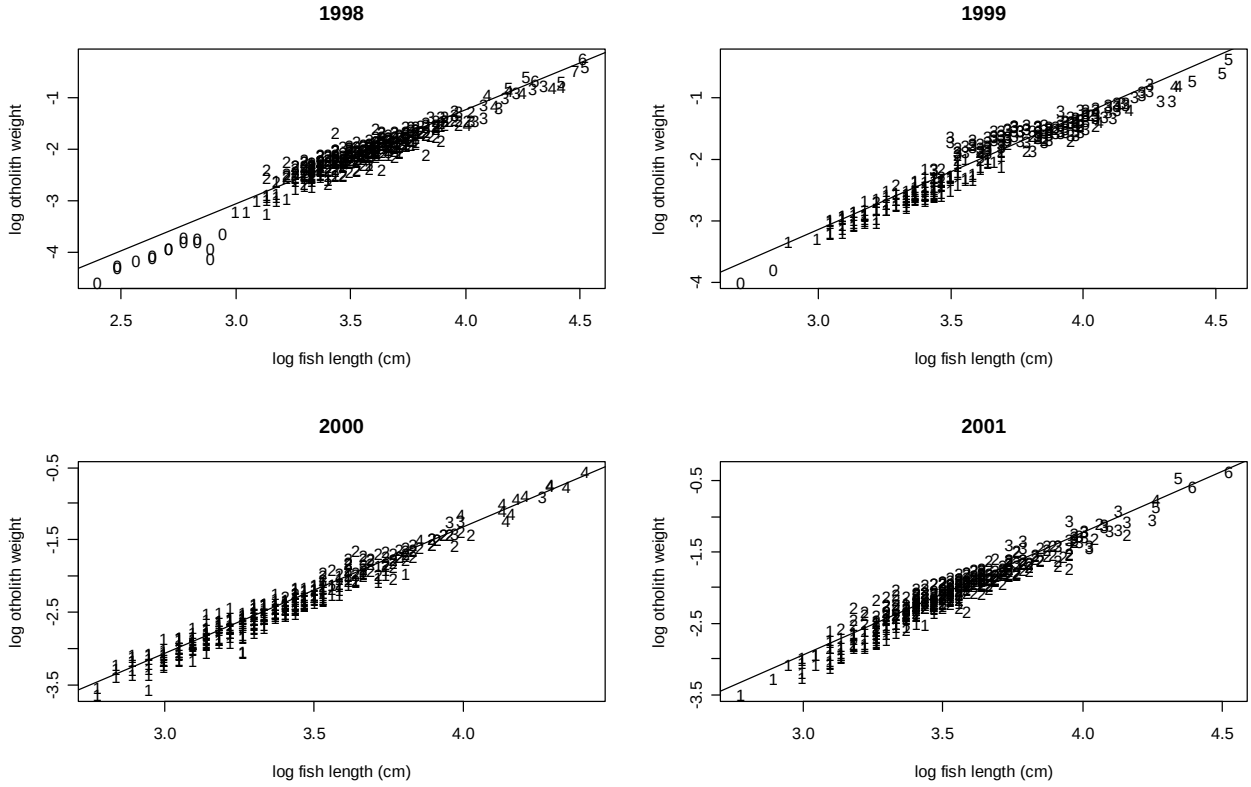

Figure 44. The relationship between age, log fish length and log otolith weight for EFGS survey data 1998-2001. The numbers on the plots indicate the age while the lines indicate the linear regression lines.

Method

A method using discriminant analysis was considered to estimate the unknown age distribution in a production sample including covariates as fish length and otolith weight

based on a calibration sample for which age as well as covariates are known. In the following the method is described for the random sample case using the EFGS data available. To test the goodness of the method data for each year were divided into two equal parts using one part as calibration and the other part as production sample. For the calibration sample the linear discriminant analysis procedure, the R packages, lda and predict.lda (Venable & Ripley 2002; R Development Core Team 2008), was used to predict the posterior probabilities

$P(A_i = a \mid (L_i, W_i)$ a = (0,1,…,maximum age)

where

A_i, L_i and W_i denotes the age, the fish length and the otolith weight respectively of fish number "i".

The age composition in the production sample simply was estimated by the averages

$$\frac{1}{n}\sum_{i=1}^{n} P(A_i = a \mid (L_i, W_i)$$ a = (0,1,…,maximum age)

The estimated age composition was compared to the true age composition. This cross-validation procedure was repeated 500 times and the variance of the age composition was calculated. The mean is not calculated as the procedure is non-biased and hence the mean close to zero.

Results

As an example results for 2001 are given in table 3 showing the 95% confidence limits of the estimated age composition:

Table 7: Upper and lower 95% confidence limits for estimated age composition.

Age	Lower 95% confidence limit	Upper 95% confidence limit
1	0.17	0.27
2	0.65	0.77
3	0.02	0.09
4	0	0.01
5	0	0.02
6	0	0.02

The estimation procedure will be given as an R function.

References

Venables, W. N. & Ripley, B. D., 2002. Modern Applied Statistics with S. Fourth edition. Springer.

R Development Core Team, 2008. R: A language and environment for statistical computing. R Foundation for Statistical Computing, Vienna, Austria. ISBN 3-900051-07-0, URL http://www.R-project.org.

- **Conditional model for age structure estimation from global otolith features and physical fish characteristics**

Principle and Method

For each species, the material is composed of a set of fish for which we have the age estimated by an expert reader and a set of measurements coming from physical fish characteristics (fish length, fish weight,…), global otolith features (otolith weight,…) and otolith shape information extracted automatically from the otolith image (otolith area, major axis length,…). In the following, we will consider the age estimated by expert reader as the ground truth and we will use it for training and estimate the validity of our method.

The goal of the conditional model is to estimate the age structure of a fish set for which the set of measurements is available for the whole data set and the age estimated by expert is only available for a part of this set. The aged samples are used as training set and the others as testing set.

To build a conditional model framework, we first compute the mean distance of a test sample to the k-nearest neighbours of each class (figure 45). The distance is computed using an Euclidean distance in the normalised feature space. The nearest neighbours are chosen among the training samples. For each sample s_i of the testing set we now have a set of distance $d_{i,j}$ to each class:

$$s_i \rightarrow \{d_{i,j}\} \text{ with } i \in \{1,...,ns\} \text{ and } j \in \{1,...,nc\}$$

where ns is the number of samples in the testing set and nc the number of class.

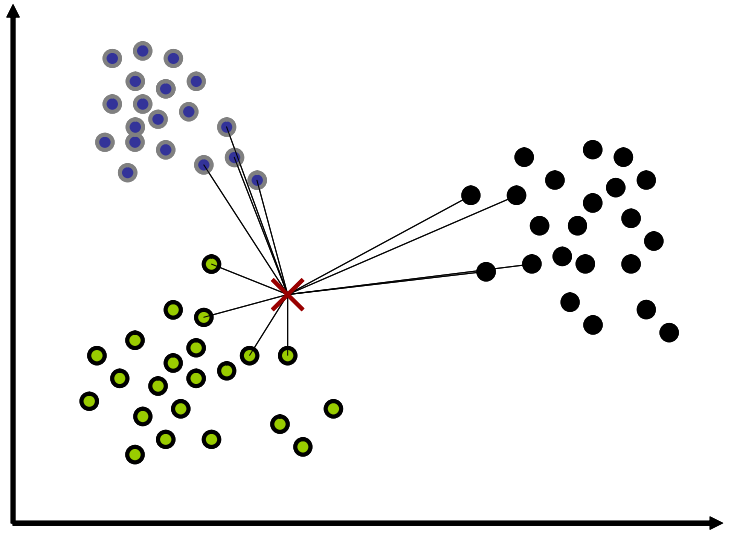

Figure 45: Example of k-nearest neighbours algorithm in a two dimensional feature space (with k=4 and 3 classes). To classify a test sample (red cross), its distance to the k-nearest neighbours is computed.

Intuitively, for a given class, the smallest this mean distance the highest the probability of belonging to the class for this test sample. So in a second step, we apply an exponential

function on the mean distance and normalise it, so that for each sample s_i of the testing set, we obtain the probability P_j of belonging to each class:

$$s_i \rightarrow P_{i,j} = \frac{e^{-\alpha.d_{i,j}}}{\sum_{k=1}^{nc} e^{-\alpha.d_{i,k}}}$$

where α is an exponential factor set to 20 in our experiments.

Finally, to obtain the age structure of the whole data set, we sum the probability P_j among all testing samples. For each age class j, we obtain the age proportion A_j:

$$A_j = \sum_{i=1}^{ns} P_{i,j}$$

In a routine framework, where the maximum of precision is needed, we also add the data from training samples by considering the age estimated by experts with a probability of 1. But to test and validate our method, we will compare the age proportion estimated on the testing set with age proportion estimated by experts on the whole data set as describes in the next section.

Test and results

To test and validate the conditional model, we randomly divide the available data set into a training set and a testing set. To analyse the precision of the results, we have run 100 different simulations each based on a new random sampling of 50% of the data for training and 50% for testing.

The following results present the mean age proportion estimated after these 100 simulations and the corresponding standard deviation compared with the "true" age proportion resulting from expert readers' estimations. For some species where age estimations from several readers are available, we show the age proportion resulting from each reader so that one can compare the variability of our method regarding the inter-reader variability. For a fair comparison, we also present the number of fish used in each estimation. For example, for Icelandic plaice, the age proportion based on estimations of 3 expert readers has a limited validity because of the small number of fish used.

Eastern channel plaice

Eastern channel plaice 2006 - quarter 1

	2-	3	4	5	6+	Nb fishes
True	0,11	0,18	0,16	0,26	0,29	238
Estimated	0,06	0,21	0,15	0,32	0,26	238
Standard deviation	0,03	0,04	0,04	0,05	0,04	238

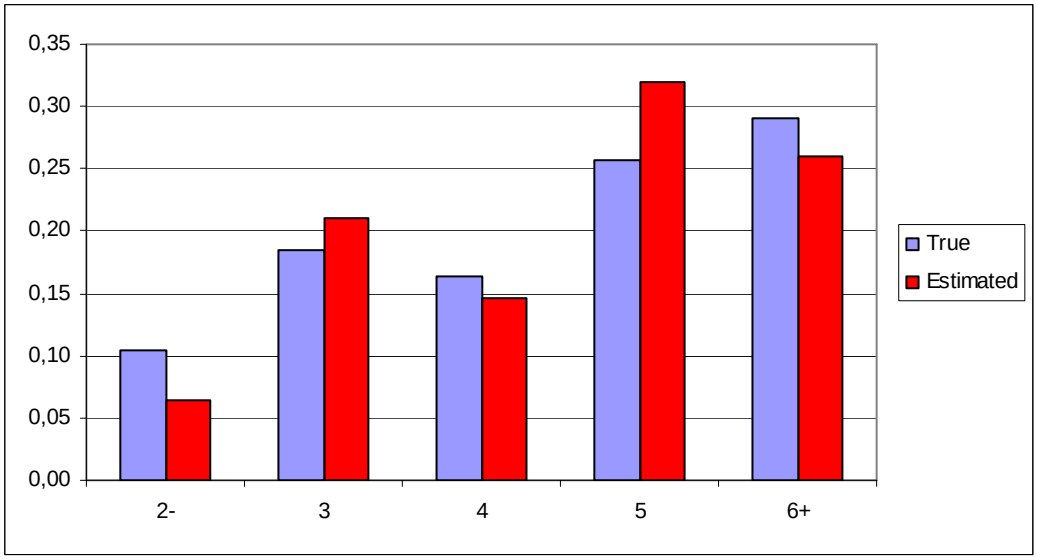

Eastern channel plaice 2006 (whole year)

	2-	3	4	5	6+	Nb fishes
True	0,31	0,29	0,13	0,16	0,11	907
Estimated	0,32	0,35	0,09	0,13	0,10	906
Standard deviation	0,02	0,02	0,01	0,01	0,01	906

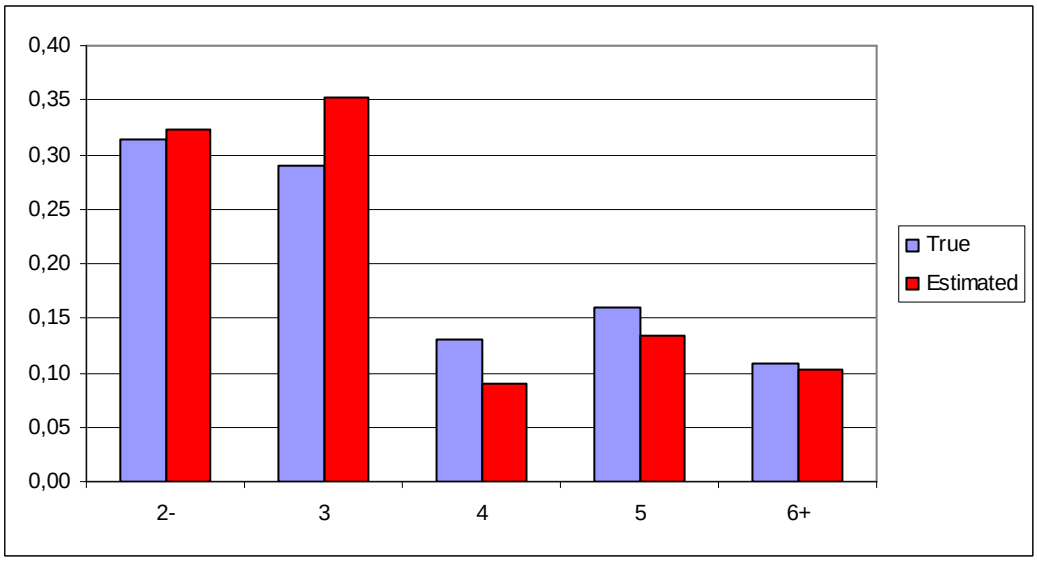

Icelandic plaice

Icelandic plaice 2006 (Q1)

	4-	5	6	7+	Nb fishes
Expert 1 (EF)	0,09	0,13	0,41	0,38	246
Expert 2 (AJ)	0,09	0,12	0,39	0,39	234
Expert 3 (AB)	0,14	0,21	0,43	0,21	14
Estimated	0,05	0,12	0,43	0,41	251
Standard deviation	0,03	0,04	0,04	0,04	251

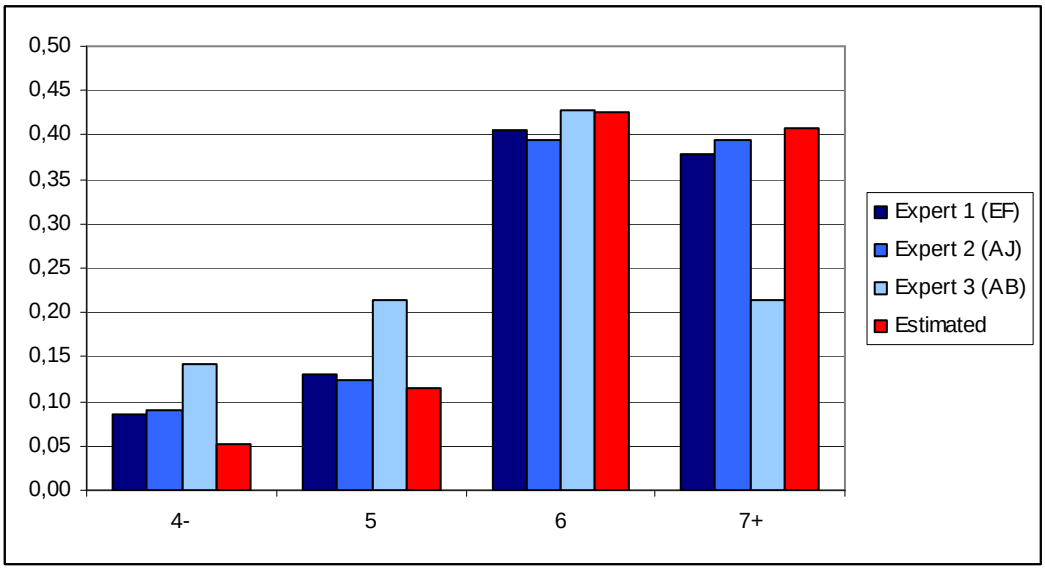

Icelandic plaice 2006 (whole year)

	4-	5	6	7+	Nb fishes
Expert 1 (EF)	0,32	0,19	0,27	0,22	982
Expert 2 (AJ)	0,31	0,18	0,26	0,25	910
Expert 3 (AB)	0,44	0,24	0,19	0,13	84
Estimated	0,36	0,14	0,31	0,19	994
Standard deviation	0,03	0,02	0,03	0,03	994

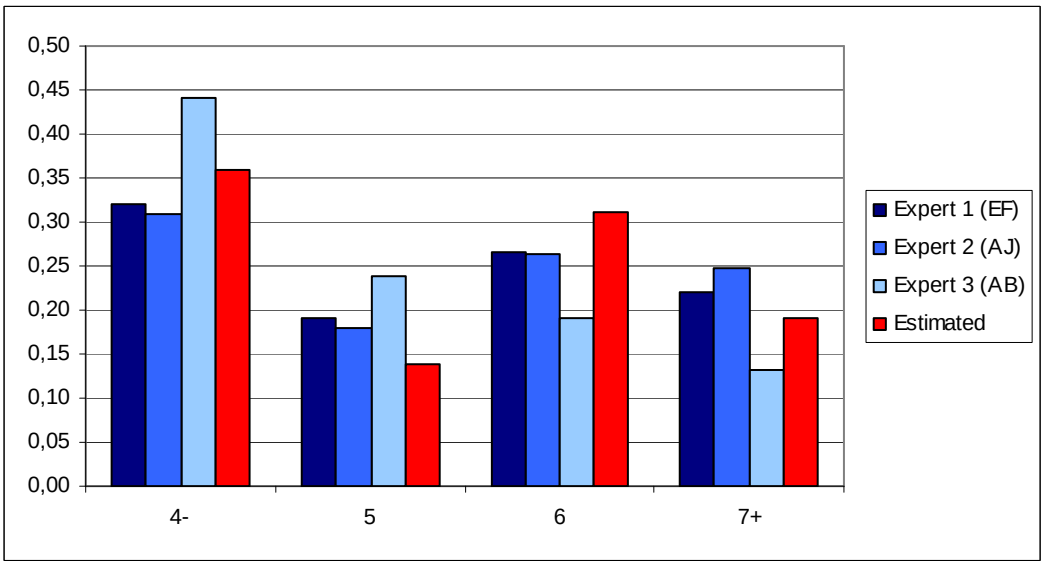

Deviations from the project work programme in WP2

The work programme in WP2 is targeted to automatize the acquisition of otolith images, extraction of 2D growth structures and individual or structure ageing. We can say that, even the extraction of 2D structures and the results on automated ageing are not as good as it was planned (see WP4 results), there has been a great advance in the methodologies needed in an operational fish ageing tool: the methods to segment the otolith image from the background and to detect the *nucleus* work for all the test datasets used in this project, the most suitable radials for age classification and the angular sectors have been particularized for each species, and the individual age classifier has been designed, implemented and made available for commercialisation purposes. Additionally, the conditional model has been designed from the scratch and is easier to understand than already existing methods that use kernel classifiers. This last point seemed important to us, since the more common users of these tools will have a biology background, and our experience is that classification methods based on classical approaches have a greater diffusion than complex ones.
Even that the extraction of 2D structures, contrast invariant representation and the automated growth demodulation doesn't perform as expected, they have allowed us to introduce new methodologies and research directions that, once refined, will benefit the other deliverables already available, like the feature discrimination algorithm. This effect can increase the performance of the overall ageing system and also help to develop smarter computer vision tools for otolith image analysis.

There are no deviations from the project and in addition an evaluation of the pre-processing algorithms was carried out. The developed algorithms have successfully been applied to the test case images of North Sea cod and Eastern Channel plaice.

The subtasks are given below, from the report from AFISA 2nd meeting (AZTI) November 7-9 2007, San Sebastian:

- **T2** Pre-processing: resp. IMR
  - Image alignment: resp. IMR
    - Input: database
    - Output: aligned images, name: ImgName_A.xxx
  - Background subtraction/contour determination: resp. IMR
    - Input: image
    - Output: image (zero value for the background), name: ImgName_BS.xxx, quality label
  - 2D Growth-adapted filtering: resp. Ifremer
    - Input: image
    - Output: image, name: ImgName_GAF.xxx
  - Low-pass image filtering: resp. IMR
    - Input: image
    - Output: image, name: ImgName_LPF.xxx

For the North East Arctic cod, in addition, the news analyses were carried out.

- **Image alignment and Background subtraction/contour determination**

The m-scripts were carried out. The m-scripts are built in a logical order, where the output from one m-file is a natural input to the next. As an example the background subtraction and contour determination is a logical start before image alignment, because minimum distortion should be introduced before the contour is determined.
The additional m-scripts outside the listed subtasks were developed, for example algorithms that transforms (x,y)-coordinates from the original image to the aligned image.

Description of "trial" species material for NS cod and plaice

The NS cod material consists of 760 otolith images, whereof 347 taken with reflected, saturated light (S) and 413 with reflected light (R). 347 of these overlapped and have been analyzed with the developed m-files. The images are rather big (3 Mpix), but the otoliths cover just a small part of the images (less than 10% of area).

The plaice material consisted of 586 otolith images: 197 S-images, 195 R-images and 194 images with translucent light (T). Of these, 193 otoliths were imaged by all 3 light settings and have been analyzed. These images are smaller than the cod images (1 Mpix), but the otolith pixel area are bigger. The otoliths are also rather aligned along the major ellipse axis compared to the more rotated NS cod otoliths.

Each NS cod image file (tif) consisted of an (n x m) matrix, and not the standard (n x m x 3 array). I did not manage to visualize the images by any of my Microsoft image visualization tools. In addition, 247 of the otoliths had images of uint16 format (min value = 0, max value = 65535), while 100 had images of uint8 format. All the m-files are based on uint8 format, so to convert from uint16 to uint8 I applied the matlab-code:

```
Im8 = uint8(double(im16/256));
```

Each plaice image file (tif) consisted of an (n x m x 3) array, where the 3 matrices involved are identical (equal r, g and b components in a gray tone image) and it was no problem to visualize them in standard Microsoft image visualization programs. The otoliths had images of int8 format (min value = -128, max value = 127). I first reduced the image array to a matrix by the matlab command.

```
Im2 = im1(:,:,1);
```

Then the image matrix was transformed to uint8 format by the commands.

```
Im3 = double(im2) + 128;
Im8 = uint8(mod(im3 + 127, 255));
```

These commands are not implemented in the m-files, where the input images are required to be on uint8 format. If needed, the format manipulation can easily be implemented in the codes on a later stage.

Brief description of developed m-files

preproc_BS.m
background subtraction and contour detection
Input
ims = saturated image matrix
imt = translucent (or reflected) image matrix
lev = threshold level, 0 < lev < 1, for segmentation of otolith
radius = radius of "smoothing circle"
Output
ims_BS = bw image matrix of otolith with black background
imt_BS = gray tone image matrix of otolith with black backgr.
cx,cy = vectors with x- and y- coordinates of contour
param = parameters
param_hd = explanation of param content

Comment: Optimal choice of input parameters lev and radius must be found be trial and error. For the NS cod lev = 0.9 and radius = 5 appeared to work well in most, but not all cases. For plaice the corresponding result was lev = 0.7 and radius = 5. Too large (small) lev-values produce too small (large) otoliths. Too large (small) radius –values produce too smooth (noisy) contours.

preproc_imrot.m
Image alignment along major ellipse axis
Input
ims_BS = cleaned saturated image from preproc_BS.m
imt_BS = cleaned gray tone image from preproc_BS.m
rotangle = param(4) from preproc_BS.m
Output
ims_A = aligned saturated image
imt_A = aligned gray tone image

Comment: The aligned images are bigger than the original ones

preproc_imred.m
Reduction of image size
Input
ims_A = aligned image from preproc_imrot.m
imt_A = aligned image from preproc_imrot.m
nopixext = pixel extension of otolith frame u/d,l/r
Output
ims_red = reduced and aligned saturated (bw) image
imt_red = reduced and aligned graytone image
rowmin = minimum row number of otolith
colmin = minimum col number of otolith

Comment: The reduced images will in many cases be several times smaller than the aligned images. The output rowmin and colmin are needed as input to imrotxy2imredxy (see below). As default value for nopixext I have used nopixext = 50.

preproc_imxy2imrotxy.m
Transforms coordinates in original image to coordinates in aligned image
Input
(x,y) = (x,y)-coordinates in original image to be transformed
nrow = number of rows in original image
ncol = number of columns in original image
Output
(xrot,yrot) = (x,y)-coordinates in aligned (rotated) image

preproc_imrotxy2imredxy.m
Transforms coordinates from aligned image to reduced image
Input
(xrot,yrot) = (x,y) coordinates in aligned image
rowmin,rowmax = output from imred.m
Output
(xred,yred) = coordinates in aligned and reduced image

Application example: North Sea cod

.

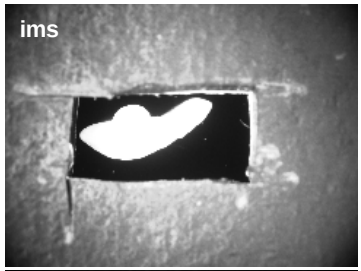

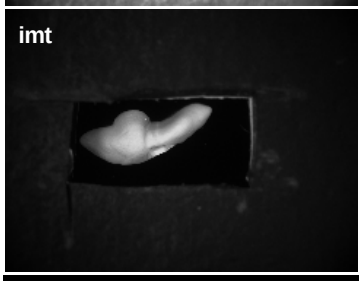

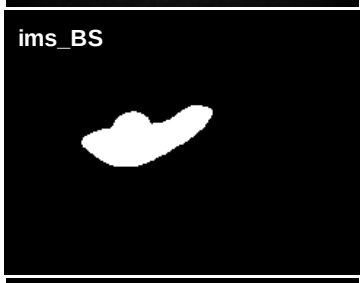

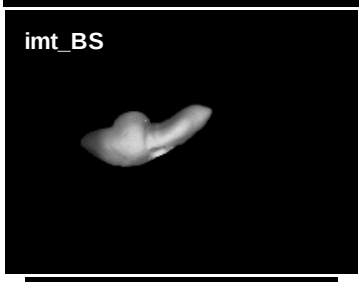

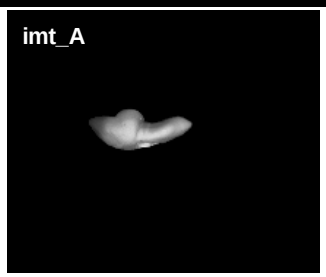

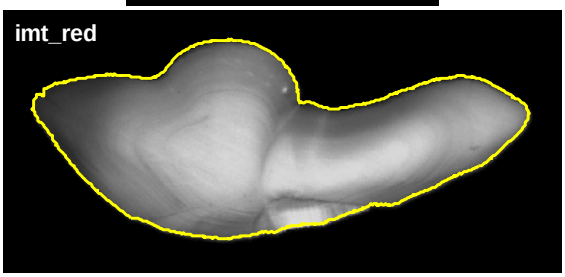

Input files:
ims: COD_NS_2000_S_RS_010001.tif
imt: COD_NS_2000_S_R_010001.tif

ims_BS and imt_BS are outputs from **preproc_BS.m** with lev = 0.9 and radius = 5 as input parameter values.

Imt_A is output from **preproc_imrot.m** with ims_BS and imt_BS as inputs along with the parameter rotangle = param(4) = 14.9307 deg (output from **preproc_BS.m**).

Imt_red is output from **preproc_imred.m** with ims_A and imt_A as inputs along with nopixext = 50. A minimum rectangular frame around otolith is first produced, and this frame is then extended with 50 pixels left, right, up and down. The image has been somewhat cut at right during the copying process to word.

The contour coordinates (xred,yred) for the contour shown in yellow are found from the following sequence:

Original contour coordinates cx and cy are output from **preproc_BS.m**

Rotated contour coordinates xrotand yrot are output from **preproc_imxy2imrotxy.m** with x = cx and y = cy as input.

Rotated and reduced contour coordinates xred and yred are output from **preproc_imrotxy2imredxy.m** with xrot and yrot as input.

▪ 2D Growth-adapted filtering

A 2D Growth-adapted filtering was carried out and tested.

Test on the North Sea cod images set

Computation time

As our algorithm needs the images taken with saturated light, we test the adapted filtering on the 347 images taken under reflected light for which an overlapping saturated image is available. It took about 32 hours to filter the entire set so between 5 and 6 minutes per image. This time includes all preprocessing steps (Background subtraction, growth direction field reconstruction) and the growth-adapted filtering.

Error rate

The adapted filtering algorithm itself can't really completely fail but of course highly depends on the quality on its inputs given by: the result of the background segmentation, the growth direction field reconstruction and the position of the *nucleus*. Regarding the position of the *nucleus*, the filter takes the position annotated by experts directly from the *iid* file and is therefore considered as true.

To increase speed, the background segmentation was applied on reduced images (half size) with lev=0.9 and radius=5 (corresponding to a radius of 10 in normal size). The algorithm fails on 2% of the dataset1 (7 images among the 347 NS cod images tested). An error is defined here when the resulting shape is clearly not an otolith. This error rate is low regarding the difficulty of NS cod image set. Indeed the otolith is small on the image (sometimes less than 10% of the area) and on saturated light images, the otolith is surrounded with a lot of noisy bright shapes.

The quality of the background segmentation in terms of distance between the real contour and the extracted contour is hard to compute because it would needs a ground truth manually annotated contour. Visually, we can see that the main shape is generally preserved while the contour is under-estimated, that is to say that the most border part of the otolith is generally lost. But this has a rather low influence on the final filtering quality.

The growth direction field reconstruction cannot be completely false but its quality is important for the quality of the adapted filtering. The quality of the obtained field is rather hard to estimate and was not measured here.

Result

The figure below (Fig. 46) shows the whole adapted filtering process with intermediate results for cod image number 140022:

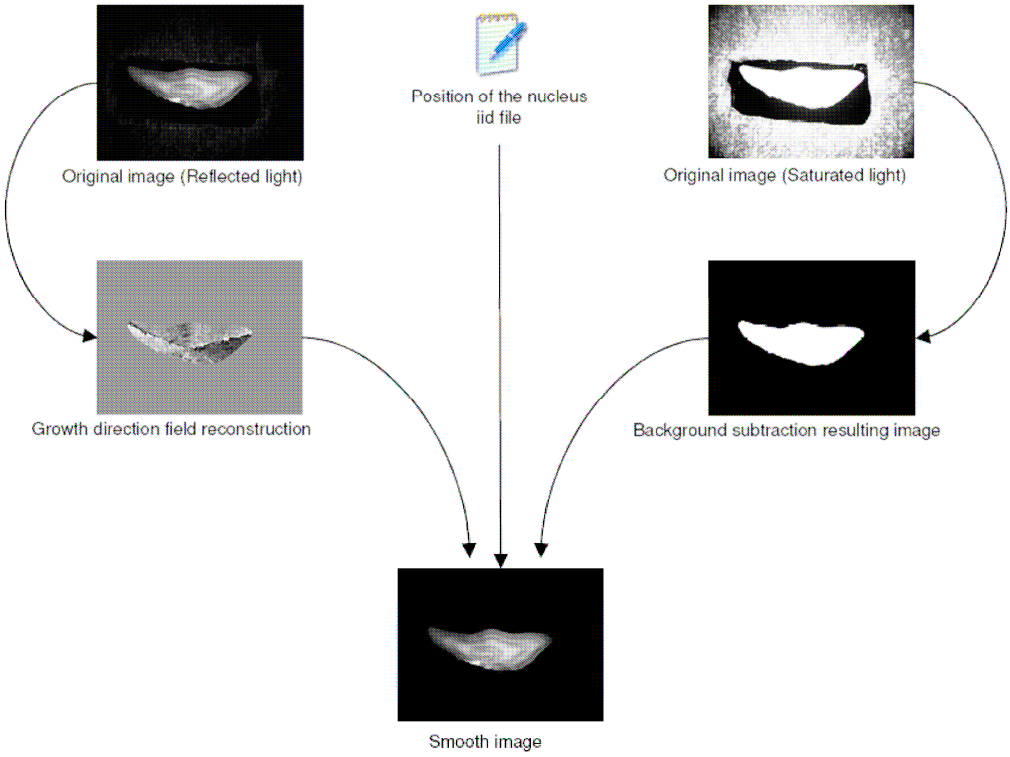

Figure 46: Process of the whole adapted filtering process with intermediate results for cod image number 140022.

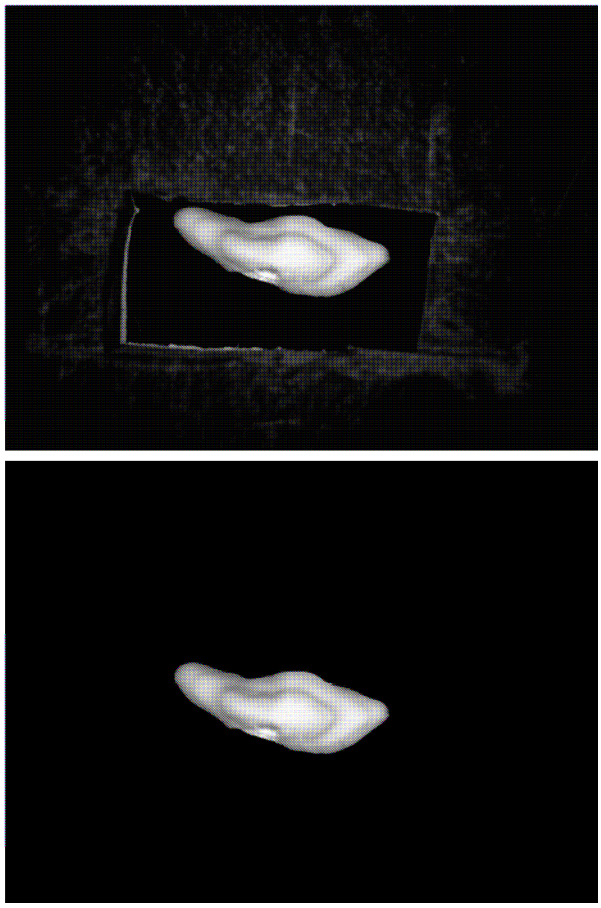

Figure 47: Growth-adapted filtering results on Image Cod with a number: 125014. (Up: original image. Down: filtered image).

Test on the Eastern Channel plaice whole otolith images set

Error rate

The filter was test on the 192 plaice images for which the 3 images (saturated, transmitted and reflected light) and the iid file were available. (The iid file is missing for image 611). To increase speed, the background segmentation was applied on reduced images (half size) with lev=0.7 and radius=5 (corresponding to a radius of 10 in normal size). The algorithm works well on the 192 images (0% error rate).

Result

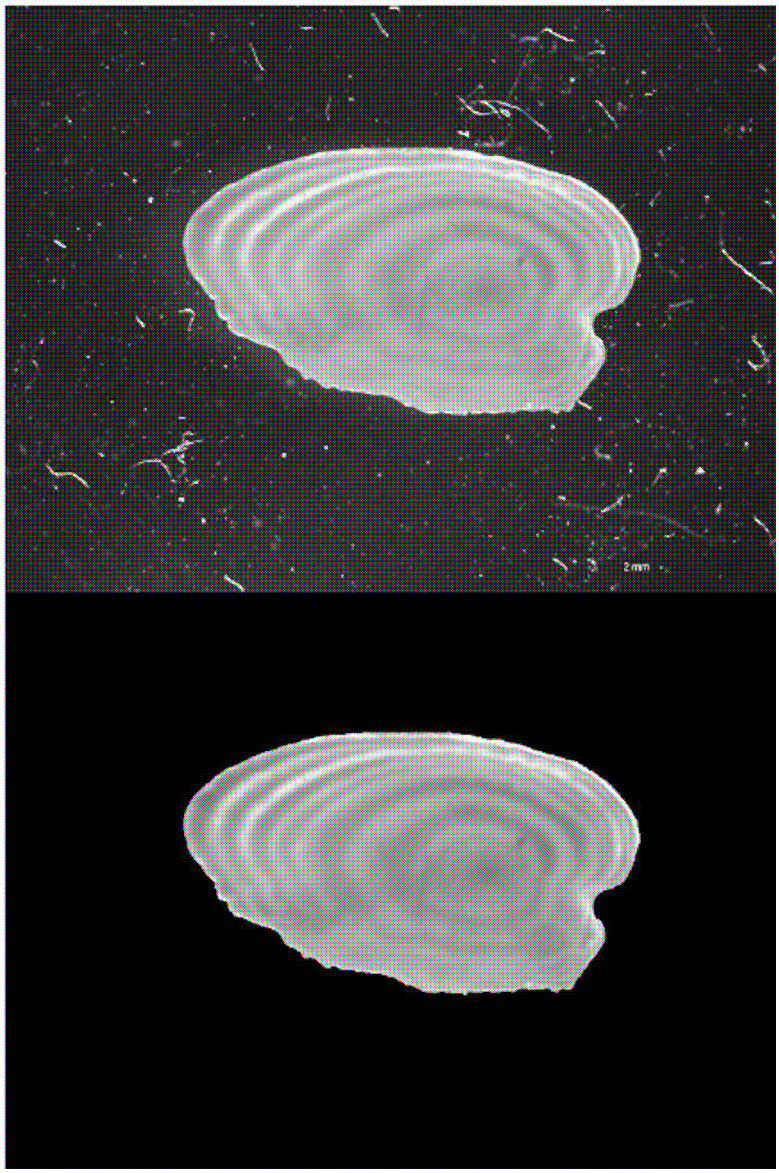

Figure 48: Growth-adapted filtering results on Image Plaice with a number: 510. (Up: original image. Down: filtered image).

This pre-processing was necessary for the good realisation of Workpackage 2.

▪ Estimation of age from morphometric variables of North East Arctic (NEA) cod

Methodology

Based on the developed tools for automatic detection of the contour as well as the core of the images of vertical otolith sections, the following three basic otolith morphometric variables were considered for estimation of fish age:

1) pixel area, *A*, enclosed by contour
2) ratio, $F = a/b$, between minor and major axes in best ellipse fit to contour
3) angle, *D*, between lines from core to the two most distant contour points

The three variables are illustrated in Figure 49 The purpose of the investigation was to examine if better estimation of age could be obtained by the morphometric image variables above than by the fish length and/or fish weight. One motivation for applying variables 2 and 3 (*F* and *D*) was that it appeared that the shape of the otolith sections becomes more bended with age, i.e., a decreasing (increasing) value of *D* (*F*) with age.

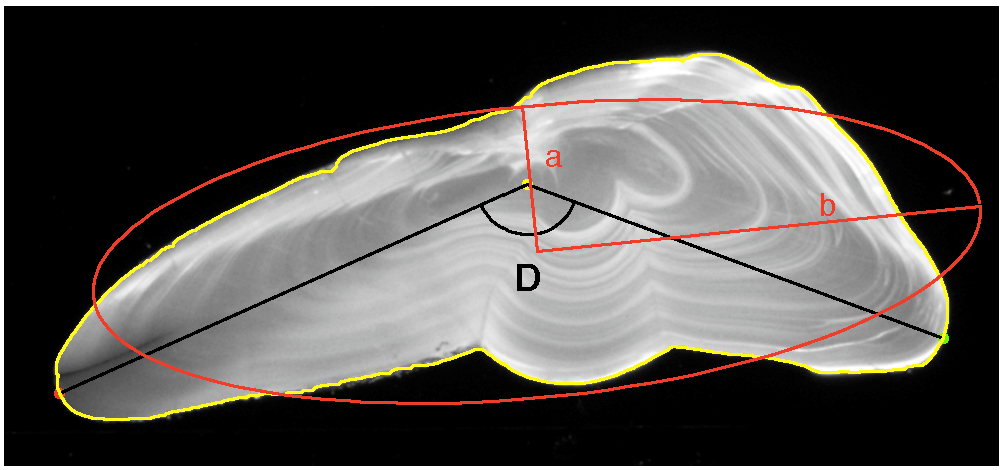

Figure 49: An example of North Sea Arctic cod otolith cross section image defining the morphometric variables 1) pixel area within closed contour (yellow), 2) ratio $F = a/b$ between half minor (*a*) and half major (*b*) axes of best fitted ellipse (red), and 3) bending angle *D* between lines from core to most distant contour points.

Let *x* be any predictor for age and let $y = \log(age)$ be based on ages read by experienced readers, and assume that a linear model for the correspondence between *x* and *y* is reasonable. By nature, *y* will normally have a coarser resolution than the predictor, *x*. Ages are given by a limited number of integer values, while a predictor like pixel area has a much finer resolution, i.e., span a much larger range of values.

To obtain linearity between *x* and *y*, we set $x = \log(A)$, *F*, *D*, $\log(L)$ or $\log(W)$, where *L* and *W* denote fish length (cm) and fish weight (gram), respectively. The general linear model is then

(1) $$y_p = a + bx \Rightarrow age_p = round\left(\exp\left(y_p\right)\right)$$

Where round means rounded to the nearest integer. Because we have stochasticity in both *x* and *y*, Ricker's estimator (1973) for the slope *b* is applied:

(2) $\hat{b} = std(y)/std(x)$

And *a* is estimated by

(3) $\hat{a} = \bar{y} - \hat{b}\bar{x}$

Where overbar denotes arithmetic average over the individual otoliths. A weighted least square principle is applied to estimate optimal weights w_1,..., w_k:

(4) $Q = \sum_{i=1}^{n} \left(age_i - w_1 age_{p1} - \mathsf{L} \; - w_k age_{pk} \right)^2$

And the weights are calculated by minimizing *Q* with regard to w_1,..., w_k:

(5) $\underline{w} = \begin{bmatrix} w_1 \\ \mathsf{M} \\ w_k \end{bmatrix} = M^{-1}\underline{c}$

With

(6) $M = \{M_{ij}\}, \quad M_{ij} = \overline{age_{pi} \cdot age_{pj}}$

$\underline{c} = \begin{bmatrix} c_1 \\ \mathsf{M} \\ c_k \end{bmatrix}, \quad c_j = \overline{age \cdot age_{pj}}$

The weighted age estimator then becomes:

(7) $age_p = \sum_{j=1}^{k} w_j age_{pj}$

As an estimator for the all over precision of the predictor, the following was used:

(8) $S = \sqrt{\sum_{i=1}^{n} \left(age_i - age_{pi} \right)^2 / (n - 2k)}$

The all over bias was estimated by the equation

(9) $bias = \frac{1}{n} \sum_{i=1}^{n} \left(age_{pi} - age_i \right)$

Where a negative (positive) value indicates that the estimator underestimated (overestimated) the average age

Results

From a total of 1992 images of North east Arctic (NEA) cod 1823 contained meaningful values of all the variables and were thus included in the analysis. Based on the otolith variables (morphometrics) we obtained

$S_{\text{morph}} = 0.85$ years

Which is substantially better than the value

$S_{\text{LW}} = 1.01$ years

Based on the fish length and weight. Also the all over bias was better for the morphometric estimator (bias = -0.032 yrs) than for the *LW*-estimator (bias = -0.077 yrs), though both were small. On an age by age basis the comparison was more varied, and the *LW*-estimator was superior for one year old fish. The age frequency distributions showed the same trend with a total of 98 of 1823 observations deviating from the age reading distribution in the morphometric case, and a total of 138 mismatch observations in the length-weight case (Figure 50).

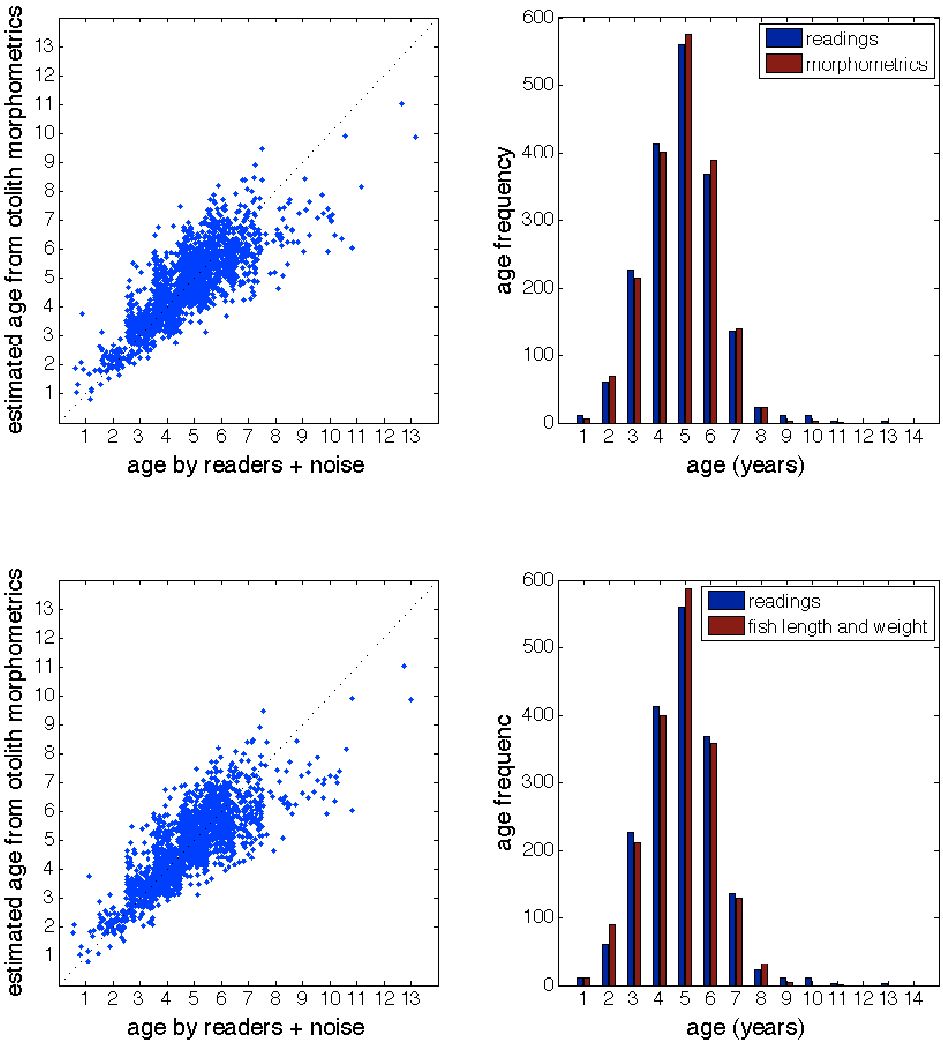

Figure 50: Correspondence between estimated age (age_p) and age based on readings (age). In the left panel a uniform random value between -0.5 and 0.5 is added to the reader based ages (horizontal direction). Upper panels: predicted ages from morphometrics. Lower panels: predicted ages from total fish length and fish weight.

Conclusion

The results indicate interesting potentials for improving automatic ageing from simple shape analysis of the contour of the cross section of NEA cod. Potentials based on entire otoliths before breaking is documented by P. Doering-Arjes *et al.* (2008). A scope for future work is to combine different approaches to improve automated ageing.

References

Doering-Arjes, P., Cardinale, M. and Mosegaard, H. 2008. Estimating population age structure using otolith morphometrics: a test with known-age Atlantic cod (Gadus morhua) individuals. Can. J. Fish. Aquat. Sci. **65**: 2342-2350.

Ricker, W.E. 1973. Linear regressions in fishery research. Journal of the Fisheries Research Board of Canada, 30: 409:434.

▪ Circularization and superposition of otolith images to reveal similarities within trawl hauls applied to North East Arctic cod

Background

It was decided in the AFISA project to maintain the information of each otolith, if available, of cruise track and time and location of the actual trawl haul from which the otoliths were taken. The reason for this was the possibility of having strong dependence between the individuals in one and the same haul, e.g. due to a common life history, especially for young fish. Such a dependency could have a potential for improving automatic ageing as well as for behavioural studies.

Methodology

Based on the developed tools for automatic detection of the contour, the otolith images were standardized to common size and orientation by fitting an ellipse to the contour with common gravitation centre as that of the area enclosed by the contour. The otolith images were then rotated with horizontal axis along the major ellipse axis, and scaled to a common extension of the fitted ellipses. In this way standardized images of the otoliths were produced with common size (401 x 801 pixels), and with the ellipse origin in the centre of the image.

Based on the automatic *nucleus* and contour detection from the images, these were also circularized (Panfili *et al*., 2002). Because the zones in general were easier to detect in certain regions of the image, the circularization was restricted to a 90 degrees section with the mid line from the core pointing downwards in the image (the medial direction). To convert the quarter-circles to entire circles, 3 techniques were tried: 1) Stretching, 2) Mirroring to obtain half circle and then stretch, 3) First mirroring to obtain half circle, then mirroring the half circle to obtain circle. In this report the attention is restricted to the latter technique. The reason that circles are suitable is just by subjective experience, and the latter technique also leaves the smoothest joints among the three circularization techniques.

Results

Figure 1, upper panel, shows the result of superimposing 1991 images. Note that the image is remarkably characteristic for an individual otolith image from NEA cod, though the superimposed image is somewhat blurred. It clearly illustrates the non-homogeneous intensity background that is typical for the individual images. In fact a major original motivation to create a superimposed image was to see if this could be used to homogenise the background of the individual images. An example is shown in Figure 51, lower panel, where an original image after standardization (mid panel) is divided by the superimposed image. As is seen, homogenization is obtained at least for large parts of the image, though some saturation problems have arisen close to the contour.

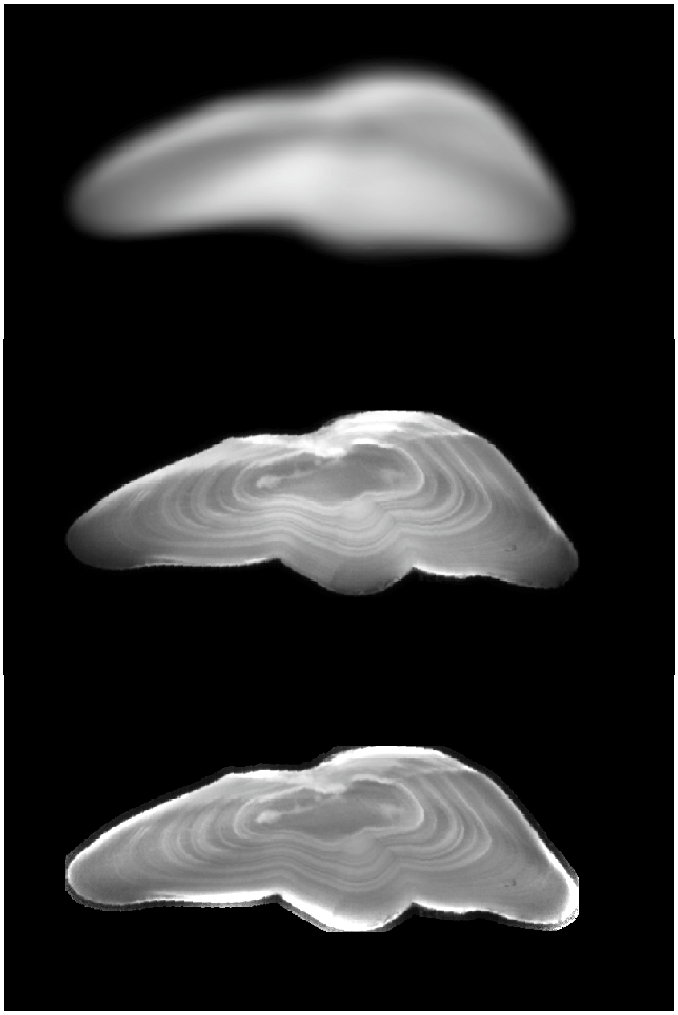

Figure 51: Upper panel: 1991 superimposed otolith images of North East Arctic cod. Mid panel: Example of an otolith image illustrating the inhomogeneous background intensity. Lower panel: Image in mid panel divided by the upper image to homogenise background.

In Figure 52, upper panel, shown the 90 degree section of an otolith to be circularized, and the result of the circularization is shown in the lower panel. In this case the age determined by the readers is 6 years. Note that by the chosen section we avoid much of the inhomogeneous intensity background. Due to the rather difficult and abruptly changing shape of the annual zones, however, the annual zones deviate quite much from ideal circles in the circularized image.

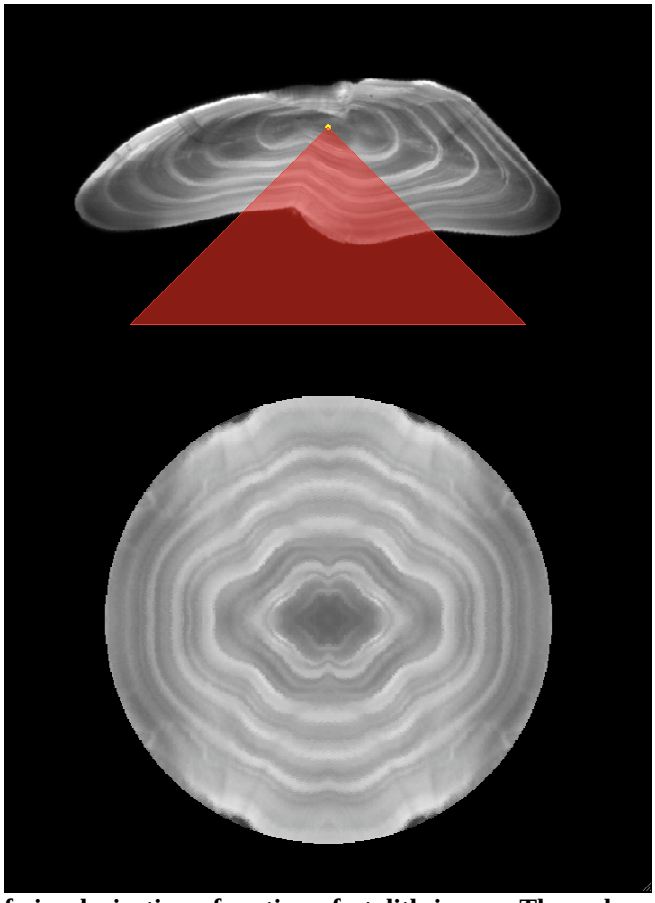

Figure 52: Illustration of circularization of section of otolith image: The red quadrant in upper panel is recognized as lower right quadrant in circle. This quarter of the circle is then flipped left-right and added, the resulting lower half circle is then flipped up-down.

An example of within haul similarity as opposed to random otoliths is shown in Figure 53. In the left panel 35 circularized otolith images of 3 years old cod are superimposed, and we clearly see 3 enhanced zones with rather equidistant radii. In the right panel, 35 3 year old otolith images from 35 random hauls are superimposed, and we see that the clear zonation in the left panel has disappeared, probably due to higher variation in growth history within the latter group.

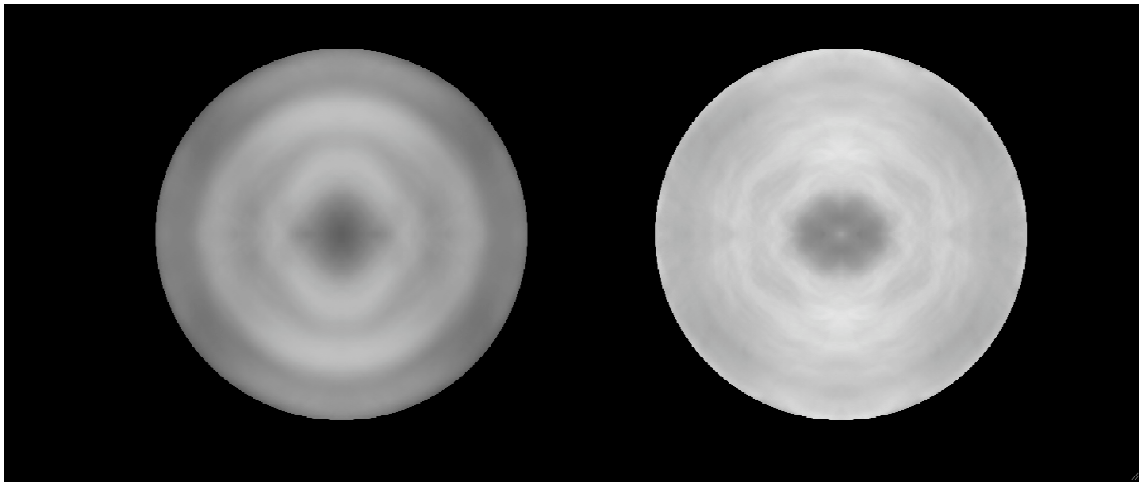

Figure 53: 35 Left panel: Superimposed circularized otolith images of North East Arctic cod of age 3 years (by readers) and from one and the same trawl haul. Right panel: 35 superimposed otolith images of 3 years old cod from 35 random trawl hauls.

Conclusion

The test case studied indicates that there might be strong similarities between standardized images of otolith sections containing annual zone information for cod of the same age that have experienced the same life history, in particular for young fish. This indicates a great potential for improving automatic ageing by clustering techniques, and also that otolith image analysis can be used for behavioural studies.

References

Panfili, J., Pontual, H.D., Troadec, H., Wright, P. 2002. Manual of Fish Sclreochronology. Editions Ifremer.

WP3 – Software integration of the developed automated ageing systems

Scientific teams involved: Partner 1, Ifremer (coordinator); Partner 2, Azti; Partner 4, Difres; Partner 5, IMR; Partner 7, UPC
Institute: Person (1) Sébastien Carbini; Kélig Mahé ; André Ogor ; Ronan Fablet (4) Henrik Mosegaard; (7) Vicenc Parisi, Antonio Soria, Père Marti

Overall objectives: The overall objective of this workpackage is to implement the algorithms developed in WP2 into a software platform dedicated to otolith processing. This includes the development three main modules:

- Task 3.1 Software module for automated acquisition of series of otolith image
- Task 3.2 Software module for the automated estimation of individual ages
- Task 3.3 Software module for the automated estimation of age structures

Deliverables:

1 TNPC module automating the acquisition of series of otolith images
2 TNPC module for the automated estimation of individual ages
3 TNPC module for the automated estimation of age structures

Start date: month 9
Completion date: month 21

Partner responsible: Partner 1, Ifremer
Partners involved: Partner 1 (Ifremer); Partner 4 (Difres); Partner 7 (UPC)
Person-months:
Status of progress: this WP has been successfully completed.

Workpackage 3 Objectives

In this work package, we will demonstrate the degree of automation of the proposed ageing systems. The automation is expected at two different levels as results of the developments carried out in WP2. As stressed above, WP2 is aimed at automating the acquisition and the processing of databases of otolith images for ageing issues:

1. We will first demonstrate the automation of the acquisition of image series (within the range of 50 samples for each series). This is aimed at reducing the cost of the acquisition of the databases of otolith images exploited by ageing systems. Typically, the sequential acquisition of single images requires about half minute per image. The automated acquisition of image series is expected to reduce this acquisition cost by a factor of five to ten. Hence, it will have a major impact on the cost-benefit analysis carried out in WP4.
2. As a second step, we will demonstrate the degree of automation of the actual ageing systems, including the estimation of the individual fish ages as well as the estimation of age structures. It will cover simultaneously the full automation of the information extraction stage and the information processing stage. It wills de demonstrated using the material in the databases provided by WP1. The automation of the acquisition of global features such as fish length and otolith weights will not be considered, though relevant procedures will de defined to optimize the associated acquisition cost.

Progress towards Objectives WP3

▪ TNPC module automating the acquisition of series of otolith images

INTRODUCTION

For research purposes, the computer vision algorithms are developed in C language with the Megawave image processing library on Linux. The acquisition platform consists in a microscope driven with the software TNPC implemented inside a Visilog framework with Microsoft Visual Basic. One of the main goals of this work was to port some computer vision algorithms developed under Linux to the acquisition platform working with Microsoft Windows.

METHODS

Cygwin is a useful tool to port linux application to windows. It contains a dynamic library (cygwin1.dll) which acts as a Linux API (Application Programming Interface) emulation layer providing substantial Linux API functionality.
The first idea was to use Cygwin to compile a dynamic library including the algorithm we wanted to port to TNPC. Then, the functions of the dynamic library could have been called from customized TNPC modules, using the visual basic framework. But the Cygwin dynamic library (cygwin1.dll) seems to be incompatible with the Visual Basic framework. Indeed, a simple addition function compiled into a dynamic library with Cygwin fails with an error on cygwin1.dll when TNPC call it, whereas it works well when the same program is compiled with Microsoft Visual Studio. Compiling the existing computer vision algorithms with Visual Studio is hard because these algorithms use functions provided by Megawave library and Linux API.
Finally, the solution we choose consist in compiling the algorithm into an independent executable program and then call this program from TNPC module. The otolith mosaic segmentation algorithm has been ported using this method and function correctly.

RESULTS

The result of this work is a module included in TNPC that can be used for acquisition of series of otolith images. A result of this acquisition is given with the results of deliverable 2.1.a.

CONCLUSION

TNPC module automating the acquisition of series of otolith images was carried out. The main difficulty of this work was to cope with incompatibility issues emerging from the use of closed proprietary software.

▪ TNPC module for the automated estimation of individual ages

INTRODUCTION

The version 4 of TNPC software presented an interface with 3 toolbars (Fig. 55).

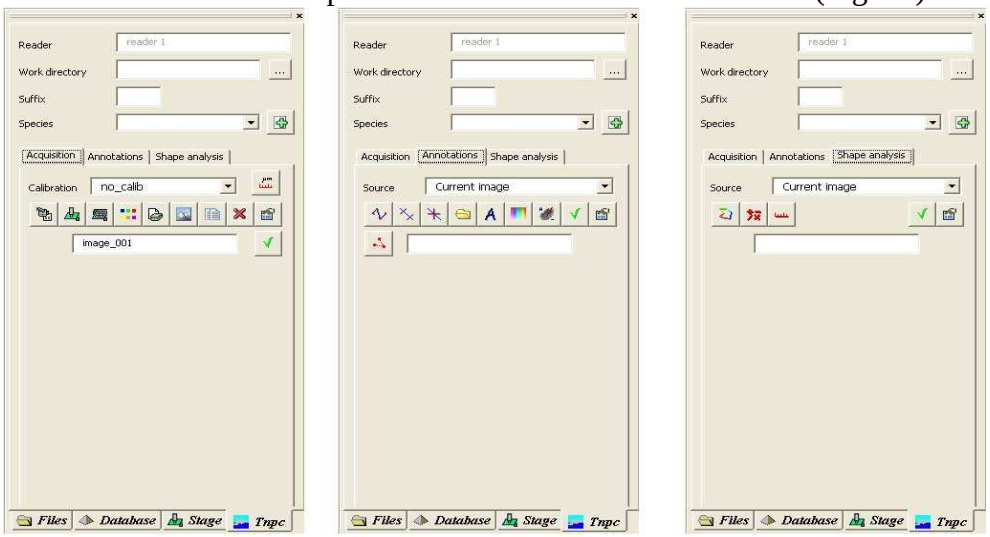

Acquisition toolbar Annotation toolbar Shape analysis toolba

Figure 55: View of the TNPC (version 4) toolbars.

To integrate 2 new modules of automation developed in the AFISA framework, a new version of TNPC was implemented under Visilog 6 (http://www.noesisvision.com/). This version 5 (Fig. 56) of TNPC was developed with 3 new toolbars in the interface.

Figure 56: Version 5 of the TNPC software.

METHODS

The algorithms chain developed under Workpackage 2 (See Deliverable D.2.4.d) has been implemented in the TNPC software.
As Visilog-based platform works on standard C/C++ codes, most of the algorithms developed in Matlab were transcribed in C++ too.
The automated estimation of individual ages, developed and integrated in TNPC, is a generic process. It can be performed in 2 successive steps: a learning procedure using a documented image data base (including images and corresponding ages) and the automated age estimation process based on otolith images. There are 2 new toolbars, the first one being devoted to the apprenticeship and the second one to for the automated estimation of individual age (Fig. 57).

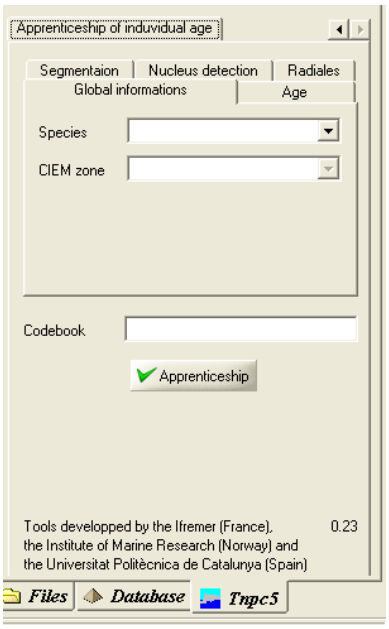

Tool bar of the learning procedure for the automated individual age estimation

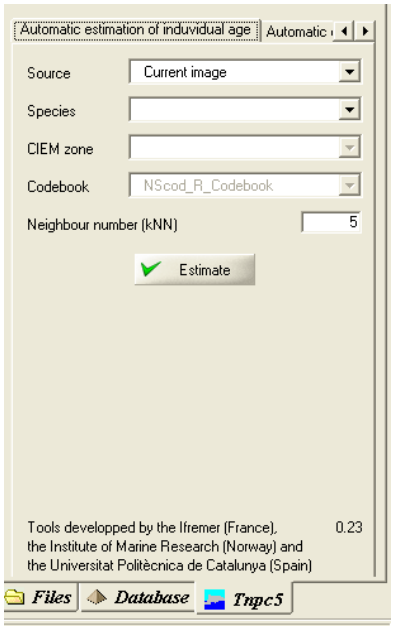

Automated estimation of individual age toolbar

Figure 57: View of the toolbars of the new TNPC module for the automated estimation of individual ages.

For the apprenticeship, 5 menus have to be documented as described subsequently (Fig. 58).

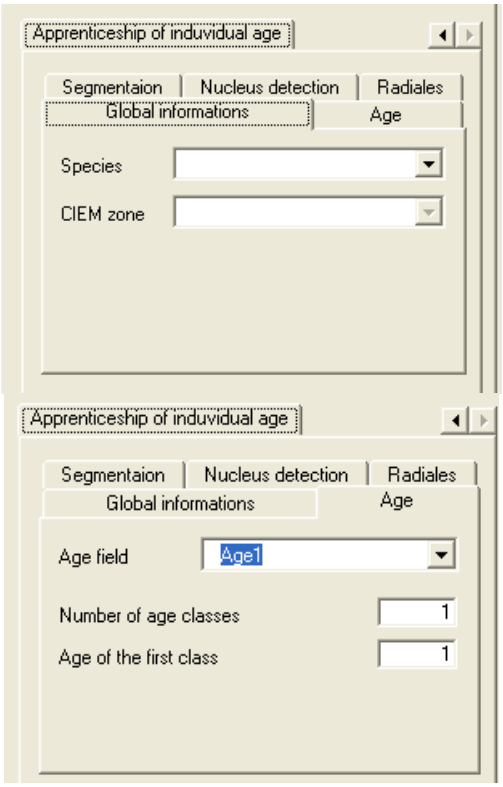

Global informations :
Allows selecting a species and a CIEM zone in lists. The list can be supplemented by the user in the file Aea_Species.cfg

Age :
Select a column in the current learning database corresponding to age data (Age field).
The number of age classes and the age of the first class need to be documented.

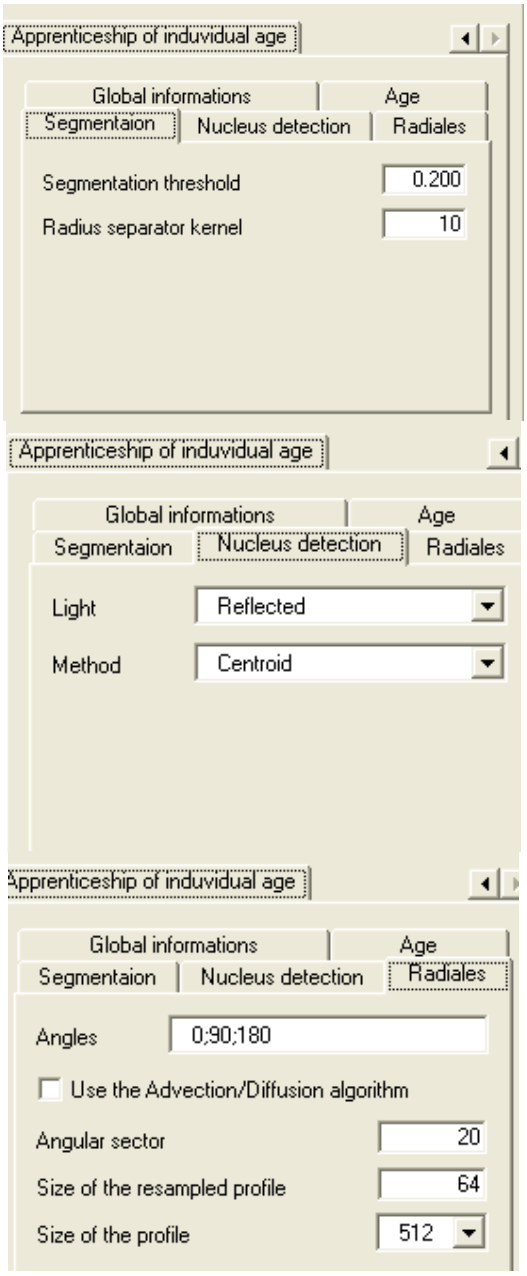

Segmentation :
Allows parametrizing the segmentation process (threshold and radius separator kernel) See deliverable D2.3.f.

Nucleus detection :
Allows specifying the light modality (images under reflected or transmitted light) and the method (centroid, morphological or empiric). See deliverable D2.3.a.

Radials :
Allow specifying the orientations of 3 radials. A method of the advection/diffusion can be used (contrast enhancement) (See Deliverable D2.3.g). An angular sector around the radials and the size of the resampled profile need to be specified. The size of the profile (64, 128, 256, 512 or 1024) is selected.
See deliverable D.2.3.d

Figure 58: View of 5 menus in the Apprenticeship of individual age toolbars.

Once these 5 menus are documented, the apprenticeship can be carried out and a codebook is created (Fig. 59).

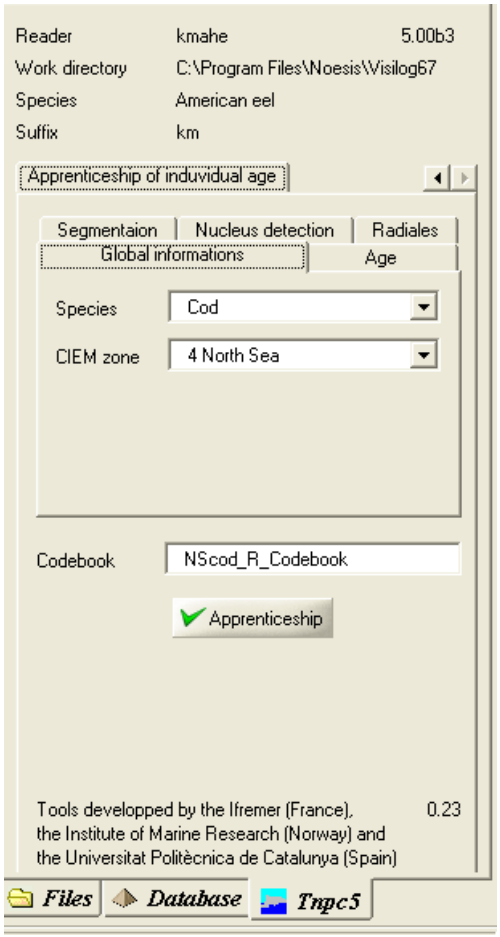

Creation of codebook :

For example
NScod_R_Codebook.cbk

NS : CIEM zone (North Sea)
cod : Species
R : light (R : Reflected, T : transmitted)

Figure 59: View of creation of codebook in the Apprenticeship of individual age toolbars.

This codebook is then used for the processing of otolith images to be 'aged' using the Automatic estimation of individual age toolbar (Fig. 60).

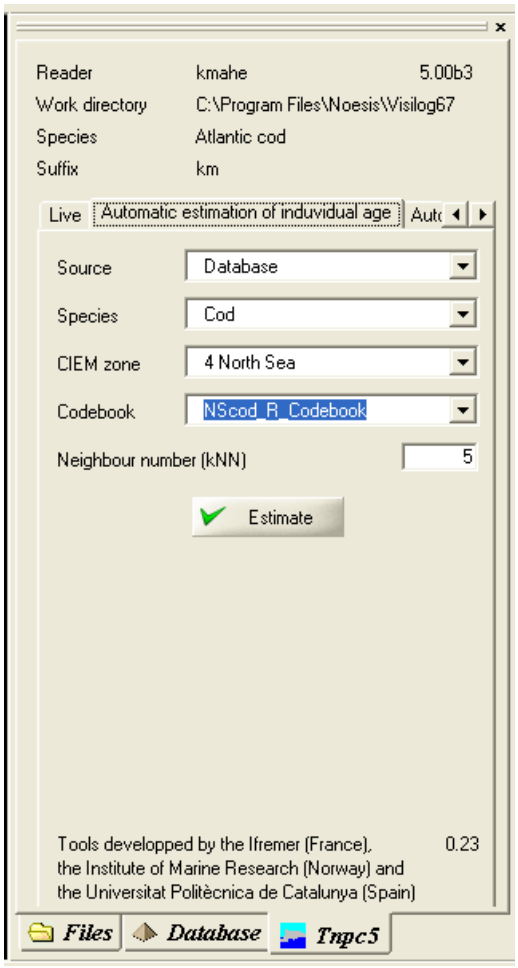

Automatic estimation of individual age :

Source : Database or Current image
Species
CIEM zone
Codebook
Neighbour number (kNN) (see deliverable D.2.4.d)

Figure 60: View of the process of automatic estimation of individual age.

The results are integrated in the current database with a new column called “AutoEstimAge”.

CONCLUSION

The main difficulty of this work was to transcribe most of the algorithms developed in Matlab in C++ codes because Visilog-based platform worked on standard C/C++ codes.
The version 5 of TNPC software now proposes a generic process for the automatic estimation of individual age from otolith interpred image database.

▪ TNPC module for the automated estimation of age structures

INTRODUCTION

The version 4 of TNPC software presented an interface with 3 toolbars (Fig. 61).

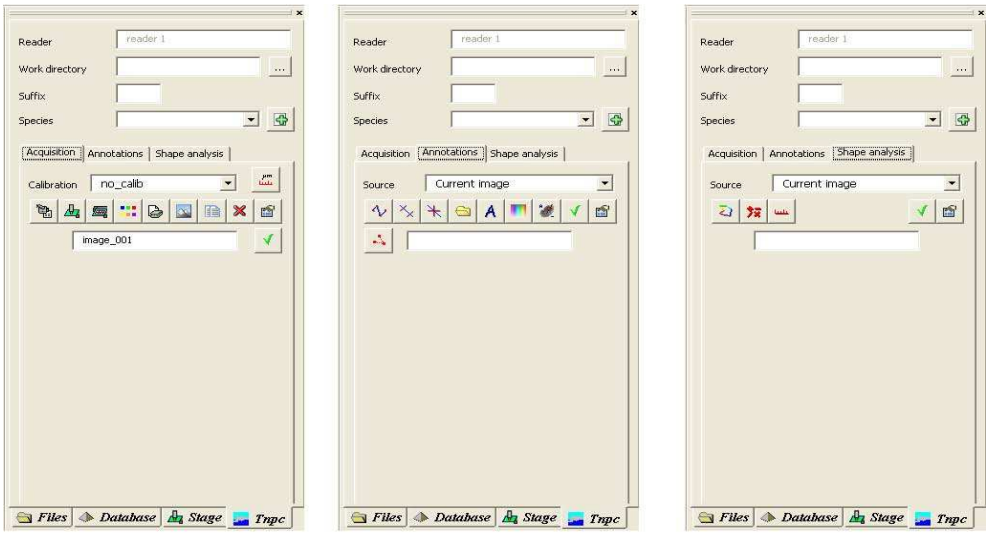

Acquisition toolbar Annotation toolbar Shape analysis toolba

Figure 61: View of the TNPC (version 4) toolbars.

To integrate 2 new modules of automation developed in the AFISA framework, a new version of TNPC was implemented under Visilog 6 (http://www.noesisvision.com/). This version 5 (Fig. 62) of TNPC was developed with 3 new toolbars in the interface.

Figure 62: Version 5 of the TNPC software.

METHODS

The algorithms of automated estimation of age structures developed within Workpackage 2 have been implemented in TNPC software. Only the conditional model (See deliverable D2.5.b) was used in TNPC software.
As the Visilog-based platform works on standard C/C++ codes, algorithms developed in Matlab had to be transcribed in C++ too.
One new toolbar has been designed for the automated estimation of age structures (Fig. 63).

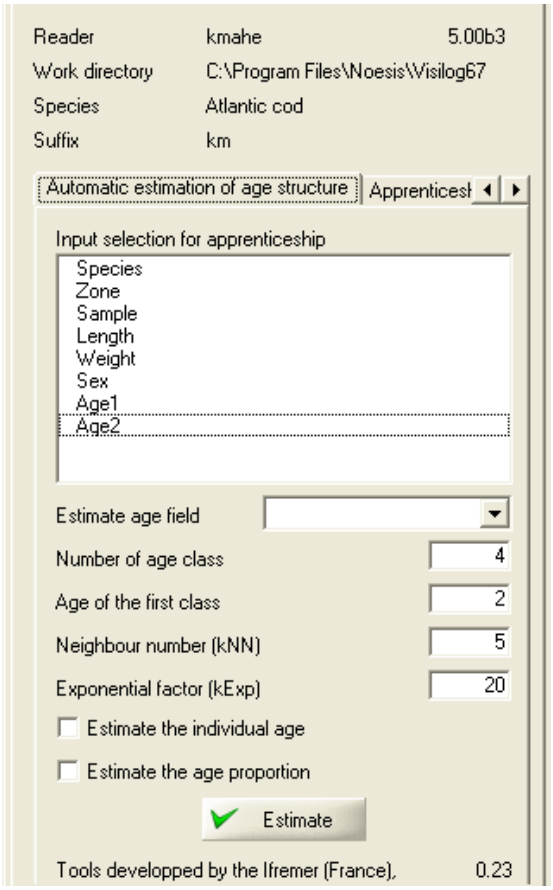

Figure 63: View of the toolbar of the TNPC module for the automated estimation of age structures.

The goal of this procedure is to estimate the age structure of a fish set with corresponding measurements (e.g. fish length) available for the whole data set. Ages estimated by expert are available for only a part of this set.

The automated estimation of age structures, developed and integrated in TNPC, is a generic process. It consists in two successive steps: a learning step using information of the database (one species, one stock) including ages estimated by readers and the age structure estimation itself. In the current database, measurements of fish characteristics (fish length, fish weight…), global otolith features (otolith weight,) and otolith shape information (otolith area, major axis length,) are selected in "Input selection for apprenticeship" (Fig. 64).

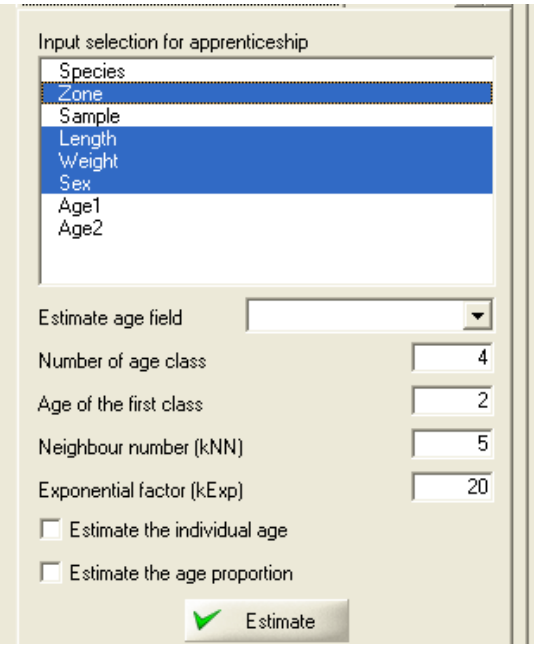

< **parameters of model**

< **choice of the parameters to be used in the learning step**
< **number of age class**
< **age of the first class**
< **neighbour number (kNN)**
<**exponential factor**

Figure 64: Selection of the parameters for the automated estimation of age structures.

This automated estimation from fish and otolith characteristics allow to obtain the age structures with "Estimate the age proportion" and the individual age with "Estimate the age proportion" as well (Fig. 64).

The results are in a spreadsheet of TNPC for the automated estimation of age structures and are integrated in the database with a new column called “AutoEstimAge_2” for the automated estimation of individual age.

CONCLUSION

The main difficulty of this work was to transcribe most of the algorithms developed in Matlab in C++ codes because Visilog-based platform worked on standard C/C++ codes.
The version 5 of TNPC software presents a generic process for the automatic estimation of age structures. The same process can be used to consider the individual age.

Deviations from the project work programme in WP3

The 3 modules were integrated into software TNPC (version 5). There are no major deviations. The mixture model developed with AD-Model-builder script could not be integrated in TNPC. The conditional model from global otolith features and physical fish characteristics, was used for age structure estimation and moreover for the automated estimation of individual ages,

WP4 - Cost-benefit analysis of the proposed solution for ageing automation

Scientific teams involved: Partner 1, Ifremer; Partner 2, Azti, Partner 3, Cefas; Partner 4, Difres (coordinator); Partner 5, IMR; Partner 6, MRI, Partner 7, UPC
Institute: Person (1) Kélig Mahé; Ronan Fablet (2) Unai Cottano; (3) Sally Warne; (4) Karin Hűssy; (5) Hans Høie; Alf Harbitz; (6) Elías Guðmundsson; (7) Vicenc Parisi, Antonio Soria, Père Marti.

Overall objectives: The overall objective of this workpackage is to perform a cost-benefit analysis of the proposed automated ageing systems for the considered case-studies. It includes four tasks:

- Task 4.1 Tools for evaluating costs, precision and accuracy of automated ageing systems
- Task 4.2 Application of cost-benefit analysis to case study I (cod)
- Task 4.3 Application of cost-benefit analysis to case study II (plaice)
- Task 4.3 Application of cost-benefit analysis to case study II (anchovy)

Deliverables:

1.a Template for cost-benefit analysis based on different objective functions

1.b Parameterization, to case-studies I, II and III, of the automated estimations of individual ages

1.c Parameterization, to case-studies I, II and III, of the automated estimation of age structures

2 Cost-benefit analysis for case study I (cod)

3 Cost-benefit analysis for case study II (plaice)

4 Cost-benefit analysis for case study III (anchovy)

Start date: month 1
Completion date: month 24

Partner responsible: Partner 4 (Difres)
Partners involved: All partners
Person-months:
Status of progress: this WP has been successfully completed.

Workpackage 4 Objectives

In this work package we will demonstrate 1) the consistency of automated age reading by comparing results among laboratories considering all major steps where variation may be expected to influence consistency. 2) Further we will develop tools to examine both accuracy and precision in the results relevant for stock assessment, and we will compare results between experienced age readers and the automated age estimation from one or several systems. 3) Finally we will provide an analysis of costs in relation to achieving different levels of accuracy and precision and compare cost-benefits of different systems.

1. In a coordination between WP1, WP3 and WP4 the entire line of automation, including handling of preparations, digitised image acquisition and age reading will be performed at two or more different labs on a series of the same or closely related material (e.g. right and left otolith from the same fish). The results will be analysed in WP4 and add to the basis of error estimation for the different systems. The performances of the ageing systems will be assessed with respect to different sources of variability:

a. The impact of the choice of preparation modes of increasing costs will be investigated by comparing whole or sectioned otoliths in the plaice CS, as well as surface treatment in the cod CS (polished, wet, dry etc.)
b. The impact of variations in illumination during the image acquisition step will be investigated by comparing results associated with different standardized light settings such as reflected, transmitted, and/or polarised conditions, as well as angle of light source to otolith surface, otolith orientation and camera sensitivity to illumination specifications.

2. The construction of tools for the examination of precision and accuracy will specifically address the most essential parameter for stock assessment, i.e. the estimated age structure. The basic concept is that a sample of otolith material with information about individual age probabilities is used to calibrate a production sample representative of a specific population component (e.g. age composition in the catch or in a survey). Three different strategies will be elaborated depending on the information type in the calibration material and the production sample. These three strategies are as follows:
    a. Strategy SA: Traditional age reading from whole and/or sectioned otolith annual ring counting. Errors are calculated based on either known age material or on the variation between different readers from different institutes analysing the same material.
    b. Strategy SB: Automated estimation of individual ages from descriptors of 1D and 2D otolith signals related to seasonal variability of the concentric formation of annual growth structures (WP2.3 and WP2.4) supported by models of physical growth laws for otolith accretion (WP 2.2). Errors are estimated in relation to individual known age material or distributions of otolith shape and size from fish with an estimated individual age probability distribution.
    c. Strategy SC: Automated estimation of age structures from global otolith features (e.g. otolith weight or morphometrics) and fish size (WP 2.2 and 2.5). The uncertainty by age group is estimated by the models depending partly on variability in translation from distribution of otolith features and fish size to age structure and partly on inherent uncertainty in true age of the calibration material.
3. The last component is to produce a template for the identification and the analysis of the costs, and the associated uncertainties at different time/ age stratified sampling levels necessary for the calculation of the disaggregated precision of age estimation. The three main strategies are compared with respect to the variance of the estimated age for fixed total costs. If possible, the calculations should be based on optimum resource allocation for each of the three strategies of otolith analysis.
    a. Costs are carefully monitored within WP1 and learning/adjustment curves are estimated for non routine components. Total costs include both investments and the age disaggregated running costs of the analyses on a routine basis.
    b. To demonstrate the application of a strategy in the specific situation of each case study, the models are parameterized from the performance of extracting the correct age structures within each strategy, and the analyses of benefit-cost relationship are carried through based on the specific conditions (i.e. sample structure, known age material etc.) for each case study.
    c. The relationship between the age disaggregated error structures and total costs will be analysed. The optimum sampling strategy will be investigated for different types of objective functions assigning different weights to for instance recruitment or adult fish.

Progress towards Objectives WP4

▪ Template for cost benefits analysis of age determination methods.

The purpose of the analysis is to determine and compare the efficiency of the three age determination methods for cod in the North Sea, Northeast Arctic cod, Plaice in the Eastern Channel, Icelandic plaice and anchovy in the Bay of Biscay. The analysis of the efficiency of a method includes analysis of how optimum sampling procedures can be obtained.

The three methods are

1. Traditional analysis counting year rings of otoliths.
2. Age Determination based on fish length and otolith weight.
3. Automatic age reading

To evaluate the three methods we assume that sufficiently many fish/otoliths are analysed to obtain an age-length keys for each the stocks considered. For a given stock the efficiency or precision of a method could be based on the goodness of the age-length key. To define the concept of the goodness we need to define an object function, which quantifies the goodness. A straightforward way to define such a function is connected to estimation of the age distribution from a given length distribution (for instance the length distribution of total national catch in numbers for a given quarter) applying the age-length key obtained. In case of method 2 the otolith weight is necessary as well. If the error distribution of an age determination method is known or estimated this should be accounted for in the evaluation of methods.
In the present cost benefits template the error distribution is assumed to be known from analyses elsewhere in the project. The object function will also be applied to obtain the optimum stratified sample allocation of the resources available for given costs, which will used in the comparison of the three methods.

To define the object function the methods 1 and 3 can treated similarly, while method 2 has to be considered separately.

Formulation of the object function for methods 1 and 3

We assume that the length composition, N_l which should be converted o age, is known without error because this probably does not effect the comparison of the three age determination methods.
The variables used are defined below in the section on notation.

Age determination without error

For the simple situation, where the age determination error distribution is unknown, one may assume that the age is determined correctly without any error. In this case the object function is relatively simple:
Let N_l be the known length distribution, which should be converted to the age distribution. Further, let $(n_{l,a}^{obs})_{l,a}$ be the matrix defining a given age-length key, where $n_{la,}^{obs}$ is the number of

fish of length *l* determined to be *a* year old from a sample $n_l = \sum_{l=1}^{L} n_{l,a}^{obs}$ fish of length *l*. The number fish by age is as usual estimated by

$$\hat{N}_a = \sum_{l=1}^{L} N_l * p_{l,a}^{obs}$$

Where

$$p_{l,a}^{obs} = \frac{n_{l,a}^{obs}}{n_l}$$

As $n_{l,-}^{obs} = (n_{l,a=0}^{obs},...,n_{l,a=A}^{obs})$ for given n_l is multinomially distributed we have that the variance and covariance of $\hat{N}_a$ are estimated by

$$V(\hat{N}_a \mid (n_l)) = \sum_{l=1}^{L} \frac{N_l^2 p_{l,a}^{obs}(1 - p_{l,a}^{obs})}{n_l}$$

$$COV(\hat{N}_a, \hat{N}_b \mid (n_l)) = -\sum_{l=1}^{L} \frac{N_l^2 p_{l,a}^{obs} p_{l,b}^{obs})}{n_l}$$

The object function, *O*, is now defined as the variance of the weighted sum of estimated *N* at age, $\hat{N}_a$:

$$O = V(\sum_{a=0}^{A} w_a \hat{N}_a) = \sum_{l=1}^{L} \frac{B_l}{n_l} \qquad (1)$$

Where

$$B_l = N_l^2 (\sum_{a=0}^{A} w_a^2 p_{l,a}^{obs}(1 - p_{l,a}^{obs}) - 2\sum_{a=1}^{A} w_a p_{l,a}^{obs} \sum_{b=0}^{a-1} w_b p_{l,b}^{obs}) \qquad (2)$$

And where w_a is user defined weight priorities associated with the age groups. If these priority weights are defined as weight at age, the object function to be minimized is the total weight of the $(N_l)_l$ fish.
Alternatively the object function may be defined as the weighted sum of variances:

$$O_1 = \sum_{a=0}^{A} w_a V(\hat{N}_a) = \sum_{l=1}^{L} \frac{C_l}{n_l} \qquad (3)$$

Where

$$C_l = N_l^2 \sum_{a=0}^{A} w_a^2 p_{l,a}^{obs} (1 - p_{l,a}^{obs}) \qquad (4)$$

Total costs for a given method are divided into fixed and variable costs:

$$c_{tot} = c_{fix} + \sum_{l=1}^{L} c_l n_l \qquad (5)$$

Where c_{tot} and c_{fix} respectively are total and fixed costs, while c_l denotes the variable unit costs for determining one fish of length *l*.
The optimum stratified allocation of samples by length, n_l^{opt} (in this case the optimum number of otoliths by length analysed) can be calculated by minimizing the object function (1) or (2) with respect to the distribution by length, $(n_l)_l$, for given total costs expressed in equation (5).

It is well known (Raj, 1968) that that the optimum solution for the object function (1) is:

$$n_l^{opt} = (c_{tot} - c_{fix}) \frac{\sqrt{\frac{B_l}{c_l}}}{\sum_{l=1}^{L} \sqrt{B_l c_l}} \qquad (6)$$

Insertion of the optimum solution (6) into the object function (1) gives the minimum value of the objective function, O^{opt}

$$O^{opt} = \frac{(\sum_{l=1}^{L} \sqrt{B_l c_l})^2}{c_{tot} - c_{fix}} \qquad (7)$$

If instead the total number of otoliths read, n_{tot} is given the optimum is:

$$n_l^{opt} = n_{tot} \frac{\sqrt{B_l}}{\sum_{l=1}^{L} \sqrt{B_l}} \qquad (8)$$

And the minimum objective function correspondingly becomes

$$O^{opt} = \frac{(\sum_{l=1}^{L} \sqrt{B_l})^2}{n_{tot}} \qquad (9)$$

For the present case for which it is assumed that both age determination methods are correct without any errors, methods 1 and 3 can of course be compared just by comparing total costs

of the methods. When comparing all three methods the resulting optima defined in eq. (7) should be applied.

Known age determination error distribution

Assume now that the possible length dependent age determination error distribution, $V_l = ((v_{l,a,b}))$ has been estimated elsewhere in the project or guessed ($v_{l,a,b}$ is the probability that a fish of true age *a* is determined to be *b* year old). To facilitate the calculations we further assume that V_l is known without error.

Let $n_{l,-}^{true} = (n_{l,0}^{true},...,n_{l,A}^{true})$ and be the vector denoting the true age composition of a sample of n_l fish of length *l*. Let $p_{l,-}^{true} = (p_{l,0}^{true},...,p_{l,A}^{true}) = n_{l,-}^{true} / n_l$ denote the corresponding probabilities defining the true age-length key. The relation between the true and the observed age-length keys is:

$$p_{l,-}^{true} V_l = p_{l,-}^{obs} \qquad (10)$$

This implies that the true age composition for n_l fish of length *l* can be calculated by

$$p_{l,-}^{true} = p_{l,-}^{obs} V_l^{-1} \qquad (11)$$

One can show that the elements in the calculated vector $p_{l,-}^{true}$ sum to one. However, often the elements are negative and hence the solution cannot be used as an age-length key. Instead one has to estimate the true age-length key by treating them as parameters by modelling the relationship between the observed age composition data and these parameters. The model suggested is:

Using equation (10) the vector $n_{l,-}^{obs}$ for given number of fish in the sample of length *l*, n_l follows the multinomial distribution:

$$n_{l,-}^{obs} \mid n_l \sim \text{Multinomial}(\ n_l, \sum_a p_{l,a}^{true} v_{l,a,b=0},..., \sum_a p_{l,a}^{true} v_{l,a,b=A}\ ) \qquad (11)$$

It is easy to show that the probabilities in the distribution sum to one: $\sum_b \sum_a p_{l,a}^{true} v_{l,a,b} = 1$

The likelihood function for all length groups then is:

$$L((n_{l,a}^{obs})_{l,a} \mid (n_l)_l) = \prod_l \binom{n_l}{n_{l,0}^{obs} \ldots n_{l,A}^{obs}} \prod_b (\sum_a p_{l,a}^{true} v_{l,a,b})^{n_{l,b}^{obs}} \qquad (13)$$

In principle the parameters $(p_{l,a}^{true})_{l,a}$ can be estimated by minimizing eq. (13) with respect to the parameters. However, as the number of observations equals the number of parameters one has to reduce the number of parameters. This can be in several ways. One way to do this is to relate the parameters (the true age-length key) to the growth:

Assume that the growth can be described by a von Bertalanffy growth equation, i.e.

$$L_t = L_\infty(1-e^{-k(t-t_0)})$$

In the present context we simply assume that all fish in the sample follow the same growth curve. Variation around the curve obviously occurs because of variation of individual growth i.e. variation of individual growth parameters. The individual growth variations are not directly modelled here, but is treated as stochastic variation around a common growth curve and hence the growth parameters estimated should be considered as the mean of all individuals.
For a given length *l* the corresponding age is

$$t(k, L_\infty, t_0 \mid l) = t_0 - \frac{1}{k}\ln(1-\frac{l}{L_\infty})$$

We now assume that the age distribution for the given length group follows a log normal distribution with log mean equal to $(\log(t(k, L_\infty, t_0 \mid l))$ and log variance equal to $\alpha + \beta(l - \bar{l})$ (we expect the variance to increase with increasing size). We therefore express the parameters $(p_{l,a}^{true})_{l,a}$ as functions of the von Bertalanffy parameters and the variance in the log normal distributions as follows:

Let

$$F(k, L_\infty, t_0, \alpha, \beta \mid a, l) = F_{\log\, normal}\,(a+1, \log \text{ mean } = \log(\, t(k, L_\infty, t_0 \mid l)), \log \text{ sd} = \alpha + \beta(l - \bar{l}))$$

Where $F_{\log \text{ normal}}$ is the cumulated log normal distribution

For a given age group *a* the true age-length key parameters could then be expressed as the difference between the cumulated value in the distribution for age *a*+1 minus the corresponding value for age *a*:

$$p_{l,a}^{true} = F(k, L_\infty, t_0, \alpha, \beta \mid a+1, l) - F(k, L_\infty, t_0, \alpha, \beta \mid a, l) \qquad (14)$$

Insertion of the parameters (eq. (14)) into the likelihood function (13) results in a likelihood, $L(k, L_\infty, t_0, \alpha, \beta)$, depending on the five parameters mentioned. These parameters are estimated by maximum likelihood.
The validity of the age distribution for a given length group, which here is assumed to be log normal, could be investigated by simulation with varying von Bertalanffy parameters and recruitment and accounting for the length selection induced by commercial exploitation pattern.
Another and simpler way to reduce the number of parameters is to assume that neighbouring length groups have the same age distribution. This assumption may be weaker and more correct if the age distribution does not follow a distribution with a single modus as the log normal or another continuous distribution,
When the true age-length key has been estimated by maximum likelihood the comparison of the three methods and the calculation of the optimum stratified solution should be carried out as in the case with known age determination error distribution, where $(p_{l,a}^{obs})_{l,a}$ should be replaced by $(\hat{p}_{l,a}^{true})_{l,a}$.

Method 2

Formulation of the object function for method 2 deviates from the other methods because analyses of otolith length and weight replace the determination of the number of year rings. How the variances $V(\hat{N}_a)$ included the object function should be calculated for this method has not yet been solved. However, the object function is the same as for the other two methods, i.e. equation (1) or (3).

Notation

Let

n_l indicate the number of fish sampled of length *l.*

$n_{l,a}^{obs}$ indicate the number of fish sampled of length *l* and determined to be *a* year old.

$p_{l,a}^{obs} = \frac{n_{l,a}^{obs}}{n_l}$ indicate the proportion of fish sampled of length *l* and determined to be *a* year old.

$n_{l,a}^{true}$ indicate the true number of fish sampled of length *l* and age *a*.

$p_{l,a}^{true} = \frac{n_{l,a}^{true}}{n_l}$ indicate the true proportion of fish sampled of length *l* and age *a*.

N_l indicate the number of fish of length *l* from the length distribution which should be converted to the age distribution.

$\hat{N}_a$ indicate the estimated number of fish at age *a*.

$V_l = (v_{l,a,b})_{l=1,\ldots,L\ a,b=0,\ldots A}$ indicate the age determination error distribution, a (A+1)*(A+1) matrix where $v_{l,a,b}$ is the probability that a fish of length *l* and of true age *a* is estimated to be *b* year old. This implies that $\sum_{b=0}^{A} v_{l,a,b} = 1$ for all *l* and *a*.

A indicate the oldest age group considered.

L indicate the number of length groups

O indicate the object function.

$V(\hat{N}_a)$ indicate the variance of $\hat{N}_a$.

w_a indicate the chosen objective function weights associated with the importance of a given age group.

c_{fix} indicate fix costs.

c_l indicate length dependant variables costs.

c_{tot} indicate total costs.

REFERENCES

Raj, D. 1968. Sampling theory. Tata McGraw- Hill Publising Company Ltd. Bombay.

- **Parametrisation to case-studies I, II and III of the automated estimation of individual ages.**

Introduction

In this work package we intended to demonstrate 1) Tools to examine accuracy and precision of different ageing method's results for stock assessment, 2) compare results between experienced age reader and the automate age estimation and 3) provide an analysis of the costs in relation to achieving different levels of accuracy and precision. In this deliverable, the parameterisation in relation to the "benefit" of the cost-benefit will be reported. The examinations of precision and accuracy have specifically addressed the most essential parameter for stock assessment – the estimated age structure.

Materials and Methods

Two methods for estimating individual ages of stocks used in fish stock assessment and other scientific purposes were evaluated with respect to cost effectiveness. Below, the first two methods are the newly developed methods which were evaluated in relation to the traditionally used age length key – the third method. The methods considered were:

1. Automated age determination using digitized images of otoliths.

2. The conditional method using nearest neighbour to age classify a stock based on fish length and weight and a range of otolith measurements.

3. The traditional age length key using age and fish length information only.

Methodology for comparisons of methods

To evaluate the goodness of the four methods considered the following simulation procedure was carried out:

For a given stock and period, usually a quarter, data on fish length and weight, otolith characteristics as weight, area etc. and the age determined by expert readers were available for a random sample of fish. This sample was randomly divided into two groups of equal size, for which one group was used as learning data with the age included and the second was used as testing data for which the age information were excluded. For each of the three methods the age distribution in the combined learning and testing sample (i.e. the original random sample available) was estimated based on these data. This procedure was repeated 100 times and thus resulting in 100 estimates of the age distribution in the combined learning and testing sample. As the "true" age distribution is known in this combined sample the goodness of the methods can be evaluated.

Two measures have been applied as measure of goodness: Mean squared error (MSE) and relative bias (RB):

MSE and RB have been calculated for each age group. The two measures are defined as follows:

Consider a given method, stock and age group. Let p_i , i = 1, 2,…, 100 denote the proportion of the age group for each of the 100 simulation and let P denote the "true" age proportion. We then have

$$MSE = E(p-P)^2 \approx \frac{1}{n}\sum_{i=1}^{n}(p_i - P)^2 = \frac{1}{n}\sum_{i=1}^{n}(p_i - \overline{p})^2 + VAR(p)$$

$$RB = 100 * \frac{\overline{p} - P}{P}$$

Where E denotes the expectation of p and n denotes the number of observations. As defined here the relative bias, RB, denotes the relative bias in per cent.

MSE is a measure which includes both the biasness and the variation of a method: A small MSE indicates a good method.

Data analysed

Data for two plaice stocks, two cod stocks and one anchovy stock were analysed: English Channel and Icelandic plaice, North Sea and North East Arctic cod and Bay of Biscay anchovy. The fish measured were obtained as random samples from Scientific surveys in the North Sea (IBTS), the Icelandic waters, North East Arctic Sea and Bay of Biscay.

In order to obtain homogenous data (i.e. individual fish data for which the relationship between age, length, otolith weight and other otolith characteristics is the same) fish caught in the same year and quarter were selected. Data for one quarter for each of the species have been analysed. In general, the species specific quarters with the most fish available have been chosen. The age of each fish was determined by expert age readings and was considered as the true age. This implies that the "true" age distribution was considered known without error in the sample considered. The data used in the analyses by stock and method are shown in table 8.

In principle the same data was used for the three methods. For the automated age reading method a few otoliths were excluded from the analysis because of problems with the digitized otolith images. For the conditional method and the age length key data used was almost the same. From table 9 it appears that the difference between the true age distributions for the four methods is insignificant. Furthermore, when evaluating the methods the true age distribution for each method separately is applied, which implies that the measures of goodness, mean squared error and relative bias, are comparable.

Results

Summary data for the results are given in table 9 and 10 and are illustrated in Fig. 65. For the conditional model analysis in general only fish length and otolith weight were included in the analyses because this gave the best estimates of the "true" age distribution.

Table 8: Data used in the age distribution analyses by species and method

			Method		
Stock	Number of observations available	Stock data analysed	Automated	Conditional	Age length key
Eastern Channel Plaice	237	Age range	$2^{-} - 6^{+}$	$2^{-} - 6^{+}$	$2^{-} - 6^{+}$
		Year-quarter	2006 1. quarter	2006 1. quarter	2006 1. quarter
		Measurements Included	Age	Fish length otolith weight, area, major and minor axes and perimeter	Age and length
Icelandic Plaice	251	Age range	$4^{-} - 7^{+}$	$4^{-} - 7^{+}$	$4^{-} - 7^{+}$
		Year and Quarter	2006 1. quarter	2006 1. quarter	2006 1. quarter
		Measurements Included	Age	Fish length and weight otolith weight, area, major and minor axes and perimeter	Age and length
North Sea Cod	311	Age range	$1- 3^{+}$	$1- 3^{+}$	$1- 3^{+}$
		Year and Quarter	2001 3. quarter	2001 3. quarter	2001 3. quarter
		Measurements Included	Age	Fish length and weight otolith weight	Age and length
North east Atlantic Cod	527	Age range	$2^{-} - 7^{+}$	$2^{-} - 7^{+}$	$2^{-} - 7^{+}$
		Year and Quarter	2001 1. quarter	2001 1. quarter	2001 1. quarter
		Measurements Included	Age	Fish length and weight otolith weight, area, major and minor axes	Age and length
Bay of Biscay Anchovy	312	Age range	$1 – 2^{+}$	$1 – 2^{+}$	$1 – 2^{+}$
		Year and Quarter	2004 2. quarter	2004 2. quarter	2004 2. quarter
		Measurements Included	Age	Fish length and weight otolith weight, area, major and minor axes and perimeter	Age and length

Table 9: True and estimated age proportion in per cent by stock, method and age.

	Age	Method					
Stock		Automated		Conditional		Age length key	
		True age proportion	Age proportion	True age proportion	Age proportion	True age proportion	Age proportion
Eastern Channel Plaice	2^-	11.74	10.24	10.50	6.44	10.55	10.59
	3	18.22	22.22	18.49	20.96	18.57	18.47
	4	16.60	15.57	16.39	14.58	16.46	16.28
	5	25.10	38.59	25.63	31.96	25.74	25.98
	6^+	28.34	14.20	28.99	26.06	28.69	28.69
Icelandic Plaice	4^-	9.15	5.90	7.57	5.22	7.57	7.66
	5	13.31	12.41	14.34	11.54	14.34	14.30
	6	40.33	47.07	39.44	42.55	39.44	39.73
	7^+	37.21	35.04	38.65	40.69	38.65	38.22
North Sea Cod	1	22.86	23.88	22.43	22.80	23.47	23.42
	2	70.48	76.59	70.64	71.30	68.81	68.64
	3^+	6.67	0	6.92	5.90	7.72	7.94
North east Atlantic Cod	2^-	4.64	1.50	4.36	2.32	4.36	4.41
	3	16.11	13.15	18.03	17.84	18.03	18.21
	4	26.85	35.35	26.00	28.04	26.00	25.89
	5	22.59	27.01	20.87	23.28	20.87	20.70
	6	17.78	17.53	17.84	17.39	17.84	17.86
	7^+	12.04	5.83	12.90	11.13	12.90	12.92
Bay of B. anchovy	1	68.34	73.28	69.77	85.98	69.87	70.12
	2^+	31.66	27.25	30.23	14.02	30.13	29.88

Table 10: Mean squared error (MSE) and relative (%) by method, stock and age

MSE*1000	Age	Method		
Stock		Automated	Conditional	Age length key
Eastern Channel Plaice	2^-	0.45	2.69	0.28
	3	2.13	2.27	0.52
	4	2.24	1.93	0.58
	5	21.3	6.20	0.78
	6^+	21.1	2.25	0.59
Icelandic Plaice	4^-	1.28	1.68	0.21
	5	0.63	2.62	0.43
	6	6.09	2.88	1.09
	7^+	1.96	2.26	0.89
North Sea Cod	1	0.40	0.66	0.31
	2	4.04	0.71	0.36
	3^+	4.44	0.21	0.12
North east Atlantic Cod	2^-	1.02	0.58	0.02
	3	1.47	0.32	0.16
	4	8.32	0.87	0.25
	5	2.83	1.09	0.33
	6	0.70	0.41	0.22
	7^+	4.12	0.69	0.15
Bay of B. anchovy	1	3.44	29.26	0.32
	2^+	2.94	29.26	0.32

Relative bias (%)		Automated	Conditional	Age length key
Eastern Channel Plaice	2^-	-12.81	-38.69	0.37
	3	21.96	13.36	-0.51
	4	-6.19	-11.01	-1.08
	5	53.73	24.71	0.92
	6^+	-49.91	-10.13	-0.02
Icelandic Plaice	4^-	-35.56	-31.00	1.14
	5	-6.77	-19.57	-0.31
	6	16.70	7.88	0.72
	7^+	-5.83	5.30	-0.84
North Sea Cod	1	4.47	1.65	-0.22
	2	8.68	0.92	-0.25
	3^+	-100.0	-14.77	2.92
North east Atlantic Cod	2^-	-67.64	-46.84	1.06
	3	-18.39	-1.02	1.04
	4	31.35	7.86	-0.42
	5	19.54	11.52	-0.81
	6	-1.37	-2.51	0.13
	7^+	-51.58	-13.74	0.15
Bay of B. anchovy	1	7.23	23.22	0.35
	2^+	-13.94	-53.60	-0.82

Figure 65a: Mean squared error, MSE, and relative bias by method and age for Eastern Channel and Icelandic plaice. Age length key: Solid line. Francis and Campana: Dashed line. Conditional method: Thick dotted line. Automated age reading: Dotdashed line.
(Note: the solid line, Francis and Campana is a method which estimates age structure, and discussed in D4.1.c)

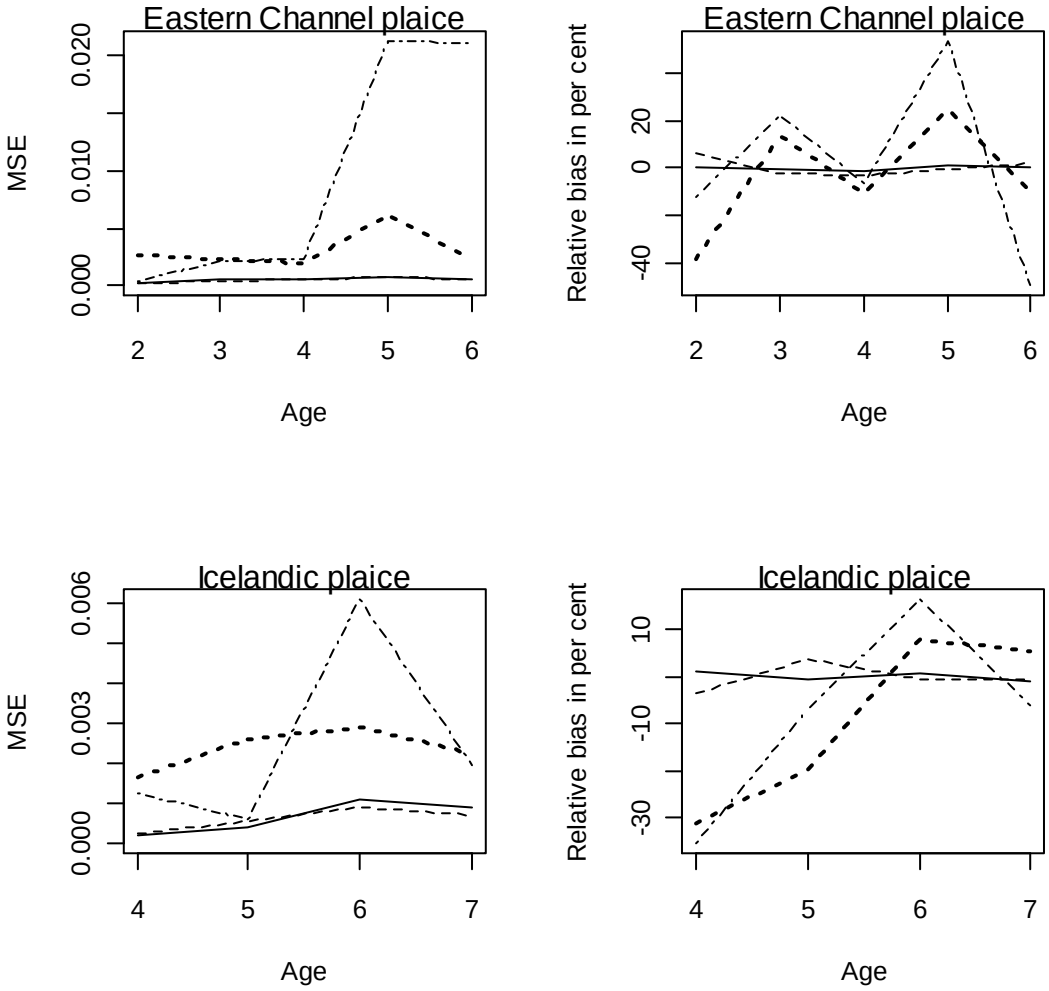

Figure 65b: Mean squared error, MSE, and relative bias by method and age for North Sea and North east arctic cod. Age length key: Solid line. Francis and Campana: Dashed line. Conditional method: Thick dotted line. Automated age reading: Dotdashed line. (Note: the solid line, Francis and Campana is a method which estimates age structure, and discussed in D4.1.c)

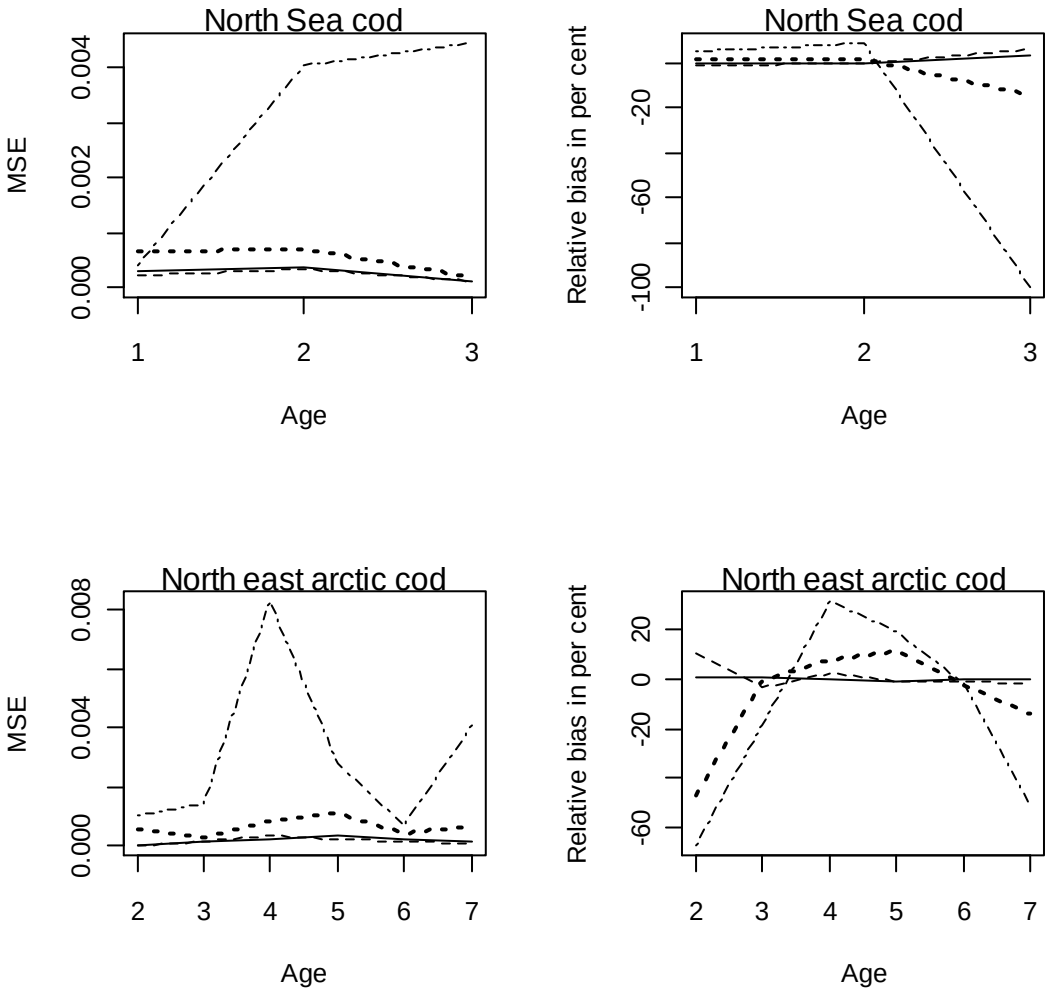

Figure 65c: Mean squared error, MSE, and relative bias by method and age for Bay of Biscay anchovy. Age length key: Solid line. Francis and Campana: Dashed line. Conditional method: Thick dotted line. Automated age reading: Dotdashed line. (Note: the solid line, Francis and Campana is a method which estimates age structure, and discussed in D4.1.c)

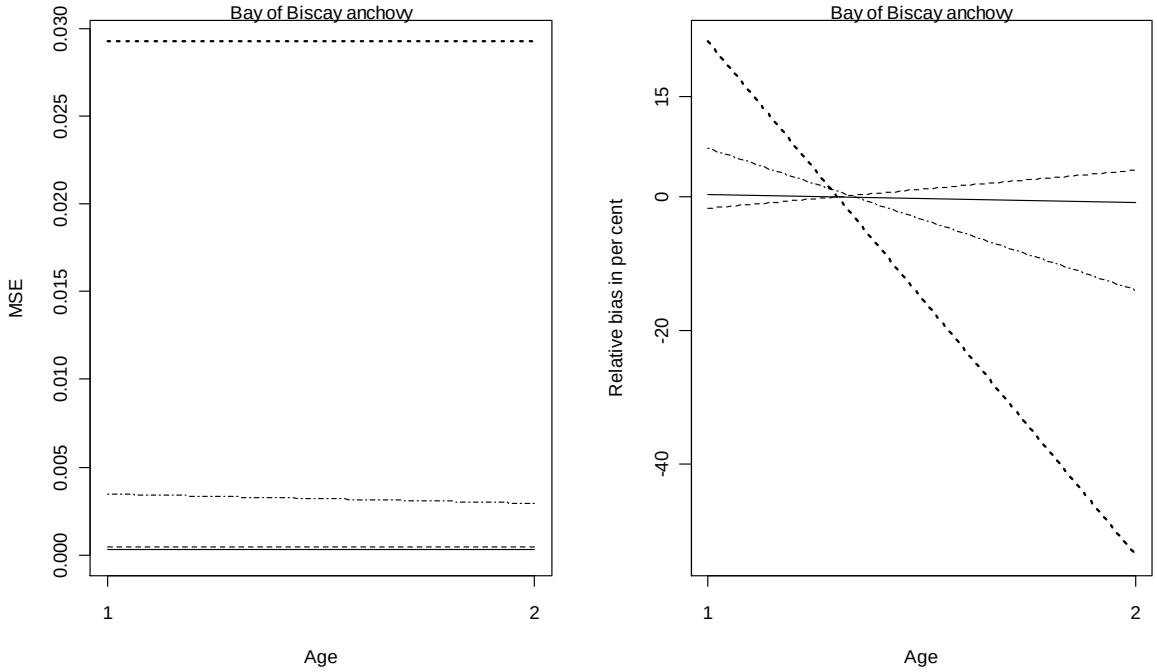

The results show that the traditional age length key (ALK) is the best methods as the MSE is less than MSE for the conditional and the automated age reading methods for all stocks and all age groups. The bias plots further show that the two latter methods are more biased than the ALK.

The ALK is apparently the best method, at least in terms of benefit as it is practically unbiased. The mean absolute relative bias of all five stocks and age groups is 2.8%.

The conditional method is significantly biased for the small ages for the two plaice stocks and for North east arctic cod age groups 2, 3 and 7^+ and for anchovy while the bias is limited for North Sea cod.

For the automated age reading method the bias is very large for some age groups all stocks considered: For instance the bias for Eastern Channel plaice for ages 5 and 6 is about 40% and about -50% and -60% for North east arctic cod age groups 2 and 7^+ respectively. For anchovy the bias is limited.

Conclusions

The age length key seems to be preferable to the conditional and the automated age reading method. Especially the latter method developed so far for cod and plaice is too biased to be used in practical assessment. It is an open question whether the bias for cod and plaice could be reduced by increase of the number of fish analysed.

All automated methods are based on the use of a testing sample, where only images and otolith biometrics are available and a learning sample, where also individual ages are known. The demand for this two-sample data structure – and particularly adequate sample sizes within the learning sample - turned out to be a factor which highly influenced the outcome of this project. We have learned that it is absolutely necessary to have a learning sample with good coverage within all age- and length classes in order to be useful and provide reliable results. Using no less than half of the data available for this project as learning sample proved to be an absolute minimum regarding data requirement. For this reason, it was not possible to evaluate the optimal constellation of sample sizes and data coverage for the learning- and testing samples.

▪ Parametrisation to case-studies I, II and III of the automated estimation of age structures.

Introduction

In this work package we intended to demonstrate 1) Tools to examine accuracy and precision of different ageing method's results for stock assessment, 2) compare results between experienced age reader and the automate age estimation and 3) provide an analysis of the costs in relation to achieving different levels of accuracy and precision. In this deliverable, the parameterisation in relation to the "benefit" of the cost-benefit will be reported. The examinations of precision and accuracy have specifically addressed the most essential parameter for stock assessment – the estimated age structure.

Materials and Methods

The only method chosen for the estimation of the age structure within a population, and not individual ages, was the Length-Mediated Mixture Model developed by Francis and Campana (2004), hence forward referred to as mixture model. This method was evaluated in comparison with the other methods described in D4.1.b and was accordingly evaluated with respect to cost effectiveness. Thus the only method considered was:

1. The mixture model of Francis and Campana using the same type of information as the conditional method.

Methodology for evaluation of the benefit of the method

To evaluate the goodness of the method considered the following simulation procedure was carried out:

For a given stock and period, usually a quarter, data on fish length and weight, otolith characteristics as weight, area etc. and the age determined by expert readers were available for a random sample of fish. This sample was randomly divided into two groups of equal size, for which one group was used as calibration data with the age included and the second was used as production data for which the age information were excluded. The age distribution in the

combined calibration and production sample (i.e. the original random sample available) was estimated based on these data. This procedure was repeated 100 times and thus resulting in 100 estimates of the age distribution in the combined calibration and production sample. As the "true" age distribution is known in this combined sample the goodness of the methods can be evaluated.

Two measures have been applied as measure of goodness: Mean squared error (MSE) and relative bias (RB):

MSE and RB have been calculated for each age group. The two measures are defined as follows:

Consider a given method, stock and age group. Let p_i , i = 1, 2,…, 100 denote the proportion of the age group for each of the 100 simulation and let P denote the "true" age proportion. We then have

$$MSE = E(p-P)^2 \approx \frac{1}{n}\sum_{i=1}^{n}(p_i - P)^2 = \frac{1}{n}\sum_{i=1}^{n}(p_i - \overline{p})^2 + VAR(p)$$

$$RB = 100 * \frac{\overline{p} - P}{P}$$

Where E denotes the expectation of p and n denotes the number of observations. As defined here the relative bias, RB, denotes the relative bias in per cent.

MSE is a measure which includes both the biasness and the variation of a method: A small MSE indicates a good method.

Data analysed

Data for two plaice stocks, two cod stocks and one anchovy stock were analysed: English Channel and Icelandic plaice, North Sea and East Arctic cod and Bay of Biscay anchovy. The fish measured were obtained as random samples from Scientific surveys in the North Sea (IBTS), the Icelandic waters, North East Arctic Sea and Bay of Biscay.

In order to obtain homogenous data (i.e. individual fish data for which the relationship between age, length, otolith weight and other otolith characteristics is the same) fish caught in the same year and quarter were selected. Data for one quarter for each of the species have been analysed. In general, the species specific quarters with the most fish available have been chosen. The age of each fish was determined by expert age readings and was considered as the true age. This implies that the "true" age distribution was considered known without error in the sample considered. The data used in the analyses by stock are shown in table 11.

From table 12 it appears that the difference between the true age distributions for the mixture model method is insignificant.

Results

Summary data for the results are given in table 12 and 13 and are illustrated in Fig. 66. For the mixture analysis of Francis and Campana in general only fish length and otolith weight were included in the analyses because this gave the best estimates of the "true" age distribution.

Table 11: Data used in the age distribution analyses by species and method

			Method
Stock	Number of observations available	Stock data analysed	Francis and Campana
Eastern Channel Plaice	237	Age range	2^{-} - 6^{+}
		Year-quarter	2006 1. quarter
		Measurements Included	Log length and otolith weight
Icelandic Plaice	251	Age range	4^{-} - 7^{+}
		Year and Quarter	2006 1. quarter
		Measurements Included	Log fish length otolith weight and area
North Sea Cod	311	Age range	1- 3^{+}
		Year and Quarter	2001 3. quarter
		Measurements Included	Log fish length log otolith weight
North east Arctic Cod	527	Age range	2^{-} - 7^{+}
		Year and Quarter	2001 1. quarter
		Measurements Included	Log fish length log otolith weight
Bay of Biscay Anchovy	312	Age range	1 – 2^{+}
		Year and Quarter	2004 2. quarter
		Measurements Included	Fish length otolith major axis

Table 12: True and estimated age proportion in per cent by stock, method and age.

	Age	Method	
Stock		Francis and Campana	
		True age proportion	Age proportion
Eastern Channel Plaice	2^-	10.55	11.22
	3	18.57	18.11
	4	16.46	15.91
	5	25.74	25.54
	6^+	28.69	29.22
Icelandic Plaice	4^-	7.57	7.32
	5	14.34	14.90
	6	39.44	39.33
	7^+	38.65	38.45
North Sea Cod	1	23.47	23.27
	2	68.81	68.58
	3^+	7.72	8.15
North east Arctic Cod	2^-	4.36	4.83
	3	18.03	17.46
	4	26.00	26.67
	5	20.87	20.64
	6	17.84	17.70
	7^+	12.90	12.70
Bay of B. anchovy	1	69.87	68.69
	2^+	30.13	31.31

Table 13: Mean squared error (MSE) and relative (%) by method, stock and age

MSE*1000	Age	Method
Stock		Francis & Campana
Eastern Channel Plaice	2^-	0.19
	3	0.47
	4	0.56
	5	0.74
	6^+	0.56
Icelandic Plaice	4^-	0.28
	5	0.59
	6	0.89
	7^+	0.71
North Sea Cod	1	0.23
	2	0.36
	3^+	0.12
North east Arctic Cod	2^-	0.06
	3	0.17
	4	0.34
	5	0.22
	6	0.16
	7^+	0.09
Bay of B. anchovy	1	0.43
	2^+	0.43

Relative bias (%)		Francis & Campana
Eastern Channel Plaice	2^-	6.36
	3	-2.44
	4	-3.33
	5	-0.79
	6^+	1.85
Icelandic Plaice	4^-	-3.26
	5	3.86
	6	-0.30
	7^+	-0.49
North Sea Cod	1	-0.88
	2	-0.34
	3^+	5.67
North east Arctic Cod	2^-	10.73
	3	-3.14
	4	2.6
	5	-1.12
	6	-0.77
	7^+	-1.61
Bay of B. anchovy	1	-1.69
	2^+	3.92

Figure 66a: Mean squared error, MSE, and relative bias by method and age for Eastern Channel and Icelandic plaice. Age length key: Solid line. Francis and Campana: Dashed line. Conditional method: Thick dotted line. Automated age reading: Dotdashed line. (Note: For comparison with results from the other ageing methods, estimates based on individual age estimation are also shown.)

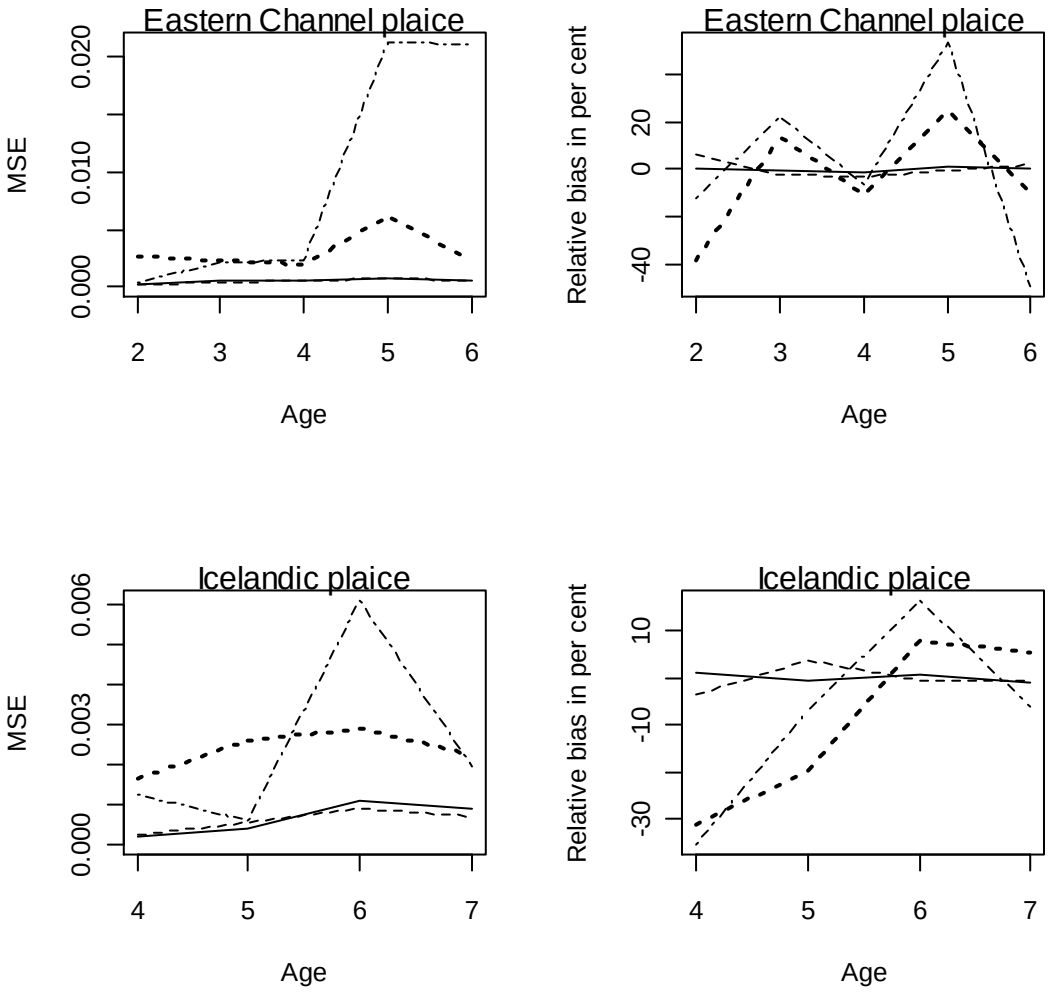

Figure 66b: Mean squared error, MSE, and relative bias by method and age for North Sea and North east arctic cod. Age length key: Solid line. Francis and Campana: Dashed line. Conditional method: Thick dotted line. Automated age reading: Dotdashed line. (Note: For comparison with results from the other ageing methods, estimates based on individual age estimation are also shown.)

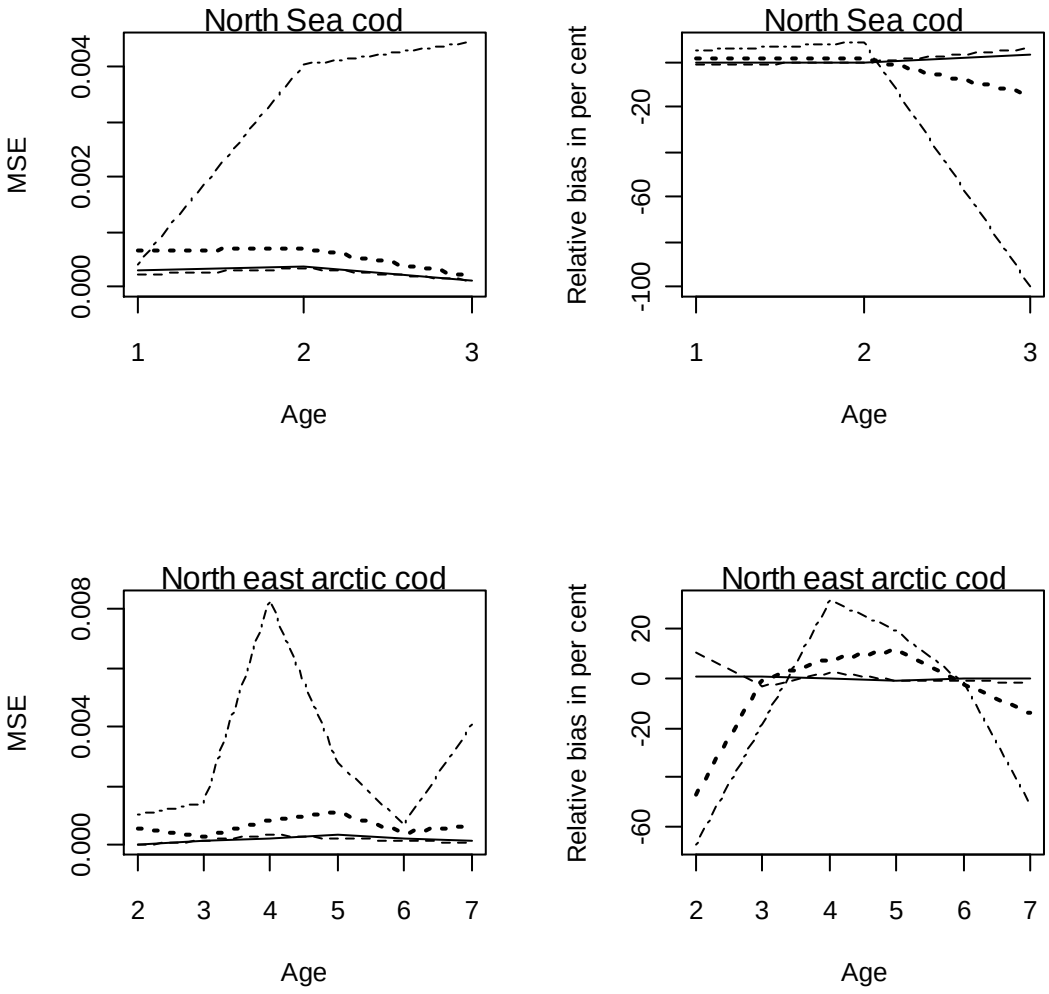

Figure 66c: Mean squared error, MSE, and relative bias by method and age for Bay of Biscay anchovy. Age length key: Solid line. Francis and Campana: Dashed line. Conditional method: Thick dotted line. Automated age reading: Dotdashed line.(Note: For comparison with results from the other ageing methods, estimates based on individual age estimation are also shown.)

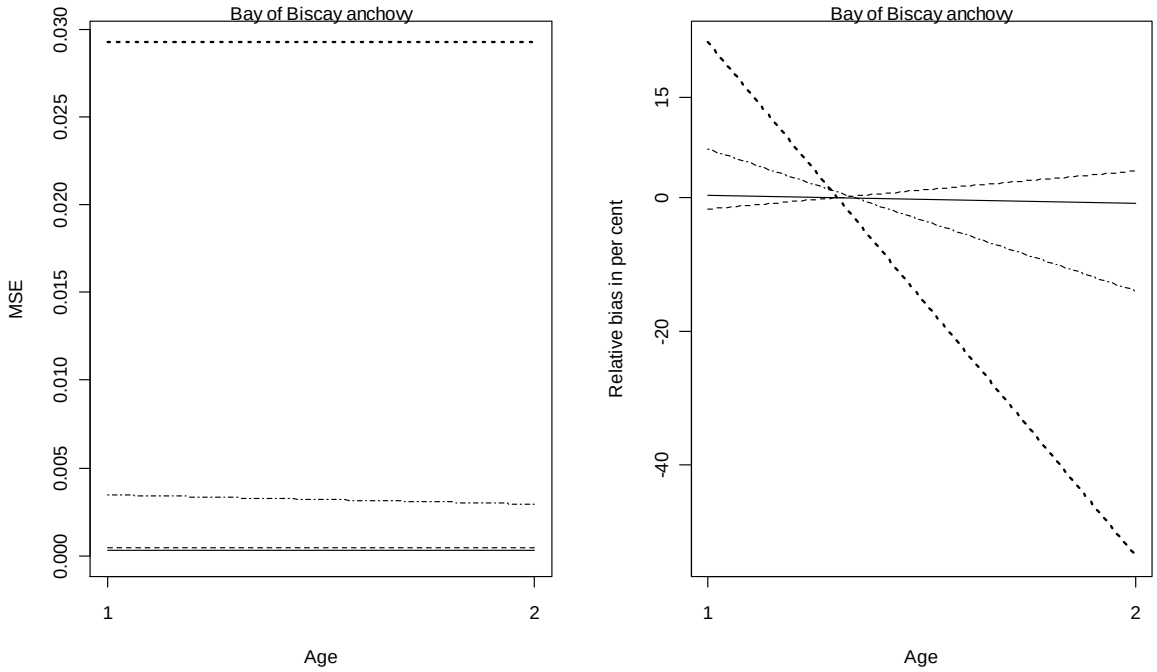

The results show that the traditional age length key (ALK) and the mixture model of Francis and Campana are the best methods as their MSE are less than MSE for the conditional and the automated age reading methods for all stocks and all age groups. The bias plots further show that the two latter methods are more biased than the ALK and mixture methods.

The ALK is a bit better than mixture model as it is practically unbiased. The biasness of the mixture model is, however, very small: The mean absolute relative bias of all five stocks and age groups is 2.8%.

The conditional method is significantly biased for the small ages for the two plaice stocks and for North east arctic cod age groups 2, 3 and 7^+ and for anchovy while the bias is limited for North Sea cod.

For the automated age reading method the bias is very large for some age groups all stocks considered: For instance the bias for Eastern Channel plaice for ages 5 and 6 is about 40% and about -50% and -60% for North east arctic cod age groups 2 and 7^+ respectively. For anchovy the bias is limited.

Conclusions

The age length key and mixture model methods seem to be preferable to the conditional and the automated age reading method.

All automated methods, both with respect to estimation of individual age and age structures are based on the use of a production (or testing) sample, where only images and otolith biometrics are available and a calibration (or learning) sample, where also individual ages are known. The demand for this two-sample data structure and particularly adequate sample sizes within the calibration/learning sample - turned out to be a factor which highly influenced the outcome of this project. We have learned that it is absolutely necessary to have a calibration/learning sample which good coverage within all age- and length classes to be useful. Using no less than half of the data available for this project as calibration sample proved to be an absolute minimum regarding data requirement. For this reason, it was not possible to evaluate the optimal constellation of sample sizes and data coverage for the calibration/learning- and production/testing samples.

▪ Cost-benefit analysis for case study I

1. Introduction

The cost-effectiveness of different ageing methods was evaluated by comparison of costs and associated bias in age structure of these method - based on the same setups of data structure across all methods.
Four methods estimating the age composition of North East Arctic cod (NEAC), North Sea cod (NSC) and Faroese Plateau (FOC) used for stock assessment and other scientific purposes were evaluated with respect to cost effectiveness. The methods considered were:

1. The traditional age length key using age and fish length information only

2. Automated age determination using digitized images of otoliths

3. The conditional method using nearest neighbour to age classify a stock based on fish length and weight and a range of otolith measurements

4. The mixture model (Francis and Campana, 2004) using the same type of information as the conditional method

2. Materials and Methods

Cost
Within WP1, costs associated with the different methods of age determination were monitored carefully. Both fixed costs related to particularly equipment and variable costs related to the different steps in the line of work were monitored. In order to evaluate the cost-effectiveness of the four methods only the variable costs associated with the preparation of individual otoliths and the four methods were used.

Benefit

To evaluate the goodness of the four methods considered the following simulation procedure was carried out:

Data on fish length and weight, otolith characteristics as major axis length, area etc. and the age determined by expert readers were available for a random sample of fish. This sample was randomly divided into two groups of equal size, for which one group was used as calibration data with the age included and the second was used as production data for which the age information were excluded. For each of the four methods the age distribution in the combined calibration and production sample (i.e. the original random sample available) was estimated based on these data. This procedure was repeated 100 times and thus resulting in 100 estimates of the age distribution in the combined calibration and production sample. As the "true" age distribution is known in this combined sample the goodness of the methods can be evaluated.

Two measures have been applied as measure of goodness: Mean squared error (MSE) and relative bias (RB):

MSE and RB have been calculated for each age group. The two measures are defined as follows:

Consider a given method and age group. Let p_i , i = 1, 2,…, 100 denote the proportion of the age group for each of the 100 simulation and let P denote the "true" age proportion. We then have

$$MSE = E(p-P)^2 \approx \frac{1}{n}\sum_{i=1}^{n}(p_i - P)^2 = \frac{1}{n}\sum_{i=1}^{n}(p_i - \overline{p})^2 + VAR(p)$$

$$RB = 100 * \frac{\overline{p} - P}{P}$$

Where E denotes the expectation of p and n denotes the number of observations. As defined here the relative bias, RB, denotes the relative bias in per cent.

MSE is a measure which includes both the biasness and the variation of a method: A small MSE indicates a good method.

In order to obtain homogenous data (i.e. individual fish data for which the relationship between age, length, and otolith characteristics is the same) fish caught in the same year and quarter were selected, in this case 1st quarter of 2001 was selected. The age of each fish was determined by expert age readings and was considered as the true age. This implies that the "true" age distribution was considered known without error in the sample considered. The data used in the analyses by method are shown in table 14.

Table 14: Data used in the age distribution analyses by species and method

			Method			
Stock	Nr. of obs. available	Stock data analysed	Automated	Conditional	Francis and Campana	Age length key
NSC	311	Age range	1- 3^+	1- 3^+	1- 3^+	1- 3^+
		Year and Quarter	2001 3. quarter	2001 3. quarter	2001 3. quarter	2001 3. quarter
		Measurements Included	Age	Fish length and weight otolith weight	Log fish length log otolith weight	Age and length
NEAC	527	Age range	2^- - 7^+	2^- - 7^+	2^- - 7^+	2^- - 7^+
		Year and Quarter	2001 1. quarter	2001 1. quarter	2001 1. quarter	2001 1. quarter
		Measurements Included	Age	Fish length and weight otolith weight, area, major and minor axes	Log fish length log otolith weight	Age and length
FOC [1, 2]	254	Age range	-	1-6	-	1-6
		Year and Quarter	-	not relevant	-	not relevant
		Measurements Included	-	Fish length otolith weight	-	Fish length otolith weight

[1] The contrast between transparent and opaque zones was too low for automatic zone detection.

[2] A requirement for the Mixture analysis is that otolith weight and fish length data are normally distributed within ages. Data from the Faeroe cod stock violated this requirement and Mixture analysis was therefore not possible.

3. Results

Cost

The variable costs associated with the different steps in the line of work for the four methods are given below in Table 15. It should be noted that the costs of "automated age determination" are associated with the production of high quality images and thus the same for both automated age estimation and Conditional model analysis. All methods involve a calibration/learning sample, and it is therefore necessary to include the cost for manual age reading in each of the methods.

Table 15: Variable costs in Euro pr. fish for measuring fish characteristics.

	Cost (€ per otolith)		
Process	NSC	NEAC	FOC
Measuring length and weight and manual age reading	2.81	5.88	2.85
Automated age determination and manual age reading	3.93	10.46	5.61
Automated age determination	2.83	7.92	4.31
Tag/recapture and pen-rearing			17.00

The table shows that the expenses pr fish for automated age determination including manual age reading are higher than measuring length, otolith weight and age, as used by the other methods.

Benefit

Summary data for the results are given in Table 16 and 17 and are illustrated in Fig. 67. The results showed that the traditional age length key (ALK) and the mixture model of Francis and Campana (2004) are the best methods as their MSE are less than MSE for the conditional and the automated age reading methods for all age groups and for all cod stocks. The largest MSE occur in the automated age estimation, while the Conditional model ranges between the two groups. With respect to bias, all methods perform almost equally well in North Sea cod for age classes 1 and 2, but bias increases dramatically for age class 3, with respect to conditional method and even more so for the automated estimation. A similar picture emerges in NEAC cod and FO cod. This may be attributable to the fact that contrast between transparent and opaque structures decreases with fish age. In the NEAC cod there seems to be an additional problem with the determination of the first winter rings, in that these age classes are also subject to heavy bias.

Table 16: True and estimated age proportion in per cent by method and age.

	Age	Method							
Stock		Automated		Conditional		Mixture model		Age length key	
		True age proportion	Age proportion	True age proportion	Age proportion	True age proportion	Age proportion	True age proportion	Age proportion
NSC	1	22.86	23.88	22.43	22.80	23.47	23.27	23.47	23.42
	2	70.48	76.59	70.64	71.30	68.81	68.58	68.81	68.64
	3^{+}	6.67	0	6.92	5.90	7.72	8.15	7.72	7.94
NEAC	2^{-}	4.64	1.50	4.36	2.32	4.36	4.83	4.36	4.41
	3	16.11	13.15	18.03	17.84	18.03	17.46	18.03	18.21
	4	26.85	35.35	26.00	28.04	26.00	26.67	26.00	25.89
	5	22.59	27.01	20.87	23.28	20.87	20.64	20.87	20.70
	6	17.78	17.53	17.84	17.39	17.84	17.70	17.84	17.86
	7^{+}	12.04	5.83	12.90	11.13	12.90	12.70	12.90	12.92
FOC [1, 2]	1	-	-	11.81	9.77	-	-	11.81	2.23
	2	-	-	30.71	26.47	-	-	30.71	26.30
	3	-	-	15.35	17.20	-	-	15.35	18.01
	4	-	-	19.29	16.07	-	-	19.29	27.06
	5	-	-	11.81	15.98	-	-	11.81	21.55
	6	-	-	11.02	14.51	-	-	11.02	4.85

[1] The contrast between transparent and opaque zones was too low for automatic zone detection.

[2] A requirement for the Mixture analysis is that otolith weight and fish length data are normally distributed within ages. Data from the Faeroe cod stock violated this requirement and Mixture analysis was therefore not possible.

Table 17: Mean squared error (MSE) and relative (%) by method, stock and age

MSE*1000	Age	Method			
Stock		Automated	Conditional	Francis and Campana	Age length key
NSC	1	0.40	0.66	0.23	0.31
	2	4.04	0.71	0.36	0.36
	3^+	4.44	0.21	0.12	0.12
NEAC	2^-	1.02	0.58	0.06	0.02
	3	1.47	0.32	0.17	0.16
	4	8.32	0.87	0.34	0.25
	5	2.83	1.09	0.22	0.33
	6	0.70	0.41	0.16	0.22
	7^+	4.12	0.69	0.09	0.15
FOC [1, 2]	1	-	0.93	-	9.32
	2	-	2.52	-	3.47
	3	-	1.25	-	1.25
	4	-	1.65	-	6.71
	5	-	2.62	-	1.30
	6	-	2.17	-	3.90

Relative bias (%)		Automated	Conditional	Francis and Campana	Age length key
NSC	1	4.47	1.65	-0.88	-0.22
	2	8.68	0.92	-0.34	-0.25
	3^+	-100.0	-14.77	5.67	2.92
NEAC	2^-	-67.64	-46.84	10.73	1.06
	3	-18.39	-1.02	-3.14	1.04
	4	31.35	7.86	2.6	-0.42
	5	19.54	11.52	-1.12	-0.81
	6	-1.37	-2.51	-0.77	0.13
	7^+	-51.58	-13.74	-1.61	0.15
FOC [1, 2]	1	-	-17.31	-	1.48
	2	-	-13.81	-	0.67
	3	-	12.03	-	0.07
	4	-	-16.68	-	-0.27
	5	-	35.29	-	-0.70
	6	-	31.63	-	-0.17

[1] The contrast between transparent and opaque zones was too low for automatic zone detection.

[2] A requirement for the Mixture analysis is that otolith weight and fish length data are normally distributed within ages. Data from the Faeroe cod stock violated this requirement and Mixture analysis was therefore not possible.

Figure 67: Mean squared error, MSE, and relative bias by method and age for North Sea cod, North East Arctic cod and Faeroe Plateau cod. Age length key: Solid line. Francis and Campana: Dashed line. Conditional method: Thick dotted line. Automated age reading: Dotdashed line.

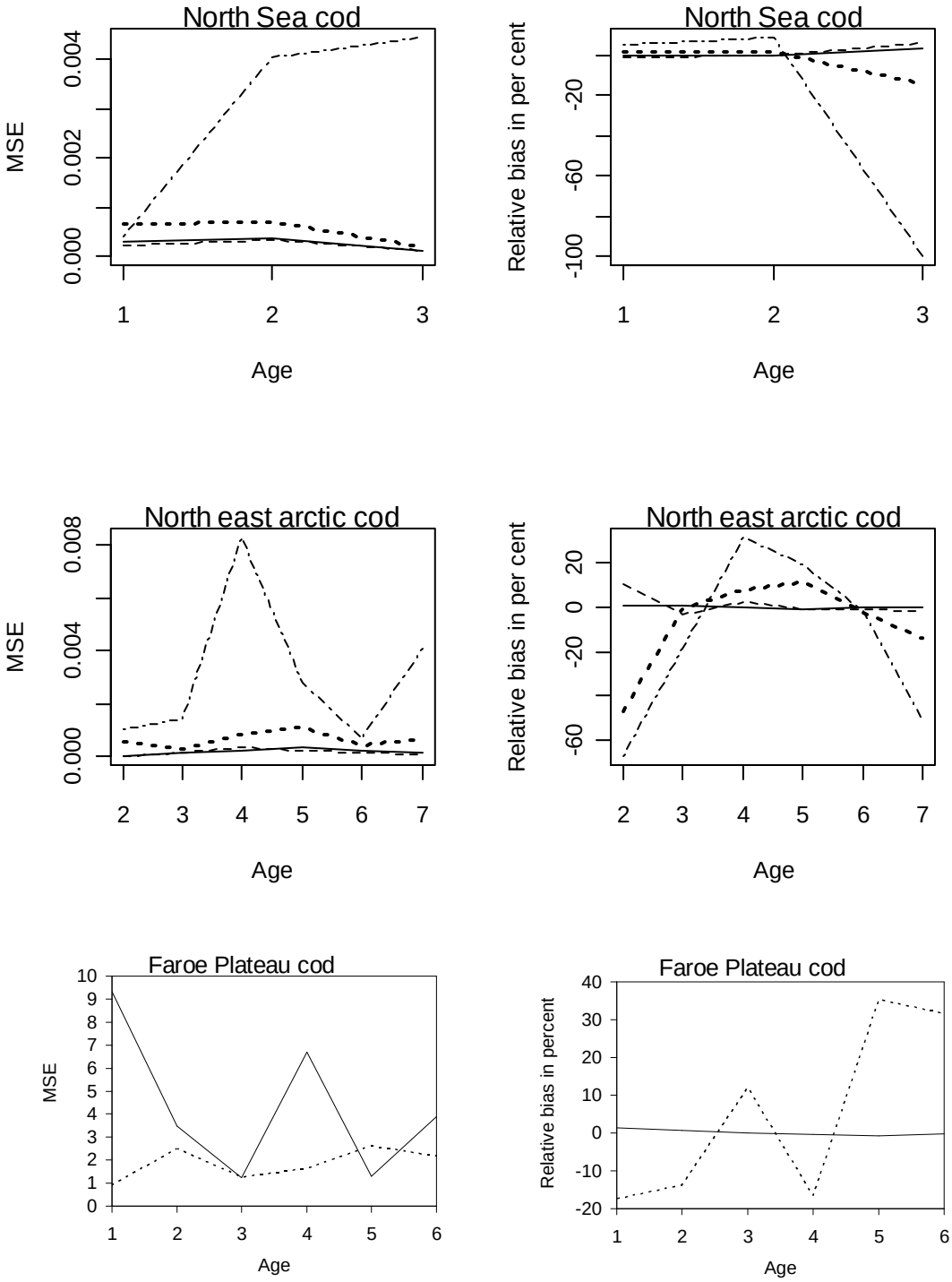

Precision and accuracy between age readers:
Since there is no known age material available for the North Sea cod, it is not possible to evaluate accuracy of individual readers or an ageing strategy. But precision between readers was evaluated for the year 2001. In this stock, age determination is considered as relatively easy due to clearly defined zonations. The results (Table 18) indicate, that this particularly applies to fish older than age 1, as the classification error as proportion of deviating age estimates between two readers. Age estimates of reader 1 were assumed to be true, due to this reader's great expertise.

Table 18: Classification error of traditional age readings in North Sea cod, disaggregated by age.

Age	Total nr	Proportion
1	108	0.14
2	290	0.02
3	18	0.00

Similarly, the precision between readers was evaluated for the Faeroe Plateau cod stock based on the age readings of two Danish, one Swedish and one Faroese expert readers. The classification errors in proportion of the total analysed otoliths for all readers, as well as the mode of these readings are shown in Table 19. The results clearly show that the Faroese readers achieve higher accuracy, but only if information on catch date and fish length is available.

Table 19: Classification error of traditional age readings with different levels of background information in Faeroe Plateau cod. FPP= Faeroe Plateau, pen-reared, FPR= Faeroe Plateau, recapture, DK1,2= Danish readers, Se= Swedish reader, FO= Faroese reader. Information level: Low= no information, Intermediate = fish length only, High= fish length and capture date.

Sample size		146	29
Level of information	Reader	FPP	FPR
Low	DK1	0.53	0.92
Low	DK2	0.61	0.44
Low	SE	0.49	0.32
Low, but expert on cod populations	FO	0.00	0.87
Intermediate	DK1	0.58	0.40
Intermediate	DK2	0.23	0.54
Intermediate, but expert on cod population	FO	0.01	0.05
High	DK1	0.63	0.82
High	DK2	0.25	0.70
Mode ($DK1_{low}$, $DK2_{low}$, SE_{low}, $DK2_{intermed}$, $DK2_{intermed}$)		0.22	0.41
Mode (all readings)		0.05	0.48

This table was published in similar for in Doering-Arjes *et al*. (2008)

Discussion

North East Arctic cod:

NEAC are managed using age-based models. In general terms, acquisition of age data from otolith readings has a high associated cost and some additional problems like the impact of ageing errors particularly when readings have to be done by different laboratories and readers.

Five national institutions are currently involved in estimate age of NEAC which are used in assessment; Norway, Russia, Germany, Spain and Poland, where the two former national institutions estimate age from most of the otoliths. NEAC otoliths are regarded as a rather difficult to interpret with the inclusion of many false zones. International otolith exchange of NEAC otoliths arranged in 2005-2006 (Woods, 2006) revealed rather low precision of age estimate with average percent agreement relative to modal age of 61% and average CV 26%. Inter-reader bias test showed that there are significant differences in age estimates between readers from different institutions. Precision of age estimate between Russian and Norwegian age readers, which produces the majority of the age estimates for assessment of NEAC, is monitored annually and is regarded as satisfactory although there is sign of relative bias between the institutions (Zuykova *et al*. 2009). An automated age system for NEAC otoliths could improve age consistency and thereby reducing the subjective interpretation of the otolith structures.

As is seen from the results, however, automated ageing by the method analyzed cannot be justified due to the much larger variance as well as bias compared to the other (and cheaper) methods. The pessimistic results can be explained by the fact that the cod otolith images have particular complications in terms of a non-homogenous brightness background, complicating the possibility of segmenting the annual zones by intensity thresholding. In addition, the shapes of the zones are partially very abrupt as opposed to the smooth zones in for example plaice otoliths. The different zones in one and the same otolith also may vary substantially in shape. NEAC experience low temperature, and also low temperature amplitude, resulting in low somatic growth rate. This is manifested in the otoliths as narrow growth increments and low contrast between winter and summer zones in many cases which complicates automatic segmenting of the zones. There is also often a problem with non-annual (false) zones, which when misinterpreted gives overestimated fish ages.

Manual age reading of NEAC is also superior to automated age determination in terms of costs. Although much time is invested in training new readers for manual age determination due to the complexity of the otolith morphology, the reading procedure itself is cost-effective. This is mainly due to reduced time spent on otolith preparation by the method of manually breaking the otoliths prior to age reading.

North Sea cod:

The experience from institutes working with central North Sea cod otoliths is that they are relatively easy to read and produce digitised images with clear annual growth structures. No known-age material exists for this stock, so the focus within this stock was on the precision between strategies. The analyses are based on otolith samples from standard sectioning of imbedded otoliths. Digitised images were produced after careful evaluation of the optimal light settings.

For the evaluation of between-reader precision, the age estimates of a relatively inexperienced reader were used, together with those with a highly experienced reader. This reader had over

30 years of experience and remarkable consistency in readings, thus his readings were used as reference ages. Precision between readers is very high, particularly in fish older than age 1.
For these reasons it is not surprising that the ALK method yielded highly precise and unbiased results. The Mixture model and the Conditional model performed likewise very well. The mean estimated age proportions of the Mixture model did not differ significantly from the true proportions. A single run of the model for which data in the production data set is not used indicates that if the calibration and the production samples are of the same size the uncertainty obtained using only the calibration sample can be reduced with 20% using the information contained in the production sample. As the production sample most often is much bigger that the calibration sample the Mixture model seems to constitute a useful exploitation of the data available. At the same time, the costs associated with these precisions are relatively low. With the data available, it was not possible to evaluate the best combination of calibration- and production sample. But from the present results it is evident, that for North Sea cod, the Mixture model approach is worth further examination.
Surprisingly, the automated age estimation based on image analysis performed not as well as anticipated based on the high-contrast images available. Particularly for the oldest age class, bias was considerable. This seems to indicate that the standard procedure used for age determination (embedding in polyester resin, sectioning and covering with glass slide) does not yield images of sufficient quality for automatic zone detection. It also highlights that the human eye has the ability to integrate visual information over an entire image, and are thus able to follow structures that may not easily be recognised by the algorithms developed so far.

In conclusion, from the results obtained within the AFISA project, we have learned that manual age reading by expert readers seems superior to automated age determination both in terms of benefit (i.e.) precision, but also in terms of costs. Although much time is invested in training new readers for manual age determination due to the complexity of the otolith morphology, the reading procedure itself is cost-effective.

Faeroe Plateau cod:
The sample of the Faeroe cod is not comparable with the other stocks, since these samples originate from fish that were reared, marked and either released into the wild or kept in pen-cages. Thus, the fish were all hatched the same year, but were recaptured after different numbers of year at liberty. The age/length relationships thus obtained may therefore differ significantly from distributions within traditional samples, where the “endpoint” is the same, but hatch dates differ. The material consists of 109 recaptured fish and 142 pen-reared fish. Pen-reared fish were sampled once a year, while recaptures occurred throughout the year (Doering-Arjes *et al*., 2008). These known-age cod otoliths were used for demonstrating accuracy and precision of the different strategies.
What is striking in this stock, compared to the other cod stocks, is the large error associated with traditional age reading (and thus the MSE in the ALK method). Classification errors of 1-5% have been documented for expert Faroese readers, if the reader was provided with detailed information on catch date fish size, but much higher if this information was not provided (Doering-Arjes *et al*., 2008). This is caused by the formation of the transparent “winter ring”, which is out of phase with the annual cycle. Depending on the time of the year the fish was captured, the final transparent ring has either to be counted – or neglected. For a reader not used to read the Faroese cod stock (as in the case of the Danish and Swedish readers), accuracy is between 40-50%, regardless of the degree of background information. This may be one of the reasons that MSE in the ALK is much larger compared to the other

stocks. This result certainly highlights the fact that traditional age reading in Faroese cod should only be done by well-trained, experienced readers.
The large error in age reading has its direct cause in the visual appearance of the otolith. Sea surface temperatures in Faeroe waters range between 7 ^{o}C. in winter and 10 ^{o}C. in summer. This amplitude in temperature range is very small compared to that found in other geographical areas. Since the otolith microstructure is strongly linked to this temperature cycle, it is not surprising that the contrast between opaque and transparent zones is extremely limited. This lack in contrast is also the reason that the development of an automated ageing system based on otolith images may never be successful – or even impossible - for the Faroese cod stocks.
With respect to the estimation of age structures, the Conditional model based on otolith weight and fish length did not result in conclusive results. Both error and bias were relatively large. Age proportions were underestimated for ages 1, 2 and 4, and overestimated in age 3. In ages 5 and 6, overestimation was the highest in all stocks. It is impossible to evaluate, whether this is a result of the sample setup (common birth date, different years of capture). It is known that there is a highly significant year effect which affects otolith growth rate (and thus also otolith shape) in Faroese cod (Cardinale *et al*., 2004). The fact that fish from the present data set all originated from the same year may have led to a more uniform fish- and otolith size distribution within individual age classes – which in turn be the reason for the large bias. For this method to be a useful option to replace the traditional ALK, it is necessary with an evaluation of the effect of sample origin. Also larger samples sizes are needed for proper calibration of the training sample.

In conclusion, the results from the Faeroe cod stock demonstrate the urgent need for the establishment of known-age material, as the bias in all methods is considerable – and larger than in the other stocks, where age was assumed to be reliably estimated by expert readers. The disadvantage of such an exercise is the large costs per otolith. It also shows that automated age estimation is not possible for all stocks, so that the traditional use of ALK may still be preferable in some cases.

References

Cardinale, M., Doering-Arjes, P., Kastowsky, M., Mosegaard, H. (2004) Effects of sex, stock, and environment on the shape of known-age Atlantic cod (*Gadus morhua*) otoliths. Can. J. Fish. Aquat. Sci. 61:158-167.

Doering-Arjes, P., Cardinale, M., Mosegaard, H. (2008) Estimating population age structure using otolith morphometrics: a test with known-age Atlantic cod (*Gadus morhua*) individuals. Can. J. Fish. Aquat. Sci. 65:2342-2350.

Francis R.I.C.C. and Campana S.E. (2004) Inferring age from otolith measurements: a review and a new approach. Can. J. Fish. Aquat. Sci. 61: 1269–1284.

Zuykova, N.V., Koloskova, V.P., Mjanger, H., Nedreaas, K.H., Senneset, H., Yaragina, N.A., Ågotnes, P. and Aanes, S. 2009. Age determination of Northeast Arctic cod through 50 years of history. Journal: Marine Biology Research 5: 66-74.

Woods, F. 2006. Analysis of Data from the Area II Cod (Gadus Morhua) Otolith International Exchange Scheme 2005/2006. Report to ICES group PGCCDBS.

▪ Cost-benefit analysis for case study II (plaice)

Methodology

Four methods estimating the age composition of plaice stocks used for stock assessment and other scientific purposes were evaluated with respect to cost effectiveness. The methods considered were:

5. The traditional age length key using age and fish length information only (Strategy SA).

6. Automated age determination using digitized images of otoliths (Strategy SB).

7. The conditional method using nearest neighbour to age classify a stock based on fish length and weight and a range of otolith measurements (Strategy SC).

8. The mixture model (Francis and Campana, 2004) using the same type of information as the conditional method (Strategy SC).

To evaluate the goodness of the four methods considered the following simulation procedure was carried out:

Data on fish length and weight, otolith characteristics such as major axis length, area etc. and the age determined by expert readers were available for a random sample of fish. This sample was randomly divided into two groups of equal size, of which one group was used as calibration data with the age included and the second was used as production data for which the age information was excluded. For each of the four methods the age distribution in the combined calibration and production sample (i.e. the original random sample available) was estimated based on these data. This procedure was repeated 100 times and thus resulting in 100 estimates of the age distribution in the combined calibration and production sample. As the "true" age distribution is known in this combined sample the goodness of the methods can be evaluated.

Two measures have been applied as measures of goodness: Mean squared error (MSE) and relative bias (RB):

MSE and RB have been calculated for each age group. The two measures are defined as follows:

Consider a given method and age group. Let p_i, i = 1,2,…, 100 denote the proportion of the age group for each of the 100 simulation and let P denote the "true" age proportion. We then have

$$MSE = E(p-P)^2 \approx \frac{1}{n}\sum_{i=1}^{n}(p_i - P)^2 = \frac{1}{n}\sum_{i=1}^{n}(p_i - \overline{p})^2 + VAR(p)$$

$$RB = 100 * \frac{\bar{p} - P}{P}$$

Where *E* denotes the expectation of *p* and *n* denotes the number of observations. As defined here the relative bias, RB, denotes the relative bias in per cent.

MSE is a measure which includes both the biasness and the variation of a method: A small MSE indicates a good method.

In order to obtain homogenous data (i.e. individual fish data for which the relationship between age, length, and otolith characteristics is the same) fish caught in the same year and quarter were selected, in this case the 1st quarter of 2006 was selected. The age of each fish was determined by expert age readings and was considered as the true age. This implies that the "true" age distribution was considered known without error in the sample considered. The data used in the analyses by method are shown in table 20.

Table 20: Data used in the age distribution analyses by species and method

			Method			
Stock	Number of observations available	Stock data analysed	Automated	Conditional	Francis and Campana	Age length key
Eastern Channel Plaice	237	Age range	2^{-} - 6^{+}	2^{-} - 6^{+}	2^{-} - 6^{+}	2^{-} - 6^{+}
		Year-quarter	2006 1. quarter	2006 1. quarter	2006 1. quarter	2006 1. quarter
		Measurements Included	Age	Fish length, otolith weight, area, major and minor axes and perimeter	Log length and otolith weight	Age and length
Icelandic Plaice	251	Age range	4^{-} - 7^{+}	4^{-} - 7^{+}	4^{-} - 7^{+}	4^{-} - 7^{+}
		Year and Quarter	2006 1. quarter	2006 1. quarter	2006 1. quarter	2006 1. quarter
		Measurements Included	Age	Fish length and weight otolith weight, area, major and minor axes and perimeter	Log fish length otolith weight and area	Age and length

Results

Summary data for the results are given in table 21 and 22 and are illustrated in Fig. 68.

The results show that the traditional age length key (ALK) and the mixture model of Francis and Campana are the best methods as their MSE are less than MSE for the conditional and the automated age reading methods for both stocks and all age groups. The bias plots further show that the two latter methods are more biased than the ALK and mixture methods.

The ALK is a bit better than mixture model as it is practically unbiased. The biasness of the mixture model is, however, very small

The conditional method is significantly biased for the small ages for the two plaice stocks.

For the automated age reading method the bias is very large for some age groups for all stocks considered: For instance the bias for Eastern Channel plaice for ages 5 and 6 is about 40% and about -50% and -60%.

Table 21: True and estimated age proportion in per cent by method and age.

	Age	Method							
Stock		Age length key		Automated		Conditional		Francis and Campana	
		True age %	Age %	True age %	Age %	True age %	Age %	True age %	Age %
Eastern Channel Plaice	2^-	10.55	10.59	11.74	10.24	10.50	6.44	10.55	11.22
	3	18.57	18.47	18.22	22.22	18.49	20.96	18.57	18.11
	4	16.46	16.28	16.60	15.57	16.39	14.58	16.46	15.91
	5	25.74	25.98	25.10	38.59	25.63	31.96	25.74	25.54
	6^+	28.69	28.69	28.34	14.20	28.99	26.06	28.69	29.22
Icelandic Plaice	4^-	7.57	7.66	9.15	5.90	7.57	5.22	7.57	7.32
	5	14.34	14.30	13.31	12.41	14.34	11.54	14.34	14.90
	6	39.44	39.73	40.33	47.07	39.44	42.55	39.44	39.33
	7^+	38.65	38.22	37.21	35.04	38.65	40.69	38.65	38.45

Table 22: Mean squared error (MSE) and relative (%) by method, stock and age.

MSE*1000		Method			
Stock	Age	Age length key	Automated	Conditional	Francis and Campana
Eastern Channel Plaice	2^-	0.28	0.45	2.69	0.19
	3	0.52	2.13	2.27	0.47
	4	0.58	2.24	1.93	0.56
	5	0.78	21.3	6.20	0.74
	6^+	0.59	21.1	2.25	0.56
Icelandic Plaice	4^-	0.21	1.28	1.68	0.28
	5	0.43	0.63	2.62	0.59
	6	1.09	6.09	2.88	0.89
	7^+	0.89	1.96	2.26	0.71

Relative bias (%)		Age length key	Automated	Conditional	Francis and Campana
Eastern Channel Plaice	2^-	0.37	-12.81	-38.69	6.36
	3	-0.51	21.96	13.36	-2.44
	4	-1.08	-6.19	-11.01	-3.33
	5	0.92	53.73	24.71	-0.79
	6^+	-0.02	-49.91	-10.13	1.85
Icelandic Plaice	4^-	1.14	-35.56	-31.00	-3.26
	5	-0.31	-6.77	-19.57	3.86
	6	0.72	16.70	7.88	-0.30
	7^+	-0.84	-5.83	5.30	-0.49

Figure 68: Mean squared error, MSE, and relative bias by method and age for Eastern Channel and Icelandic plaice. Age length key: Solid line. Francis and Campana: Dashed line. Conditional method: Thick dotted line. Automated age reading: Dotdashed line.

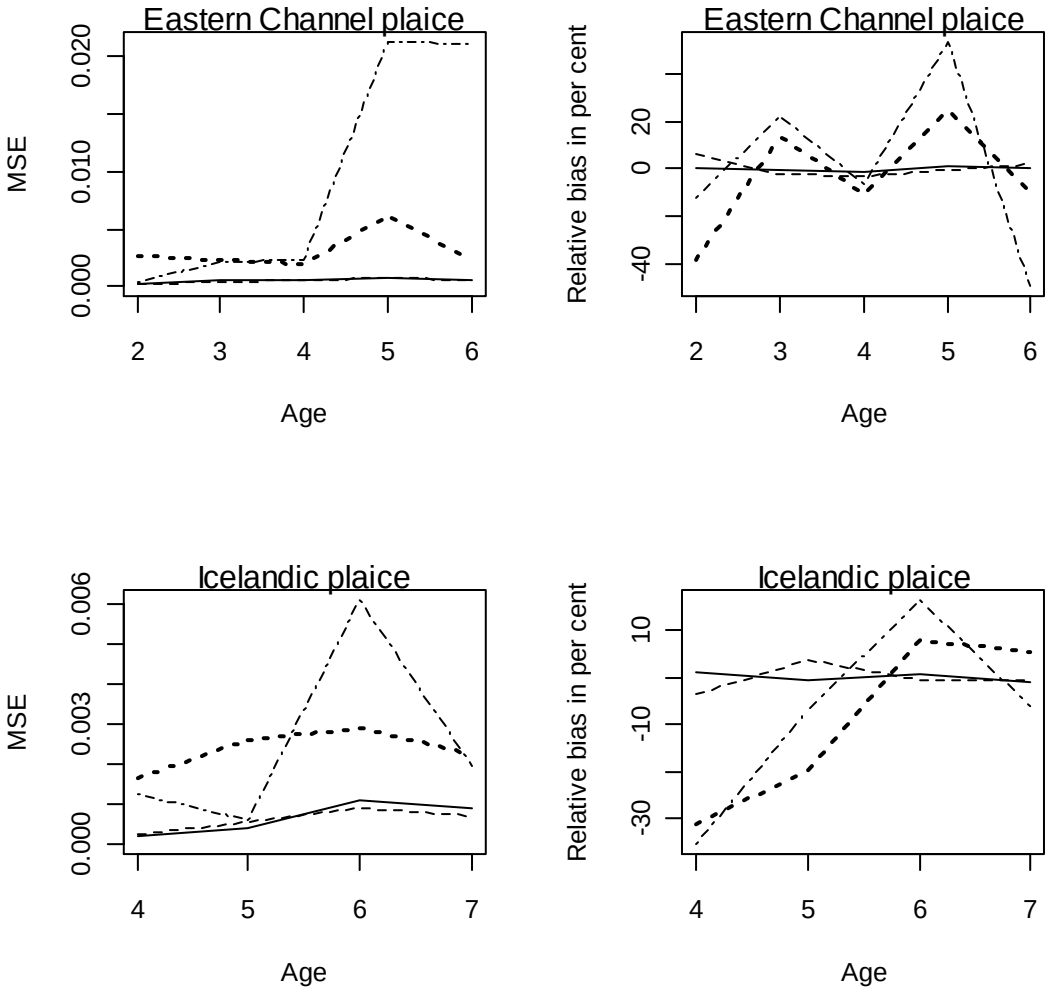

Discussion

***Eastern Channel and Icelandic Plaice*:**
The age length key and mixture model methods seem to be preferable to the conditional and the automated age reading methods. In particular the automated age reading method developed so far for plaice is too biased to be used in practical assessment. It is an open question whether the bias for plaice could be reduced by increase of the number of fish analysed.
In order to further enlighten the potential of the methods, the variable costs in connection with the methods are given in table 23.

Table 23: Variable costs in Euro pr. fish by stock for measuring fish characteristics.

Process	E. Channel Plaice	Icelandic Plaice
Measuring length and weight and manual age reading	2.13	5.37
Automated age determination and manual age reading	2.47	6.24
Automated age determination	1.38	3.03

The table shows that the expenses per fish for automated age determination including manual age reading are higher than measuring length, otolith weight and age, as used by the other methods. On the other hand for plaice the expenses of automated age reading for a production sample is lower than for the other methods. Hence, if the automated method could be significantly improved it could be a potential candidate for plaice.

The mixture model applies both a calibration and a production data set, while the age length key applies the calibration data set only. This may imply that the ALK may be preferable because it is cheaper than the mixture model. However, the comparisons carried out assumed that the production data set is of the same size as the calibration data set. Hence, it is still an open question whether an increase of the production sample may improve the performance of the mixture model so much that the ALK is outperformed. To examine that requires further data on fish and otolith characteristics or simulations.

Like for most of European fish stocks, Eastern Channel and Icelandic plaice are managed using age-based models. In general terms, acquisition of age data from otolith readings has a very high associated cost and some additional problems like the impact of ageing errors especially when reading has to be done by different laboratories and readers.

In the case of Eastern Channel Plaice only two European institutes (CEFAS and IFREMER) are involved in the interpretation of otoliths for stock assessment and both of them participate in inter-calibration workshops. The results of the 2002 workshop on VIId plaice age determination indicated that the level of agreement and precision for individual plaice age reading was very satisfactory between the institutes contributing to the assessment with an average agreement of 85.7 %. Despite these good results in terms of accuracy and precision it is true that expenses associated with traditional age interpretation are high and that problems

could arise with the incorporation of new readers. Therefore, the development of automated ageing systems would provide a means to standardize ageing among laboratories and readers and to control ageing consistency while reducing the cost of the acquisition of age data, training of new readers, etc.

From the results obtained in this study, the age-length keys method (ALK) seems to be the best methodology among the tested ones, since it has got the lower error associated to the calculation of plaice age structure. Moreover it has to be considered that although previous calibration it is needed, age interpretation based on somatic length and weight reduces the cost associated to age analysis since cost related to otolith extraction could be partially eliminated. So, the cost would be even lower than those showed in table 4 (2.13 € per fish for Eastern Channel Plaice and 5.37 € for Icelandic Plaice). Nevertheless, we have also to consider that those results refer exclusively to a sample obtained for one year, one quarter and five age classes and that error would probably increase when inter-annual variability would be include in the analysis. The inclusion of older ages would increase significantly the error since the decreasing in growth rates for older fish will reduce the difference in length among older age groups. Although additional analysis would need to be done, the ALK method seems to be adequate when huge quantities of plaice coming from homogeneous samples (same year and season and area) have to be aged.

Regarding automated ageing methodology; the error obtained, is low up to age 4 then rises significantly. However the cost associated with the automated methodology is lower than that associated with the traditional methods of age determination. Therefore, at this point it seems that there is some potential for the automated method to provide results that could offer similar precision for fish up to age 4 at a lower cost than traditional methods. After age 4 the bias increases significantly for the automated method and so the results are poorer from a cost benefit point of view. The advantages that the automated methodologies give in terms of objectivity in readings and reduction of costs in terms of training of new readers must be taken into account. Therefore, it can not be discarded that a higher degree of automation in the image acquisition processes and a further improvement of the automated methodologies could lead to a reduction in the cost/benefit ratio for automated methodologies in future in the case of eastern channel and Icelandic plaice.

The conditional method using nearest neighbour to age classify plaice based on fish length and weight and otolith characteristic does not offer any additional advantage except the objectivity of the methodology. The error associated to this method is very high, and cost levels are similar to that showed for automated methodologies. In the case of the Francis and Campana's mixture method the cost are similar but in contrast it offers very good results in terms of precision.

The comparison of the two methods with lowest error (ALK and the mixture model) indicates that the ALK may be preferable with regard to plaice stocks because it is cheaper than the mixture model. In general terms, from the results obtained in this study additional work seems to increase precision at a lower cost so advantages associated to the elimination of reader's subjectivity may lead to lower cost/benefit ratios in the case of Eastern Channel and Icelandic plaice stocks. Both ALK and mixture models give very low error levels.

The comparisons carried out assumed that the calibration data set is of the same size as the production data set, which has a deep influence on final cost. Furthermore if we consider the advantage of the objectivity and the reduction of training expenses a significant reduction of

cost-benefit ratios of these methodologies compared to traditional one would be expected. To examine that requires further data on fish and otolith characteristics or simulations.

References

Fablet, R., Le Josse, N. (2005) Automated fish age estimation from otolith images using statistical learning, Fisheries research, 72(2-3): 279-290.

Francis R.I.C.C. and Campana S.E. (2004) Inferring age from otolith measurements: a review and a new approach. Can. J. Fish. Aquat. Sci. 61: 1269–1284.

▪ Cost-benefit analysis for case study III (anchovy)

Methodology

Four methods estimating the age composition of anchovy stocks used for stock assessment and other scientific purposes were evaluated with respect to cost effectiveness. The methods considered were:

9. The traditional age length key using age and fish length information only (Strategy SA).

10. Automated age determination using digitized images of otoliths (Strategy SB).

11. The conditional method using nearest neighbour to age classify a stock based on fish length and weight and a range of otolith measurements (Strategy SC).

12. The mixture model (Francis and Campana, 2004) using the same type of information as the conditional method (Strategy SC).

To evaluate the goodness of the four methods considered the following simulation procedure was carried out:

Data on fish length and weight, otolith characteristics as major axis length, area etc. and the age determined by expert readers were available for a random sample of fish. This sample was randomly divided into two groups of equal size, for which one group was used as calibration data with the age included and the second was used as production data for which the age information were excluded. For each of the four methods the age distribution in the combined calibration and production sample (i.e. the original random sample available) was estimated based on these data. This procedure was repeated 100 times and thus resulting in 100 estimates of the age distribution in the combined calibration and production sample. As the "true" age distribution is known in this combined sample the goodness of the methods can be evaluated.

Two measures have been applied as measure of goodness: Mean squared error (MSE) and relative bias (RB):

MSE and RB have been calculated for each age group. The two measures are defined as follows:

Consider a given method and age group. Let p_i, i = 1,2,…, 100 denote the proportion of the age group for each of the 100 simulation and let P denote the "true" age proportion. We then have

$$MSE = E(p-P)^2 \approx \frac{1}{n}\sum_{i=1}^{n}(p_i - P)^2 = \frac{1}{n}\sum_{i=1}^{n}(p_i - \overline{p})^2 + VAR(p)$$

$$RB = 100 * \frac{\overline{p} - P}{P}$$

where E denotes the expectation of p and n denotes the number of observations. As defined here the relative bias, RB, denotes the relative bias in per cent.

MSE is a measure which includes both the biasness and the variation of a method: A small MSE indicates a good method.

In order to obtain homogenous data (i.e. individual fish data for which the relationship between age, length, and otolith characteristics is the same) fish caught in the same year and quarter were selected, in this case 2nd quarter of 2004 was selected. The age of each fish was determined by expert age readings and was considered as the true age. This implies that the "true" age distribution was considered known without error in the sample considered. The data used in the analyses by method are shown in table 24.

Table 24: Data used in the age distribution analyses by species and method

			Method			
Stock	**Number of observations available**	**Stock data analysed**	**Age length key**	**Automated**	**Conditional**	**Francis and Campana**
Bay of Biscay Anchovy	312	**Age range**	$1 - 2^+$	$1 - 2^+$	$1 - 2^+$	$1 - 2^+$
		Year and Quarter	2004 2. quarter	2004 2. quarter	2004 2. quarter	2004 2. quarter
		Measurements Included	Age and length	Age	Fish length and weight otolith, area, major and minor axes and perimeter	Fish length otolith major axis

Results

Summary data for the results are given in table 25 and 26 and are illustrated in Fig. 69. The results showed that the traditional age length key (ALK) and the mixture model of Francis and Campana (2004) are the best methods as their MSE are less than MSE for the conditional and the automated age reading methods all age groups of anchovy.

Table 25: True and estimated age proportion in per cent by method and age.

	Method							
Age	**Age length key**		**Automated**		**Conditional**		**Francis and Campana**	
	True age %	**Age %**	**True age %**	**Age %**	**True age %**	**Age %**	**True age %**	**Age %**
1	69.87	70.12	68.34	73.28	69.77	85.98	69.87	68.69
2^+	30.13	29.88	31.66	27.25	30.23	14.02	30.13	31.31

Table 26: Mean squared error (MSE) and relative (%) by method, stock and age

		Method			
Error estimation	**Age**	**Age length key**	**Automated**	**Conditional**	**Francis and Campana**
MSE*1000	1	0.32	3.44	29.26	0.43
	2^+	0.32	2.94	29.26	0.43
Relative Bias (%)	1	0.35	7.23	23.22	-1.69
	2^+	-0.82	-13.94	-53.60	3.92

Figure 69: Mean squared error, MSE, and relative bias by method and age for Bay of Biscay anchovy. Age length key: Solid line. Francis and Campana: Dashed line. Conditional method: Thick dotted line. Automated age reading: Dotdashed line.

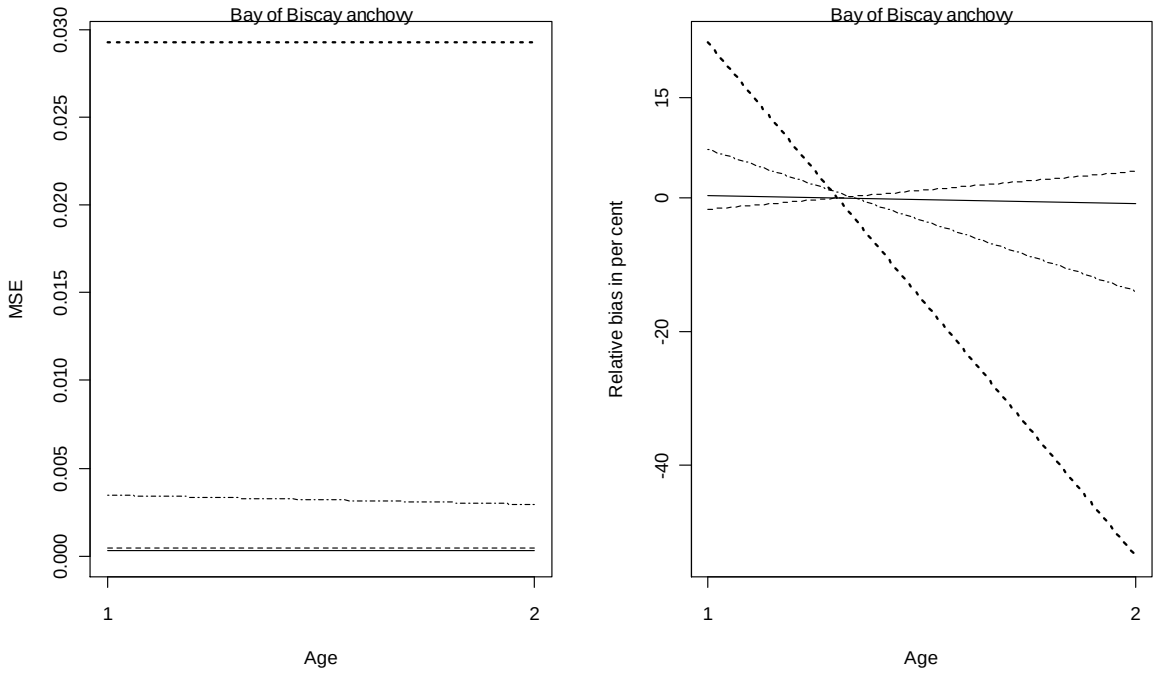

Cost associated to the different age estimation methodologies are indicated in Table 27.

Table 27: Variable costs in Euro pr. fish for measuring fish characteristics.

Process	Cost (€)
Measuring length and weight and manual age reading	6.50
Automated age determination and manual age reading	9.71
Automated age determination	7.74

Discussion

Like for most of European fish stocks, anchovy in the Bay of Biscay are managed using age-based models. In general terms, acquisition of age data from otolith readings has a very high associated cost and some additional problems like the impact of ageing errors specially when readings has to be done by different laboratories and readers.

In the case of anchovy only three European institutes (IEO, AZTI and IFREMER) are involved in the interpretation of anchovy otoliths for stock assessment and all of them participate in inter-calibration workshops. The results of the last workshop on anchovy otolith indicated that the level of agreement and precision for individual anchovy age reading determinations was highly satisfactory with an average agreement of 92.7 % among readers of these three institutes (Uriarte *et al*., 2002a, b, 2006). Despite these good results in terms of accuracy and precision is true that expenses associated to traditional age interpretation are high and that problems could arise with the incorporation of new readers. Therefore, the

development of automated ageing systems would provide a mean to standardize ageing among laboratories and readers and to control ageing consistency while reducing the cost of the acquisition of age data, training of new readers, etc.

In this context, anchovy appears to be well adapted to automated methods based on classification settings (Fablet & Le Josse, 2005). Otolith morphology has been shown to be clearly related to age but due to the presence of numerous checks or false rings, the interpretation of these otoliths depends on the discrimination of actual growth rings from the latter. This problem has frequently exposed among experts readers in anchovy workshops (Urairte *et al*., 2002 a, b, 2007). For the above mentioned reasons, the anchovy case-study may be considered within the framework of the AFISA project as a relevant case-study to test for the robustness of the proposed automated systems.

From the results obtained in this study, the age-length keys method (ALK) seems to be the best methodology among the tested ones, since it has got the lower error associated to the calculation of anchovy age structure. Moreover it has to be considered that although previous calibration it is needed, age interpretation based on somatic length and weight reduces the cost associated to age analysis since cost related to otolith extraction could be partially eliminated. So, the cost would be even lower than those showed in table 4 (6,5 € per fish). Nevertheless, we have also to consider than those results refers exclusively to a sample obtained for one year, one quarter and two age classes and that error would probably increase when inter-annual variability would be include in the analysis. The inclusion of ages 3 (or even 4) would increase significantly the error since the decreasing in growth rates for old anchovy will reduce the difference in length among older ages groups (2 and olders). Although additional analysis would be necessary to be done, the ALK method seems to be adequate when huge quantities of anchovy coming from homogeneous samples (same year and season and area) have to be aged.

Regarding automated ageing methodology, the error obtained, is low. Nevertheless, the cost associated to automated methodology is higher as a consequence of the image acquisition processes. Therefore, at this point does not seem that the result obtained by automated methodologies for age estimation in anchovy can improve the results in terms of precision or cost obtained by traditional methodology, having poorer results from the cost-benefit point of view. In any case, it cannot be forgotten the advantages that automated methodologies gives in terms of objectivity in readings and reduction of costs in terms of training of new readers. Therefore, it can not be discarded that a higher degree of automation in the image acquisition processes and a further improvement of the automated methodologies could lead to reduce the cost/benefit ratio for automated methodologies in future in the case of anchovy.

The conditional method using nearest neighbour to age classify anchovy stock based on fish length and weight and otolith characteristic does not offer any additional advantage except the objectivity of the methodology. The error associated to this method is very high, overestimating age 1 in more than 20% and cost levels are similar to that showed for automated methodologies. In the case of the Francis and Campana's mixture method the cost are similar but in contrast it offers very good results in terms of precision.

The comparison of the two methods with lowest error (ALK and the mixture model) indicates that the ALK may be preferable because it is cheaper than the mixture model. In general terms, from the results obtained in this study additional work seems to increase precision at a lower cost so as advantages associated to the elimination of reader's subjectivity may lead to

lower cost/benefit ratios in the case of anchovy stock in the Bay of Biscay. Both ALK and mixture models give very low error levels, although imply higher cost than traditional methodology. However, the comparisons carried out assumed that the production data set is of the same size as the production data set which has a deep influence on final cost. Hence, it is still an open question whether an increase of the production sample may improve the performance of the mixture model so much that the traditional methodology is outperformed. Furthermore if we consider the advantage of the objectivity and the reduction of training expenses a significant reduction of cost-benefit ratios of these methodologies compared to traditional one would be expected. To examine that requires further data on fish and otolith characteristics or simulations.

References

Fablet, R., Le Josse, N. (2005) Automated fish age estimation from otolith images using statistical learning, Fisheries research, 72(2-3): 279-290.

Francis R.I.C.C. and Campana S.E. (2004) Inferring age from otolith measurements: a review and a new approach. Can. J. Fish. Aquat. Sci. 61: 1269–1284.

Uriarte, A., Blanco, M. Cendrero, O. Grellier, P. Millán, P.,Morais, A. Rico, I. (2002a).Report of the Workshop on anchovy otoliths from subarea VIII and division IXa (Annex to PELASSES report EU study Project -EC DG XIV Contract nº99/010 and Working Document to the ICES Working Group on the assessment of Mackerel, Horse Mackerel, Sardine and Anchovy. Copenhagen, 10-19 September 2002.).

Uriarte, A. (2002b). Report of the 2001 Anchovy otolith exchange programme from Sub-area VIII and division IXa. (Annex to PELASSES report EU study Project -EC DG XIV Contract nº99/010).

Uriarte, A., Dueñas, C., Duhamel, E., Grelier, P., Rico, I., and B. Villamor, 2007. 2006 ANCHOVY OTOLITH WORKSHOP. Working Document to the 2007 ICES Planning Group on Commercial Catch, Discards and Biological Sampling (PGCCDBS) (5-9 March).

Deviations from the project work programme in WP4

The objective of WP4 was to evaluate the cost-effectiveness of different ageing methods, compare the different methods and estimate optimal setup in relation to sample sizes for calibration- and production samples.

Comparison between methods: For the Faeroe cod, the automated ageing was not possible, both with respect to individual ages based on image analysis and the age structure based on mixture analysis. This was attributable to the poor contrast in otolith visual appearance for the former, and non-normally distributed data in the latter. Since two methods did not yield acceptable results, a full evaluation of the cost-effectiveness was not possible for this stock.

Optimal setup All automated methods are based on the use of a testing sample, where only images and otolith biometrics are available and a learning sample, where also individual ages are known. The demand for this two-sample data structure – and particularly adequate sample sizes within the learning sample - turned out to be a factor which highly influenced the outcome of this project. We have learned that it is absolutely necessary to have a learning sample with good coverage within all age- and length classes in order to be useful and provide reliable results. Using half of the data available for this project as learning sample proved to

be an absolute minimum regarding data requirement. For this reason, it was not possible to evaluate the optimal constellation of sample sizes and data coverage for the learning- and testing samples. This lack of sufficient data was a problem associated with all stocks.

Consortium management

Co-ordination activities

During this first year, 2 meetings took place at the beginning and at month 8th. There were 2 meetings during the second period at month 18th and at month 23rd.

April 2007 meeting

The management of the project during the first year started in April 2007 (12-13) by a plenary meeting hosted by Ifremer, centre of Brest. This meeting gathered all scientists involved in the project and representing the 7 partners.

The aim of the meeting was to have an overview of the project realisation and of planning and tasks of the first year. A focus was carried out on the acquisition of the images and the associated databases (WP1) and the realisation of the algorithms.

The agenda of the meeting is provided hereafter :

April 12

09h00-09h30	Welcome / Short presentations of the participants	R. Fablet (Ifremer)
09h30-10h00	Administrative and financial guidelines from the EC	N. Vanden Eynden (EC)
10h15-10h30	*Coffee break*	
10h30-10h45	Overview of project organization and management Objectives for the first period (M1 to M9)	R. Fablet (Ifremer)
10h45-12h00	WP1: otolith data collation (Standardisation issues) - Otolith preparation protocols - Image acquisition protocols - Interpretation acquisition protocols - Data storage formats	R. Millner (CEFAS)
12h30-14h00	*Lunch*	
13h30-14h00	TNPC demo	A. Ogor (Ifremer)
14h00-14h45	WP1 & CS1: cod CS 2. Otolith data and CS objectives 3. Review of the information available for the considered stocks (stock characteristics, biological traits, ageing protocols) : ▪ North Sea cod ▪ Faeroe cod ▪ North East Artic cod	H. Mosegaard (DIFRES) R. Millner (CEFAS) H. Mosegaard (DIFRES) H. Hoie (IMR)
14h45-15h30	WP1 & CS1: plaice CS 4. Otolith data and CS objectives 5. Review of the information available for the	R. Millner (CEFAS)

	considered stocks (stock characteristics, biological traits, ageing protocol)	
	6. English Channel plaice	R. Millner (CEFAS)
	7. Iceland plaice	G. Thordarsson (MRI)
15h30-16h15	WP1 & CS3: anchovy CS 8. Otolith data and CS objectives 9. Review of the information available for the considered stock : Bay of Biscay anchovy	D. Mendiola (AZTI)
16h15-16h45	*Coffee break*	
16h45-17h30	WP1 : discussion & synthesis	R. Millner (CEFAS)
09h00-09h30	SC meeting	

April 13

09h00-09h30	SC meeting restitution	R. Fablet (Ifremer)
90h30-10h00	WP4: strategy and protocols for collating information conc cost benefit analysis	H. Mosegaard (DIFRES)
10h00-10h30	*Coffee break*	
10h30-10h45	WP2: algorithm developments 4) Overall objectives 5) WP organization	R. Fablet (Ifremer)
10h45-11h00	WP2: automated acquisition of image series (Task 2.1) - Objectives - Current development	R. Fablet (Ifremer)
11h00-12h00	WP2: otolith growth modelling (Task 2.2) - Objectives - Related work - Discussion concerning objectives and collaborations from M1 to M9	A. Christensen (DIFRES)
12h15-13h30	*Lunch*	
13h30-14h30	WP2: information extraction in images (Task 2.3) - Objectives - Related work - Discussion concerning objectives and collaborations from M1 to M9	R. Fablet (Ifremer) / A. Arbitz (IMR)
14h30-15h30	WP2: automated estimation of individual ages (Task 2.4) - Objectives - Related work - Discussion concerning objectives and collaborations from M1 to M9	V. Parisi (UPC)

15h30-16h00	*Coffee break*	
16h00-17h00	WP2: automated estimation of age structures (Task 2.5) - Objectives - Related work - Discussion concerning objectives and collaborations from M1 to M9	H. Mosegaard (DIFRES)
17h00-17h30	Ending word	R. Fablet

November 2007 meeting

In November 2007 (7-9), the second plenary meeting hosted by Azti, San Sebastian. This meeting gathered all scientists involved in the project and representing the 7 partners.

The aim of the meeting was to have an overview of the WP progress during the first 8 months and of the actions planned for 2008.

The agenda of the meeting is provided hereafter :

November 7

09h30-10h00	Welcome, presentation reminder on AFISA agenda	R. Fablet (Ifremer)
10h00-10h15	AFISA website presentation	A. Ogor (Ifremer)
10h15-10h30	Coffee Break	
10h30-12h30	WP1 and CS progress - deliverables results by stock - Schedule for completion of WP1 - Issues discussion	R. Millner (CEFAS)
12h30-14h00	Lunch	
14h00-17h00	parallel meetings : -DB acquisition and storage, cost-benefit issues (WP1) -shared code library (WP2)	 WP1 participants WP2 participants
17h00-18h00	plenary restitution	

November 8

09h00-12h00	Task-by-task progress of WP2	
	Task 2.1: image acquisition system (Ifremer)	S. Carbini (Ifremer)
	Task 2.2: otolith growth modelling (DIFRES, Ifremer)	H. Mosegaard (DIFRES) R. Fablet (Ifremer)
	Task 2.3: information extraction (Ifremer, IMR, UPC)	R. Fablet (Ifremer)
	Task 2.4: Estimation of individual fish ages (UPC, Ifremer)	V. Parisi (UPC)
12h00-14h00	Lunch	
15h00-17h00	WP2: definition of the structure of the shared library	WP2 participants
17h00-19h00	Steering Committee (SC) meeting	

November 9

09h00-12h00 Synthesis

12h00-14h00 Lunch

September 2008 meeting

In September 2008 (15-19), the third plenary meeting hosted by MRI, Reykjavik. This meeting gathered all scientists involved in the project and representing the 7 partners.

The aim of the meeting was to have an overview of the WP progress during the first 18 months and of the actions planned for 2009.

The agenda of the meeting is provided hereafter :

15th of September

Morning

Summary of the project by Kélig Mahe (Ifremer)
Welcome by Elias Gudmundsson (MRI)
Plenary meeting:

- description of the work advances:
- description of the algorithms made by UPC (Vicenç Parisi)
- description of the algorithms made by Ifremer (Sébastien Carbini)
- description of the algorithms made by the IMR (Alf Harbitz)
- description of the mixture and conditional models for age structure estimation made by the DTU (Karin Hüssy)
- description of the cost/benefit analysis made by the DTU (Karin Hüssy)

Afternoon

WP2 work session
WP4 work session

16th of September

Morning

Plenary session:

- Tasks and schedules anchovy otoliths observation and tests of some algorithms.

Afternoon

WP2 work session
WP4 work session

17th of September

Morning and Afternoon

WP2 work session

18th of September

Morning

Plenary meeting:

- presentation of the tests and analyses of the WP2 (UPC, IFREMER, IMR)
- to define the deadlines for each task to realise
- assessment of the deliverables of the second period

February 2009 meeting

In February 2009 (24-26), the fourth plenary meeting hosted by UPC, Vila Nova. This meeting gathered all scientists involved in the project and representing the 7 partners except DTU.

The aim of the meeting was to have an overview of the WP progress before the end of Afisa project and the work during the last month.

The agenda of the meeting is provided hereafter :

Tuesday (24 February)

09h30-09h45 : Welcome
09h45-11h00 : Plenary meeting : Workpackage 2 (Presentation of results)
description of the chain algorithms (Vicenç Parisi & Sébastien Carbini)
11h00-11h30 : Workpackage 2 (Presentation of results)
conditional model for age structure estimation from global otolith features and physical fish characteristics (Sébastien Carbini)
11h30-12h00 : Plenary meeting : Workpackage 3 (Presentation of results)
Software module for the automated estimation (Sébastien Carbini & Kélig Mahé)
13h00-14h30 : lunch
14h30-17h00 : Plenary meeting : Workpackage 4 (Discussion)
17h00-17h30 : Plenary meeting : Deliverables of second period
17h30-18h00 : Plenary meeting : Final Reports : documents for each partner
18h00-18h30 : Plenary meeting : Deviations of AFISA Project

Wednesday (25 February)

09h00-10h00 : Plenary meeting : Workpackage 4 (discussion with DTU Team)
10h00-13h00 : Work session (WP2 & WP4)
13h00-15h00 : Lunch
15h00-16h00 : Workpackage 2 (presentation of conditional model with new analyses)
16h00-18h30 : Plenary meeting : Final Reports : documents for each partner

Thursday (26 February)

09h00-10h30 : Plenary meeting : Workpackage 4 (discussion with DTU Team)
10h30-12h00 : Plenary meeting : Deliverables of second period and final reports

Consortium management tasks

The consortium agreement of the project AFISA was signed by all the partners at the beginning of 2008. This delay is explained by the change of management and the statute's modification of a partner (Danish Institute for Fisheries Research, Partner 4).

- Amendment n° 1 to the contract (10/07/2007) : Technical University of Denmark (DTU) takes over the rights and obligation of Danish Institute for Fisheries Research (DIFRES, Partner 4).

- Amendment n° 2 to the contract (08/04/2008): Change of article 11 with for the coordinator : Kelig.Mahe@ifremer.fr and Ramiro.Gonzales@ifremer.fr ; Change of coordinator's details with Institut Français de Recherche pour l'Exploitation de la Mer, represented by Mr. Jacques Serris, Deputy Managing Director.

These changes don't have any impact on the project objectives.

Project timetable and status

The Tasks 2.4 and 2.8 were longer to optimise the results of Workpackage 2. So, the Tasks 3.2 and 3.3 were moved at the end of the project (Tab. 28).

Table 28: Workpackages - Plan and Status Barchart

PROJECT BARCHART and STATUS

Acronym: **AFISA**

Contract N° **44132**

(to be frontlined to show status at project reviews)

(any previous revisions to be attached if original plans are revised)

		3 m	6 m rep	9 m	12 m rep	15 m	18 m rep	21 m rep	Final 24 m
		Duration							
Workpackage 1:	**Data collation**								
Task 1.1	Cod database								
Task 1.2	Plaice database								
Task 1.3	Anchovy database								
Task 1.4	Comprehensive cost-budget information								
Workpackage 2:	**Algorithms**								
Task 2.1	Automated acquisition of series of otolith images								
Task 2.2	Otolith growth modelling								
Task 2.3	Automated extraction of structures of interest in otolith images								
Task 2.4	Automated estimation of individual fish ages								
Task 2.5	Automated estimation of age structures from statistical distribution of otolith features								
Workpackage 3:	**Software integration**								
Task 3.1	Software module for automated acquisition of series of otolith image								
Task 3.2	Software module for the automated estimation of individual ages								
Task 3.3	Software module for the automated estimation of age structures								
Workpackage 4:	**Cost-benefit analysis**								
Task 4.1	Tools for evaluating costs, precision and accuracy of automated ageing systems								
Task 4.2	Application of cost-benefit analysis to case study I (Cod)								
Task 4.3	Application of cost-benefit analysis to case study II (Plaice)								
Task 4.4	Application of cost-benefit analysis to case study III (Anchovy)								

Comments and information on co-ordination activities

The project management and animation is carried out through a Ifremer web site. A public access presents the objectives and progress of the project to the general public :
http://www.ifremer.fr/lasaa/anglais/aAFISA.htm
This site has a private access (wiki system) for the Afisa consortium that acts as a management and information sharing tool:
http://www.ifremer.fr/lasaa/Afisa/wikiafisa/wiki/index.php

The data exchanges between the partners of the Afisa consortium are carried out using DVD or FTP.

For a public, there is as well an European commission web site:
http://ec.europa.eu/research/fp6/ssp/afisa_en.htm

Policy Implemantation Plan

The AFISA (Automated Fish Ageing) project is targeted on SPP Call 5A, area 1.3, "Modernisation and sustainability of fisheries, including aquaculture-based production systems", Task 3 "Objective model-based and computer-assisted age determination technology for fish:"
The Common Fisheries Policy (CFP) relies on the assessment of fish stock status. Age estimation plays a very important role in the age-based assessment of many stocks in the North Atlantic which are assessed annually using age-based sequential population analysis models (eg Extend Survivor Analysis XSA). Annual age-length keys which are used to estimate catch-at-age data and age structure catch per-unit-effort (CPUE) indices as well as maturity at age used to estimate the spawning stock biomass are key inputs for the exploited stock assessment models. The quality of this age-related data is then a crucial aspect for improving the results of the CFP. Consequently, the demonstration of the readiness of automated systems for routine ageing will significantly contribute to the objectives of the CFP at different levels.
The benefits expected from the implementation of automated ageing systems are then important. More precisely, the impact of the associated improvements in terms of ageing quality, especially regarding quality control and quality assurance issues, is expected at different levels as detailed below:

- Ageing automation reduces the cost of the acquisition of age-related, as it will be exemplified within this project for the selected case-studies. Therefore, effort allocation could be optimized, for instance to increase the number of aged samples, or to reallocate the effort to related issues (e.g., ageing validation and accuracy issues). This aspect clearly contributes to the framework of the fisheries data collected by the EU, under EU Council Regulation 1543/2000 and the subsequent Commission Regulation 1639/2001 amended by 1581/2004;
- Expected improvements, especially quality assurance and quality control of ageing procedures, will first result in improved stock assessment models which will deliver more accurate stock forecasts and management advices. Such results will permit better adjustments of the TACs (Total Allowable Catches) and consequently improve the use of the production capacities to contribute to a sustainable fisheries management;
- Such improvements will also contribute to a better knowledge of the actual population status, both in qualitative and quantitative terms. As such, it will contribute to environmental monitoring, e.g. within the framework of the European Marine Strategy;
- Age-related data also participate to the evaluation of the effect of anthropogenic impacts and/or global change on natural populations at the individual level. Therefore, an improved quality of age data issued from the operational use of automated ageing systems will be a relevant contribution for the determination of the maximum sustainable yield within the framework of the CFP (e.g. Council Regulation (EC) No 2371/2002**)**;
- The considered case-studies species are, at least for two of them, namely, cod and anchovy (cf. Council Regulation 423/2004 and Commission Regulation 1539/2005)), species for which the

status of the stocks are critical. Hence, the improvement of ageing quality as well as the characterization of ageing uncertainty are of key importance for delivering accurate stock forecasts important for management advices (e.g. recovery plans);

- The combination of automated ageing systems to fisheries information systems will also clearly contribute to the data collection regulation implemented by EU under Council Regulation 1543/2000 and the subsequent Commission Regulation 1639/2001 amended by 1581/2004;
- As stressed by the objectives of EU concerted action TACADAR (2006), means for the accreditation and the certification of fish age determination are investigated at the European level. Automated ageing systems are clearly key contributions to these issues;
- The recommendation issued from EU concerted action EFARO/MUTIFISHARE (QLRT-2001-01353) meeting "How can otolith research contribute at improving fisheries sciences?" held in December 2004 further stress the relevance of this project with respect to the CFP.

After 2 years, an assessment of AFISA Project can be established :

- A database of 6729 otoliths has been digitized (transmitted and reflected light) and interpreted by the European readers in three case studies : a) Cod (*Gadus morhua* ; Faeroes, North Sea, North East Arctic) b) Anchovy (*Engraulis encrasicolus* ; Bay of Biscay) c) Plaice (*Pleuronectes platessa*, Eastern Channel, Iceland). These images could be an important tool for the exercises of calibrations among laboratories, especially for anchovy because for this species readers do not routinely produce images. This set of images could be used for the future development of automation and other applications.
- During this project, 7 laboratories (IFREMER, France; AZTI, Spain; CEFAS, England; DTU, Denmark; IMR, Norway; MRI, Iceland; UPC, Spain) acquired the TNPC software dedicated to the images analysis of otoliths. The use of this software could be included in quality insurance and quality control of ageing procedures which are associated with fish age estimation for each laboratory and during the exchanges among laboratories (Green Paper, Integrating the Common Fisheries Policy in the broader maritime policy context).
- A module automating the acquisition of a series of otolith images was carried out in the TNPC software. This application reduces the acquisition costs of images.
- A fish age classifier and a conditional model were carried out and then integrated in TNPC software in order to automatically obtain age estimations from images. This process is generic and able to be applied to all species. Although high percentages of agreement between readers and models resulted for the plaice and the cod, they are not so significant for anchovies. Thus, this tool is usable for certain species but it has a potential to be improved in the future for all species.
- A Matlab – C library of functions, fully documented and tested, has been compiled. It implements all the algorithms and methods developed in order to improve the otolith images, extract the 1D and 2D signals and process them to compute the most discriminant features for classification.
- This project shows that computer vision and image processing can decrease the acquisition cost of age-related data in many cases and can be a great tool to aid in the interpretation and quality improvement of otolith image information, for those cases where individual age estimation or age structure computation doesn't yield as good results as expert or traditional age-length keys.

Delivery of the First year reports

The consortium submits the following reports of the Commission for the first reporting period in May 2008:

1) the periodic activity report which includes:
   - ❖ publishable executive summary
   - ❖ plan for using and disseminating the knowledge
2) the periodic management report
   - ❖ justification of the resources deployed by each contractor
   - ❖ Form C statement set out in Annex VI
   - ❖ A summary financial report consolidating the claimed costs of all the contractors in an aggregate form, based on the information provided in Form C
3) the periodic report on the distribution of the community's contribution
4) Interim science and society reporting questionnaire
5) Interim reporting questionnaire on workforce statistics
6) Interim socio-economic reporting questionnaire
7) Deliverables

Delivery of the Second year reports

The consortium submits the following reports of the Commission for the second reporting period in May 2009:

8) the periodic activity report which includes:
   - ❖ publishable executive summary
   - ❖ plan for using and disseminating the knowledge
9) the periodic management report
   - ❖ justification of the resources deployed by each contractor
   - ❖ Form C statement set out in Annex VI
   - ❖ A summary financial report consolidating the claimed costs of all the contractors in an aggregate form, based on the information provided in Form C
10) the periodic report on the distribution of the community's contribution
11) Interim science and society reporting questionnaire

12) Interim reporting questionnaire on workforce statistics
13) Interim socio-economic reporting questionnaire
14) Deliverables

Delivery of the whole period reports

The consortium submits the following reports of the Commission for the whole reporting period in May 2009:

15) Publishable final activity report which includes:
    - ❖ publishable executive summary
    - ❖ plan for using and disseminating the knowledge
16) the management report
    - ❖ justification of the resources deployed by each contractor
    - ❖ Form C statement set out in Annex VI
    - ❖ A summary financial report consolidating the claimed costs of all the contractors in an aggregate form, based on the information provided in Form C
17) the report on the distribution of the community's contribution
18) Final science and society reporting questionnaire
19) Final reporting questionnaire on workforce statistics
20) Final socio-economic reporting questionnaire
21) Deliverables

Annex I – Plan for using and disseminating the knowledge

Section 1 - Exploitable knowledge and its Use

Overview table

Exploitable Knowledge (description)	Exploitable product(s) or measure(s)	Sector(s) of application	Timetable for commercial use	Patents or other IPR protection	Owner & Other Partner(s) involved
Digital processing for calcified structures with the module of	TNPC software (version 5)	laboratories of science (sclerochronology)	2009	Licence of software	IFREMER and Noesis company

Exploitable Knowledge (description)	Exploitable product(s) or measure(s)	Sector(s) of application	Timetable for commercial use	Patents or other IPR protection	Owner & Other Partner(s) involved
automation					

Ifremer and Noesis society developed TNPC 4.0 software since 2005. During the Afisa project, the development of algorithms for fish ageing automation from otolith features is realised. The estimation of individual ages and the age proportion, was integrated into the software TNPC 5.0 developed by the Noesis company (http://www.noesisvision.com/index_en.htm) allowing an automated system for the acquisition of otolith image series and age estimation. For some species such as plaice, the automation could be usable from the perspective of bias and costs of age data.

Section 2 – Dissemination of knowledge

Overview table

Planned/ actual Dates	Type	Type of audience	Countries addressed	Size of audience	Partner responsible /involved
31/12/07	Database of annotated otoliths	other partners in the project			3
25/09/07	TNPC User Guide	other partners in the project			1
25/09/07	TNPC step by step	other partners in the project			1
21/01/08	TNPC version 4.2	other partners in the project			1
17/01/08	AFISA Computer Vision Library	other partners in the WP2			1

Section 3 - Publishable results

Publications

Doering-Arjes, P., Cardinale, M. & Mosegaard, H., 2008. Estimating population age structure using otolith morphometrics: a test with known-age Atlantic cod (*Gadus morhua*) individuals. Can. J. Fish. Aquat. Sci. 65: 2342-2350.

Fablet, R., Chessel, A., Carbini, S., Benzinou, A. & de Pontual, H. 2009. Reconstructing individual shape histories of fish otoliths: a new image-based tool for otolith growth analysis and modeling Fisheries Research, 96(2-3):148-159.

Hüssy, K., 2008. Otolith shape in juvenile cod (*Gadus morhua*): Ontogenetic and environmental effects. Journal of Experimental Marine Biology and Ecology. 364: 35-41.

Symposium

Carbini, S., Chessel, A., Benzinou, A., Fablet, R., Mahé, K. & De Pontual, H., 2008. A review of image-based tools for automatic fish ageing from otolith features, Colloque "Approche Systémique des Pêches", Boulogne-sur-mer, France, 5-7 September.

Harbitz, A. & Høie, H., 2009. Age distribution of North East Arctic cod estimated from the contour of otolith section images. 4th International Otolith Symposium, Monterey, USA, 24-28 August.

Harbitz, A., 2009. A generic ad-hoc algorithm for automatic nucleus detection from the otolith contour. 4th International Otolith Symposium, Monterey, USA, 24-28 August.

Mahé, K. (coord.), 2008. AFISA Automated FISh Ageing (2007-2009), Colloque "BIOMARINE", Toulon & Marseille, France, 20-24 October.

Mahe, K., Parisi, V., Carbini, S., De Pontual, H., Soria, J.A., Cotano, U., Harbitz, A., Fablet, R., 2009. Automated Fish Ageing (AFISA). 4th International Otolith Symposium, Monterey, USA, 24-28 August.

Parisi, V., Carbini, S., Soria, J.A. & Fablet, R., 2009. Otolith image classification and conditional models for fish ageing: plaice and cod case studies. 4th International Otolith Symposium, Monterey, USA, 24-28 August.

Workshops

Carbini, S. & Parisi, V, 2009. Conditional models. 4th AFISA Workshop, Vilanova i la Geltrú, Spain, 23-27 February.

Carbini, S., & Mahé, K., 2009. TNPC 5.0 : new version and automatisation. 4th AFISA Workshop, Vilanova i la Geltrú, Spain, 23-27 February.Christensen, A., Thyg Mosegaard, H., esen, U.H. & Worse, L. A. 2007. Otolith growth modelling. 1st AFISA Workshop, Brest, France, 12-13 April.

Fablet, R., Benzinou, A., Chessel, A. Dzonou, R., Lorrain, A., Pecquerie, L., de Pontual, H. & Rodin, V. 2007. A numerical model for the formation of fish otoliths. 2nd AFISA Workshop, San Sebastian, Spain, 7-9 November.

Gudmundsson, E. 2007. Plaice in Icelandic waters. 1st AFISA Workshop, Brest, France, 12-13 April.

Harbitz, A. 2007. Automatic segmentation of age zones in North East Arctic Cod (NEAC) otoliths. 1st AFISA Workshop, Brest, France, 12-13 April.

Hoie, H & Harbitz, A. 2007. Cod of the Barents Sea area. 1st AFISA Workshop, Brest, France, 12-13 April.

Mendiola, D. 2007. Anchovy of the Bay of Biscay. 1st AFISA Workshop, Brest, France, 12-13 April.

Millner, R. & Warnes, S. 2007. Collation of otolith material and creation of databases of annotated images of otoliths. 1st AFISA Workshop, Brest, France, 12-13 April.

Millner, R. & Warnes, S. 2007. North Sea Cod (CIEM IV). 1st AFISA Workshop, Brest, France, 12-13 April.

Millner, R. & Warnes, S. 2007. Plaice of the Eastern English Channel (CIEM VIId). 1st AFISA Workshop, Brest, France, 12-13 April.

Mosegaard, H. 2007. Otolith growth modelling. 1st AFISA Workshop, Brest, France, 12-13 April.

Parisi, V & Soria, J.A., 2008. Evaluation of developed algorithms. 3rd AFISA Workshop, Reykjavic, Iceland, 15-19 September.

Parisi, V, Carbini, S. & Soria, J.A., 2009. Automated fish age estimation results. 4th AFISA Workshop, Vilanova i la Geltrú, Spain, 23-27 February.

Reports

Carbini, S. 2007. Automation of the fish age estimation starting from otoliths images. *ENIB Final Report, N° Contract : 07 20 733 051,* 28p.

Fablet, R. & Ogor, A., 2007. TNPC : Digital Processing of Calcified Structures v4.2. 57p. (http://www.ifremer.fr/lasaa/TNPC/engmanuel_tnpc42.pdf)

Mahé, K., Dufour, J. L. & Ogor, A., 2007. T.N.P.C. 4.2 : Step by step user guide, Ifremer Report, 29p. (http://www.ifremer.fr/lasaa/TNPC/Tnpc4_2English.htm)